CORA Cork Open Research Archive
Cartlann Taighde Oscailte Chorcaí

| | |
|---|---|
| Title | High resolution wave and tidal energy resource assessment in the Irish and western UK waters |
| Authors | Furlong, Rebecca |
| Publication date | 2021-10-19 |
| Original Citation | Furlong, R. 2021. High resolution wave and tidal energy resource assessment in the Irish and western UK waters. MRes Thesis, University College Cork. |
| Type of publication | Masters thesis (Research) |
| Rights | © 2021, Rebecca Furlong. - https://creativecommons.org/licenses/by-sa/4.0/ |
| Download date | 2026-11-17 11:41:57 |
| Item downloaded from | https://hdl.handle.net/10468/13209 |

UCC
University College Cork, Ireland
Coláiste na hOllscoile Corcaigh

# Ollscoil na hÉireann, Corcaigh

National University of Ireland, Cork




High Resolution Wave and Tidal Energy Resource Assessment in the Irish and Western UK waters.

Thesis presented by

Rebecca Furlong

for the degree of

Masters by Research

University College Cork

School of Engineering & Architecture

Head of School/Department: Dr Jorge Oliveira

Supervisor(s): ROSS O'CONNELL, DR. JIMMY MURPHY

2021

# Contents

Declaration ..... I

Preface ..... II

Acknowledgements ..... III

Abstract ..... IV

List of Figures ..... V

List of Tables ..... IX

List of Equations ..... X

List of Acronyms ..... XI

1. Introduction ..... 1

1.1 Aims and Objectives ..... 2

1.2 Outline of Thesis ..... 2

1.3 Research output and novel contributions ..... 3

2. Literature Review ..... 4

2.1 Introduction to Literature Review ..... 4

2.2 Waves and Wave Energy ..... 5

2.2.1 Wave parameters for wave resource assessment ..... 7

2.2.2 Wave Energy Converters (WEC's) ..... 8

2.2.3 Technology and Commerciality ..... 12

2.3 Tides and Tidal Energy ..... 13

2.3.1 Tidal Energy ..... 15

2.3.2 Tidal Energy Converter's (TEC's) ..... 18

2.4 Data Availability ..... 22

2.4.1 Modelling Techniques for Wave Energy Resource Assessment ..... 22

2.4.2 Modelling Techniques for Tidal Energy Resource Assessment ..... 23

2.5 Introduction to Online GIS ..... 23

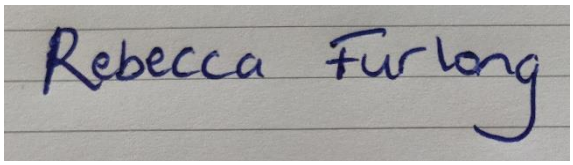
2.5.1 Spatial Analysis ..... 23

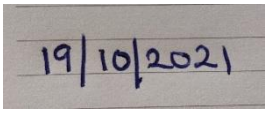
2.6 Wave and Tidal Resource Assessment ..... 28
3 Data and Methodology ..... 31
3.1 Software ..... 31
3.2 Study Area ..... 31
3.3. Wave Data ..... 32
3.3.1 Validation of Wave Data ..... 33
3.3.2 Wave Assessment ..... 40
3.4 Tidal Data ..... 47
3.4.1 Tidal Data Validation ..... 47
3.4.2 Tidal Assessment ..... 49
3.4.2.1 Tidal Current Analysis ..... 49
3.4.2.2 Tidal Power Analysis ..... 50
4 Results ..... 52
4.1 Wave Results ..... 52
4.1.1 Wave Power Resource Analysis ..... 52
4.1.2 Seasonal Analysis of the Wave Parameters ..... 55
4.1.3 Comparison between IBI and NWS Models ..... 68
4.2 Tidal Results ..... 75
4.2.1 Tidal Current Analysis ..... 75
4.2.2 Tidal Power Resource Analysis ..... 78
4.2.3 Total Tidal Energy ..... 84
4.3 Updated Resource Assessment ..... 86
4.3.1 Wave Resource ..... 86
4.3.2 Tidal Resource ..... 86
4.4 Importance for MRE Industry ..... 87
4.5 Comparison with other datasets ..... 88
5 Conclusions and Recommendations ..... 92

5.1 Methodology ..... 94
5.2 Data Limitations ..... 95
5.3 Recommendations for future work ..... 96
References ..... 98
Appendix ..... 104
1 - Publication of Paper related to research ..... 104
2 – Figures ..... 114
3 – Tables ..... 131
4 – IBI Scripts ..... 134
5 – NWS Scripts ..... 154

## Declaration

This is to certify that the work I am submitting is my own and has not been submitted for another degree, either at University College Cork or elsewhere. All external references and sources are clearly acknowledged and identified within the contents. I have read and understood the regulations of University College Cork concerning plagiarism and intellectual property.

Signed: 


Date: 

# Preface

This thesis was submitted to the Department of Engineering at University College Cork for a degree of Masters by Research. The thesis was completed under the supervision of Dr. Jimmy Murphy and Ross O'Connell

The work was completed as part of the SELKIE project under Work Package 4. SELKIE is a new €4.2m cross-border project aiming to boost the marine energy industry in Wales and Ireland. Selkie is bringing together leading researchers and businesses to improve the performance of Wave and Tidal marine energy devices in Ireland and Wales. The SELKIE project has received funding from the European Union's European Regional Development Fund through the Ireland Wales Cooperation programme.

## Acknowledgements

I would firstly like to thank my main supervisor Dr. Jimmy Murphy of the School of Engineering in UCC and Lead Technical Engineer of the Lir National Ocean Test Facility (Lir NOTF) in the SFI MaREI Centre. His advice, guidance, and feedback during the process of undertaking the thesis has been essential and appreciated. I would also like to thank my colleague and mentor on SELKIE work package 4 Ross O'Connell whose advice and guidance has been vital to the work that I undertook for this project.

I would like to thank the team at Copernicus Marine Service for their technical help with the wave data downloads, particularly Elena and David whose help was greatly appreciated. I would also like to thank Kieran Lyons at the Irish Marine Institute for his help with the tidal data download. The data from both Copernicus Marine Service and the Irish Marine Institute was freely provided and it goes without saying that this study couldn't have been undertaken without it.

I would like to thank Marco Guerrini at MaREI for his help and advice with regards to the tidal modelling in MATLAB, it was greatly appreciated. I would like to thank Rory Scarrott and James Fitton at UCC for their helpful advice regarding ArcGIS and ArcGIS Enterprise, it was much appreciated. My thanks also go to Felix Butschek for his advice regarding modelling in MATLAB and R. Finally, my thanks go to the other research students at the department in UCC, the weekly coffee catch ups were very helpful in keeping the spirits up during difficult times.

Finally, I would like to thank my family and close friends, who have motivated me and encouraged me to pursue this research masters. I would like to thank them for their never-ending support and for taking the time to read the many drafts of this thesis that I have shared with them.

## Abstract

As island countries, both Ireland and the UK have long and extensive coastlines, making offshore renewable energy easily accessible. Previous studies in the area have shown that there is resource availability for both wave and tidal energy in UK and Irish waters, with an abundant wave resource off the west coast of Ireland and a well-known tidal resource within the Irish and Celtic Seas. The Irish Climate Action Plan 2019 set out that 70% of electricity would come from renewable sources by 2030, meaning that research and development that is ongoing in the offshore industry is key to reaching that target. This study aims to create new, updated GIS layers showing both the wave and tidal energy resource as well as the parameters needed to compute them, including significant wave heights, wave energy periods and tidal current speeds. The Copernicus Marine Service recently updated two models that now contain wave spectrum data at high resolutions, both less than 5 kilometres, and long hindcasts of greater than 20 years. The accessibility of this data means that the wave energy resource can be modelled very accurately at high resolutions, a parameter that is hugely important for marine renewable energy developers to gain an understanding of potential deployment site characteristics. Data for tidal resource analysis is available through the Irish Marine Institute and is based on a ROMS model. This study has shown that the Copernicus models correlate very well with each other, and it is possible to create resource layers for use in GIS with the data. This information is imperative for marine renewable energy developers at a first stage so they can have a thorough understanding of the resource availability and conditions available at a proposed site. Having resource information available within a GIS tool can give developers a spatial overview of where the best resource is available, while the GIS can also provide valuable information such as the location of the closest grid connections and the nature of the underlying bedrock, all factors that can influence the location of a wave or tidal farm.

# List of Figures

Figure 2.1 Study area for high resolution wave and tidal energy resource assessment. ..... 4
Figure 2.2 A figure from Aquaret showing the wave resource distribution across Europe (Aquaret, 2012a). ..... 5
Figure 2.3 Global wave resource distribution in kW/m (Bombora, 2020)..... 6
Figure 2.4 Characteristics of Waves (A Level Geography, 2018)..... 6
Figure 2.5 Example of an attenuator device (Aquaret, 2012). ..... 8
Figure 2.6 The figure on the left hand side shows the Archimedes Waveswing (AWS Ocean Energy, 2021). The figure on the right hand side shows how a point absorber looks on the ocean floor (Aquaret, 2012)..... 9
Figure 2.7 The figure on the left hand side shows the Langlee device (Langlee Wave Power AS, 2013). The figure on the right hand side showsshowing how an oscillating wave surge converter would look on the ocean floor. (Aquaret, 2012). ..... 9
Figure 2.8 An illustration showing how an Oscillating Water Column works (Aquaret, 2012). ..... 10
Figure 2.9 The Ocean Energy OE35 Buoy which is an example of a floating oscillating water column (OceanEnergy, 2020). ..... 10
Figure 2.10 The figure on the left hand side shows the WaveDragon device (Tethys, 2021). The figure on the right hand side shows an example of an overtopping device (Aquaret, 2012)..... 11
Figure 2.11 An illustration showing how a submerged pressure differential works (Aquaret, 2012) ..... 11
Figure 2.12 The Wello Penguin (Wello, 2021) ..... 12
Figure 2.13 An illustration of how the rotating mass device works (Aquaret, 2012)..... 12
Figure 2.14 An illustration of the global mean daily tidal range (Minesto AB, 2021b). ..... 13
Figure 2.15 An illustration showing the global distribution pattern of Diurnal, Semi-Diurnal and Mixed Tides (Webb, 2021). ..... 14
Figure 2.16 Two figures showing both the spring and neap cycles. The figure on the left-hand side shows the spring cycle, where the sun, moon and earth are aligned resulting in larger variations in the tide. Then figure on the right shows the neap tidal cycle where..... 14
Figure 2.17 An illustration showing the tidal stream resource distribution for Europe. Source:(EMEC, 2021c). ..... 16

Figure 2.18 Depth Averaged Peak Spring Tidal Currents around the island of Ireland (SEAI, 2004)..... 17
Figure 2.19 The figure on the left hand side shows the SeaGEN turine (Simec Atlantis, 2021). The figure on the right hand side is an illustration of a horizontal axis turbine where the blades of the turbine are parallel to the current direction. (EMEC, 2021). ..... 18
Figure 2.20 Sabella D10 Horizontal axis turbine (Sabella, 2021). ..... 19
Figure 2.21 An illustration of a vertical axis turbine (EMEC, 2021). ..... 19
Figure 2.22 An illustration of an oscillating hydrofoil (EMEC, 2021)..... 20
Figure 2.23 The figure on the left hand side shows the Flumill device that was tested at Shapinsay Sound in the UK in 2011 (EMEC, 2021). The figure on the right shows an illustration of an Archimedes screw type tidal energy converter (EMEC, 2021)..... 20
Figure 2.24 Minesto DG500 Tidal Kite (Minesto AB, 2021). ..... 21
Figure 2.25 Minesto DG100 Tidal Kite (Minesto AB, 2021) ..... 21
Figure 2.26 Wales Marine Planning Portal showing Annual Average Tidal Power (British Crown and OceanWise Ltd, 2020)..... 25
Figure 2.27 Ireland Marine Atlas showing Mean Theoretical Wave Energy Resource (Marine Institute, 2015). ..... 25
Figure 2.28 Ireland Marine Atlas showing Tidal layers that are currently available (Marine Institute, 2015). ..... 26
Figure 2.29 This map shows the significant wave height and direction in 237 locations placed at approximately 100 km intervals some 50 to 100 km off Europeand#39;s coastline. The observations of wave height and direction were collected using the altimeter sensors carried by the ERS-1, ERS-2, Topex/Poseidon and Geosat satellites available in the waveclimate.com database. From these observations, averages were calculated in a 200 by 200 kilometre box centred on each location (European Union, 2021). ..... 27
Figure 2.30 This map displays the average tidal amplitude, half of the height difference between low and high tide, in 237 locations placed at approximately 100 km intervals some 50 to 100 km off Europe's coastline. The observations were calculated using a tidal model derived from eight years of satellite altimeter measurements as well as tidal gauge measurements from approximately 7300 coastal stations (European Union, 2021). ..... 28
Figure 2.31 Peak Spring Tide current velocity. (Lewis, 2015) ..... 30
Figure 3.1 Study Area for high resolution wave and tidal energy resource assessment in the Irish and Celtic Seas. ..... 32

Figure 3.2 Details of the Atlantic Iberian Biscay Irish Ocean Wave Reanalysis model from the Copernicus Marine service that was used for the modelling of the wave resource (CMEMS, 2021). ..... 33
Figure 3.3 Details of the Atlantic European North West Shelf Wave Physics Reanalysis model from the Copernicus Marine service that was used for the modelling of the wave resource (CMEMS, 2021). ..... 33
Figure 3.4 Location of the coastal (orange dots) and deep water (green dots) buoys included in the IBI qualification during the whole period (01/01/1993 - 31/12/2019). Source: (Baladrón, 2020). ..... 35
Figure 3.5 Detailed figure showing the location of the buoys that Copernicus used for their validation study of the IBI model. Note: The co-ordinate information for these buoys was taken from the CMEMS dashboard, the location information for all 11 buoys within UK.... 36
Figure 3.6 Tables from the CMEMS validation study showing results for the Irish sub region for Significant Wave Heights Source: (Baladrón, 2020). ..... 37
Figure 3.7 Tables from the CMEMS validation study showing results for the Irish sub region for Wave Periods. Source: (Baladrón, 2020)..... 37
Figure 3.8 Verification statistics for significant wave height comparison versus open waters in-situ observations.(Tonanai & Saulter, 2021)..... 38
Figure 3.9 Results from the validation study carried out by O'Connell.R, 2021. The results in table a show NWS values and table B shows IBI values. ..... 40
Figure 3.10 Grid Index for NetCDF data downloads from the Copernicus Website. ..... 41
Figure 3.11 Individual GeoTIFF datasets for Wave Power (prior to merging unto final output layer)..... 43
Figure 3.12 Input parameters for the IBI model data for ArcGIS Pro ‘Mosaic to New Raster’ toolbox that is used for merging GeoTIFF files into final raster dataset. ..... 44
Figure 3.13 ArcGIS Pro 'Raster Calculator' tool that is used during the conversion process. 45
Figure 3.14 ArcGIS Pro 'Int' tool that is used during the conversion process..... 45
Figure 3.15 ArcGIS Pro 'Raster to Polygon' tool that is used during the conversion process. 46
Figure 3.16 ArcGIS Pro 'Field Calculator' tool that is used during the conversion process. .. 46
Figure 3.17 The comparison of the tidal constituent data between the tidal gauges and the ROMS model as part of the validation study (Nagy, H. 2020). ..... 48
Figure 4.1 Scatter plot showing the relationship between the mean wave power (kW/m) for the IBI and NWS models, with the IBI model showing in the map on the top right and the NWS map on the bottom left of the page. ..... 52

Figure 4.2 Mean wave power resource in kW/m for the study area, calculated using the 20 year hindcast data from the Copernicus IBI model..... 54
Figure 4.3 Mean wave power resource in kW/m for the study area, calculated using the 20 year hindcast data from the Copernicus NWS model. ..... 54
Figure 4.4 Seasonal statistical analysis for the winter datasets for IBI and NWS..... 56
Figure 4.5 Significant wave heights (m) for each season: summer, spring, autumn and winter. Values were modelled using 20 year IBI dataset..... 57
Figure 4.6 Significant Wave Heights(m) for each season: summer, spring, autumn and winter. Values were modelled using 20-year NWS dataset. ..... 58
Figure 4.7 Statistical analysis of the spring wave periods for both the IBI and NWS models. ..... 60
Figure 4.8 Scatter diagram showing R sqared value for IBI and NWS data for wave periods for spring once outlier points have been removed. ..... 61
Figure 4.9 Mean Wave Energy Period (s) for each season: summer, spring, autumn and Winter. Values were modelled using 20-year IBI dataset. ..... 62
Figure 4.10 Mean Wave Energy Period (s) for each season: summer, spring, autumn and winter. Values were modelled using 20-year NWS dataset. ..... 62
Figure 4.11 Scatter diagram showing R squared value for IBI and NWS data for wave power for the winter layers. ..... 64
Figure 4.12 Mean wave power resource in kW/m for each season: summer, spring, autumn and Winter. Values were modelled using 20 year IBI dataset..... 67
Figure 4.13 Mean wave power resource in kW/m for each season: summer, spring, autumn and winter. Values were modelled using 20 year NWS dataset. ..... 67
Figure 4.14 Comparison sites that have been chosen to review the IBI and NWS mean wave power resource results..... 68
Figure 4.15 Comparison of mean wave power in kW/m between the IBI Model and the NWS Model for the Northwest Coast of Ireland, just west of Donegal. ..... 69
Figure 4.16 Comparison of mean wave power in kW/m between the IBI Model and the NWS Model for the Wave Hub Pembrokeshire Demonstration Zone off the SW Coast of Pembrokeshire in Wales..... 70
Figure 4.17 Comparison of mean wave power in kW/m between the IBI Model and the NWS Model for the Irish Sea SW of the Isle of Man..... 72
Figure 4.18 Comparison of mean wave power in kW/m between the IBI Model and the NWS Model for the West Wave Deployment Zone off the SW coast of Ireland. ..... 73

Figure 4.19 Mean Spring Current Velocity (m/s) that has been calculated using a 1 year time series of data from the Irish Marine Institute ROMS model. ..... 75
Figure 4.20 Mean peak current velocity (m/s) - (calculated over the whole year irrespective of mean or spring periods) that has been calculated using a 1 year time series of data from the Irish Marine Institute ROMS model. ..... 77
Figure 4.21 Mean neap peak current velocity (m/s) that has been calculated using a 1 year time series of data from the Irish Marine Institute ROMS model. ..... 78
Figure 4.22 Mean Tidal Power (W/m2). ..... 80
Figure 4.23 Mean Tidal Power (W/m2) showing areas of interest mainly within the Irish and Celtic Seas. ..... 81
Figure 4.24 Mean tidal power sites of interest continued. ..... 82
Figure 4.25 Mean Neap Tidal Power (W/m2). ..... 83
Figure 4.26 Mean Spring Tidal Power (W/m2). ..... 83
Figure 4.27 Total Energy (MWh) for the study area: calculated using data from the Irish Marine Institute ROMS model. ..... 84
Figure 4.28 Total Spring Energy (MWh) for the study area: calculated using data from the Irish Marine Institute ROMS model. ..... 85
Figure 4.29 Total Neap Energy (MWh) for the study area: calculated using data from the Irish Marine Institute ROMS model. ..... 85
Figure 4.30 Comparison between wave energy resource dataset that has been created as part of this study and the datasets that are currently available through the Irish Marine Atlas and the Wales Marine Planning Portal. ..... 89
Figure 4.31 Comparison between tidal energy resource dataset that has been created as part of this study and the datasets that are currently available through the Irish Marine Atlas and the Wales Marine Planning Portal. ..... 91

## List of Tables

Table 4.1 Comparison table between IBI mean wave power (kW/m) and NWS mean wave power (kW/m) for the 5 points that have been selected. ..... 55
Table 4.2 Comparison table showing the mean significant wave heights for winter and summer from the IBI model and the NWS model for the 5 comparison points. ..... 59
Table 4.3 Comparison table showing the mean significant wave heights for spring and autumn from the IBI model and the NWS model for the 5 comparison points. ..... 59

Table 4.4 Comparison table showing the mean wave energy periods (Te) for winter and summer from the IBI model for the 5 comparison points. ..... 63
Table 4.5 Comparison table showing the mean wave energy periods (Te) for spring and autumn from the IBI model for the 5 comparison points. ..... 63
Table 4.6 Comparison table showing the mean wave power resource (kW/m) for winter and summer from the IBI model for the 5 comparison points. ..... 66
Table 4.7 Comparison table showing the mean wave power resource (kW/m) for spring and autumn from the IBI model for the 5 comparison points. ..... 66
Table 4.8 Comparison table of mean wave power in kW/m between the IBI Model and the NWS Model for the Northwest Coast of Ireland, just west of Donegal. ..... 69
Table 4.9 Comparison table of mean wave power in kW/m between the IBI Model and the NWS Model for the Wave Hub Pembrokeshire Demonstration Zone off the SW Coast of Pembrokeshire in Wales. ..... 71
Table 4.10 Comparison table of mean wave power in kW/m between the IBI Model and the NWS Model for the Irish Sea SW of the Isle of Man. ..... 72
Table 4.11 Comparison table of mean wave power in kW/m between the IBI Model and the NWS Model for the West Wave Deployment Zone off the SW coast of Ireland. ..... 73
Table 4.12 Comparison table for the 5 points that have been selected across the study area showing mean and max values for spring current velocity, neap current velocity and peak current velocity. ..... 78
Table 4.13 Comparison table for the 5 points that have been selected across the study area showing hourly mean tidal power, hourly mean spring tidal power and hourly mean neap tidal power. ..... 79
Table 4.14 Comparison table for the 5 points that have been selected across the study area showing Annual Tidal Power, Annual Spring Tidal Power and Annual Neap Tidal Power. . 86

## List of Equations

Equation 1 Wave Power ..... 7
Equation 2 A simplified equation for regular wave power, for regular sea states. ..... 7
Equation 3 Wave power per unit width of a wave crest. ..... 7
Equation 4 Mean power of a tidal current per unit area. ..... 17
Equation 5 Simplified equation of mean power of a tidal current. ..... 17

# List of Acronyms

ADCP – Acoustic Doppler Current Profiler

AEP – Annual Energy Production

CAPEX – Capital Expenditure

CMEMS – Copernicus Marine Environment Monitoring Service

EC – European Commission

ECMWF – European Centre for Medium Range Weather Forecasts

EEZ – Exclusive Economic Zone

EMEC – European Marine Energy Centre

EU – European Union

GIS – Geographic Information System

GWh – Gigawatt hours

IBI – Atlantic Iberian Biscay Irish Ocean Wave Reanalysis Model

km – Kilometer

kW/m – Kilowatts per linear meter

MFWAM – Meteo France WAve Model

MRE – Marine Renewable Energy

$ms^{-1}$ – Meters per second

MW – Megawatts

$MW/m^2$ – Megawatts per meter squared

NEMO – Nucleus for European Modelling of the Ocean

NWS – Atlantic European Northwest Shelf Wave Physics Reanalysis Model

OE – Ocean Energy Ltd.

OPEX – Operational Expenditure

ROMS – Regional Ocean Modelling System

SEAI – Sustainable Energy Authority of Ireland

SME – Small to Medium Enterprise

TEC – Tidal Energy Converter

TWh – Terawatt hour

TWh/yr - Terawatt hour per year

US – United States of America

UK – United Kingdom

WEC – Wave Energy Converter

$W/m^2$ – Watts per meter squared

# 1. Introduction

With Global and EU (European Union) protocols encouraging countries including Ireland and the UK (United Kingdom) to reduce their greenhouse gas emissions to reduce the effects of climate change, it is important now more than ever to work towards a more renewable future both for our people and our economies. Both Ireland and Wales have long coastlines, 7500km and ~2200km respectively, meaning that both countries have large areas of ocean that could potentially be accessible for MRE (Marine Renewable Energy). The areas including the Irish and Celtic Seas have been subject to ongoing research for wave and tidal energy devices over the past decade (Irish Sea has an area of ~47,000km$^2$ while the Celtic Sea has an area of ~300,000km$^2$). This study focuses on a high-resolution wave and tidal resource assessment for the Irish Coast, including the western Atlantic Coast, the Northern Irish Coast and the Irish and Celtic Seas, with the aim of using that information to inform a multi criteria decision analysis tool that is currently being developed as part of the SELKIE project. The tool is being developed as an open-source Geographic Information System (GIS), with the goal of aiding SME's (Small to Medium Enterprises) and Government bodies.

Both the Irish and Welsh governments have announced targets of having 70% of their energy coming from renewable sources by the year 2030. An estimated 7.4 TWh of renewable electricity was generated in Wales in 2018, up from 7.1 TWh the previous year. This represents 25% of all electricity generation in Wales (Regen, 2019). While there are already a number of onshore renewable energy sources such as onshore wind, geothermal and hydroelectric, one area that requires more investigation is the offshore wave and tidal sector. Eirgrid, the company that manages the electricity supply in Ireland notes that demand for electricity has been higher than ever recently, with daily demand reaching unprecedented levels in December 2020. Eirgrid's records show that consumption reached 5,112 MW for a period between 5pm and 6pm on Thursday December 3rd 2020, beating a previous record of 5,090 MW set in December 2010 (O'Halloran, 2020).

## 1.1 Aims and Objectives

This study develops a new up-to-date resource assessment layer for both wave and tidal energy for the study area which includes the west and north Atlantic coasts of Ireland as well as the Irish and Celtic Seas. As well as the updated resource assessment, detailed analysis of the wave resource and the wave parameters is carried out. Analysis of both spring and neap tidal currents are also completed. The aim is to better understand the nature of the wave and tidal resources for the study area through GIS interpretation. The GIS layers are used as a tool to help us to better understand both the spatial and temporal nature of the resource. The detailed aims include:

- To develop a wave resource layer covering the study area of the west and north Atlantic coasts of Ireland as well as the Irish and Celtic Seas. This wave resource will be generated using data from models that are available through the Copernicus Marine Service. Two models will be used, both at different resolutions, and the variability in the results will be interpreted to understand which model works best for wave resource assessment.
- To carry out detailed analysis of the seasonal trends using a 20-year time series of data in order to understand spatial and temporal patters in the wave resource, as well as in the significant wave heights and the wave periods for the study area.
- To develop a tidal resource layer covering the study area of the west and north Atlantic coasts of Ireland as well as the Irish and Celtic Seas. This tidal resource layer will be generated using data from a model that is available through the Irish Marine Institute.
- To carry out detailed analysis of the spring and neap tides in order to understand the spatial patterns for mean and max spring and neap tides for the study area.
- To understand both the spatial and temporal nature of the wave and tidal energy resource for the study area.

## 1.2 Outline of Thesis

This thesis adheres to the following format: The first section aims to cover the literature review where the work of previous authors is reviewed. The literature review aims to give a thorough understanding of what research has previously been carried out in the area of resource assessment and any gaps that may currently be there are identified. The second section aims to cover the data gathering and methodology for the resource assessment. Following this the results are discussed for both the wave and tidal resource assessments. The final section

discusses the results that have been achieved with the aim of interpreting the spatial and temporal patterns in the resource assessments and also to differentiate between which methodology is best for resource assessment. Any shortcomings from the work will be discussed also including proposing what needs to be carried out in future work.

## 1.3 Research output and novel contributions

This research was presented along with further work that is being carried out as part of SELKIE Work Package 4 at the International Coast GIS Conference which was hosted by Novia University of Applied Sciences in Raseborg on the south Coast of Finland (the conference was held online). The publication can be viewed in Appendix 1. The publication that was submitted as part of the conference was entitled:

O'Connell, R and Furlong, R. (2021) "An assessment of newly available Copernicus sea surface wave products for mapping wave energy in Irish and UK waters." Proceedings of the 14th CoastGIS International Symposium CoastGIS 2021 16-17 September 2021, Raseborg, Finland.

The specific novel contributions of this thesis include:

- GIS layers illustrating the mean wave energy resource, the seasonal significant wave heights, the seasonal wave energy period and the seasonal mean wave energy resource for the study area including Irish and UK waters.
- GIS layers illustrating the hourly mean tidal power, the annual tidal power, the spring and neap mean tidal power, the mean spring, neap and peak currents for the study area including Irish and UK waters.

# 2. Literature Review

## 2.1 Introduction to Literature Review

This literature review will examine the theory behind wave and tidal energy, as well as examples of wave and tidal technologies that are currently available for use. For wave energy, the theory behind how waves work is examined, followed by the parameters that are needed for a wave resource assessment. For tidal energy, the science behind the tides is covered followed by the parameters needed for a tidal power resource assessment. The availability of data for use for the wave and tidal energy resource assessments is then covered. The study area for the project can be seen below in Figure 2.1.

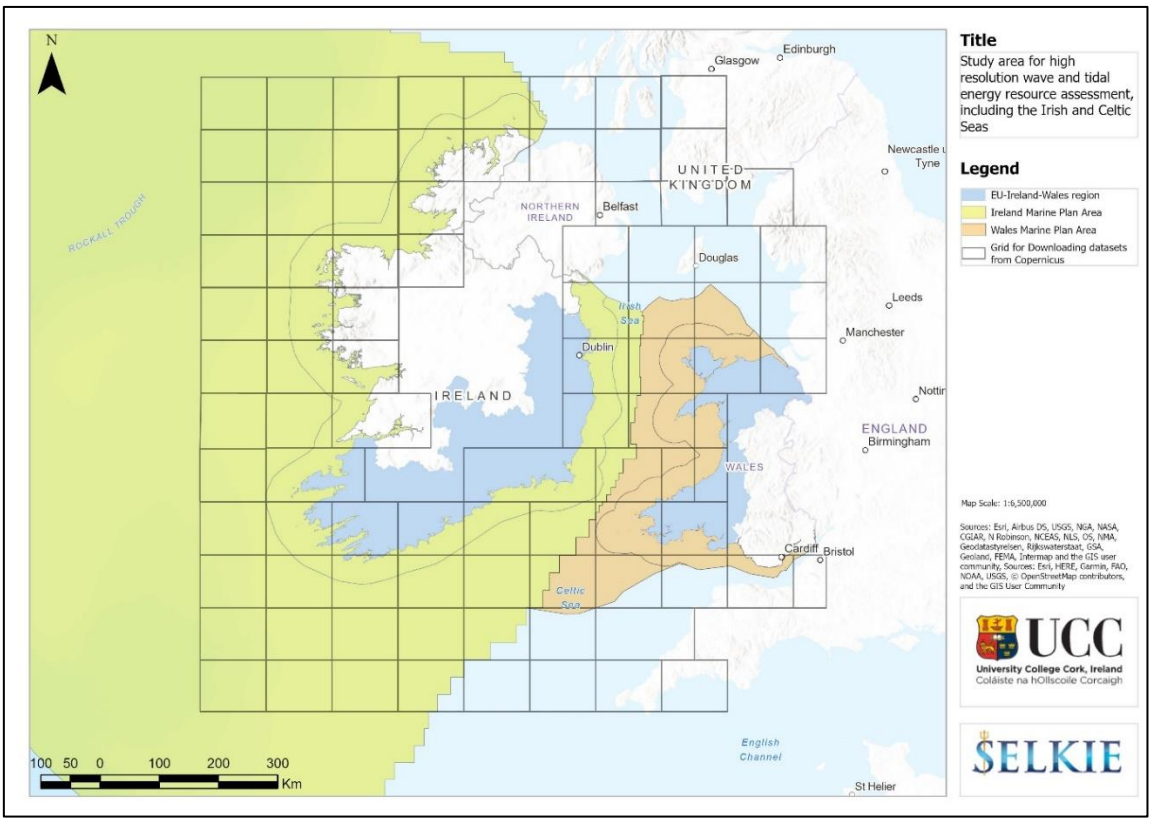



*Figure 2.1 Study area for high resolution wave and tidal energy resource assessment.*

There are currently several online GIS tools that are available for use within the study area for this project, these tools are reviewed, and it is noted how they differ from what is being carried out for this project. Any limitations identified with work that has been previously completed are noted and the proposed solutions for the work that is being completed as part of this project is discussed at the end of this section.

## 2.2 Waves and Wave Energy

Waves are generated when winds blow over the ocean and there is a transfer of energy. Larger waves tend to be more powerful, but other parameters which affect the power of a wave include the wave speed, the wavelength, wave period and the water density. The wave resource tends to be best in areas where the winds have travelled over long distances, as a result large wave resources can be seen off the west coast of Ireland (Aquaret, 2008). The general wave resource distribution for Europe can be seen in **Error! Reference source not found.** which has been produced by Aquaret.

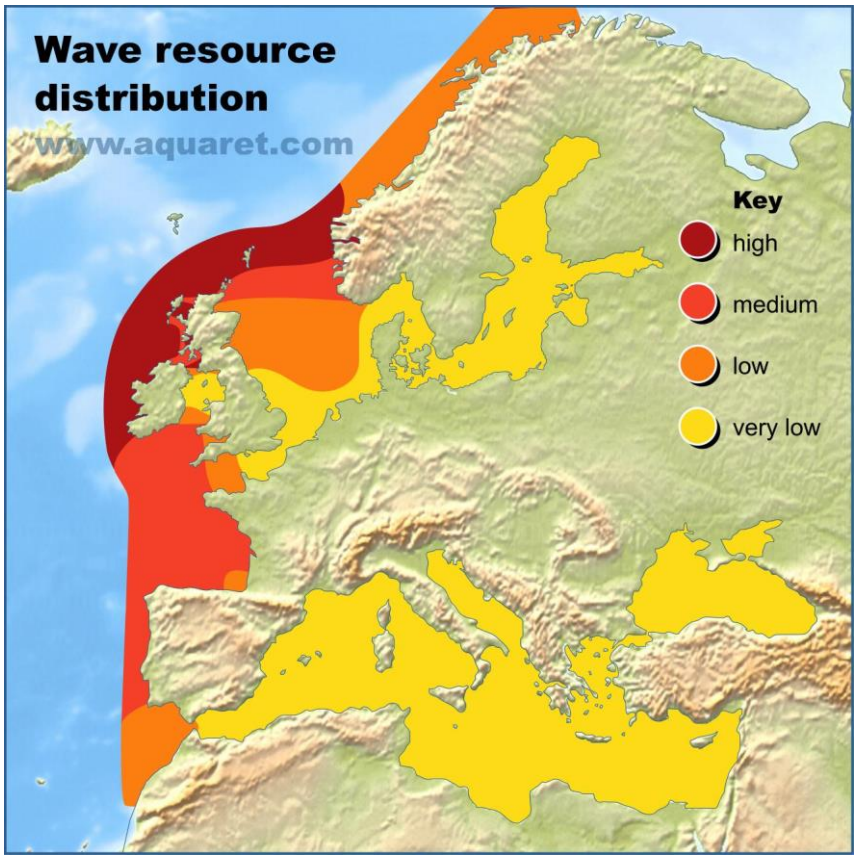



*Figure 2.2 A figure from Aquaret showing the wave resource distribution across Europe (Aquaret, 2012a).*

The global wave resource distribution in kW/m can also be seen below in Figure 2.3. This figure shows that the highest wave resource can be seen in the northern Latitudes, with values of approximately 40-60 kW/m seen in areas like the western coasts of USA, Ireland, Portugal. There are also high values between 30-60 kW/m seen off the southern coasts of Australia, Africa and also along the south west coast of Chile.

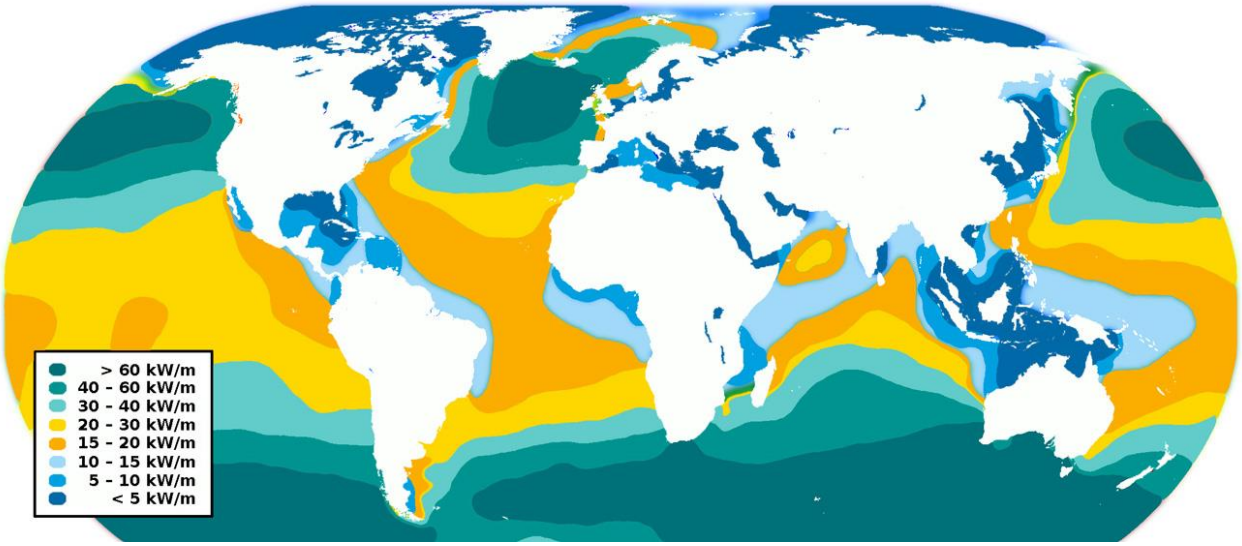



*Figure 2.3 Global wave resource distribution in kW/m (Bombora, 2020).*

Gleizon et al., (2017) acknowledged that wave activity depends largely on the fetch and is mainly concentrated between 30° and 70° north and south latitudes. The bathymetry can have an effect on the waves, as larger waves tend to occur in deeper waters. The paper also mentioned that the coastal and bathymetric irregularities seen in coastal locations can influence wave patterns and consequently can introduce small scale variability in the wave energy distribution.

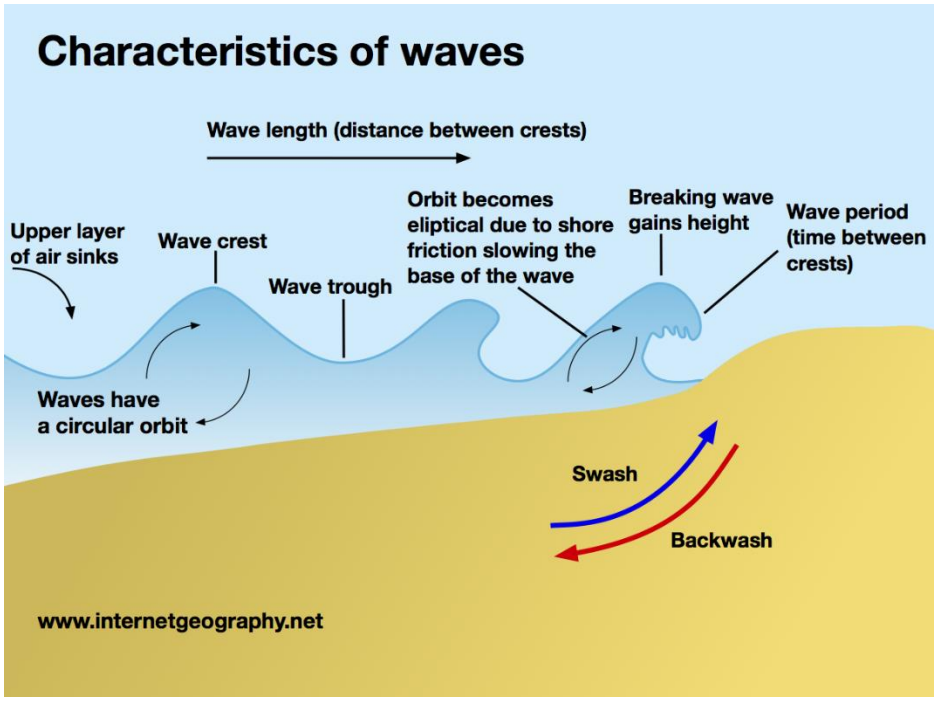



*Figure 2.4 Characteristics of Waves (A Level Geography, 2018).*

### 2.2.1 Wave parameters for wave resource assessment

Wave energy or wave power is the capture of ocean energy from the waves. This energy can then be used for electricity generation. It is estimated that ocean energy can produce between 4,000 TWh/yr and 29,500 TWh/yr in Europe (Ocean Energy - Europe, 2021). Europe consumes around 3,000TWh/yr. The variables that strongly affect the wave energy are the wave height and wave period (O'Connell et al., 2020). The wave height is the difference between the height at a wave crest and the following wave trough. The wave period is said to be the time taken (usually seconds) for two wave crests to pass the same point (Figure 2.4). A paper by Ainsworth and Juneau (2009) stated that the Significant Wave Height $H_s$ is defined as the average height of the highest one-third waves in a wave spectrum. The equation for wave power, which is the time-averaged energy flux in a system of water waves is given by Tucker, M. and Pitt (2001) as

$$P = \frac{\rho g^2}{64\pi} H_s T_e$$

*Equation 1 Wave Power*

where ρ is the density of water (in k/gm$^3$), g is the gravitational acceleration constant given as 9.8m/s, $H_s$ is the significant wave height (m), $T_e$ is the wave energy period. A simplified equation for regular sea states is given by Cahill and Lewis (2014) as

$$P = 0.49 H_s$$

*Equation 2 A simplified equation for regular wave power, for regular sea states.*

where P is the power per unit width of wave crest. This power equation was then simplified by Cahill and Lewis (2014) to give the power per unit width of a wave crest P as:

$$P = 0.49 H_s^2 T_e$$

*Equation 3 Wave power per unit width of a wave crest.*

This equation is the standard deep water power equation. It is only applicable in areas where d/ λ > ½, with d being the water depth and λ being the wavelength.

### 2.2.2 Wave Energy Converters (WEC's)

This section will give a brief overview of some of the wave energy converters (WEC's) that are currently being used to harness wave power. The types of devices include:

***M4 Wave Attenuator***

The attenuator can be seen below in Figure 2.5. The methodology for this device is that it floats perpendicular to the waves and captures energy by moving both 'arms' with the motion of the waves. An example of an 'Attenuator' type WEC is the M4 Wave buoy, a wave energy converter that has been tested both off the south coast of western Australia and also at the EMEC test site in Orkney (Santo, Taylor and Stansby, 2020).

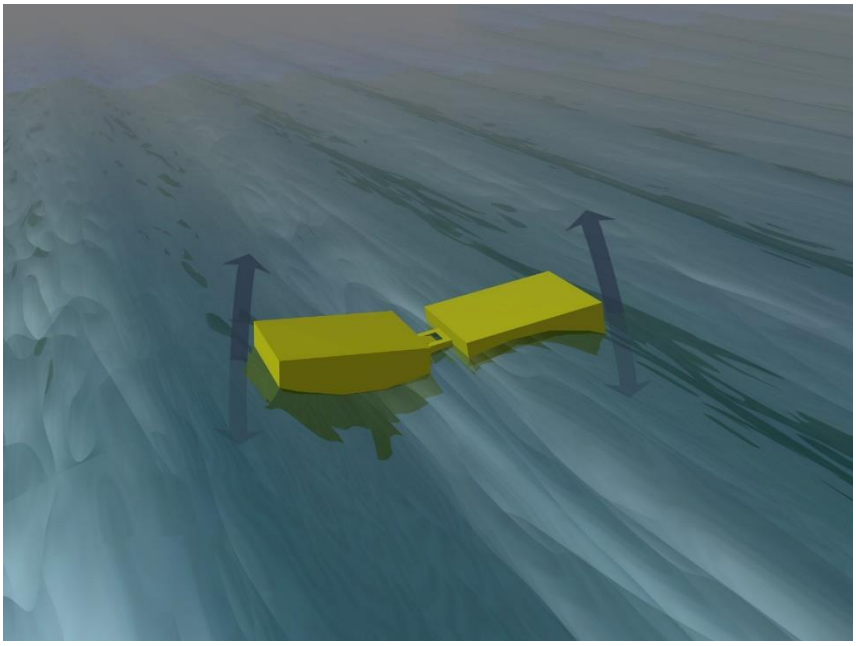


*Figure 2.5 Example of an attenuator device (Aquaret, 2012).*

***Point Absorber***

The point absorber works under the principle that wave energy is absorbed from all sides of the device as the device is pushed up and down from the energy of the wave. The device is generally moored to the sea floor. The Archimedes Waveswing submerged wave power buoy can be seen below on the left hand side of Figure 2.6. This device was tested off the coast of Portugal in 2004. It is suitable for sites with water depths >25m and it can generate power of 25-250kW (AWS Ocean Energy, 2021).

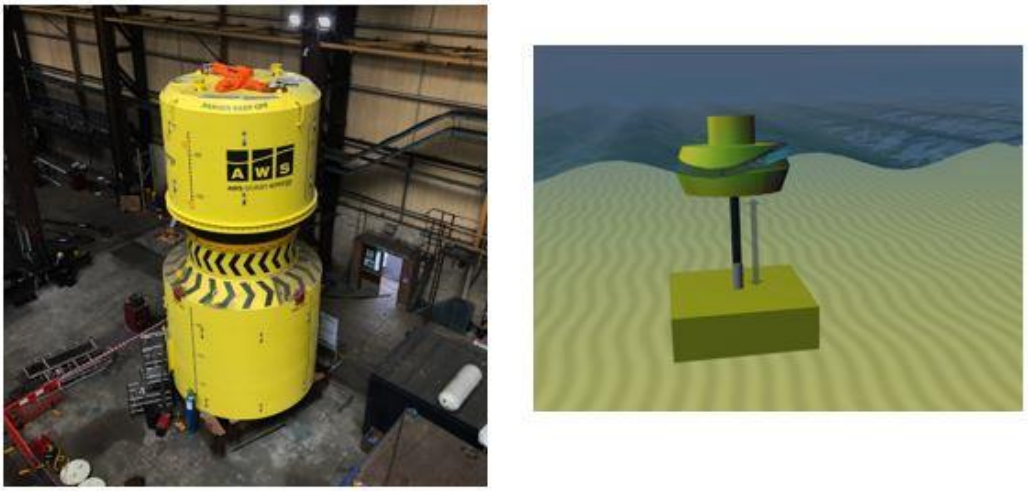


*Figure 2.6 The figure on the left hand side shows the Archimedes Waveswing (AWS Ocean Energy, 2021). The figure on the right hand side shows how a point absorber looks on the ocean floor (Aquaret, 2012).*

***Oscillating Wave Surge Converter***

The oscillating wave surge converter works on the basis that the arm of the device moves with the motion of the waves and generates the electricity. An example of an oscillating wave surge converter is the Langlee device which has been developed in Norway by Langlee Wave Power to capture energy found in deep water waves. The Langlee works as two hinged flaps attached to a moored, semi submerged frame. The flap then moves back and forward from the motion of the waves (Lavelle, John and Kofoed, 2021).

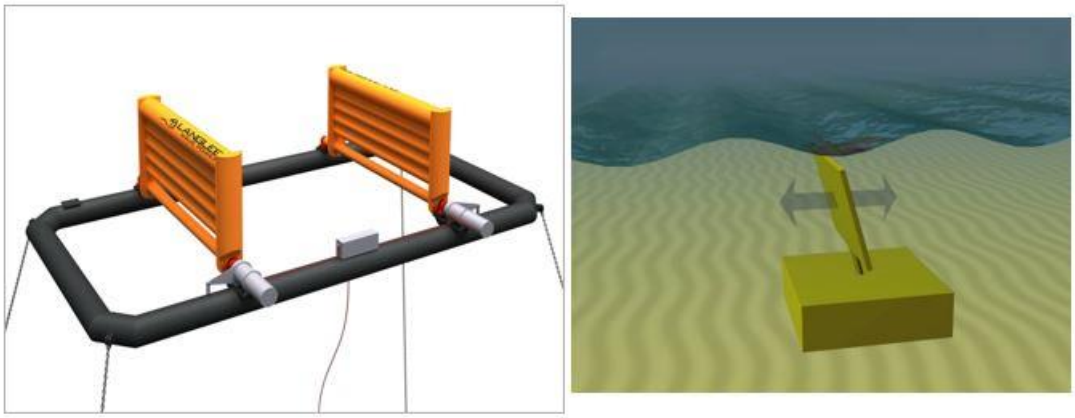


*Figure 2.7 The figure on the left hand side shows the Langlee device (Langlee Wave Power AS, 2013). The figure on the right hand side showsshowing how an oscillating wave surge converter would look on the ocean floor. (Aquaret, 2012).*

***Oscillating Water Column***

An example of an oscillating water column can be seen below in Figure 2.8. It is a hollow structure that is submerged below the surface of the water, the water then fills the chamber the pressure forces air upwards which then turns a turbine and generates energy (Falcão and Henriques, 2016). An example of an oscillating water column is the Ocean Energy OE35 buoy which has been tested in Galway Bay. It is said by Ocean Energy that Oscillating Water Column technology is the most successful and most extensively researched out of the various WEC's that are available (OceanEnergy, 2020a). The OE buoy extracts power by means of a Well's or Impulse turbine.

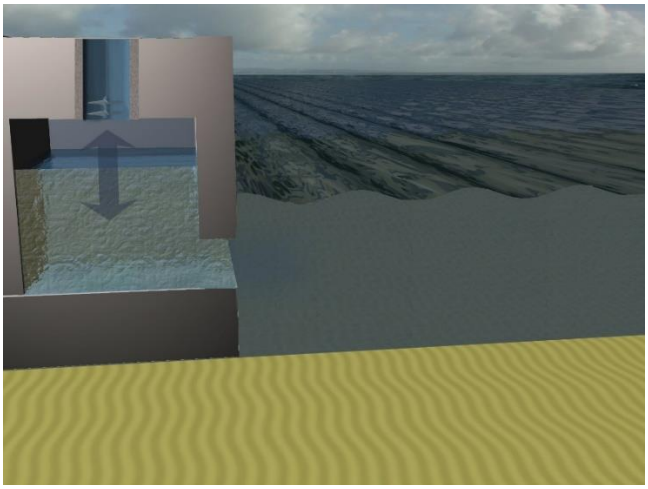


*Figure 2.8 An illustration showing how an Oscillating Water Column works (Aquaret, 2012).*



*Figure 2.9 The Ocean Energy OE35 Buoy which is an example of a floating oscillating water column (OceanEnergy, 2020).*

***Overtopping Device***

An example of a WEC of the overtopping style is the WaveDragon (Wave Dragon, 2017). The Wave Dragon is a WEC with a rated capacity of 1.5MW – 12MW. An overtopping device captures water from the waves and stores this water in a reservoir. This water is held above the sea surface level and returned to the sea via a set of turbines which generate the energy. An example of how an overtopping device works can be seen below in Figure 2.10.

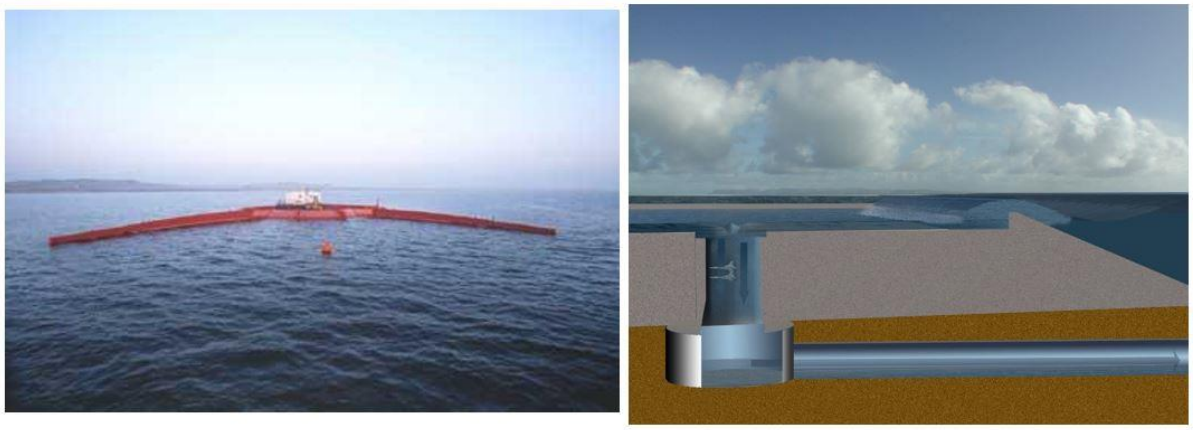


*Figure 2.10 The figure on the left hand side shows the WaveDragon device (Tethys, 2021). The figure on the right hand side shows an example of an overtopping device (Aquaret, 2012).*

***Submerged Pressure Differential***

The submerged pressure differential device is mounted on the sea floor close to the coast, it uses the pressure difference above the device that is created between wave crests and troughs. This pressure difference then causes the device to move up and down acting like a piston to generate energy (Folley et al., 2012).

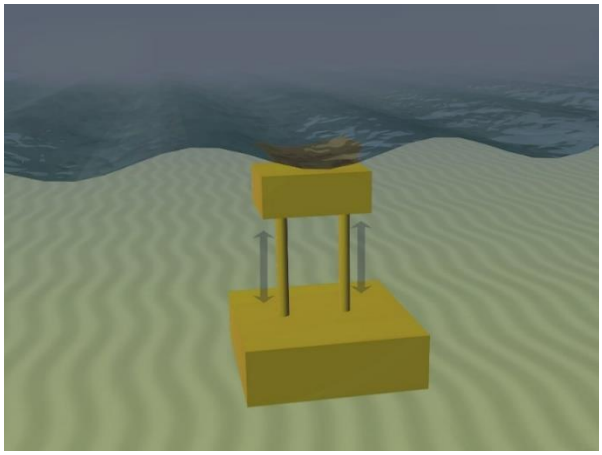


*Figure 2.11 An illustration showing how a submerged pressure differential works (Aquaret, 2012)*

***Rotating Mass***

A rotating mass device generates energy from waves travelling in any direction. This device works under the basis that a weight moves around a fixed point, driven by the power of the waves, and drives and internal rotary alternator (The Liquid Grid, 2018). An example of a rotating mass energy converter is the Finnish Wello OY Penguin device. The Penguin is 30-56m in size, is estimated to generate 0.5-1MW of energy and has survived >18m storm surge waves (Wello, 2021).



*Figure 2.12 The Wello Penguin (Wello, 2021)*

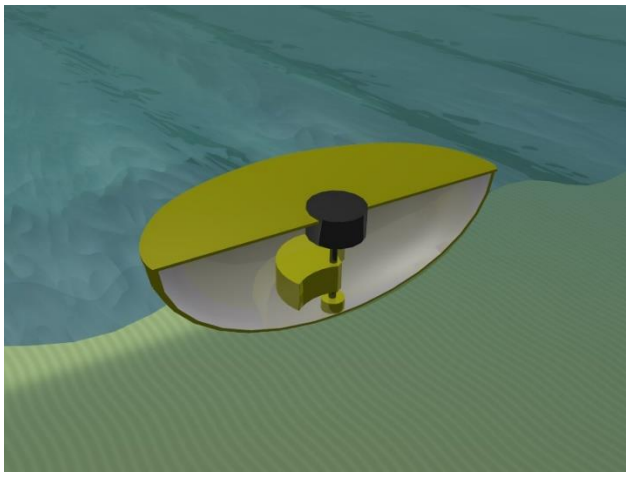


*Figure 2.13 An illustration of how the rotating mass device works (Aquaret, 2012)*

### 2.2.3 Technology and Commerciality

Many of the WEC's that have been discussed in the section above have been developed and are undergoing testing and deployment, but it is envisioned that the wave energy sector will not reach commerciality until mid-2030. Devices are currently being tested for feasibility at

sites such as the Galway Bay test site site off the western coast of Ireland and the WaveHub site off the coast of Pembrokeshire in Wales.

## 2.3 Tides and Tidal Energy

The tides are driven by the gravitational pull of the moon and the sun and can be predicted far in advance (NOAA, 2021). Tides are defined to be long period waves that travel through the ocean as a result of this gravitational pull. High tide occurs when the highest part of the wave, the crest, reaches a particular location, with low tides being the opposite, the lowest part of the wave which is known as the trough. The difference between high tide and low tide is known as the tidal range. The global mean daily tidal range can be seen below in Figure 2.14. Many tidal energy technologies that currently exist use the difference between high and low tide (the tidal range) to generate electricity, including tidal barrages such as the one at La Rance in France. Tidal range is the most established tidal energy generating technology that is currently available, but it is not suitable for global production. One reason why is it not suitable is because in most locations, such as in parts of Ireland, the tidal range is not large enough to be viable for energy production. In general the tidal range needs to be >5m to be viable for energy generation. As a result of this, the tidal energy technology that will be focused on for this project is tidal current technology (also referred to as tidal stream technology).

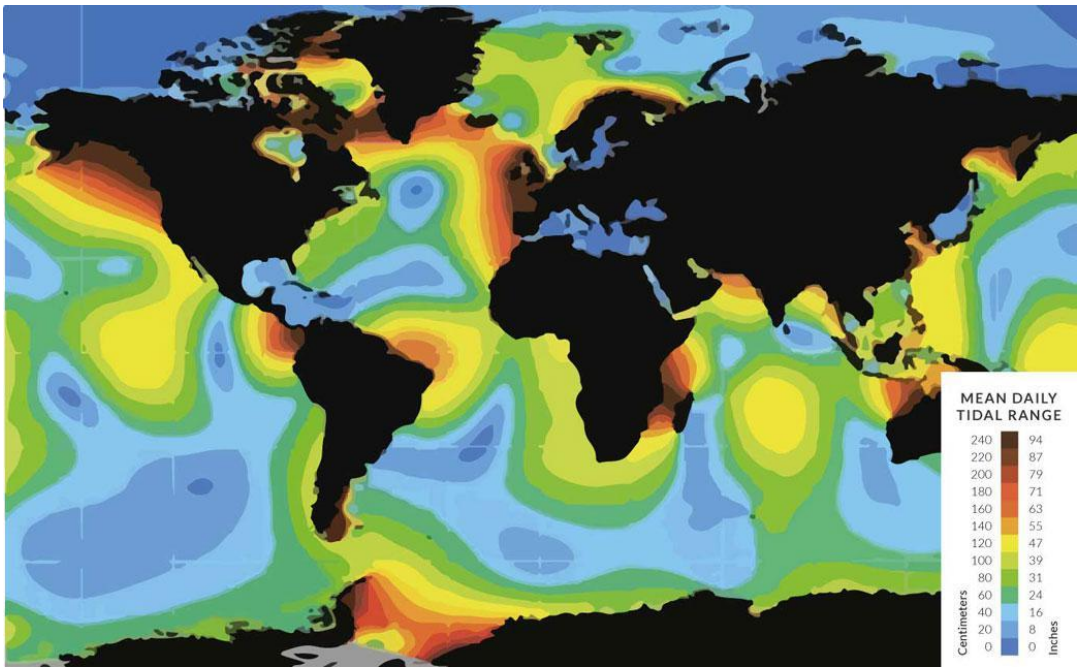



*Figure 2.14 An illustration of the global mean daily tidal range (Minesto AB, 2021b).*

Tides can be classified in three ways, as a diurnal tide, a semi-diurnal tide or a mixed semi-diurnal tide. A diurnal tide is one where there is only one high and one low tide during the day. A semi-diurnal tide has two high tides and two low tides during the day. A mixed semi diurnal tide has two high tides and two low tides each day, but the heights of each tide differ (Webb, 2021b). The global distribution of the three types of tide can be seen below in Figure 2.15.

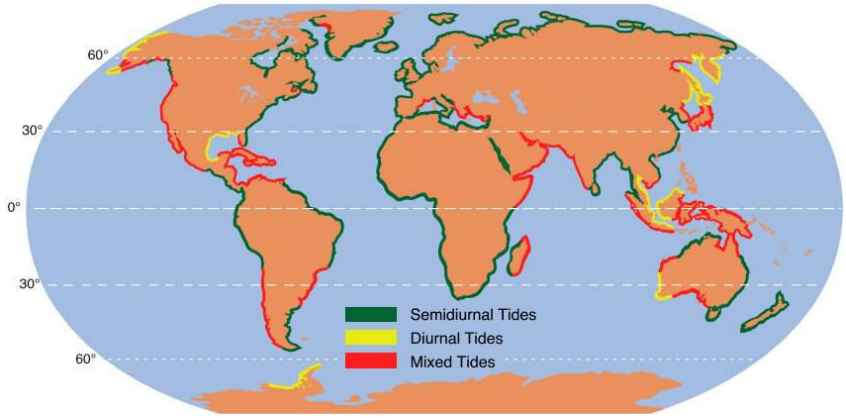



*Figure 2.15 An illustration showing the global distribution pattern of Diurnal, Semi-Diurnal and Mixed Tides (Webb, 2021).*

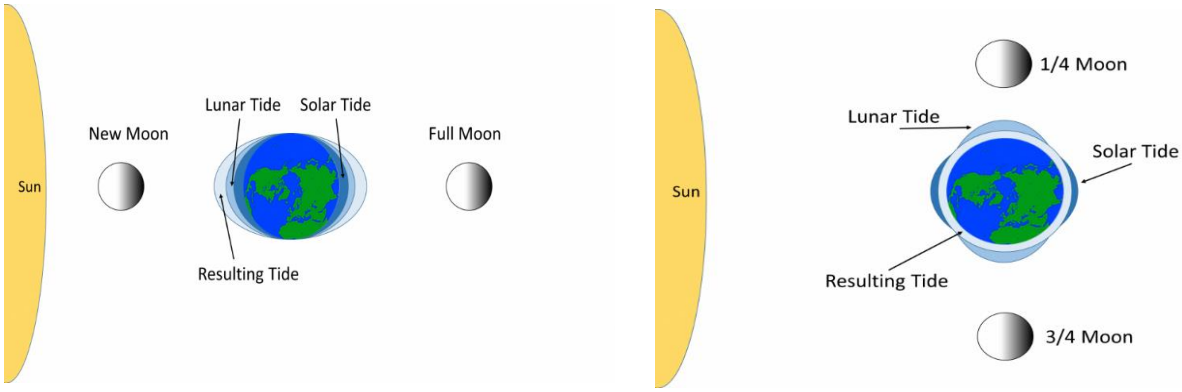



*Figure 2.16 Two figures showing both the spring and neap cycles. The figure on the left-hand side shows the spring cycle, where the sun, moon and earth are aligned resulting in larger variations in the tide. Then figure on the right shows the neap tidal cycle where*

While the classification mentioned above describes the daily differences in the tides, there is also a classification for the longer-term cycles in the tides, also known as the Spring-Neap cycle. The two main forces on the strength of the tide are the gravitational pull from both the sun and the moon. Depending on the location of either the sun or the moon with reference to the earth, there can be either a spring or a neap tidal cycle. The spring – neap cycle is mainly associated with the phase of the moon. When the sun and the moon are aligned with the Earth at 180°, their semi-diurnal components interfere constructively, giving rise to tides of larger amplitude, known as spring tides. When they are at 90° to each other, the interference is

destructive, giving rise to smaller amplitude tidal variations, called neap tides (Hendershott, 2004). A spring tide occurs during a new moon and a full moon, when the gravitational pull of the moon is at its strongest. This results in the highest variation in the tides, with high - high tides and low - low tides, occurring twice every month. The neap tide occurs during the quarter and three-quarter phases of the moon, when the sun, earth and moon are at 90° angles to each other. A neap cycle also occurs every two weeks and results in smaller variations in the tides, with low high tides and high low tides (Webb, 2021).

A tidal current, which is an important parameter in tidal energy, is the movement of water with the rising and falling tides. There are two types of tidal current, a flood current and an ebb current. A flood current occurs when the tide is flowing inward (towards high tide) and an ebb current occurs when water flows seaward (towards low tide). Parameters that affect the strength of a tidal current are the volume of water that is moving and also the size of the area that the water is moving through. In general, the largest tidal currents are seen where a large volume of water is moving through a narrow channel and the smallest currents are seen where the tide is moving across a large area (Webb, 2021).

This study will aim to focus on tidal stream energy, which is energy that is produced by the movement of the tidal currents. The tidal energy converters (TEC's) for use in tidal stream technology work in a similar way to wind turbines, with many of the TEC's having turbine blades that generate electricity from the tidal current. It is also said that tidal stream energy generation has a lower environmental impact than tidal barrages (WP Marine, 2021).

### 2.3.1 Tidal Energy

In 2015, it was stated by the Carbon Trust in the UK that 18TWh of tidal energy would be extractable within 1450km$^2$ of UK waters (Lewis et al., 2015). The affect of the solar system on the tides means that tidal stream energy is 100% predictable, which is unique for a renewable energy source. The predictability means that tidal resource can be predicted for years/decades in advance. The tidal stream resource distribution can be seen below for Europe in Figure 2.17 which was produced by Aquaret/EMEC (EMEC, 2021c). The tidal stream resource potential in the area of the Irish and Celtic Seas, as well as the English Channel area and the north of Scotland is medium-high.

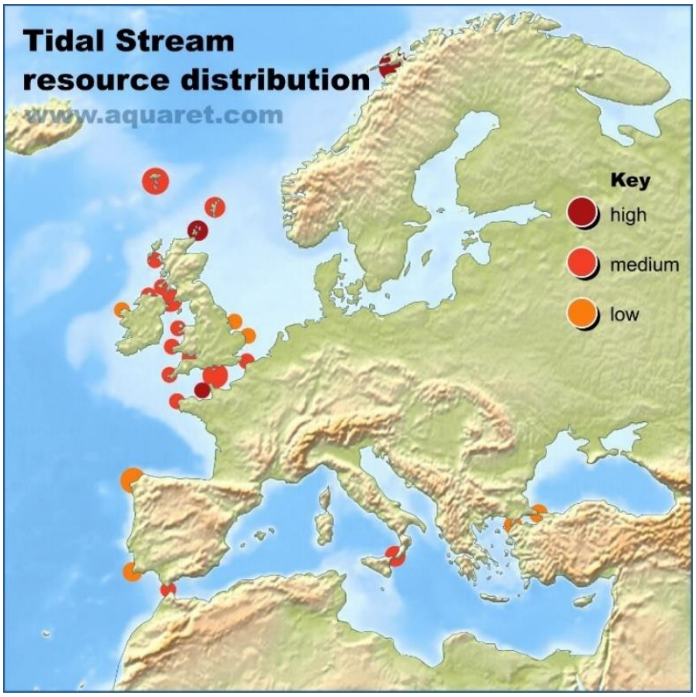



*Figure 2.17 An illustration showing the tidal stream resource distribution for Europe. Source:(EMEC, 2021c).*

A report by Blunden and Bahaj (2007) showed that tidal streams are predictable for decades provided that over a month but ideally a year worth of data is provided. Modelling methods can predict the phase, magnitude and direction of the tidal streams.

Much like with the wave resource, it is necessary to predict the tidal energy resource so that developers have an understanding of the best locations for device deployment. The parameters that are needed for tidal stream resource assessment are the tidal current speed (generally greater than 2m/s) and the depths (generally >20m) (Blunden and Bahaj, 2007). It is said that devices that need to be employed at a site with SV > 2m/s (SV = spring tide peak depth averaged velocity (m/s)) and depth >25m are first generation devices (Lewis et al., 2015). Strong tidal currents are known to scientists along the north and east coast of Ireland (the Irish and Celtic Seas). “The tidal current flow is particularly energetic entering the Irish Sea from the St. Georges Channel and the north Channel” (O’Rourke, Boyle and Reynolds, 2010). It is said that bathymetry changes and narrow headlands can cause changes in tidal currents. Large tidal currents are commonly located between land masses or adjacent to headlands (Charlier, 2003). The depth averaged peak spring tidal currents for the area around the coast of Ireland including the Irish and Celtic Seas can be seen below in Figure 2.18, showing that there are many areas including the east coast and particularly off the northern coast of Ireland where the currents are >1.5ms.

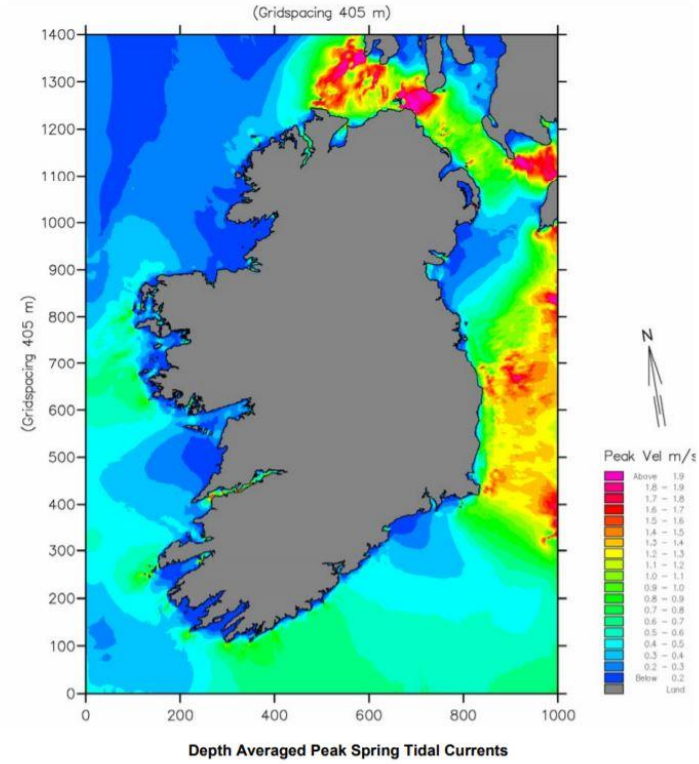



*Figure 2.18 Depth Averaged Peak Spring Tidal Currents around the island of Ireland (SEAI, 2004).*

The calculation for the mean power of a tidal current per unit area, $P_{mean}$, is given by O'Rourke, Boyle and Reynolds (2010) as:

$$P_{mean} = \frac{1}{2}\rho K_s K_n V_{peak}^3$$

*Equation 4 Mean power of a tidal current per unit area.*

where ρ is the density of seawater, $K_s$ is the velocity available factor (0.424), $K_n$ is the neap/spring factor (0.57) and $V_{peak}$ is the peak spring-tide velocity. This equation can be further simplified to be:

$$P = \frac{1}{2}\rho V^3$$

*Equation 5 Simplified equation of mean power of a tidal current.*

where ρ is the density of seawater and $V^3$ is the current velocity.

The Seagen site in north Wales (10 mw S/MCT$^{-1}$) is an example of a site that is under active development in the Irish Sea. The site has tidal currents > 2.5m/s. There was also the Seagen turbine located at Strangford Lough, which produced 11.6GWh of energy during its lifecycle prior to decommissioning in 2019. There are multiple other sites that have been identified to

be optimum for tidal energy generation including the Bristol Channel, eastern Ireland (area close to the Arklow Bank) SEAI (2004) and the tidal energy zone off the coast of Anglesey. The West Anglesey Tidal Demonstration Zones consists of 35km² of sea bed. The deployment of tidal energy converter technologies within the zone is planned to scale up over time to a potential maximum electricity generating capacity of 240MW (Marine Energy Wales, 2020).

### 2.3.2 Tidal Energy Converter's (TEC's)

Tidal stream devices use the tidal current to generate electricity. There are a number of different devices currently available, many of them similar to wind turbines that use blades to generate energy. The types of TEC's are:

***Horizontal Axis Turbine***

In a horizontal axis turbine the blades rotate around an axis that is parallel to the direction of the current flow. The device is generally moored on the ocean floor. KHI (Kawasaki Heavy Industries) tested a 1MW horizontal axis turbine in the UK in October 2010 (EMEC, 2021b).

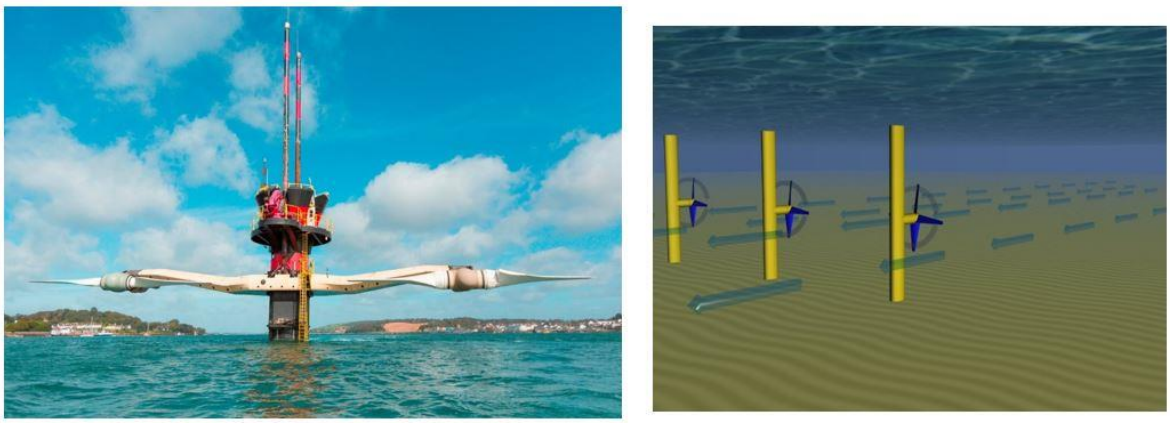


*Figure 2.19 The figure on the left hand side shows the SeaGEN turine (Simec Atlantis, 2021). The figure on the right hand side is an illustration of a horizontal axis turbine where the blades of the turbine are parallel to the current direction. (EMEC, 2021).*



*Figure 2.20 Sabella D10 Horizontal axis turbine (Sabella, 2021).*

***Vertical Axis Turbine***

A vertical axis turbine works within a horizontal plane, rotating around a horizontal axis.The device is moored on the ocean floor and the blades are perpendicular to the tidal current.

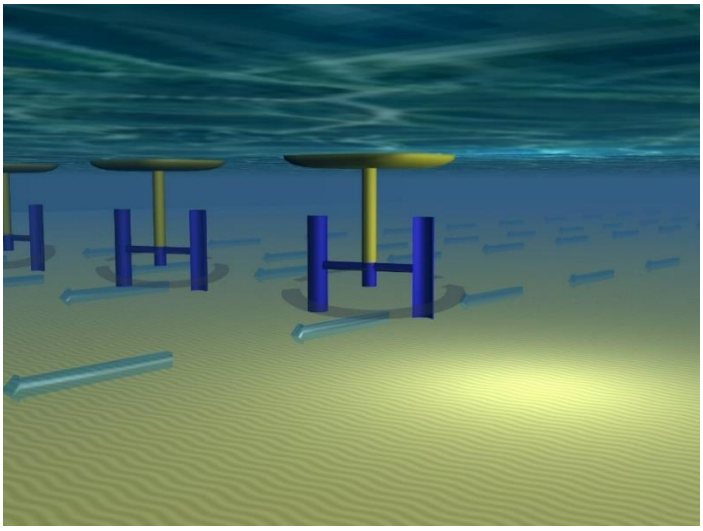


*Figure 2.21 An illustration of a vertical axis turbine (EMEC, 2021).*

***Oscillating Hydrofoil***

An oscillating hydrofoil works on the basis that the arm of the device oscillates up and down with the motion of the tidal current. The movement of the arm of the device causes fluid to flow in the hydraulic system generating electricity.

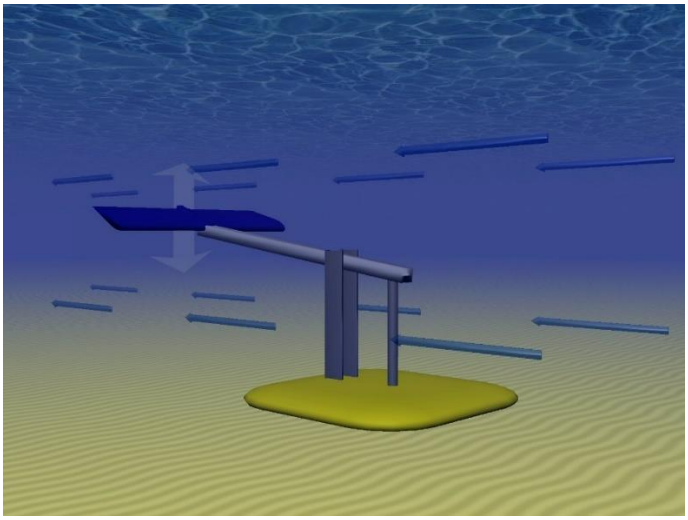


*Figure 2.22 An illustration of an oscillating hydrofoil (EMEC, 2021).*

***Archimedes Screw***

The Archimedes screw has been around now for many years and was originally designed to transfer water up a tube. The Archimedes screw tidal device works on the basis that the tidal current causes the screw to rotate, generating electricity through the spinning screw-like turbines.

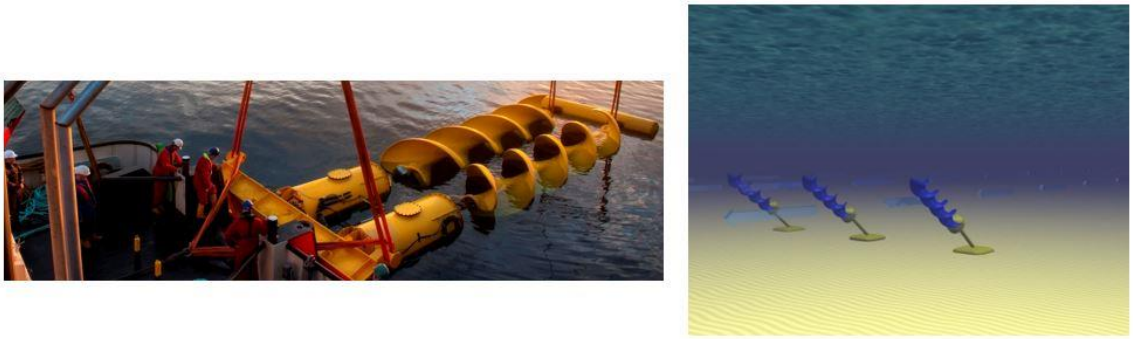


*Figure 2.23 The figure on the left hand side shows the Flumill device that was tested at Shapinsay Sound in the UK in 2011 (EMEC, 2021). The figure on the right shows an illustration of an Archimedes screw type tidal energy converter (EMEC, 2021).*

***Tidal Kite***

A tidal kite works under the principle that the current moving under the wing of the kite creates a hydrodynamic lift force. The kite carries a turbine under the wing and it 'flies' in the tidal stream generating electricity. An example of a tidal kite is the kite that has been developed by Minesto. The Minesto kite was tested in Strangford Lough in Northern Ireland in 2013, with further testing in 2018 in Holyhead, Wales. The Minesto kite is said to generate 0.5MW at commercial scale and can be either surface mounted or bottom installed (Minesto AB, 2021).




*Figure 2.24 Minesto DG500 Tidal Kite (Minesto AB, 2021).*




*Figure 2.25 Minesto DG100 Tidal Kite (Minesto AB, 2021)*

## 2.4 Data Availability

This study aimed to obtain data with a high resolution of <5km or <0.05 degrees from the Copernicus Marine Service (CMEMS -Copernicus Marine Environment Monitoring Service). CMEMS provides free information on the state of the ocean on both a global and regional scale. The service is implemented by Mercator Ocean International and is funded by the European Commission (EC). CMEMS provides vast amounts of data from satellites (including Copernicus Sentinel Satellites) from ground-based, airborne and seaborne measurement systems and from numerical models (Copernicus, 2021). While using numerical models will allow the user to create high resolution data, this method is computationally complex and can be very time consuming. CMEMS provides datasets from different numerical models which have assimilated data from in situ measurements, altimeter and satellite data. Data is now available at high resolutions that cover the study area for a range of ocean parameters including significant wave height, wave period and current speeds. Depending on the model, the data can be available for long hindcasts of more than twenty years at different time steps.

### 2.4.1 Modelling Techniques for Wave Energy Resource Assessment

Numerical modelling techniques have been employed by researchers for several years in order to model the wave energy resource at a given location. Modelling of the wave energy resource enables developers to better understand the amount of power that can be generated at a given location, the conditions at the location (extreme conditions etc.) and it can also aid with site selection for the device (to select a site where suitable amounts of power will be generated). There are a number of spectral wave models available to scientists for wave resource assessment, including SWAN (Simulating Waves Near Shore) at TU Delft, WaveWatch III, WAve Model (WAM) and Mike-21. Parameters such as significant wave height ($H_s$), mean energy wave period ($T_e$) and wave direction can be calculated using these models. This information can then be used to calculate the wave energy resource using the wave power equation which has been defined above. Some of the models are more suited to deep water applications, such as WAM and WaveWatch III, whereas SWAN was developed for use with a much smaller grid spacing in the nearshore. The models have been developed for use on local, regional and global scales. It has been said that due to the differences in the models, estimating a wave energy resource both on synoptic and local scales can be challenging, and may require a combination of the different models (Gleizon et al., 2017). Model data is available on local, regional, and global scales from CMEMS. Data can be downloaded for hindcasts that range

from 0-20+ years and parameters that are available to download include significant wave height, mean wave period, mean wave direction, swell wave period and many more. Data assimilation is included for some of the models, which means that satellite data has been fed into the models in order to improve model performance and predictions. (O'Connell et al., 2020).

### 2.4.2 Modelling Techniques for Tidal Energy Resource Assessment

Previous studies have modelled tidal energy resources using both 2D and 3D hydrodynamic models. A tidal current energy assessment was completed for Ireland by SEAI (Sustainable Energy Authority of Ireland) in 2004. A 2D numerical model of the tidal currents around Ireland was developed using Mike 21 software and was also validated using ADCP's. (Acoustic Doppler Current Profiler). A theoretical resource of 230 TWh/year was calculated for Ireland (SEAI, 2004). Data from hydrodynamic models is available to download from the CMEMS. The "Atlantic - European North West Shelf - Ocean Physics Analysis And Forecast" model that is available through the Copernicus site is produced using a forecasting ocean assimilation model, with tides, at 1.5 km horizontal resolution coupled with a wave model. The ocean model is NEMO (Nucleus for European Modelling of the Ocean), using the 3DVar NEMOVAR system to assimilate observations.

## 2.5 Introduction to Online GIS

Geospatial resources and processing functions are available in the form of online Web services (Zhao, Foerster and Yue, 2012). An online GIS system enables a large number of end users to access data and tools in order to carry out specific analyses based on the theme of the data (Hofer, 2014).

### 2.5.1 Spatial Analysis

In order for developers and members of public bodies to decide on suitable sites for deployment of wave/tidal energy devices, suitable spatial analysis must be completed. It is imperative that the analysis considers a range of factors that are likely to influence the efficiency of the device, such as environmental, geographical, and socio-economic factors. Malczewski (2007) stated

that a GIS system can often be referred to “as a decision support system involving the integration of spatially referenced data in a problem-solving environment”.

Currently, there are openly available GIS tools available online that contain wave and tidal resource information for the study area. The Wales Marine Planning portal and the Irish Marine Atlas both have environmental layers as well as resource assessment layers showing tidal and wave resources. One issue is that each tool only shows data for its own jurisdiction i.e.. the Irish Marine Atlas only shows data to the extent of the Irish Marine Plan Area and the Welsh Tool only covers western UK waters. The aim of this study will be to develop a resource layer that covers the extent of both the Irish and Welsh Marine Plan areas slightly beyond, and to have that information available in a GIS tool. Another issue that has been encountered is the lack of information available for how the resource layers were generated, the metadata of the layers is vague, and it is unknown what time series or specific parameters have been used to calculate the resource value. This information will be taken forward with this project with an emphasis being put on adding informative metadata to the layers that are being created so the user has an understanding of how the data was created.

In terms of the information that is available on the Wales Marine Planning Portal, the site contains wave data that has been supplied by the Met Office on behalf of BERR for the Atlas of UK Marine Renewable Energy Resources project. The dataset includes information about significant wave heights and full wave field power for the area of the UK Continental Shelf for a period of 7 years from 2001 – 2008 (ABPmer, 2008). The site also contains tidal data that was supplied by Proudman Oceanographic Laboratory (POL) on behalf of BERR for the Atlas of UK Marine Renewable Energy Resources project. The tidal data is available at 32 evenly spaced sigma levels through depth. The tidal dataset includes information about flow speed (m/s), power and tidal range for the area of the UK Continental Shelf. (ABPmer, 2008). The wave resource data has been modeled using data from two sources: UK Waters Wave Model (Spatial resolution 12km) and Global Model (Spatial Resolution 60km).

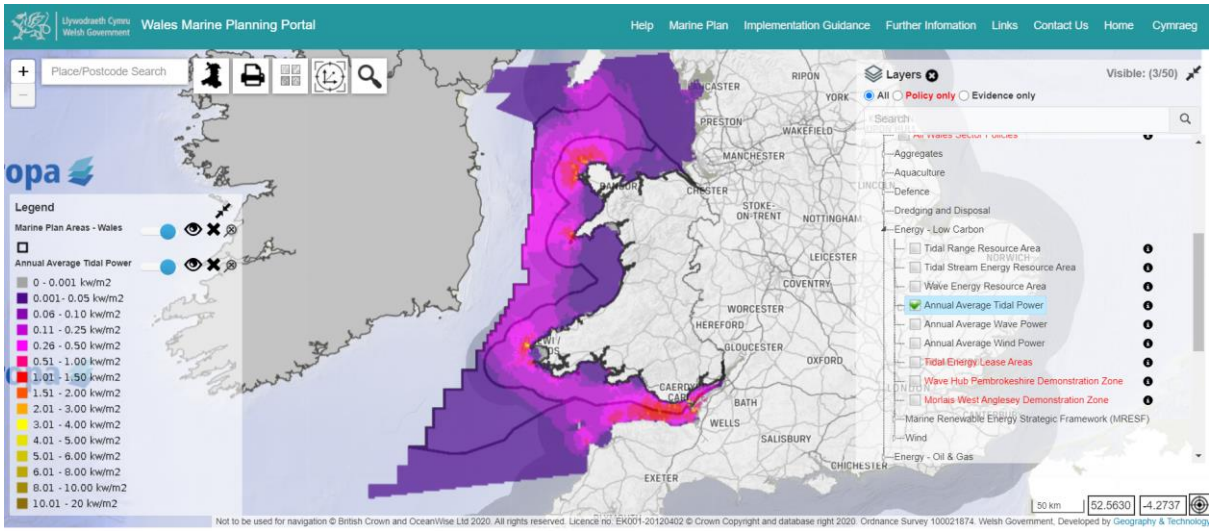



*Figure 2.26 Wales Marine Planning Portal showing Annual Average Tidal Power (British Crown and OceanWise Ltd, 2020).*

The Irish Marine Atlas has a number layers available for the wave resource and it's parameters, including but not limited to: Mean annual distribution of wave height (m), mean annual distribution of wave period (s), mean annual theoretical wave energy resource (MWh/m), mean annual technical wave power resource (Pelamis) MWh/m. It is stated in the metadata that this information covers an area known as Irish Exclusive Economic Zone (EEZ) and that the data model was produced in 2005 (Marine Institute, 2005). The metadata does not provide any further information about the dataset, including how many years of data were used to model the results.

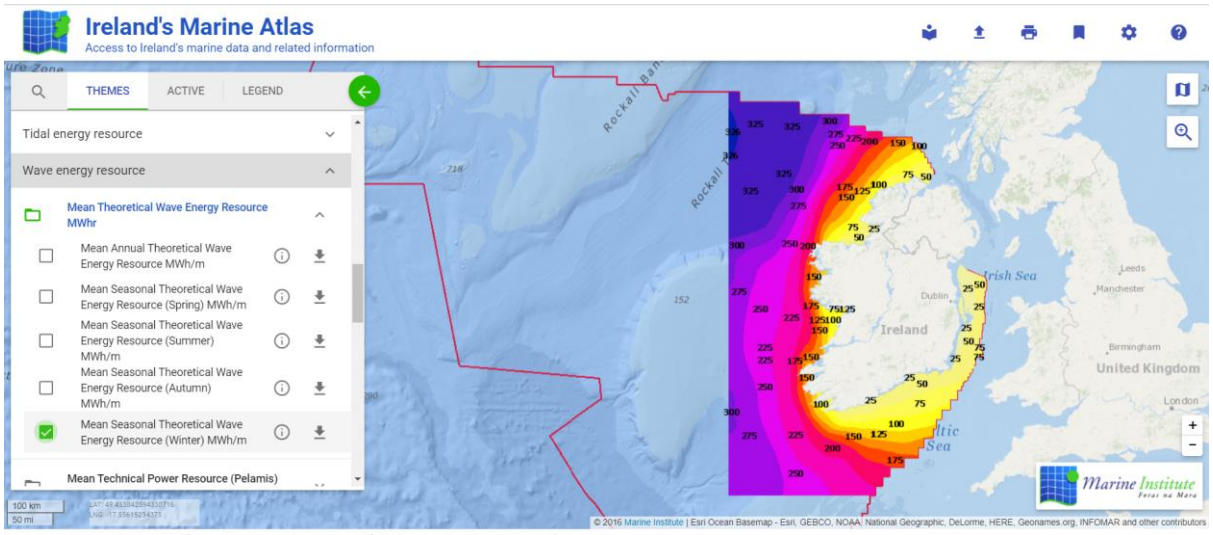



*Figure 2.27 Ireland Marine Atlas showing Mean Theoretical Wave Energy Resource (Marine Institute, 2015).*

There is limited information available in terms of the tidal energy resource, with a polygon layer for the tidal resource potential which was produced as part of the Offshore Renewable Energy Development Plan Strategic Environmental Assessment in 2014. There is limited information given on the methods or data models that were used to produce these layers, so it is unknown what spatial resolution and length of hindcasts have been used. (Ireland's Marine Atlas, 2021)

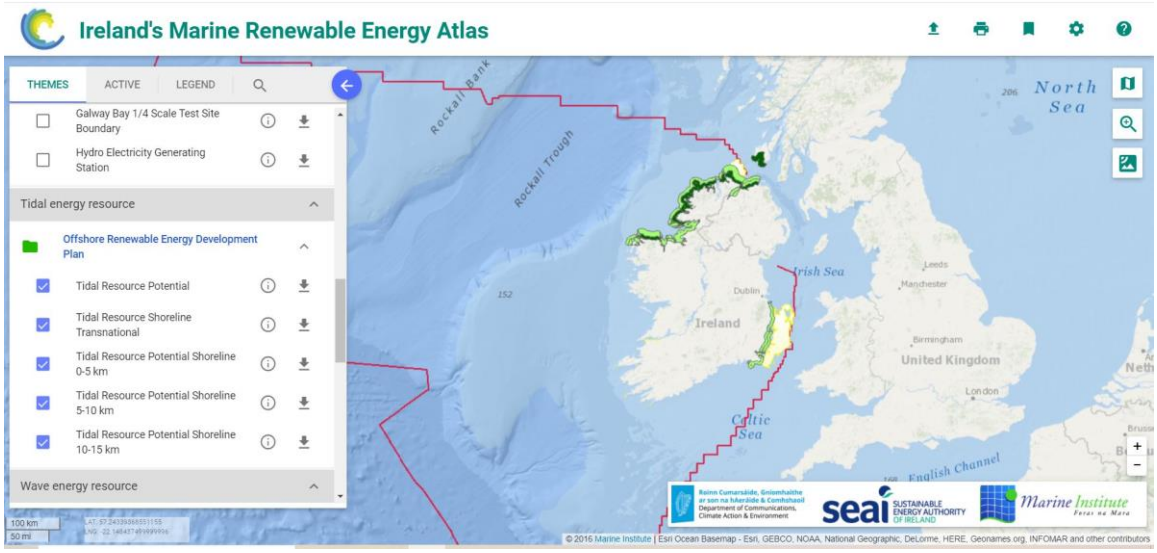



*Figure 2.28 Ireland Marine Atlas showing Tidal layers that are currently available (Marine Institute, 2015).*

There is also an online GIS tool belonging to the European Atlas for Maritime Affairs. The data that is available here is much coarser as it covers the whole of Europe. Figure 2.29 below shows the wave height and direction data which is a dataset of 237 point locations that show

significant wave height and direction. In Figure 2.30 the tidal amplitude (meters) can be seen, also shown for 237 point locations across the study area.




*Figure 2.29 This map shows the significant wave height and direction in 237 locations placed at approximately 100 km intervals some 50 to 100 km off Europeand#39;s coastline. The observations of wave height and direction were collected using the altimeter sensors carried by the ERS-1, ERS-2, Topex/Poseidon and Geosat satellites available in the waveclimate.com database. From these observations, averages were calculated in a 200 by 200 kilometre box centred on each location (European Union, 2021).*

In terms of what is currently available for the study area, the data from the various examples that were discussed is of a much coarser nature in comparison to what will be produced during this study. This study uses high resolution data that is <3km resolution for both the wave and tidal energy resource assessment. This study will also differ from previous work in that the data will cover the extent of (-)12°W – (+)2.5°W; 52°N – 49°N, covering the west and north Atlantic coasts of Ireland as well as the Irish and Celtic Seas. This study also aims to carry out detailed seasonal analysis for the wave resource, which will be useful to developers to understand the temporal variability in the resource.

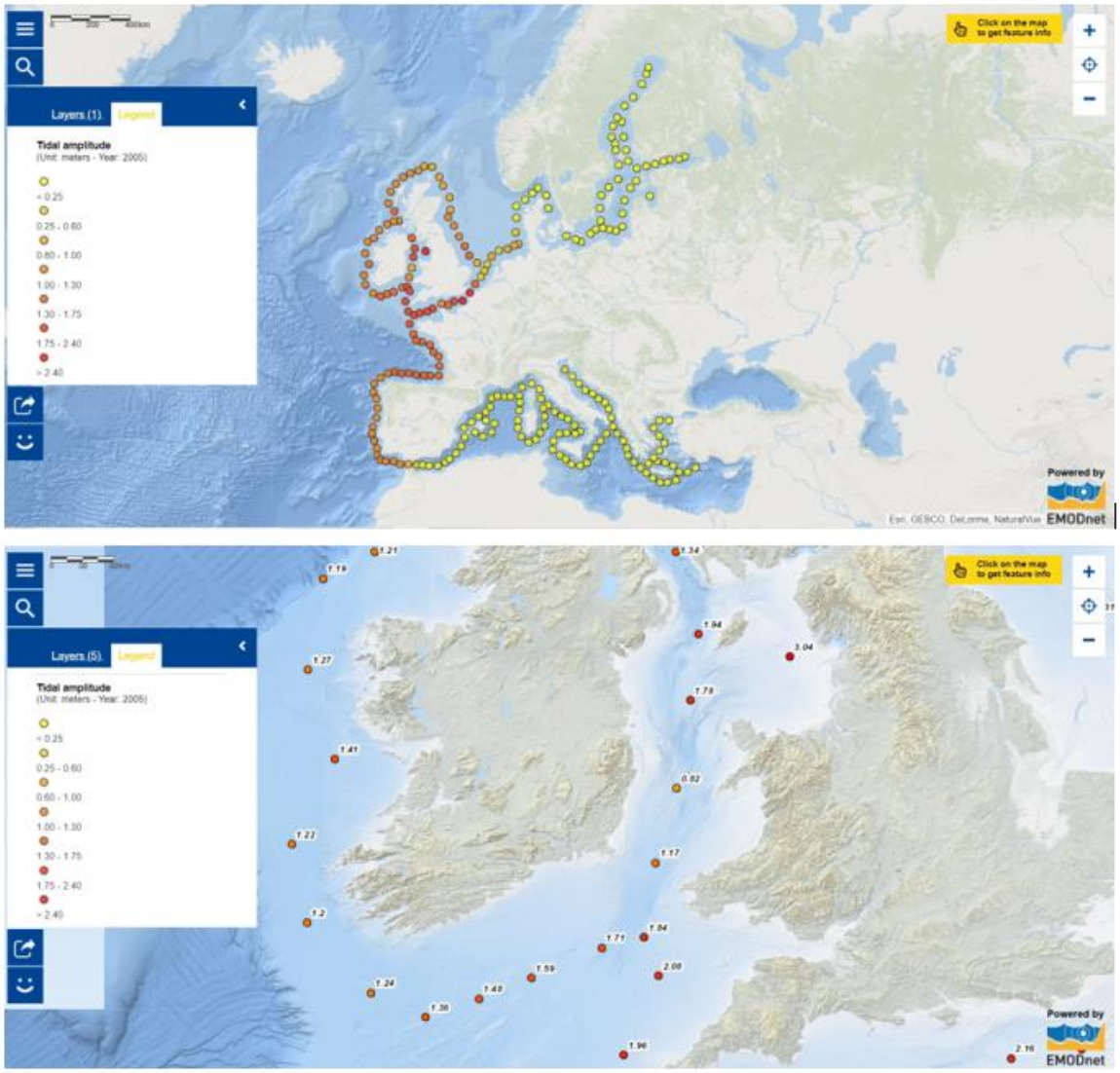



*Figure 2.30 This map displays the average tidal amplitude, half of the height difference between low and high tide, in 237 locations placed at approximately 100 km intervals some 50 to 100 km off Europe's coastline. The observations were calculated using a tidal model derived from eight years of satellite altimeter measurements as well as tidal gauge measurements from approximately 7300 coastal stations (European Union, 2021).*

## 2.6 Wave and Tidal Resource Assessment

A number of studies have carried out wave or tidal resource assessment in the area that covers the study area of this project, and it is important to understand the methodology and results of those studies to inform the work that will be carried out as part of this study.

A study by Guillou et al (2020) reviewed the benefits, limitations and potential of different methods for wave resource assessment, with particular attention paid to using satellite data for

wave resource assessment. The author identified that there are a number of sources of data currently available for wave resource assessment, including in situ data, satellite and altimeter data, hindcast and reanalysis datasets. It was stated that historical data is very valuable at the preliminary stage of a project as it is easily accessible and provides information about seasonal conditions. The author referenced a study in China's seas which used five years of satellite data to model wave energy, which was the first wave energy assessment of it's kind using satellite data. It was also noted that it is likely that there will be increased accuracy in the energy resource assessments being completed with satellite data as longer hindcasts become available (Guillou, Lavidas and Chapalain, 2020). Based on the review it was stated that hindcast and reanalysis data is very valuable for analysing wave resource at the reconnaissance stage of a project as it saves time and money in terms of setting up complex numerical models.

A resource assessment carried out by Atan et al (2018) looked at the Galway Bay Test site as well as the Westwave commercial demonstration site in off the western Irish coast. The study carried out a wave resource assessment using 12 years of data. The results present an annual mean wave power of 3 kW/m at the Galway Bay test site and 50 kW/m at the Westwave site. These results will be useful to use as a comparison for the results that are obtained from the analysis as part of this study. The author stated that a minimum of ten years of measured or modelled wave data should be used in order for the wave resource assessment to be reliable. It was stated that wave power values of up to 100 kW/m can occur in the NW Atlantic, with significant wave height values of up to 4m possible. It was also reported that seasonal variations were seen for the wave parameters of wave height and wave period, as well as in the wave power resource, with highest values seen in the winter and lowest in the summer.

A tidal resource assessment for the Irish Sea was carried out by Lewis et al, (2015). The study reported that resource assessment for tidal energy is sensitive to the model resolution, with finer resolution of <500m being the most reliable. For the study, three model resolutions were investigated; 1.1km, 0.6km and 0.3km. The study used the ROMS model, similar to the data from the Marine Institute that is used for this study. A map was provided of the peak spring tide current velocity, which was simulated using the finer resolution model, the results of which will be very useful as a comparison for this study (Figure 2.31).

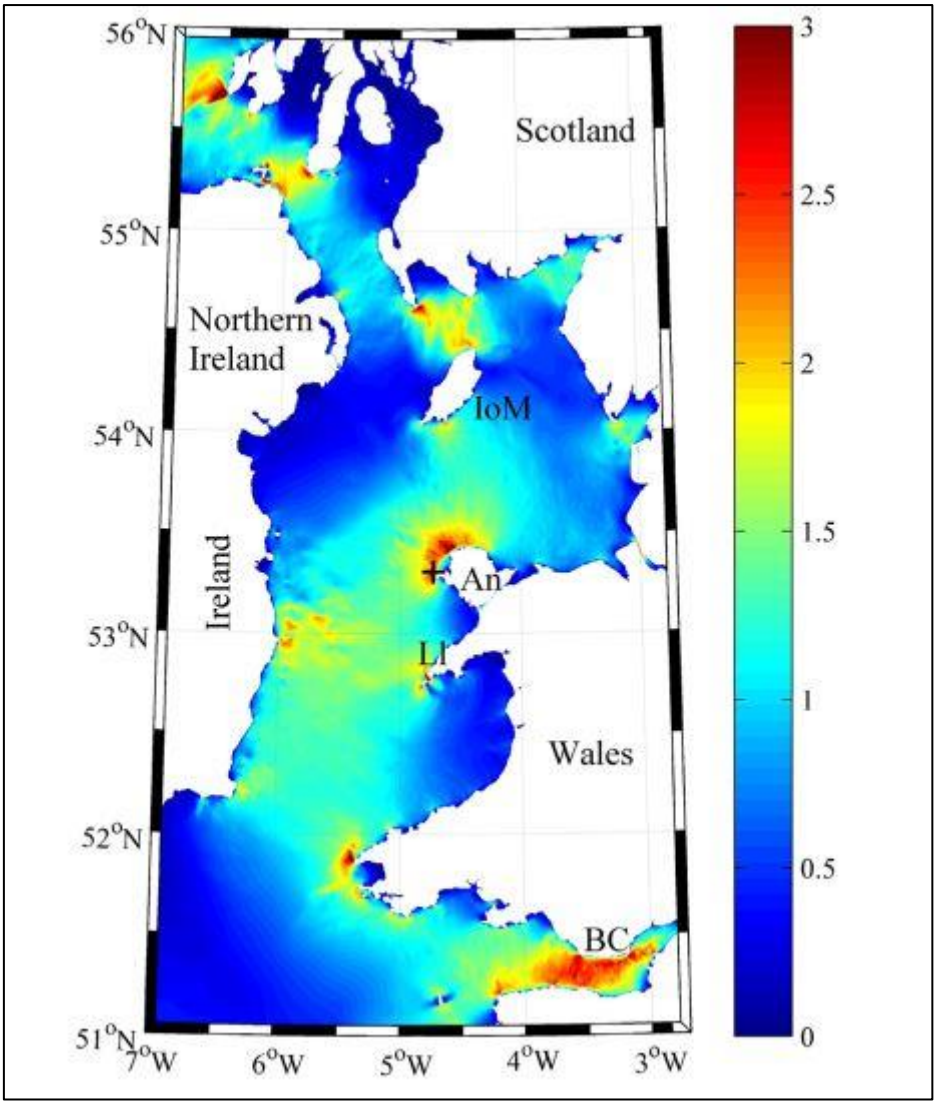



*Figure 2.31 Peak Spring Tide current velocity. (Lewis, 2015)*

# 3 Data and Methodology

In this section, the methodology for both the wave energy resource assessment and the tidal energy resource assessment will be outlined. The methodology adopted for each is quite different, so this section will be split into two main sections: one for the wave assessment and one for the tidal assessment. The rationale for each GIS layer that will be created will also be discussed.

## 3.1 Software

Two different software packages have been used as part of this study: MATLAB was used for the analysis of the data and ArcGIS Pro was used to create the GIS layers.

MATLAB was chosen because it is a software that allows the user to organize, clean, and analyze complex data sets. This study aims to use 20 years of climatological data which will result in very large datasets and MATLAB is a software that will be able to handle the complexity of the data.

ArcGIS Pro has been chosen as the GIS tool to be used for the study as it has been developed to handle raster data very well. The results from the MATLAB analysis will be converted to GIS rasters and these layers will then be added to an online web-tool. ESRI, the company who creates ArcGIS, also has ArcGIS online which will enable the user to add datasets to the web for wider use as part of the SELKIE GIS Tool.

## 3.2 Study Area

The study area aims to look at the wave and tidal energy for the Irish and Welsh EEZ's (Exclusive Economic Zone). Previous studies have shown the wave energy off the west coast of Ireland is one of the most abundant in the World, while tidal energy sources in the region are known to be plentiful (Fig 18). In terms of downloading the data, the latitude and longitude co-ordinates that were used were 12°W – 2°W; 56°N – 50°N. The extent of the datasets that will be created can be seen below in Figure 3.1.

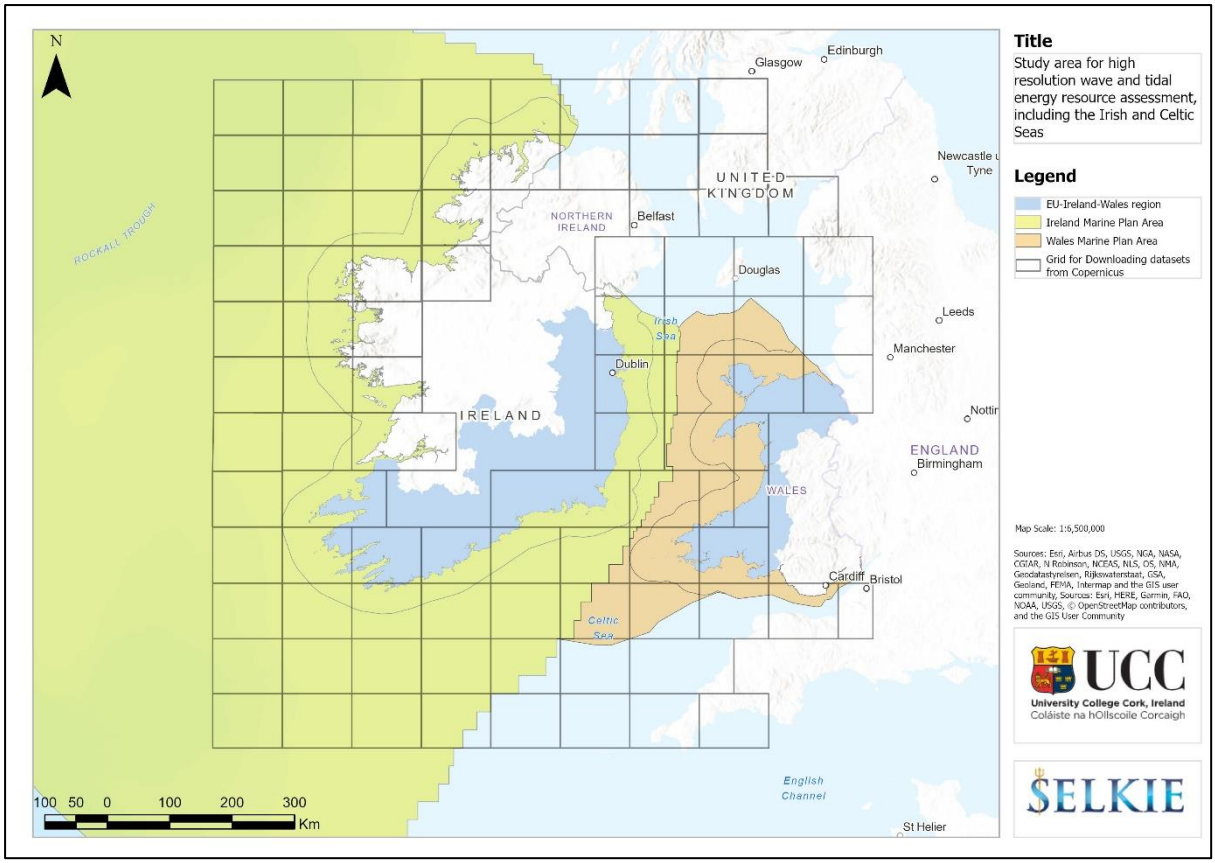



*Figure 3.1 Study Area for high resolution wave and tidal energy resource assessment in the Irish and Celtic Seas.*

## 3.3. Wave Data

Two products have been identified to be suitable for the wave resource assessment for this study. Both products are used and then a comparison will be carried out to analyze the accuracy and resolution of each product and the suitability for wave resource modelling.

The first product that was identified to be suitable for use for the wave modelling is called Atlantic – Iberian Biscay Irish – Ocean Wave Reanalysis (Product Identifier - IBI_MULTIYEAR_WAV_005_006). The product provides a multiyear high-resolution wave reanalysis product for the IBI (Iberian Biscay Irish) area with a time series starting from 01/01/1993. The model is based on the MFWAM model developed by Meteo-France (MF), with a grid of 5 km of horizontal resolution. The model is fed by the ERA 5 reanalysis wind data from ECMWF. It covers the extents (-)19°W – (+)5°W; 56°N – 26°N and has a spatial resolution of 0.05degree x 0.05degree. The product is composed of one dataset with hourly instantaneous fields, including the following variables: Wave Height, Period and Direction for total spectrum and fields of Wind Wave (or wind sea), Primary Swell Wave and Secondary Swell for partitioned wave spectra.

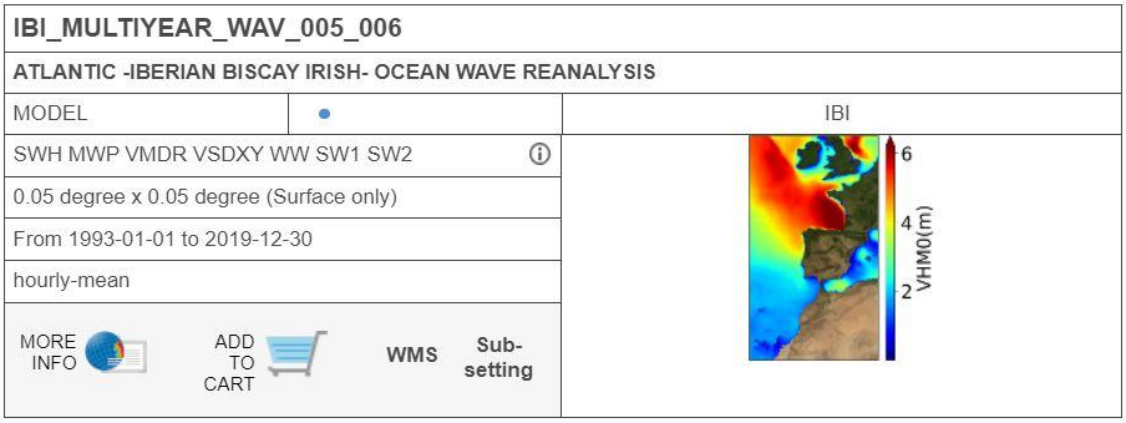



*Figure 3.2 Details of the Atlantic Iberian Biscay Irish Ocean Wave Reanalysis model from the Copernicus Marine service that was used for the modelling of the wave resource (CMEMS, 2021).*

The second product that was identified to be suitable for the wave resource modelling was the Atlantic – European North West Shelf – Wave Physics Reanalysis model, which has a product identifier of NWSHELF_REANALYSIS_WAV_004_015. The model gives a hindcast for the European Northwest Shelf area beginning from 1980 – 01 – 01 to present. The wave model used is WaveWatch III, which covers the extents of (-)16°W – (+)13°W; 62.75°N – 46°N and the resolution is ~1.5km or 0.017degree x 0.017degree.

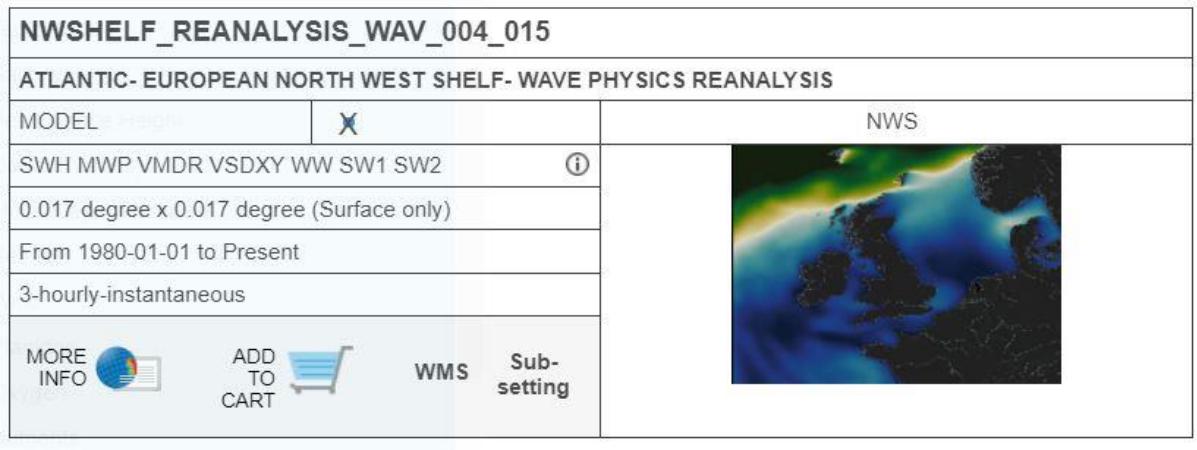



*Figure 3.3 Details of the Atlantic European North West Shelf Wave Physics Reanalysis model from the Copernicus Marine service that was used for the modelling of the wave resource (CMEMS, 2021).*

### 3.3.1 Validation of Wave Data

Validation of model data against in situ measurements is an important step as it ensures that the user has confidence in the accuracy of the dataset that is being used. Validation has not been carried out as part of this study as the data from the Copernicus website has been thoroughly validated against in situ data by the team at CMEMS as part of the model

development process. The data has also been validated as part of the paper that has been co-authored and published as part of this study - O'Connell, R and Furlong, R. (2021). The results of the validation assessments will be discussed below so that the reader can understand the accuracy of these datasets in order to better interrogate the results.

#### *3.3.1.1 CMEMS - IBI_MULTIYEAR_WAV_005_006*

For the validation that has been carried out by CMEMS, the accuracy assessment has been calculated with in situ buoys, with the period from 01/01/1993 to 31/12/2019 used for the validation study. Data from 112 mooring buoys provided by the CMEMS In-Situ TAC was used for the study. The validation study has considered buoys moored on depths less than 100 m (labelled as coastal) and those moored in deeper waters (labelled as deep water). The CMEMS validation study focused on 10 subareas across the European region which can be seen in Figure 3.4, but this study will focus on the Irish sub region. Eleven buoys in total were available for Irish and UK waters, ten coastal buoys and one deep buoy, which can be seen in Figure 3.4 (Baladrón, 2020).

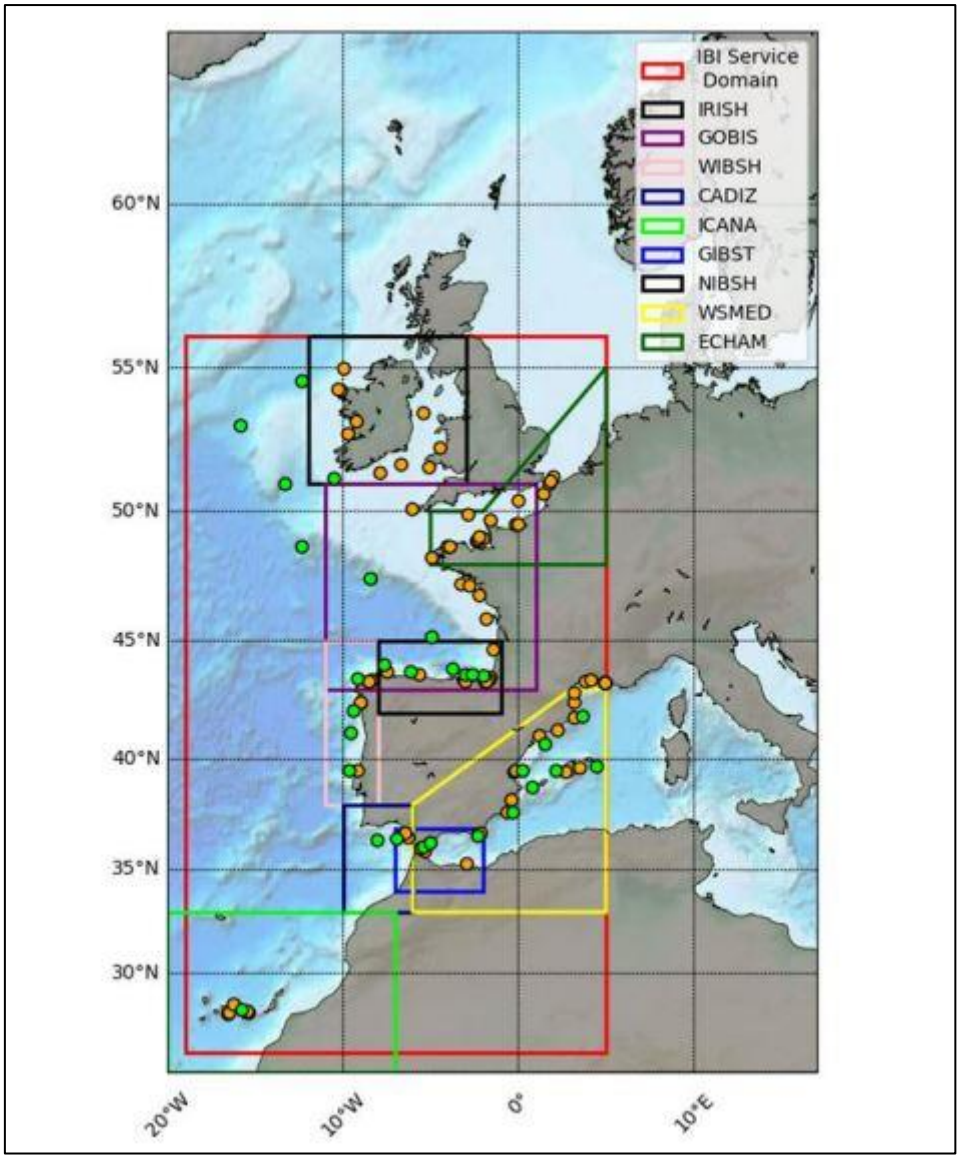



*Figure 3.4 Location of the coastal (orange dots) and deep water (green dots) buoys included in the IBI qualification during the whole period (01/01/1993 - 31/12/2019). Source: (Baladrón, 2020).*

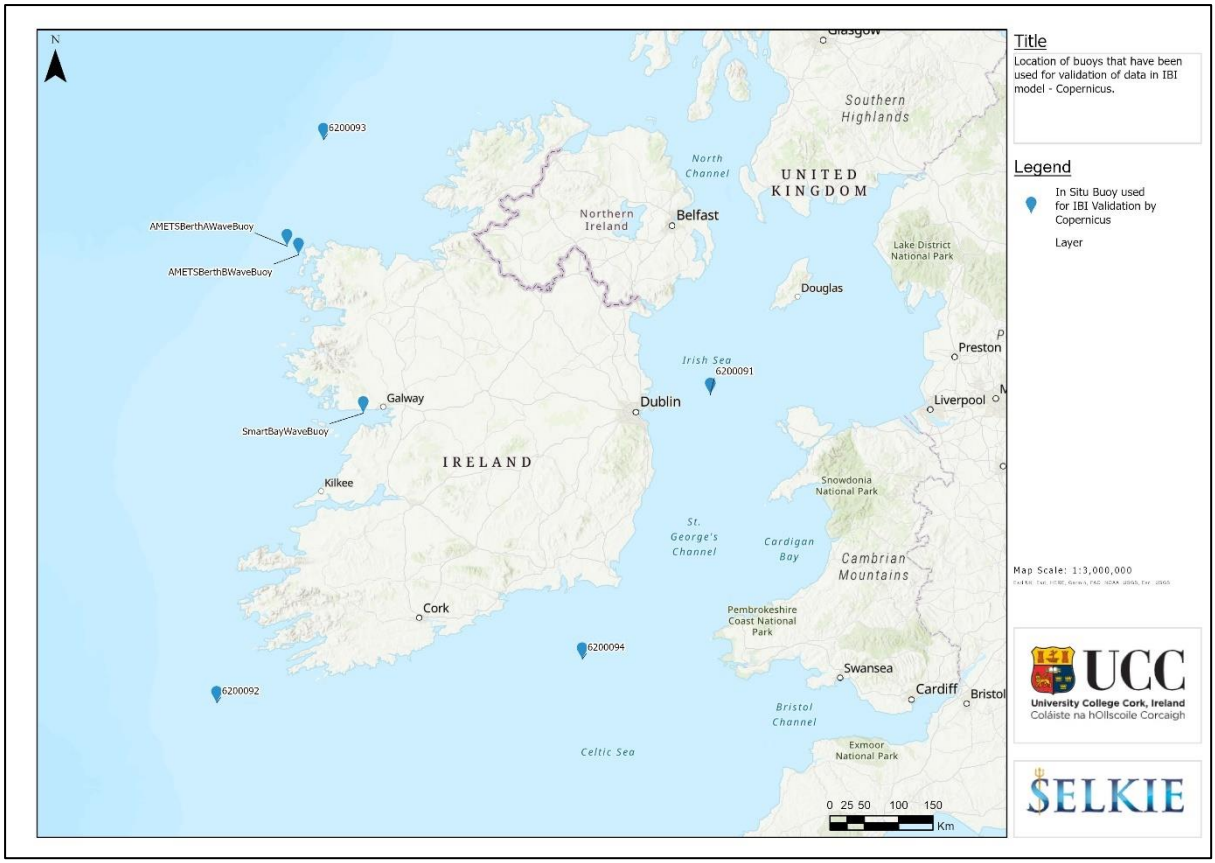



*Figure 3.5 Detailed figure showing the location of the buoys that Copernicus used for their validation study of the IBI model. Note: The co-ordinate information for these buoys was taken from the CMEMS dashboard, the location information for all 11 buoys within UK*

The results show that significant wave heights generally have good performance with high linear correlations and low scatter index in most areas. For the Irish sub region, the correlation co-efficient is >90% for all buoys, except the smart wave buoy which is the most coastal buoy in the study (correlation coefficient of 86.47%). Lower results can be seen across each of the sub areas for the coastal buoys which may be related to the wave that the waves are interacting in shallow water and the change in bathymetry close to the coastline.

| SUB-REGION IRISH | | | | | | | |
|---|---|---|---|---|---|---|---|
| MOORING BUOYS | N | BIAS (m) | RMSD (m) | SI (%) | LR SLOPE | LR OFFSET (m) | CORR (%) |
| COASTAL(10) (10)(1) (4) | 691077 | -0.13 | 0.39 | 21.34 | 0.95 | 0.21 | 95.60 |
| DEEP (1) | 115025 | -0.03 | 0.38 | 13.01 | 0.98 | 0.09 | 97.13 |
| TOTAL (11) | 806102 | -0.12 | 0.39 | 19.63 | 0.95 | 0.20 | 96.26 |

| SUB-REGION IRISH | | | | | | | |
|---|---|---|---|---|---|---|---|
| BUOY | N | BIAS (m) | RMSD (m) | SI (%) | LR SLOPE | LR OFFSET (m) | CORR (%) |
| IR_TS_MO_62091 | 12055 | -0.16 | 0.29 | 20.6 | 0.97 | 0.19 | 94.38 |
| IR_TS_MO_62093 | 87998 | 0.20 | 0.60 | 20.0 | 0.93 | 0.03 | 93.91 |
| IR_TS_MO_62094 | 10133 | -0.09 | 0.30 | 15.8 | 0.98 | 0.13 | 96.28 |
| IR_TS_MO_AMETS-weather-buoy | 2726 | -0.41 | 0.57 | 15.9 | 1.22 | -0.04 | 97.08 |
| IR_TS_MO_AMETSBerthAWaveBu | 28650 | -0.14 | 0.35 | 10.5 | 1.07 | -0.08 | 97.89 |
| IR_TS_MO_FS1-weather-buoy | 1088 | -0.12 | 0.32 | 9.00 | 0.97 | 0.21 | 96.78 |
| IR_TS_MO_SmartBayWaveBuoy | 27324 | 0.06 | 0.29 | 34.6 | 0.81 | 0.11 | 86.47 |
| IR_TS_MO_WestwaveWaveBuoy | 10684 | -0.37 | 0.52 | 12.1 | 1.14 | 0.02 | 98.18 |
| NO_TS_MO_62301 | 14383 | -0.33 | 0.45 | 23.3 | 1.19 | 0.14 | 94.15 |
| NO_TS_MO_62303 | 16688 | -0.14 | 0.32 | 16.9 | 1.01 | 0.12 | 96.48 |
| IR_TS_MO_62092 | 11502 | -0.03 | 0.38 | 13.0 | 0.98 | 0.09 | 97.13 |

*Figure 3.6 Tables from the CMEMS validation study showing results for the Irish sub region for Significant Wave Heights Source: (Baladrón, 2020).*

The results show that mean wave period scores are promising too with a minimal overestimation of 0.15 s and scatter index around 20%. The poorest performing location is at the Smart Bay Wave Buoy off the west coast of Ireland where the correlation co-efficient is 42%.

| SUB-REGION IRISH | | | | | | | |
|---|---|---|---|---|---|---|---|
| BUOYS | N | BIAS (s) | RMSD (s) | SI (%) | LR SLOPE | LR OFFSET (s) | CORR (%) |
| COASTAL (8) | 380899 | -0.20 | 1.10 | 19.65 | 0.71 | 1.71 | 82.58 |
| DEEP (1) | 116063 | -0.24 | 0.60 | 8.02 | 0.93 | 0.70 | 93.25 |
| TOTAL (9) | 496962 | -0.21 | 1.00 | 16.86 | 0.78 | 1.47 | 85.94 |

| SUB-REGION IRISH | | | | | | | |
|---|---|---|---|---|---|---|---|
| BUOYS | N | BIAS (s) | RMSD (s) | SI (%) | LR SLOPE | LR OFFSET (s) | CORR (%) |
| IR_TS_MO_62091 | 120964 | -0.82 | 1.05 | 14.98 | 0.67 | 1.99 | 74.00 |
| IR_TS_MO_62093 | 88341 | -0.10 | 0.64 | 9.12 | 0.92 | 0.65 | 91.24 |
| IR_TS_MO_62094 | 101580 | -0.34 | 0.68 | 10.62 | 0.85 | 1.11 | 90.09 |
| IR_TS_MO_AMETS-weather-buoy | 2726 | -0.29 | 0.62 | 8.37 | 0.86 | 1.17 | 91.46 |
| IR_TS_MO_AMETSBerthAWaveBuoy | 28637 | 0.16 | 0.47 | 6.37 | 0.93 | 0.31 | 94.88 |
| IR_TS_MO_FS1-weather-buoy | 1088 | 0.01 | 0.49 | 7.37 | 0.78 | 1.48 | 90.35 |
| IR_TS_MO_SmartBayWaveBuoy | 26879 | 2.23 | 2.93 | 51.55 | 0.19 | 2.56 | 42.66 |
| IR_TS_MO_WestwaveWaveBuoy | 10684 | 0.38 | 0.68 | 8.14 | 0.87 | 0.58 | 94.03 |
| IR_TS_MO_62092 | 116063 | -0.24 | 0.60 | 8.02 | 0.93 | 0.70 | 93.25 |

*Figure 3.7 Tables from the CMEMS validation study showing results for the Irish sub region for Wave Periods. Source: (Baladrón, 2020).*

### 3.3.1.2 CMEMS validation study of NWS model data

A validation study for the NWS model has been carried out by CMEMS. For the validation study, a global dataset of offshore measurements was collated, and quality controlled each month under the World Meteorological Organization – International Oceanographic Commission (WMO-IOC) Joint Commission On Marine Meteorology's operational Wave Forecast Verification Scheme (Bidlot et al. 2007, referred to as the JCOMM-WFVS). Over 400 measurement sites are registered in the system and observations over the period 01/01/2016 to 31/12/2017 are used. For the NWS model, the correlation co-efficient for the significant wave heights the Celtic-Irish Seas area is 0.952. This shows there is generally good correlation between modeled and measured data within the study area. This results also correlates well with the validation study for the IBI model which showed all correlation co-efficient for the study area being >90% (Tonanai & Saulter, 2021).

| Region | No. Samples | Observed MEAN | Observed STD | BIAS | Error RMSD | Error STD | SI | Sym. Slope | CORR |
|---|---|---|---|---|---|---|---|---|---|
| North-West Shelf Offshore | 149179 | 2.185 | 1.41 | 0.003 | 0.307 | 0.307 | 0.218 | 0.896 | 0.977 |
| Celtic-Irish Seas | 5652 | 1.221 | 0.763 | -0.080 | 0.252 | 0.239 | 0.313 | 1.049 | 0.952 |
| Central North Sea | 60443 | 1.911 | 1.181 | -0.002 | 0.275 | 0.275 | 0.233 | 0.842 | 0.974 |
| Southern North Sea | 26360 | 1.242 | 0.778 | 0.021 | 0.196 | 0.195 | 0.251 | 0.941 | 0.968 |
| North Sea Approaches | 53575 | 2.548 | 1.472 | 0.019 | 0.361 | 0.36 | 0.245 | 0.907 | 0.970 |
| UK Northwest Approaches | 19941 | 3.053 | 1.685 | -0.081 | 0.345 | 0.335 | 0.199 | 0.895 | 0.981 |
| UK Southwest Approaches | 6227 | 2.972 | 1.591 | 0.047 | 0.306 | 0.302 | 0.190 | 0.986 | 0.982 |
| English Channel | 3838 | 1.022 | 0.612 | -0.079 | 0.193 | 0.176 | 0.288 | 0.975 | 0.958 |
| Bay of Biscay | 5100 | 1.669 | 1.127 | 0.355 | 0.534 | 0.398 | 0.353 | 1.273 | 0.952 |

*Figure 3.8 Verification statistics for significant wave height comparison versus open waters in-situ observations.(Tonanai & Saulter, 2021).*

### 3.3.1.3 O'Connell, R and Furlong, R. (2021) Paper

A paper entitled "An assessment of newly available Copernicus sea surface wave products for mapping wave energy in Irish and UK waters" was presented at the 14th International Coast GIS Conference 2021 and subsequently published as part of the conference proceedings by O'Connell, R and Furlong, R. (2021). Part of the work for this study looked at validation of the IBI and NWS models with three in situ buoys (WestWave, WaveHub and West Pembrokeshire).

The results of the validation study showed that there was generally very good correlation between the NWS and IBI buoys with the average significant wave height correlation coefficient across the three sites being 0.97 for both models. The RMSE for the IBI product was slightly greater than that of the NWS product, even though the R values for both were the same. The agreement between modelled wave period and observed wave period was slightly lower than that of the significant wave height, with overall R values of 0.88 for both the NWS and IBI products. The validation study showed that the models are generally agreeing well with the observed in-situ data from the met-ocean buoys. The validation study has also shown that grid spacing of the models is an important factor, with the NWS model (which has the finer grid spacing) performing better than the IBI model in most cases. The significant wave height tends to perform better against measured data than the wave period for both NWS and IBI models. This result corresponds well with what is seen with the validation study that was carried out by CMEMS. Although the validation results proved a high level of accuracy, the WestWave site generally produced the least accurate results of the three sites for both products representing both parameters (significant wave height and wave period). This result reflects what was seen in the results of the CMEMS study, with coastal buoys showing poorer results, possibly as a result of coastal process.

(a)

| Significant Wave Height | | | | | |
|---|---|---|---|---|---|
| Buoy | $\bar{x}$ (m) | Bias (m) | RMSE | SI | *R* |
| WestWave | 2.3497 | 0.2399 | 0.4175 | 0.1777 | 0.9739 |
| WaveHub | 1.9881 | 0.0256 | 0.2666 | 0.1341 | 0.9729 |
| WestPem | 1.6660 | 0.0625 | 0.2582 | 0.1549 | 0.9709 |
| **Wave Energy Period** | | | | | |
| Buoy | $\bar{x}$ (s) | Bias (s) | RMSE | SI | *R* |
| WestWave | 7.1070 | -0.4990 | 0.8882 | 0.1250 | 0.8876 |
| WaveHub | 5.8662 | 0.1394 | 0.6752 | 0.1151 | 0.8932 |
| WestPem | 4.9107 | 0.4419 | 0.7517 | 0.1531 | 0.8853 |

(b)

| Significant Wave Height | | | | | |
|---|---|---|---|---|---|
| Buoy | $\bar{x}$ (m) | Bias (m) | RMSE | SI | *R* |
| WestWave | 2.2447 | 0.3459 | 0.4773 | 0.2126 | 0.9807 |
| WaveHub | 1.9271 | 0.0879 | 0.2846 | 0.1477 | 0.9721 |
| WestPem | 1.5824 | 0.1441 | 0.2959 | 0.1870 | 0.9715 |
| **Wave Energy Period** | | | | | |
| Buoy | $\bar{x}$ (s) | Bias (s) | RMSE | SI | *R* |
| WestWave | 7.1867 | -0.5784 | 0.8828 | 0.1228 | 0.9134 |
| WaveHub | 6.1137 | -0.1081 | 0.7410 | 0.1212 | 0.8923 |
| WestPem | 5.0130 | 0.3340 | 0.7170 | 0.1430 | 0.8754 |

*Figure 3.9 Results from the validation study carried out by O'Connell.R, 2021. The results in table a show NWS values and table B shows IBI values.*

### 3.3.2 Wave Assessment

In order to model the wave energy resource, the following wave parameters are needed: significant wave height (m) and wave energy period (s). These parameters will then be used to calculate the wave energy resource using the wave power equation which was defined in section 2.1.2 using the software application MATLAB. These wave parameters are available to download from numerical models that have been outlined in section 2.3.1. In order to download NetCDF datasets from the Copernicus website there is a download limit of 1024MB, so the datasets had to be below this threshold. It was also found through trial and error that if the datasets exceeded this size, there were difficulties with post processing of the data in

MATLAB and ArcGIS Pro. As a result, a grid was generated for the study area so that the data could be downloaded at equally spaced intervals with no overlap, the grid squares were set up to be generally 1 degree x 0.5 degree. The grid that was generated for the downloads can be seen below in Figure 3.10.

As two models were selected for the wave resource analysis so that a comparison could be made, the wave parameters needed to be downloaded for each grid cell twice, once for each model. In total, 178 NetCDF files were downloaded for the study area, 89 for each model, with each file containing information for the parameters VHM0 (Spectral significant wave height (Hm0)) and VTM10 (Spectral moments (-1,0) wave period (Tm-10)), for the time series 2000-01-01 00:00:00 to 2019-12-30 23:00:00. For the IBI model, the data was collected at hourly intervals, so each NetCDF file has a total of 175296 time steps for each parameter, covering a time series of 20 years. For the NWS model, the data was collected at 3-hourly intervals, so each NetCDF file has a total of 58440 time steps for each parameter, covering a time series of 20 years. Data was downloaded for the same geographical extents from both the IBI and NWS models.

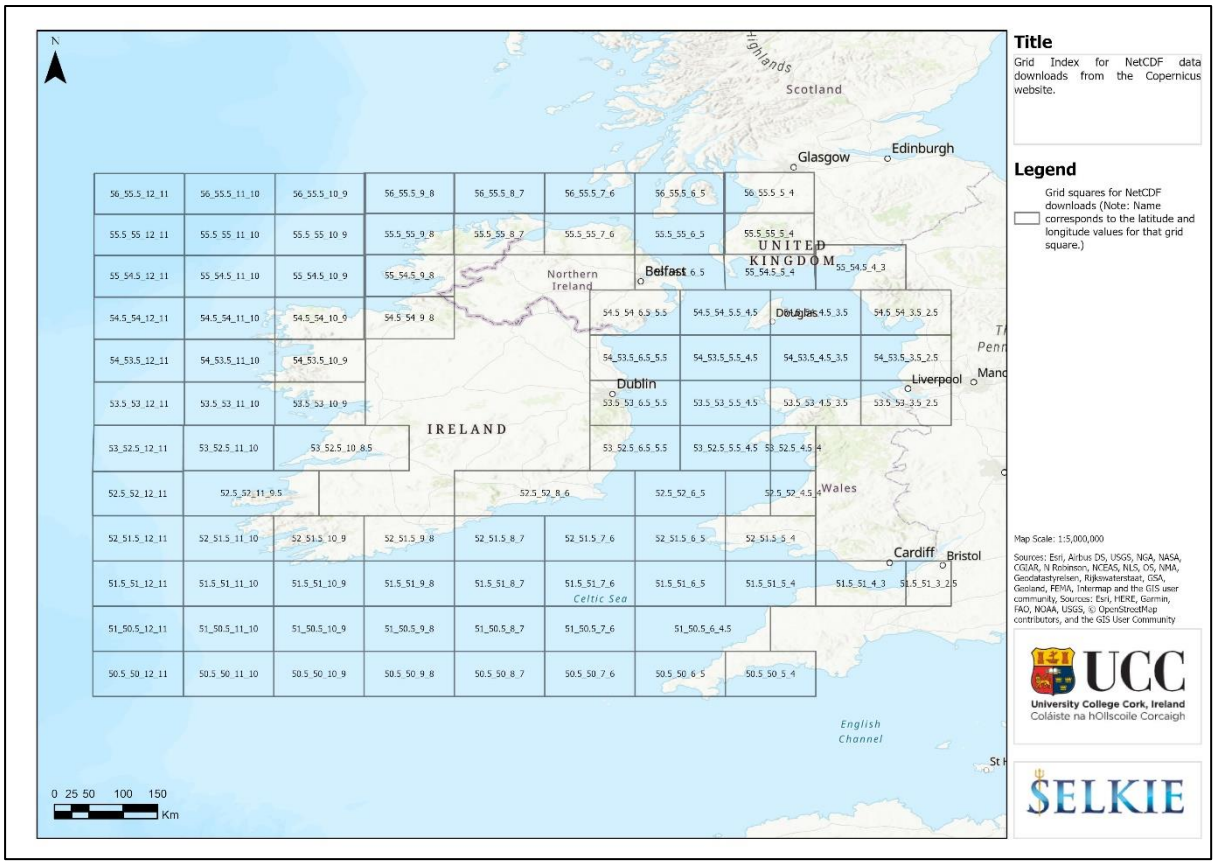



*Figure 3.10 Grid Index for NetCDF data downloads from the Copernicus Website.*

The list of GIS layers that were created can be seen in Appendix 3. These layers were selected so that a thorough understanding of the wave resource could be gained both spatially and temporally. The mean wave power layer aims to give an overall understanding of the resource spatially. The wave energy resource, as well as the significant wave height and the wave energy period were then calculated for each season, so that an understanding could be gained of the variability in the resource throughout the year. The seasons have been split into three monthly intervals: spring (March, April and May), summer (June, July and August), autumn (September, October and November) and winter (December, January andFebruary). Each of the layers that have been created as part of the wave assessment and detailed descriptions of each layer can be viewed in Appendix X.

In order to create each layer, a set of steps was followed for each of the layers. The steps are as follows:

1. The NetCDF datasets were imported to MATLAB (see appendix II for scripts) where the calculations were carried out. For each layer, a MATLAB script was created, which ran through each of the time step values for each parameter and created an output matrix of results for the study area.
2. For each grid square, the final values were then outputted to a GeoTIFF file and imported to GIS. A GeoTIFF is a file format that allows georeferencing information to

be embedded in a TIFF file. This means that the spatial information for the data will be present when opened in ArcGIS.

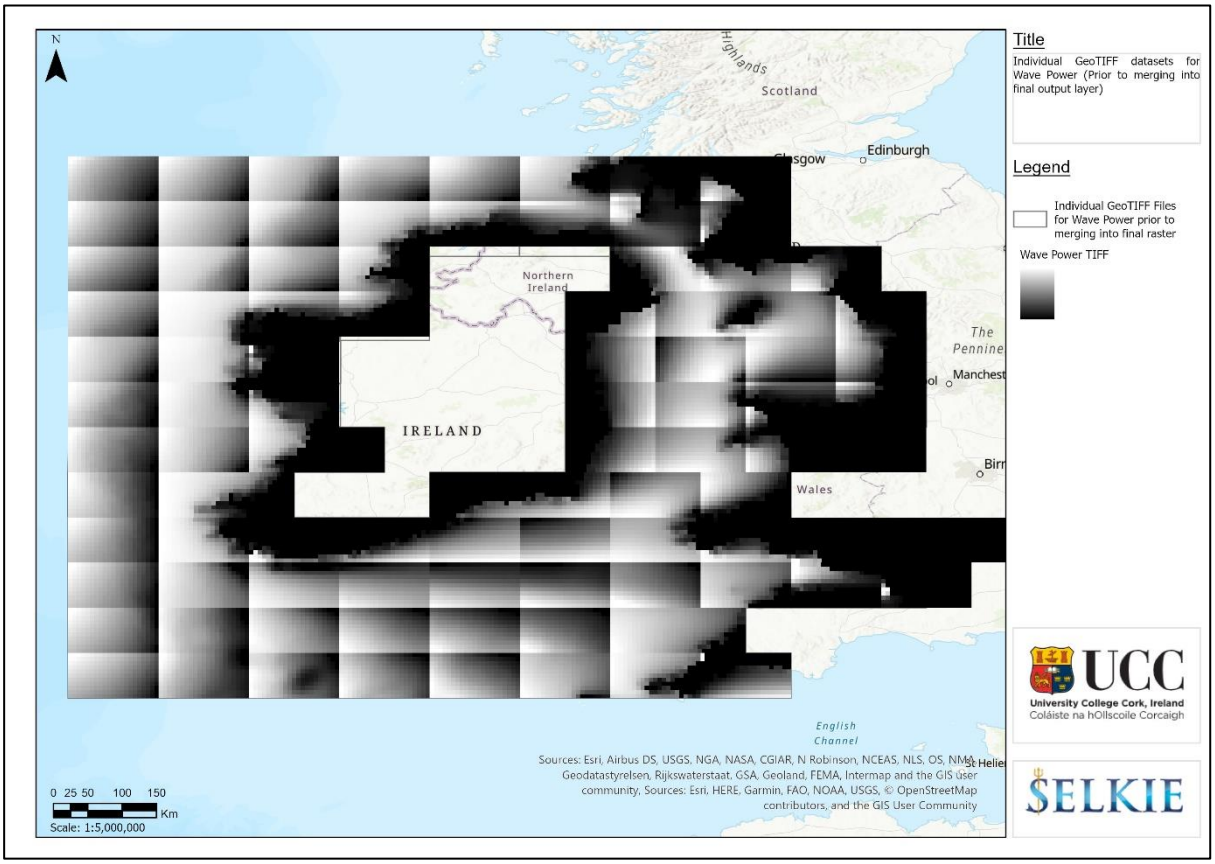



*Figure 3.11 Individual GeoTIFF datasets for Wave Power (prior to merging unto final output layer).*

3. Once there was a GeoTIFF file available for each of the 89 grid squares, they were imported to ArcGIS Pro. The GeoTIFF's then needed to be merged so that there would be one raster dataset covering the whole study area. A raster dataset is a type of spatial data that consists of a matrix of cells that are organized into rows and columns, with each cell holding a value (Environmental Systems Research Institute, 2016). In order to create the raster dataset, the tool 'Mosaic to New Raster' was used within ArcGIS Pro. As the grid spacing for the two models (the IBI model and the NWS model) was different, the inputs for the tool were also different to take into account the cell size of the output raster. The cellsize that was used for the IBI model was 0.05 and the cellsize used for the NWS model was 0.015. The following parameters were used as inputs for the tool:

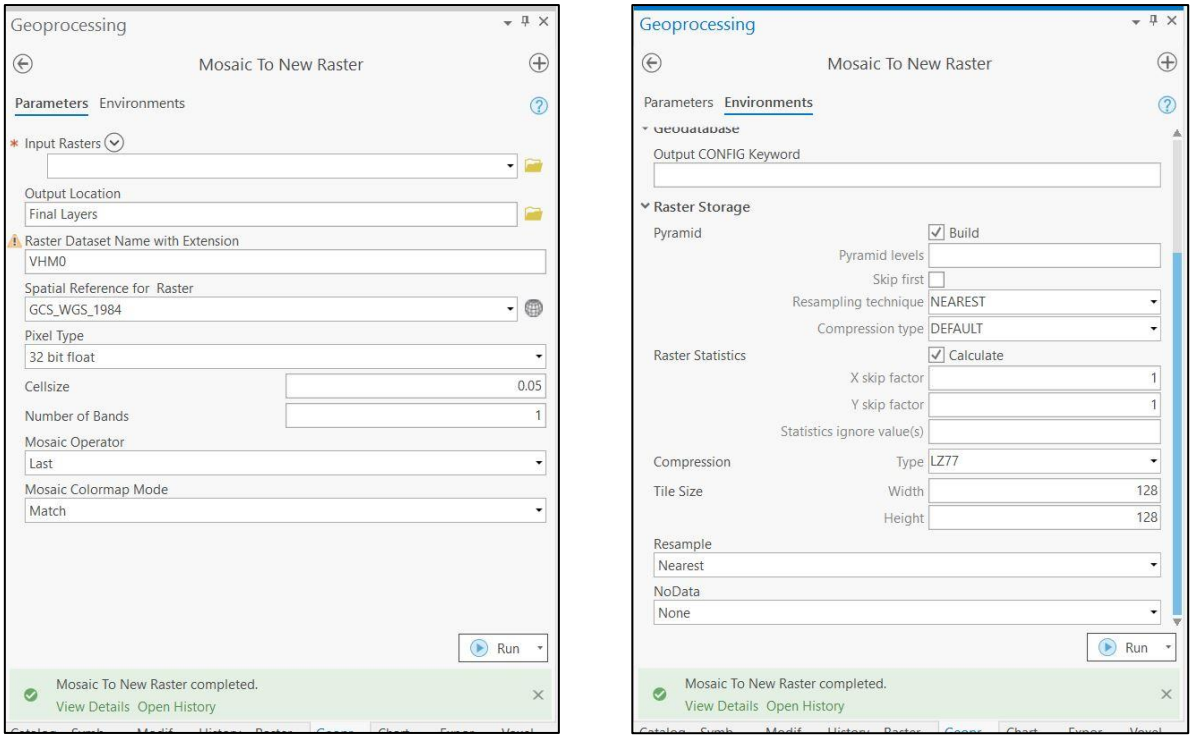



*Figure 3.12 Input parameters for the IBI model data for ArcGIS Pro 'Mosaic to New Raster' toolbox that is used for merging GeoTIFF files into final raster dataset.*

4. Once the raster was created that contained the information from all 89 GeoTIFF files,the information then needed to be converted to a polygon feature class so that the feature layer could be published to ArcGIS Online. As the raster that was created was a floating type raster, it first needed to be converted to an integer raster before the tool 'Raster to Polygon' could be used in ArcGIS Pro. The steps that were taken can be seen below:

4.1 Using the ‘Raster Calculator’, multiply the value in the raster layer by a multiple of 10 in order to remove the decimal places eg, six decimal places multiply by 1000000.

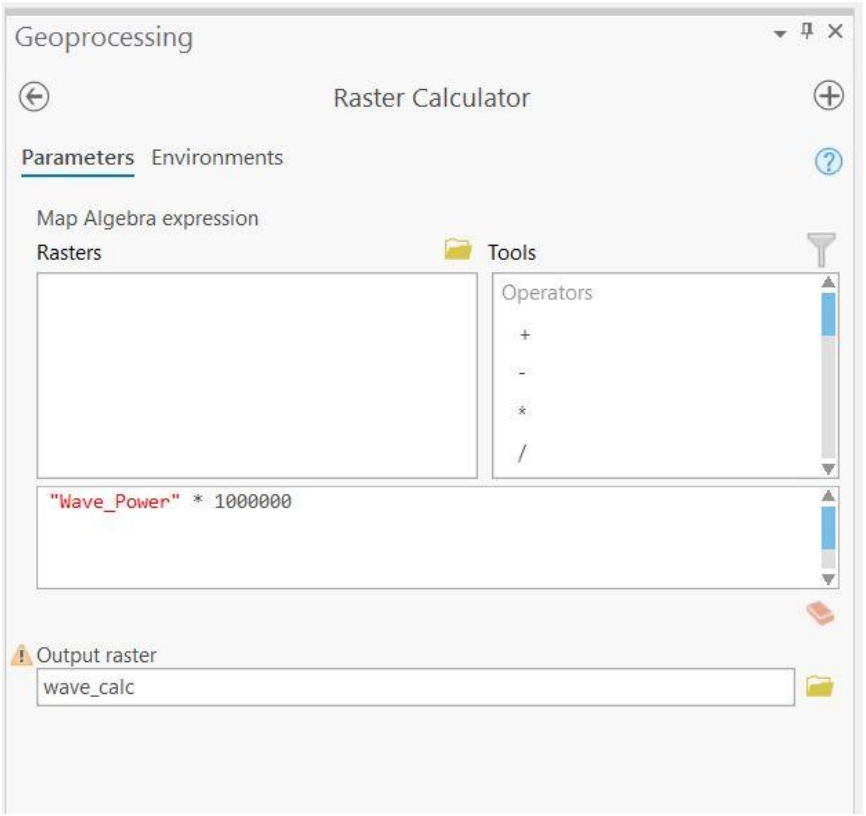



*Figure 3.13 ArcGIS Pro 'Raster Calculator' tool that is used during the conversion process.*

4.2 The floating type raster is converted to an integer type raster using the ‘Int’ tool.

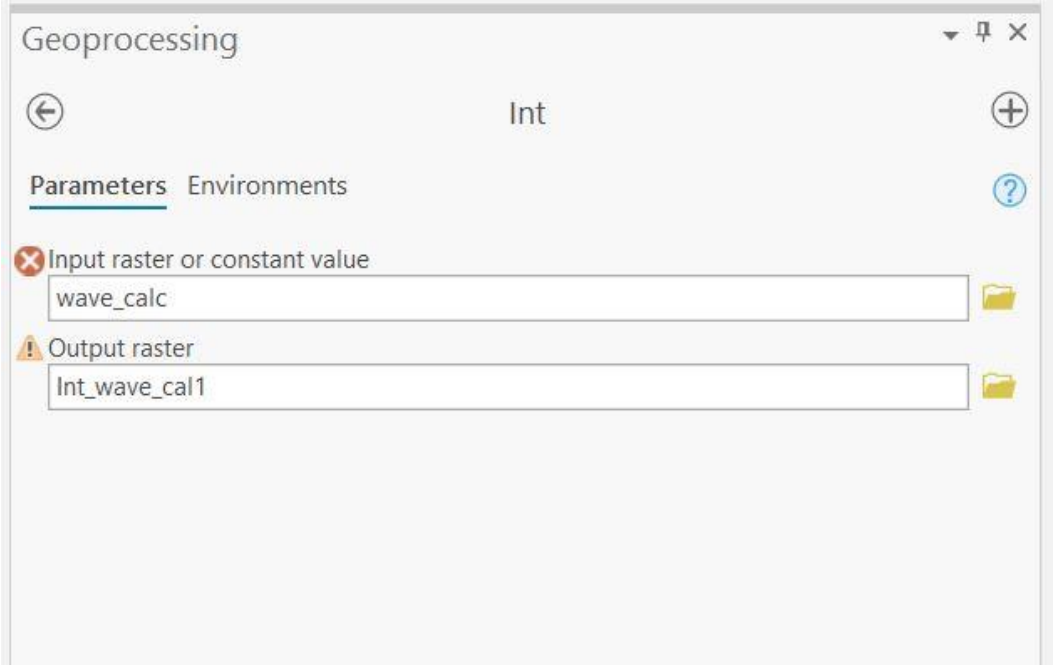



*Figure 3.14 ArcGIS Pro 'Int' tool that is used during the conversion process.*

4.3 The integer type raster is then converted to a polygon using the ‘Raster to Polygon tool.

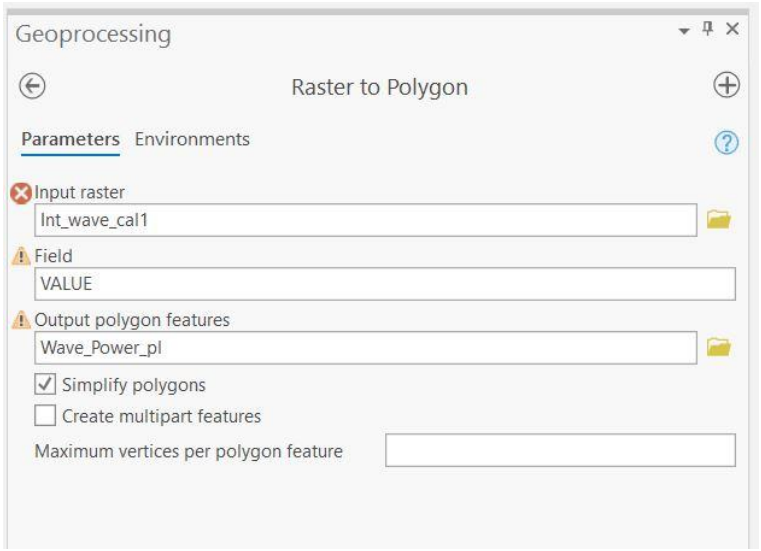



*Figure 3.15 ArcGIS Pro 'Raster to Polygon' tool that is used during the conversion process.*

4.4 The polygon feature class is then divided by 10 in order to get the original decimal values.

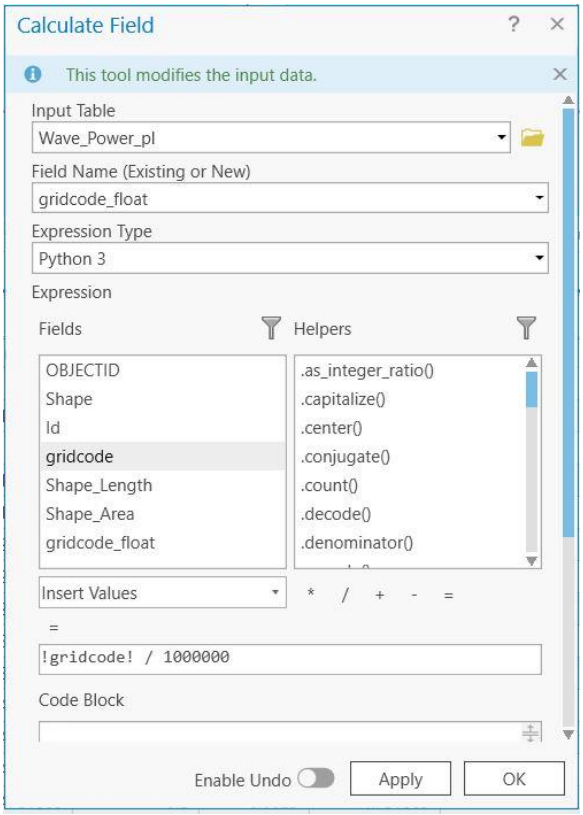



*Figure 3.16 ArcGIS Pro 'Field Calculator' tool that is used during the conversion process.*

## 3.4 Tidal Data

For the modelling of the tidal resource, current data is also available from the Irish Marine Institute ROMS hydrodynamic model (Regional Ocean Modelling System). The model is run at a resolution of 1.9km and parameters such as ocean temperature, salinity and ocean currents are available. The ROMS model that is run by the Marine Institute covers an area which includes the northeast Atlantic and all Irish waters. Surface currents are available at 1 hourly intervals (Marine Institute, 2020). ROMS (Regional Ocean Modelling System) is an open source set of oceanographic models that are used by the scientific community to model 3D ocean parameters. The model is based on the Reynolds-averaged Navier–Stokes equations.

### 3.4.1 Tidal Data Validation

A validation study has been carried out for the data available from the Irish Marine Institute ROMS model and has been published as a scientific paper, the findings of which will be discussed here (Nagy, H. 2020). The study compared the results of the ROMS model data with measured data (tide gauges, satellite data, Argo, CTD temperate and salinity profiles) and evaluated RMSE, correlation coefficient and mean error. The time period used for the validation was 1 January 2016 to 31 December 2019. There are 8 tide gauge stations which are situated around the coast of the republic of Ireland which were used to compare the Sea Surface Height parameter from the model. The results showed that in general the error with the M2 tidal constituent had an error of 0.07 for the stations on the west coast of Ireland, with a slightly higher error of 5% for the M2 amplitude in the Celtic Sea. It was determined that the S2 amplitude had a similar pattern to M2 (Nagy, H. 2020). The results of the comparison of the tidal constituests from the tidal gauges versus the ROMS model data can be seen in Figure 3.17
.

| Tidal Constituent | | Gauge | | NEA_ROMS | |
|---|---|---|---|---|---|
| | | Amp | Phase | Amp | Phase |
| Aranmore | M2 | 1.22 | 161 | 1.29 | 156 |
| | S2 | 0.44 | 194 | 0.46 | 189 |
| | N2 | 0.25 | 139 | 0.26 | 135 |
| | K1 | 0.12 | 154 | 0.14 | 142 |
| | O1 | 0.08 | 359 | 0.08 | 5 |
| | Q1 | 0.03 | 299 | 0.03 | 292 |
| Ballycotton | M2 | 1.42 | 148 | 1.26 | 146 |
| | S2 | 0.44 | 193 | 0.41 | 190 |
| | N2 | 0.26 | 128 | 0.23 | 128 |
| | K1 | 0.02 | 178 | 0.02 | 178 |
| | O1 | 0.03 | 35 | 0.02 | 55 |
| | Q1 | 0.01 | 340 | 0.01 | 348 |
| Ballyglass | M2 | 1.16 | 158 | 1.21 | 152 |
| | S2 | 0.41 | 191 | 0.43 | 185 |
| | N2 | 0.23 | 136 | 0.25 | 131 |
| | K1 | 0.14 | 122 | 0.16 | 116 |
| | O1 | 0.09 | 337 | 0.08 | 342 |
| | Q1 | 0.03 | 277 | 0.03 | 268 |
| Castletownbere | M2 | 1.12 | 131 | 1.09 | 124 |
| | S2 | 0.36 | 161 | 0.36 | 155 |
| | N2 | 0.23 | 108 | 0.22 | 101 |
| | K1 | 0.04 | 50 | 0.05 | 49 |
| | O1 | 0.01 | 279 | 0.02 | 277 |
| | Q1 | <0.01 | 185 | <0.01 | 184 |
| Dunmore East | M2 | 1.38 | 150 | 1.20 | 150 |
| | S2 | 0.45 | 199 | 0.43 | 198 |
| | N2 | 0.25 | 133 | 0.22 | 136 |
| | K1 | 0.04 | 178 | 0.04 | 177 |
| | O1 | 0.04 | 29 | 0.03 | 49 |
| | Q1 | 0.01 | 344 | 0.01 | 341 |
| Galway | M2 | 1.57 | 141 | 1.64 | 137 |
| | S2 | 0.55 | 172 | 0.58 | 170 |
| | N2 | 0.32 | 119 | 0.34 | 117 |
| | K1 | 0.09 | 76 | 0.10 | 79 |
| | O1 | 0.06 | 311 | 0.05 | 311 |
| | Q1 | 0.02 | 261 | 0.02 | 243 |
| Howth | M2 | 1.44 | 325 | 1.39 | 318 |
| | S2 | 0.41 | 357 | 0.41 | 349 |
| | N2 | 0.28 | 297 | 0.28 | 289 |
| | K1 | 0.10 | 198 | 0.11 | 187 |
| | O1 | 0.08 | 37 | 0.07 | 54 |
| | Q1 | 0.03 | 343 | 0.03 | 340 |
| Malin Head | M2 | 1.12 | 178 | 1.19 | 172 |
| | S2 | 0.42 | 206 | 0.44 | 201 |
| | N2 | 0.23 | 156 | 0.26 | 151 |
| | K1 | 0.09 | 167 | 0.11 | 154 |
| | O1 | 0.07 | 7 | 0.07 | 18 |
| | Q1 | 0.03 | 310 | 0.03 | 306 |

*Figure 3.17 The comparison of the tidal constituent data between the tidal gauges and the ROMS model as part of the validation study (Nagy, H. 2020).*

When the data was shared via the Marine Institute for this study it was pointed out that there is also a lack of measured data to use for validation purposes in this area. There is very little validation of model currents because there isn't the measured data available to compare against. The team stated that the fact that the modelled tidal heights compare well with the tide gauge data does give some confidence that the tidal currents should be accurate.

### 3.4.2 Tidal Assessment

The parameters that were analysed as part of this study aim to give a broad understanding to a developer the nature of the tidal currents within the study area as well as the tidal power availability. This data can then be used to better inform the developer as to the optimum location for tidal device site location. The mean tidal flows are then analysed, including spring and neap currents as well as the peak current values (irrespective of neap and spring periods). In order to model the potential tidal energy resource, the tidal current velocity is needed so that the tidal power can be calculated. The tidal current data was downloaded for the study area (see Figure 3.10) from the Irish Marine Institute ROMS model. The parameters that were downloaded were:

- dn: datetime in Matlab datenum format
- lon: longitude of grid points
- lat: latitude of grid points
- uB: matrix of U-component barotropic velocity
- vB: matrix of V-component barotropic velocity
- ssh: sea surface height

The data was downloaded at hourly intervals for a period of 1 year, for the time series 2020-01-01 00:00:00 to 2020-12-30 23:00:00. This data was then used in MATLAB to create a series of output layers that will be converted into GIS layers for the tidal analysis.

#### 3.4.2.1 Tidal Current Analysis

A thorough understanding of the currents at a tidal site is very important for developers as it informs them of times when power will be at its peak and when current speeds are conducive to device maintenance. The mean peak current velocity (m/s) and the maximum peak current velocity (m/s) layers were modelled in order to understand the tidal conditions irrespective of spring or neap cycles. For the mean peak current layer, the current peak velocities were selected for each time step and a mean was calculated. For the maximum peak current velocity, the maximum value across the whole time series was taken. These values are important for developers to understand the general current speeds at a site, with most tidal devices needing current speeds >2 m/s in order to produce energy. To better understand the tidal currents,

analysis was undertaken to separate the spring current values from the neap current values. To do this, a script was created in MATLAB which isolated all of the maximum values for each tidal cycle for each grid point and these values were then separated into spring and neap cycles . Having these cycles separated will enable further analysis to be completed to better understand the spatial pattern of the spring and neap cycle currents within GIS. Eight layers were created in total to better understand the tidal current cycles, four layers for the spring cycle and four layers for the neap cycle; Maximum Spring/Neap Peak Current Velocity (m/s), Mean Spring/Neap Peak Current Velocity (m/s), Total Spring/Neap Energy (MWh) and Mean Spring/Neap Tidal Power ($W/m^2$). In order to calculate the mean spring current velocity, the spring current cycles were separated for the duration of the time series and each of the velocities during the cycle was summed to get an average in m/s. The same process was repeated for the neap cycle.

#### 3.4.2.2 Tidal Power Analysis

The velocity was used to calculate the tidal energy resource using the tidal power equation which was defined in section 2.2.1 using the software application MATLAB. In total, six layers have been created to analyse the tidal power for the study area: Total Energy (MWh), Mean Tidal Power ($W/m^2$), Total Spring/Neap Energy (MWh) and Mean Spring/Neap Tidal Power ($W/m^2$) (which have been discussed in section 3.3.1). The mean tidal power was generated by calculating the tidal power at each grid point for each time step and then calculating the mean of those values over the time series to give the result in $W/m^2$. The total energy was created by calculating the tidal power at each grid point for each time step and then there was a summation of those values for the year which gives total energy in MWh. The spring cycle current values were used to calculate the Mean Spring Tidal Power, where the tidal power was calculated for each grid point using current values from each of the spring current cycles throughout the time series, and then a mean was obtained (the same process was carried out for the neap cycle to create the Mean Neap Tidal Power layer). The spring cycle current values were also used to calculate the Total Spring Energy in MWh, where the tidal power was calculated using current values from each of the spring current cycles throughout the time series, and an annual total was obtained (the same process was carried out for the neap cycle to create the Total Neap Energy (MWh) layer).

While the modelling for the wave energy layers was computationally time-consuming due to the large datasets, the tidal datasets were much smaller due to the time series only being 1 year as opposed to 20 years. This means that just one layer was created for the whole study area in MATLAB, which was then exported to GeoTIFF in order to import the data to GIS. Once the GeoTIFF was imported, steps 4.1 – 4.4 in section 3.2 were used to create the tidal GIS raster and polygon layers.

The list of tidal layers that have been created as part of this study can be seen in Appendix 3.

The GIS layers that have been created as part of this study will be added to a Web-GIS tool that is being developed as part of SELKIE WP4. In order for the end user to be able to rely on the datasets and have a thorough understanding of the methodology used and the source of the base data, thorough information has been added to the metadata of the layers. Information that has been added to the metadata of the layers includes the model that was used for the calculations (ie, the IBI/NWS/ROMS models), the hindcast that was used, the parameters that the layer is displaying and the units, the creators of the dataset and links to further information.

# 4 Results

## 4.1 Wave Results

In this section, the results of the wave power modelling are discussed. A comparison of the results is made between both the IBI and NWS models. For both models, the mean wave power resource was calculated, along with seasonal modelling of the wave power resource, the significant wave height, and the wave energy period. A number of sites have been chosen for a comparison study and these will be discussed in more detail below.

### 4.1.1 Wave Power Resource Analysis

Statistical analysis of the datasets was carried out in order to understand the correlation between the results of both models. The results of this analysis can be seen in the scatter plot in Figure 4.1.

There is a very good correlation between the mean wave power layers for the IBI and NWS model, with an $R^2$ of 0.99 for the dataset. The scatter plot with the results in Figure 4.1 displays the strong correlation between both datasets, with no outliers in the dataset. This strong correlation gives the user good confidence in the results of both models.

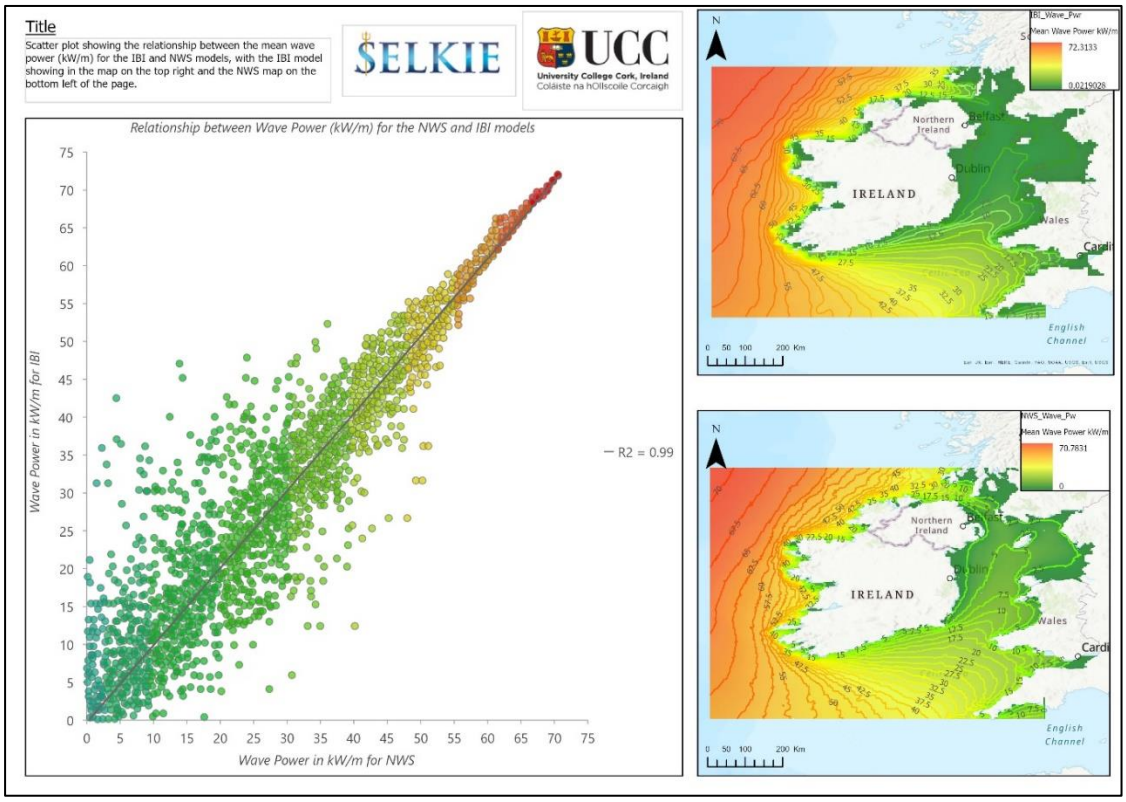



*Figure 4.1 Scatter plot showing the relationship between the mean wave power (kW/m) for the IBI and NWS models, with the IBI model showing in the map on the top right and the NWS map on the bottom left of the page.*

The mean wave power resource was calculated using the 20 year hindcast of data from both the IBI and NWS models. The results from the IBI model can be seen below in Figure 4.2 and the results from the NWS model can be seen in Figure 4.3. Both models show a similar spatial trend with the resource being greatest off the northwest coast of Ireland, and high values seen off the west and southwest coasts of Ireland also. The resource can be seen to reduce in size with the proximity to land in all areas as a result of coastal process due to wave breaking. Another factor that may have had an influence on the result in coastal regions is the grid spacing that has been used, as the larger grid spacing may not have picked up the rapid depth changes closer to the shore which will have an impact on the power result that is obtained. Five comparison points have been chosen throughout the study area and can be seen in Figure 4.2, the results of the points are in Table 4.1. The validation studies of both the IBI and NWS models have shown that the models are less efficient in coastal areas. This variability due to the grid spacing can be seen in comparison point 1 where the point is <2km from the coastline and there is 13.25% in the difference between the results of both models. Comparison point 3 which is located off the west coast of Wales shows a percentage difference of 14.21% between the two models. This point is also located in a very coastal area, where it likely to be affected by poorer reliability in the model data. The models are seen to correlate very well at the remaining three points which are located in deeper water, with differences of 1.64% for point 2, 3.81% for point 4 and 2.01% for the Celtic Sea. A reduction in power can be seen moving along the Celtic Sea northwards into the Irish Sea. Power values off the west coast of Ireland tend to be between 50-72 kW/m, with power values in the Irish Sea being less than 10 kW/m.

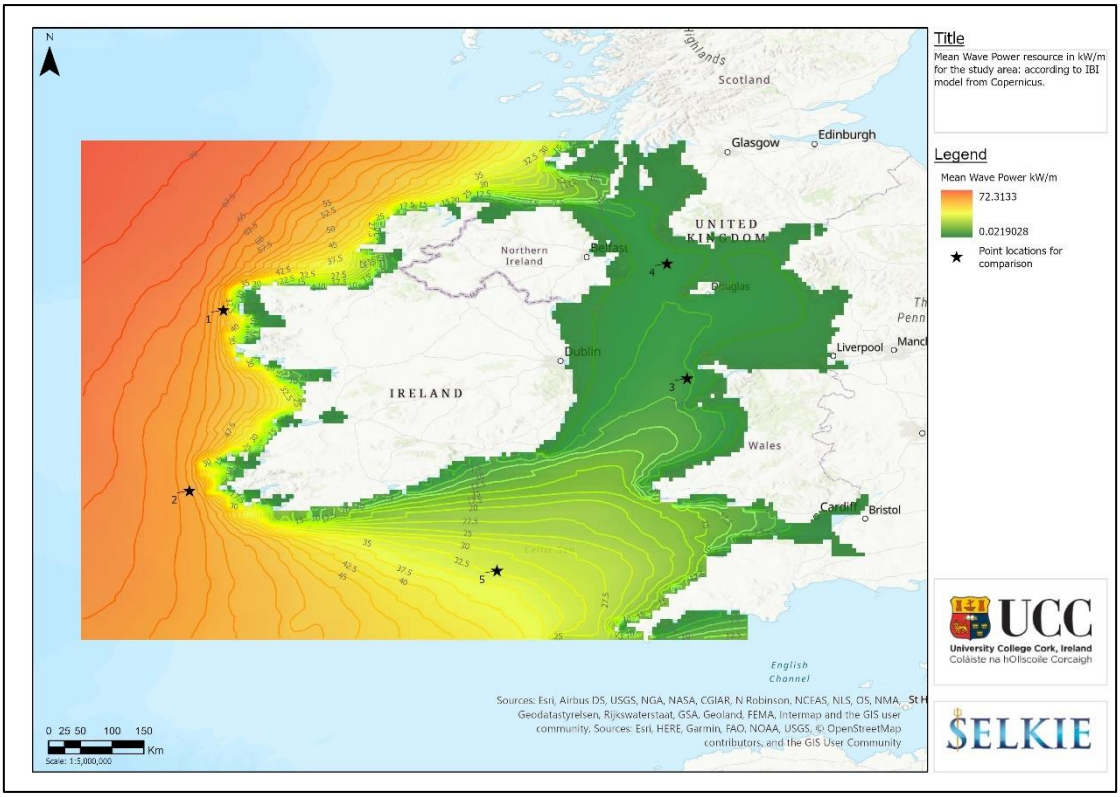



*Figure 4.2 Mean wave power resource in kW/m for the study area, calculated using the 20 year hindcast data from the Copernicus IBI model.*

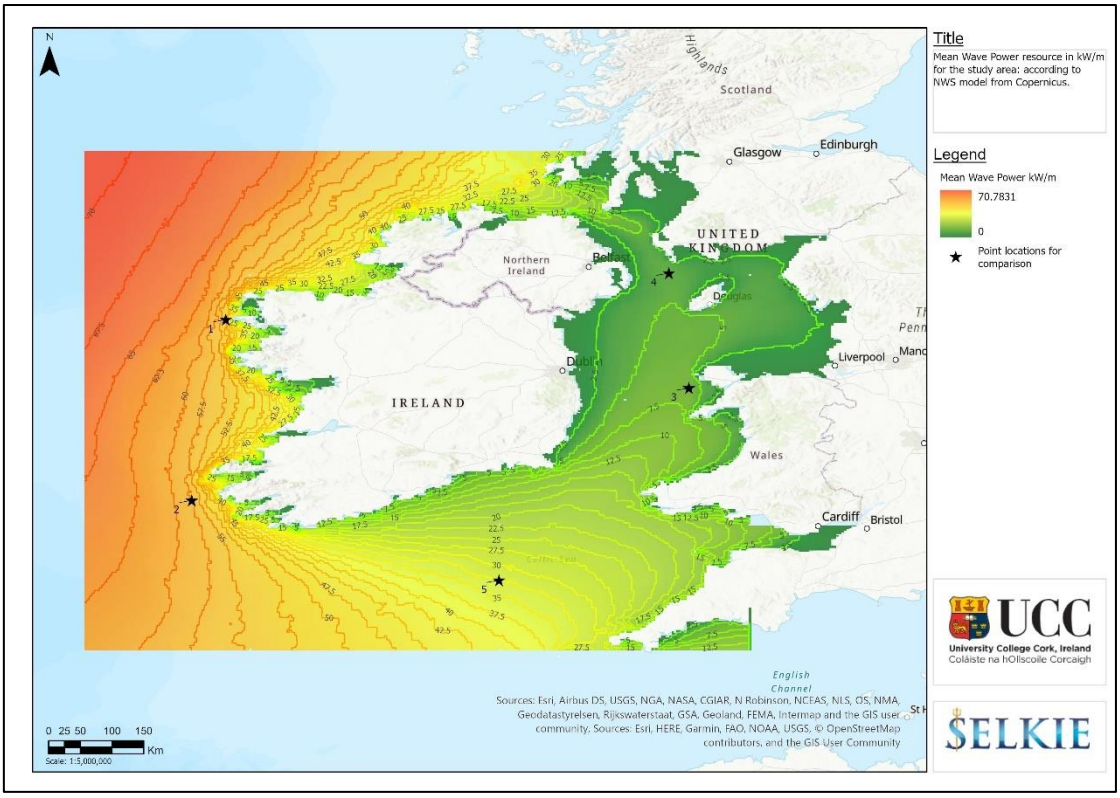



*Figure 4.3 Mean wave power resource in kW/m for the study area, calculated using the 20 year hindcast data from the Copernicus NWS model.*

| Location | IBI – Mean Wave Power kW/m | NWS– Mean Wave Power kW/m | % Difference between models |
|---|---|---|---|
| 1 - West coast of Ireland | 47.86 kW/m | 54.21 kW/m | 13.25% |
| 2 - Southwest coast of Ireland | 58.36 kW/m | 57.42 kW/m | 1.64% |
| 3 - West coast of Wales | 5.91 kW/m | 6.75 kW/m | 14.21% |
| 4 - Northwest of Isle of Man | 4.46 kW/m | 4.63 kW/m | 3.81% |
| 5 - Celtic Sea | 32.0 kW/m | 32.65 kW/m | 2.01% |

*Table 4.1 Comparison table between IBI mean wave power (kW/m) and NWS mean wave power (kW/m) for the 5 points that have been selected.*

### 4.1.2 Seasonal Analysis of the Wave Parameters

Seasonal analysis was carried out for significant wave height and wave energy period, as well as for the mean wave power. This section looks at the results that were obtained from both the IBI and NWS models for the seasonal significant wave heights as well as the seasonal wave periods.

#### *4.1.2.1 Seasonal Significant Wave Height Analysis*

Statistical analysis has also been carried out for the seasonal significant wave height (m) layers in order to better understand the correlation between the models (IBI and NWS) before analysing the results.

The scatter plot of all points for IBI and NWS for the winter months can be seen in Fig 4.4. The scatter plot shows strong correlation between both datasets for the winter months, with an $R^2$ value of 0.99. This strong correlation between the significant wave heights for both models gives the user increased confidence in the layers that have been created as part of this study.

This statistical analysis has also been carried out for the seasons of spring, summer and autumn and the figures can be seen in Appendix 2. The results for the remaining seasons reflect what has been seen for the winter datasets, with strong positive correlation between both models for each of the spring, summer, and autumn datasets. There is a 0.98 $R^2$ correlation value the summer months, there is a 0.99 $R^2$ value for the autumn months and a 0.99 $R^2$ value showing

correlation between the IBI and NWS datasets for spring. These values show that there is a strong correlation between the results from both the IBI and NW models, which corroborates the strong correlation between the two models for the seasonal significant wave heights from the validation studies.

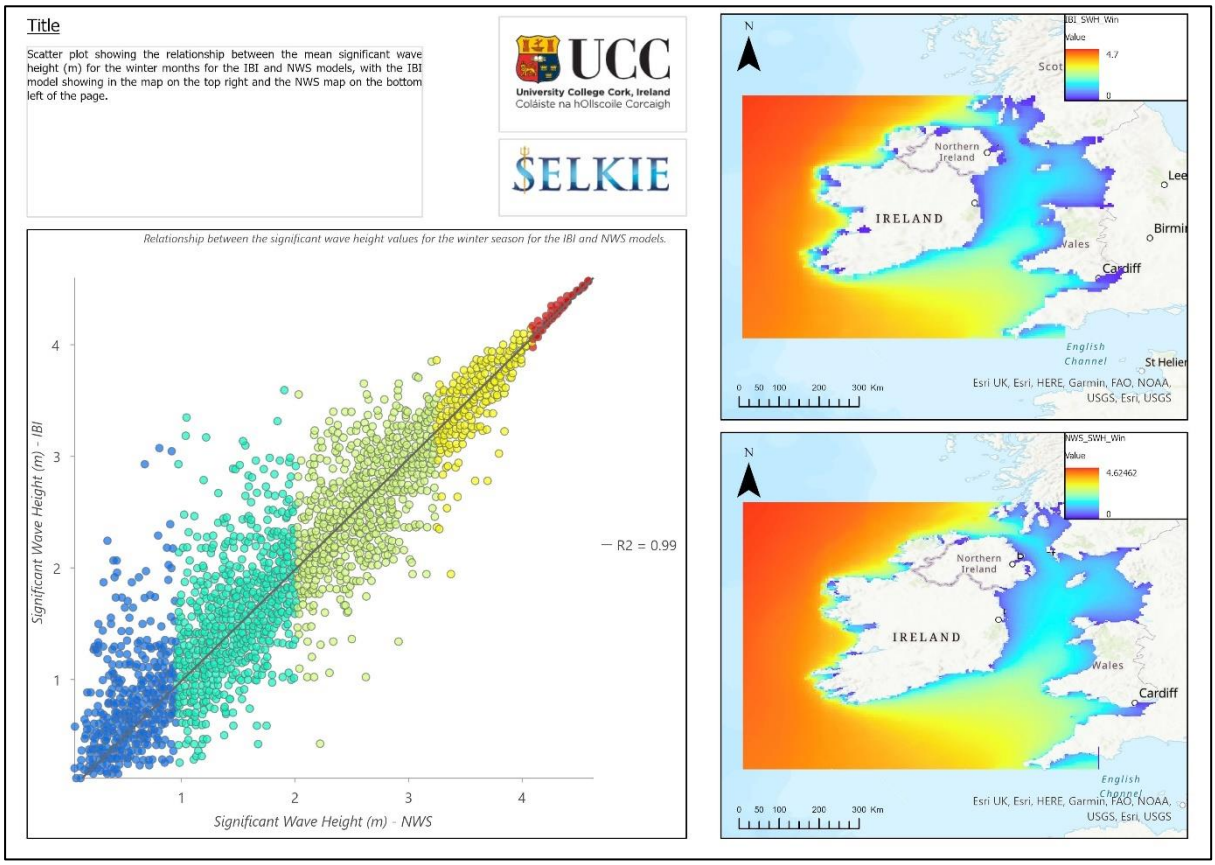



*Figure 4.4 Seasonal statistical analysis for the winter datasets for IBI and NWS.*

The seasonal significant wave heights for the IBI model can be seen below in Figure 4.5. The largest significant wave heights can be seen during winter, with values of ~4.5m seen off the west coast of Ireland and values of ~2.5m in the Celtic Sea to the west of Pembrokeshire. The wave height values tend to decrease with proximity to the coast, which is most likely as a result of the waves breaking with proximity to the shoreline. Values of ~1.5m can be seen southwest of the Isle of Man in the Irish Sea for winter. In comparison, the seasonal significant wave heights for the NWS model can be seen below in Figure 4.6. The seasonal modelling of the significant wave heights using the data from the NWS model is consistent with the results received from the IBI model. The largest values can be seen in the winter months with a maximum value of 4.7m seen off the west coast of Ireland. The spatial variability of the significant wave heights follows the same pattern as the data from the IBI model, with highest values in the NW of Ireland, decreasing south into the Celtic Sea and lowest values in the Irish

Sea. The significant wave height values from the NWS model for autumn follow a similar trend to the winter season, with the largest values seen off the NW coast of Ireland (~3.5m), slightly lower values are seen off the SW coast (~4.0m) and the lowest values are seen in the Irish Sea (< 1.5m). The significant wave heights observed in spring are only marginally lower than those in autumn for most areas, with values of ~3.0m seen off the NW coast of Ireland and the lowest values are seen in the Irish sea with ~1.0m. A difference in the spatial pattern of the significant wave heights can be seen between autumn and spring, with larger significant wave heights occurring off the northwest to west coasts of Ireland in the deeper Atlantic (>50km off the coast) for the spring months. A good correlation can be seen with the results from the NWS model, with values from spring and autumn being analogous. The significant wave heights observed in summer are the lowest of all seasons, with values not exceeding 2.1m for the whole study area. As per the spatial pattern seen for the other seasons, the largest wave heights are seen off the west coast of Ireland for the summer months, with the lowest values of ~0.5m seen in the Irish Sea.

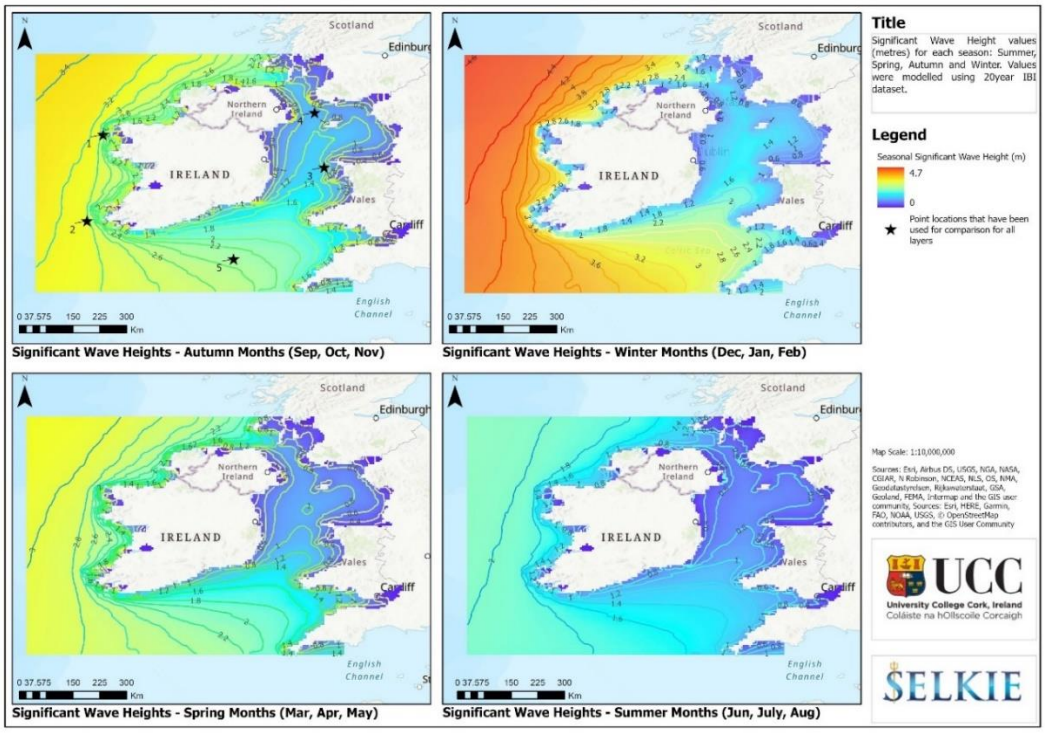



*Figure 4.5 Significant wave heights (m) for each season: summer, spring, autumn and winter. Values were modelled using 20 year IBI dataset.*

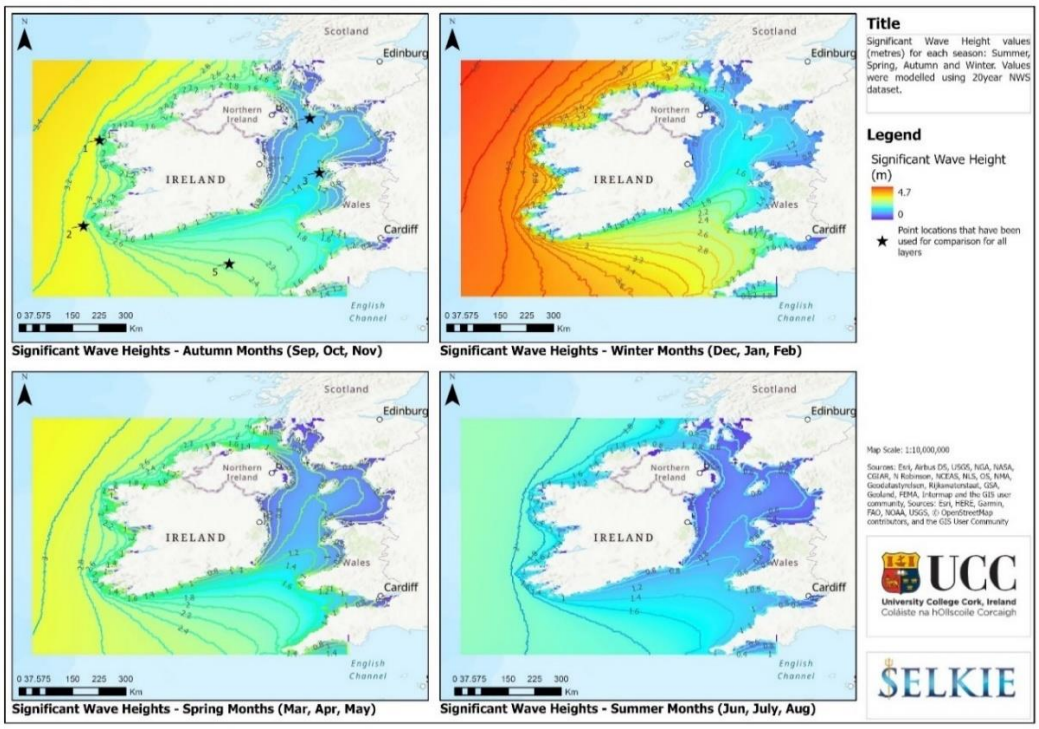



*Figure 4.6 Significant Wave Heights(m) for each season: summer, spring, autumn and winter. Values were modelled using 20-year NWS dataset.*

A comparison of the significant wave heights for the five points that have been selected can be seen in Figure 4.2 and 4.3 for both the IBI and NWS models. The largest difference seen is for point 1 located off the west coast of Ireland, with a mean of 7.92% difference seen between the two models across the four seasons. Following this is point three off the west coast of Wales in the Celtic Sea, with a mean percentage difference of 6.97%. These two points are located in coastal regions which are more likely to be affected by coastal process and inefficiencies in the models as presented in the validation studies. The three remaining points correlate very well, with the two models showing a percentage difference of 1.82% (point 2), 4.26% (point 4) and 3.42% (point5). The largest percentage difference between the values obtained for the two models is for point 1 for the spring months, with 12.03% difference seen between the two

models, which is followed closely by 11.11% difference in the two models for the autumn months.

| Location | NWS Significant Wave Height (m) - Winter | IBI Significant Wave Height (m) - Winter | % Difference Winter | NWS Significant Wave Height (m) - Summer | IBI Significant Wave Height (m) - Summer | % Difference Summer |
|---|---|---|---|---|---|---|
| 1 | 3.94m | 3.65m | 7.94% | 1.69m | 1.68m | 0.59% |
| 2 | 4.10m | 4.08m | 0.49% | 2.01m | 1.92m | 4.69% |
| 3 | 1.58m | 1.47m | 7.48% | 0.80m | 0.76m | 5.26% |
| 4 | 1.39m | 1.34m | 3.73% | 0.72m | 0.69m | 4.35% |
| 5 | 3.16m | 3.11m | 1.60% | 1.64m | 1.54m | 6.49% |

*Table 4.2 Comparison table showing the mean significant wave heights for winter and summer from the IBI model and the NWS model for the 5 comparison points.*

| Location | NWS Significant Wave Height (m) - Spring | IBI Significant Wave Height (m) - Spring | % Difference Spring | NWS Significant Wave Height (m) - Autumn | IBI Significant Wave Height (m) - Autumn | % Difference Autumns | Mean % Difference for all seasons |
|---|---|---|---|---|---|---|---|
| 1 | 2.70m | 2.41m | 12.03% | 3.00m | 2.70m | 11.11% | 7.92% |
| 2 | 2.80m | 2.76m | 1.45% | 3.08m | 3.06m | 0.65% | 1.82% |
| 3 | 1.00m | 0.93m | 7.52% | 1.27m | 1.18m | 7.63% | 6.97% |
| 4 | 0.93m | 0.89m | 4.49% | 1.17m | 1.12m | 4.46% | 4.26% |
| 5 | 2.13m | 2.06m | 3.40% | 2.33m | 2.28m | 2.19% | 3.42% |

*Table 4.3 Comparison table showing the mean significant wave heights for spring and autumn from the IBI model and the NWS model for the 5 comparison points.*

#### *4.1.2.2 Seasonal Wave Period Analysis*

Statistical analysis of the wave period datasets has been carried out in line with what was completed for the wave power and the significant wave heights. The results showed that for the seasonal wave periods there were outliers in these datasets based on the Z-scores that were calculated (Figure 4.7). The outliers were identified to be any point that had a z-score of +-3, and these were subsequently removed from the dataset. The z-score is a number that shows the relationship of a value to the mean of the dataset in terms of standard deviations. If a z-score is 0 then it is equal to the mean, if it is 3 or greater then it is ≥ 3 standard deviations from the mean (Investopedia, 222). The figure below shows the results of the analysis for the spring dataset, showing the mean and standard deviations for both the IBI and NWS models, as well as the $R^2$ value for both which was 0.96. The scatter plot and the map have identified the outlier points in blue, and it's shown in the map that the points are all lying in coastal areas. This result

coincides with the validation studies that have been carried out, where it was concluded that the model tended to be less accurate in coastal areas. One notable point is that the outliers are located within bays and not at all coastal locations, possibly showing that the models are least accurate within these areas.

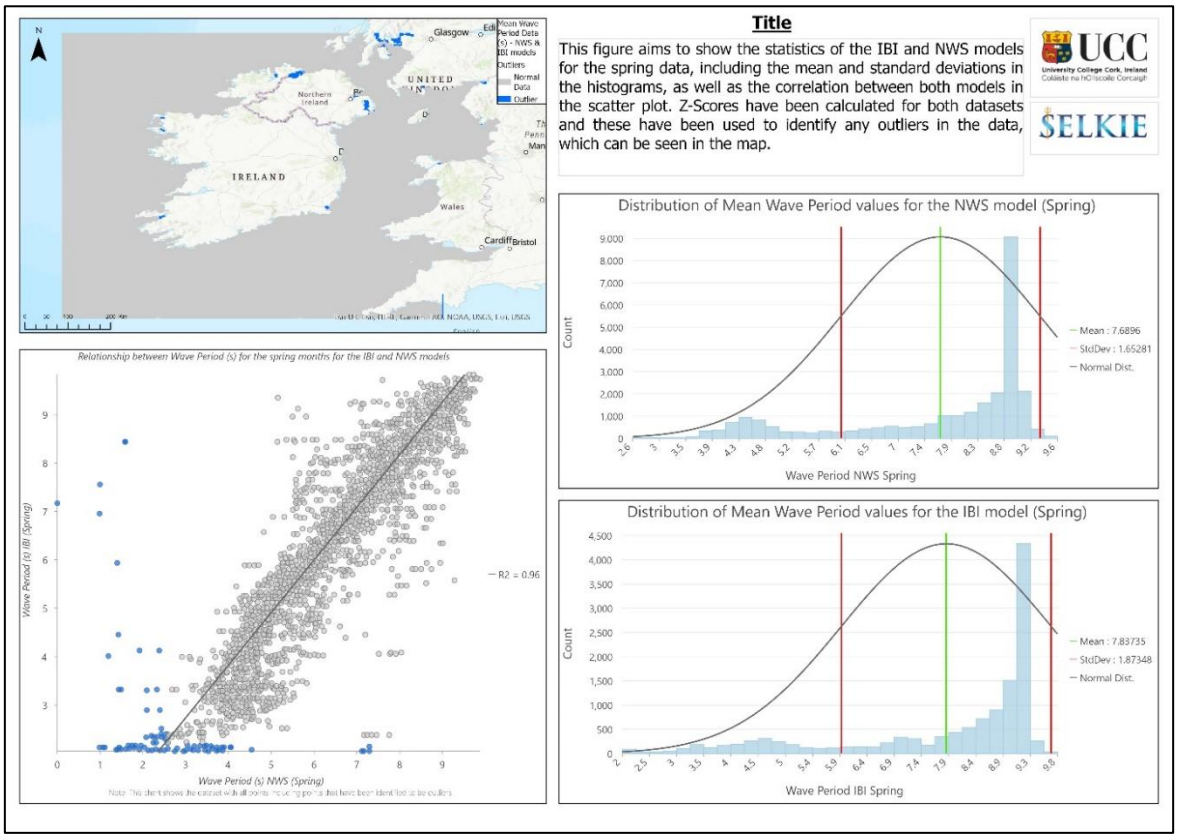



*Figure 4.7 Statistical analysis of the spring wave periods for both the IBI and NWS models.*

An important point to note based on this analysis is the locations where wave devices are likely to be located do not coincide with these areas where the outlier points are seen, which means that the models are still very useful for modelling of wave power resource for energy devices.

Once the outlier points were removed from the dataset the $R^2$ value increased to 0.97 (Figure 4.8), showing that the correlation between both datasets increased with the outlier points removed. This detailed analysis has been carried out for each season and the figures can be seen in Appendix 2. The results for the winter, spring and summer seasons were reflective of what was seen for spring, with the outliers in the datasets located in coastal regions, and once these were removed the $R^2$ values increased. Correlation between the IBI and NWS models for the wave periods is generally positive, which agrees with the validation studies that have been

referenced as part of this study. This statistical analysis has shown for the study area the IBI and NWS models correlate very well for wave periods.

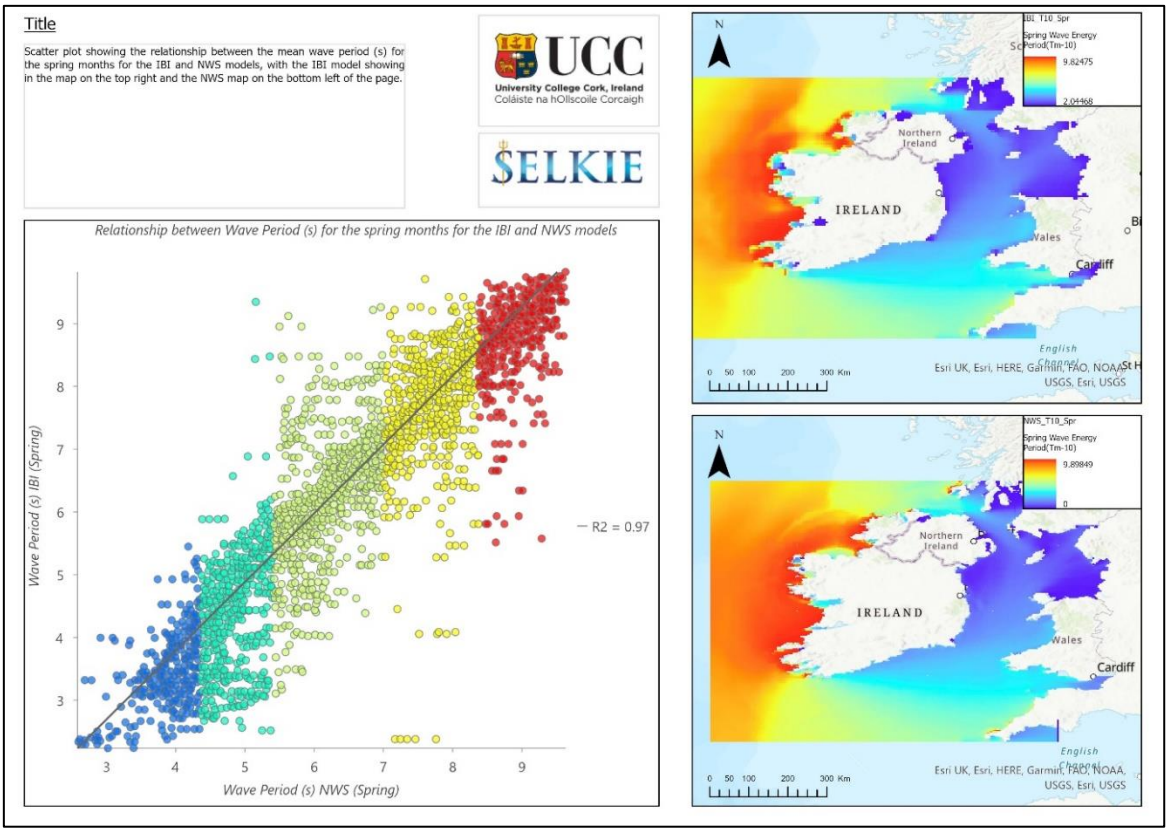



*Figure 4.8 Scatter diagram showing R sqared value for IBI and NWS data for wave periods for spring once outlier points have been removed.*

The seasonal wave energy periods ($T_e$) from the IBI model can be seen below in Figure 4.9 and the NWS model can be seen in Figure 4.10. The general spatial pattern for the wave period follows the same trend as the significant wave heights and the mean wave power, with the largest values encountered off the northwest coast of Ireland, decreasing south/southwest into the Celtic Sea and then the lowest values are encountered in the Irish Sea. The values can be seen to decrease with proximity to the coast in all locations, although this reduction is not as significant as what is seen with the significant wave heights. The greatest spatial variability across the seasons can be seen off the west coast of Ireland in the Atlantic Ocean, where different patterns can be seen for the wave period for each season. The values encountered for the winter months range from 11.5 – 2.1 seconds. The $T_e$ values for winter off the NW coast of Ireland are ~10.5s, values of ~7.0-9.0s are seen in the Celtic Sea and <5.0s in the Irish Sea. The seasons of autumn and spring are very similar, with a maximum value of 10.0s for autumn and 9.8s for spring from the IBI model. For the summer months, the lowest values for the spectral wave periods are seen, with the highest values being 7.8s for the study area.

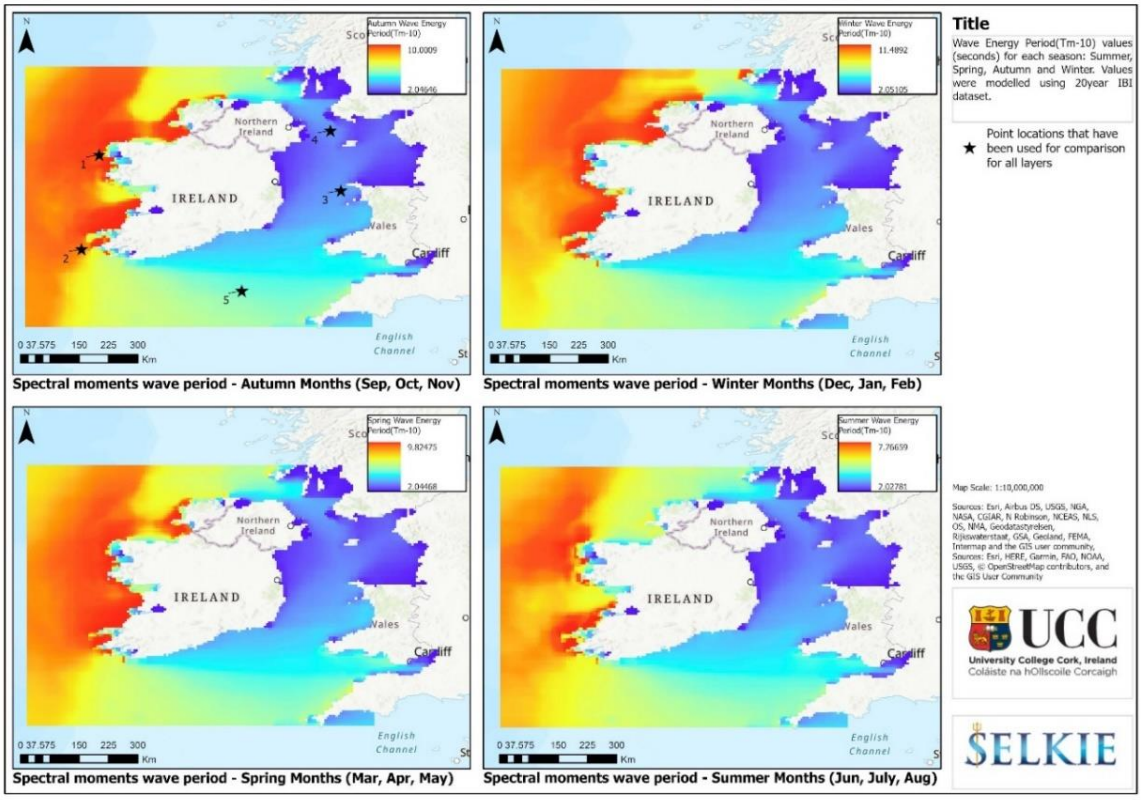



*Figure 4.9 Mean Wave Energy Period (s) for each season: summer, spring, autumn and Winter. Values were modelled using 20-year IBI dataset.*

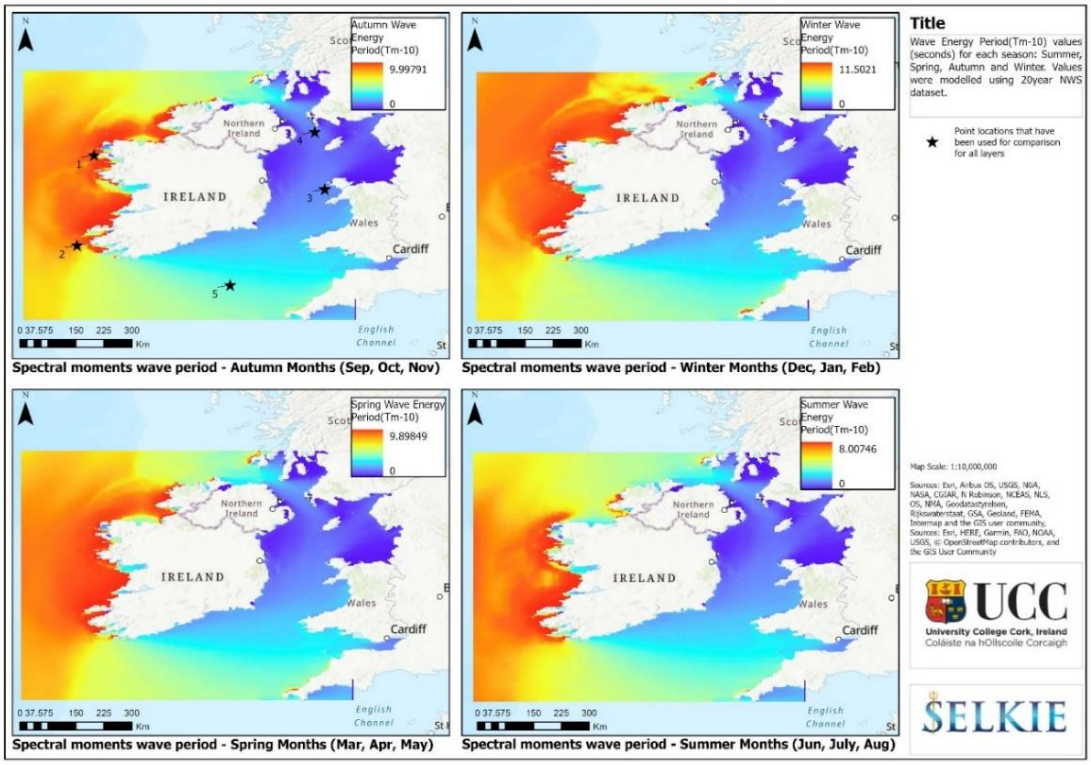



*Figure 4.10 Mean Wave Energy Period (s) for each season: summer, spring, autumn and winter. Values were modelled using 20-year NWS dataset.*

The results of the comparison between the five points across the study area can be seen in Table 4.4 and Table 4.5.

| Location | NWS– Wave Period Winter (s) | IBI – Wave Period Winter (s) | % Difference Winter | NWS– Wave Period Summer (s) | IBI – Wave Period Summer (s) | % Difference Summer |
|---|---|---|---|---|---|---|
| 1 | 10.23s | 10.71s | 4.69% | 7.59s | 7.63s | 0.53% |
| 2 | 10.04s | 10.40s | 3.59% | 7.58s | 7.62s | 0.53% |
| 3 | 6.40s | 6.45s | 0.78% | 5.08s | 5.55s | 9.25% |
| 4 | 5.53s | 5.77s | 4.34% | 4.60s | 4.71s | 2.39% |
| 5 | 9.23s | 9.54s | 3.36% | 7.07s | 7.06s | 0.14% |

*Table 4.4 Comparison table showing the mean wave energy periods (Te) for winter and summer from the IBI and NWS models for the 5 comparison points.*

| Location | NWS– Wave Period Spring (s) | IBI – Wave Period Spring (s) | % Difference Spring | NWS– Wave Period Autumn (s) | IBI – Wave Period Autumn(s) | % Difference Autumn | Mean % Difference between four seasons |
|---|---|---|---|---|---|---|---|
| 1 | 9.04s | 9.38s | 3.76% | 9.04s | 9.41s | 4.09% | 3.27% |
| 2 | 8.97s | 9.22s | 2.79% | 9.00s | 9.30s | 3.33% | 2.56% |
| 3 | 5.74s | 6.04s | 5.23% | 5.64s | 5.89s | 4.32% | 4.89% |
| 4 | 5.09s | 5.28s | 3.73% | 5.19s | 5.41s | 4.24% | 3.68% |
| 5 | 8.18s | 8.37s | 2.32% | 7.99s | 8.26s | 3.38% | 2.30% |

*Table 4.5 Comparison table showing the mean wave energy periods (Te) for spring and autumn from the IBI and NWS models for the 5 comparison points.*

The largest difference between the two models is seen for point 3 which is located off the west coast of Wales, with a mean of 4.89% difference across the four seasons. Similarly, to the differences seen for the significant wave heights and the wave power layers, the percentage differences are lowest for points 2, 4 and 5 which are located in areas of deeper water where the models are known to be more accurate.

### *4.1.2.3 Seasonal Analysis of the Wave Resource*

Statistical analysis of the seasonal wave power resource has been broadly in agreement with the seasonal wave parameter results, as well as with the mean theoretical wave power resource results. The correlation seen between the IBI and NWS models for the winter months is 0.99, which is in agreement with the results of the significant wave heights, the wave periods and also for the overall wave resource. The results from the correlation study for spring, autumn and summer can be seen in Appendix 2.

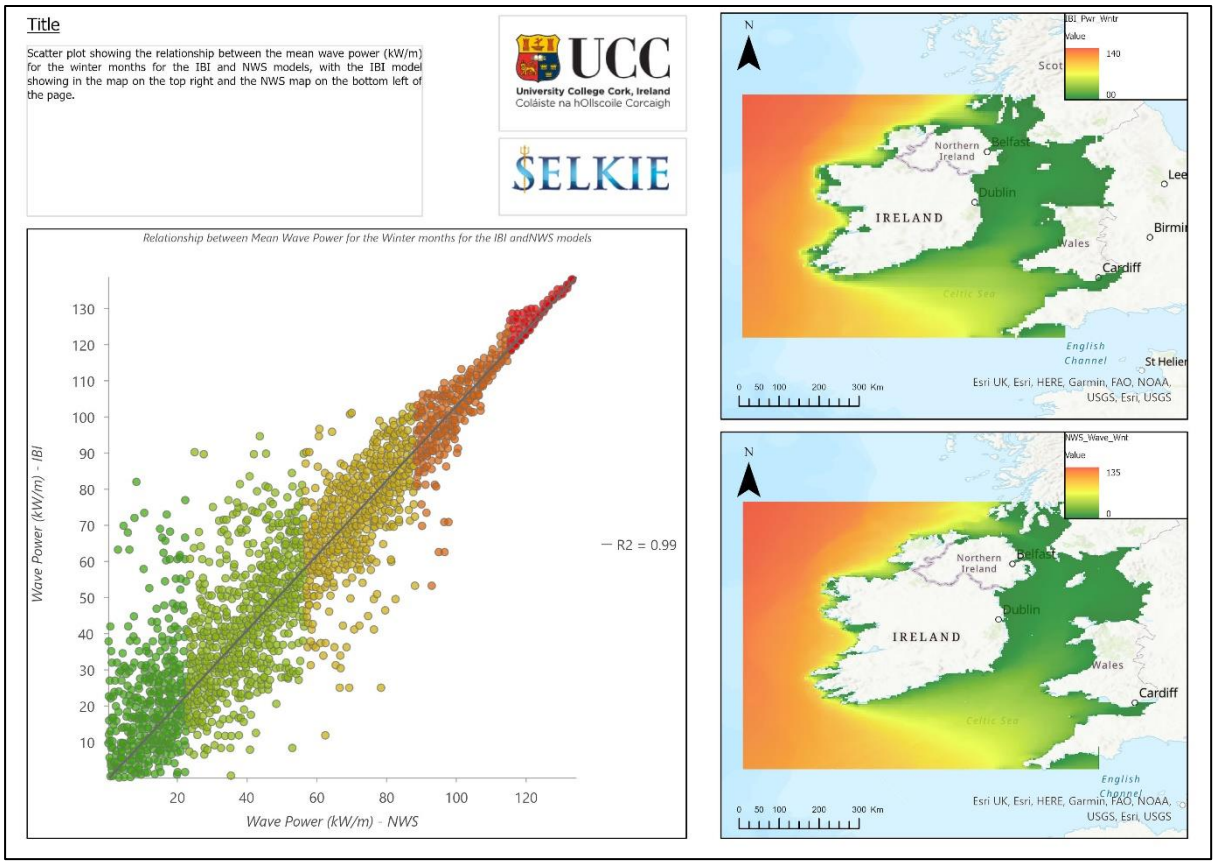



*Figure 4.11 Scatter diagram showing R squared value for IBI and NWS data for wave power for the winter layers.*

The seasonal mean wave power resource can be seen below for the IBI model in Figure 4.12 and for the NWS model in Figure 4.13. The results of the comparison between the five points across the study area can be seen in Table 4.6 and 4.7. For the results from the IBI model, the resource is seen to be most abundant in the winter months of December, January, and February, with maximum values of 140 kW/m observed off the northwest coast of Ireland, and values of approximately 30 kW/m observed in the Celtic Sea. The resource values modelled in both spring and autumn are very similar, with values of 50-70 kW/m seen off the west coast of Ireland, with the same trend persisting of the highest values presenting in the northwest of Ireland. The summer layer shows the lowest wave power resource, with the highest value of

21 kW/m seen of the NW coast of Ireland and values in the Irish and Celtic Seas not exceeding 10 kW/m. Unsurprisingly, the greatest variability can be seen between the seasons of winter and summer, with a variance of ~100 kW/m seen off the NW coast of Ireland. The same spatial pattern can be seen with the NWS model results for the seasonal analysis of the mean wave resource, with the largest values seen off the NW coast of Ireland, decreasing to the south into the Celtic Sea and the lowest values tend to be observed in the Irish Sea for all seasons. The season of winter shows the largest values for the power, with the highest values for the study area being 134kW/m. In comparison to the values seen for the winter months from the IBI data, this maximum value is 6 kW/m lower.

Based on the five points that have been chosen for the comparison study, the largest difference can be seen at point location 1 off the west coast of Ireland, with a mean difference across the four seasons of 17.31%. Following this point 3 off the west coast of Wales shows a mean difference of 13.07% between the two models across the four seasons. As with the analysis of the seasonal significant wave heights and the wave periods, these two points are reflective of areas that are close to the coast, where the models have been proven to be less efficient and where they effects of wave breaking and changes in bathymetry are more likely to effect results. The results between the IBI and NWS models are seen to be more accurate for the three points that are located in deeper waters (2, 4 and 5), with mean differences of 3.30%, 5.45% and 4.12% respectively.

| Location | NWS -Wave power resource Winter – kW/m | IBI - Wave power resource Winter – kW/m | % Difference Winter | NWS - Wave power resource Summer – kW/m | IBI - Wave power resource Summer – kW/m | % Difference Summer |
|---|---|---|---|---|---|---|
| 1 | 102.76 | 94.65 | 8.57% | 18.06 | 13.95 | 29.46% |
| 2 | 108.97 | 112.32 | 3.07% | 19.04 | 17.81 | 6.91% |
| 3 | 12.26 | 10.70 | 14.58% | 2.66 | 2.37 | 12.23% |
| 4 | 7.91 | 7.77 | 1.80% | 1.86 | 1.70 | 9.41% |
| 5 | 62.01 | 62.01 | 0.00% | 12.45 | 11.17 | 11.45% |

*Table 4.6 Comparison table showing the mean wave power resource (kW/m) for winter and summer from the IBI and NWS models for the 5 comparison points.*

| Location | NWS - Wave power resource Spring – kW/m | IBI - Wave power resource Spring – kW/m | % Difference Spring | NWS - Wave power resource Autumn | IBI - Wave power resource Autumn | % Difference Autumn |
|---|---|---|---|---|---|---|
| 1 | 44.36 | 38.12 | 16.37% | 39.70 | 45.60 | 14.86% |
| 2 | 47.00 | 47.42 | 0.89% | 55.63 | 56.92 | 2.32% |
| 3 | 4.78 | 4.12 | 16.02% | 7.17 | 6.55 | 9.47% |
| 4 | 3.47 | 3.24 | 7.10% | 5.37 | 5.19 | 3.47% |
| 5 | 26.02 | 24.92 | 4.41% | 30.67 | 30.48 | 0.62% |

*Table 4.7 Comparison table showing the mean wave power resource (kW/m) for spring and autumn from the IBI and NWS models for the 5 comparison points.*

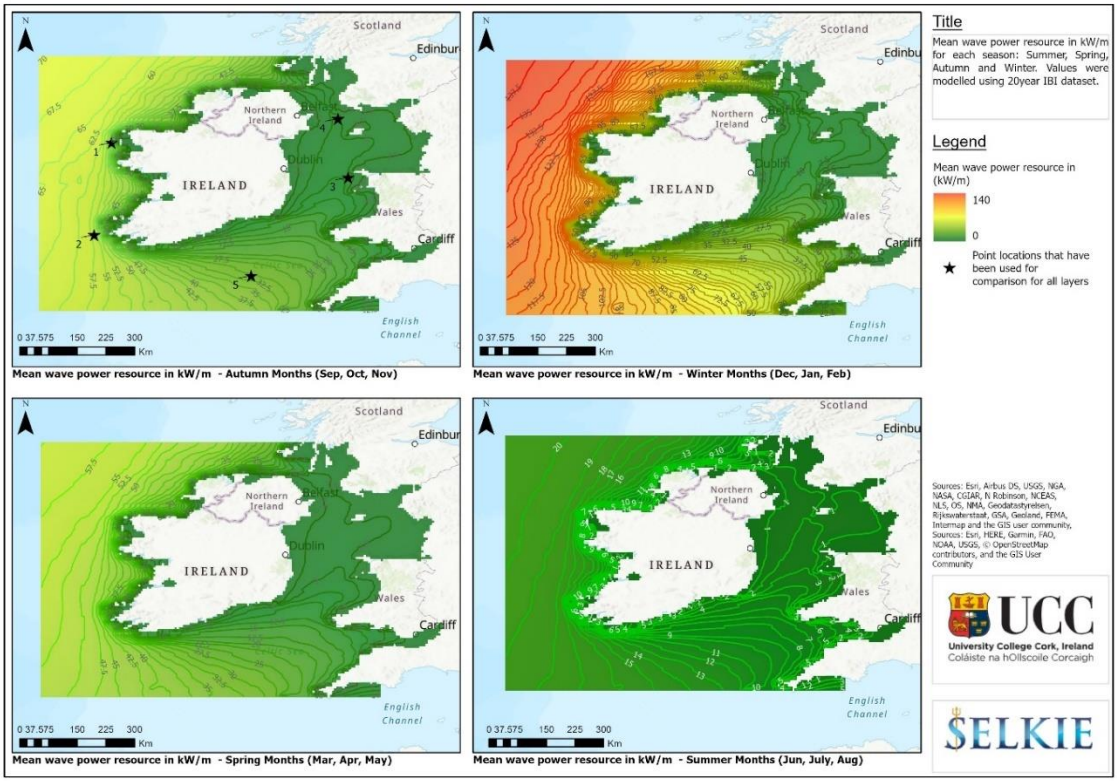



*Figure 4.12 Mean wave power resource in kW/m for each season: summer, spring, autumn and Winter. Values were modelled using 20 year IBI dataset.*

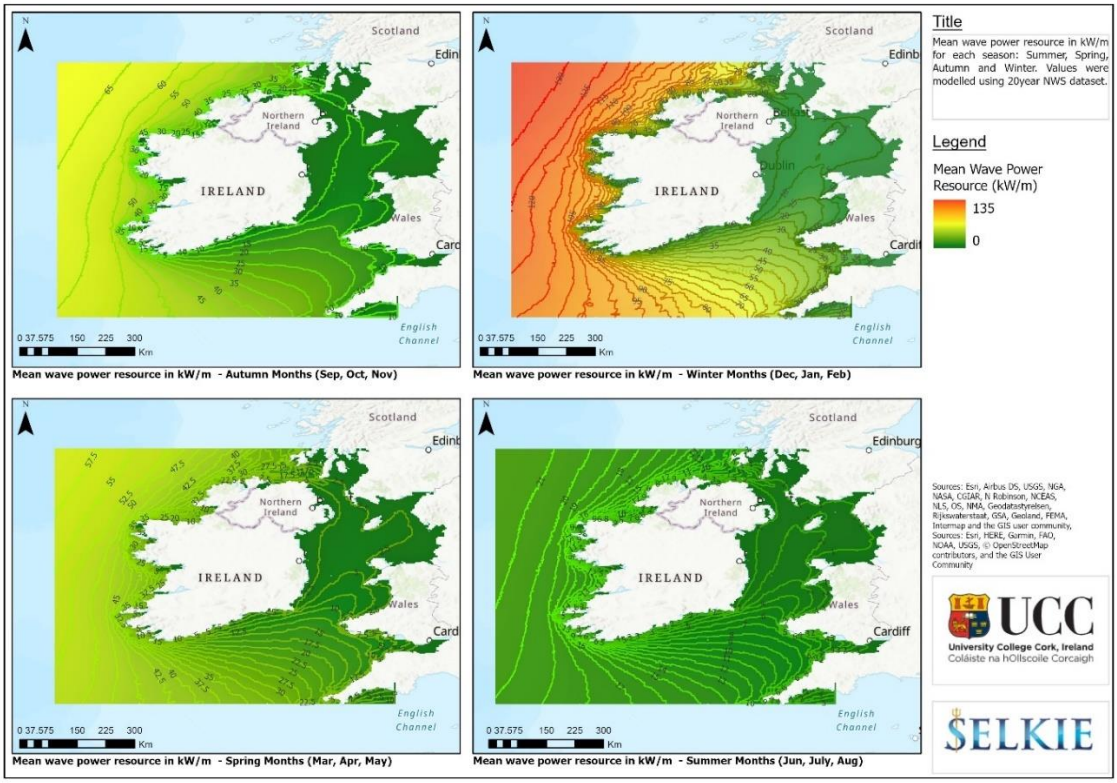



*Figure 4.13 Mean wave power resource in kW/m for each season: summer, spring, autumn and winter. Values were modelled using 20 year NWS dataset.*

### 4.1.3 Comparison between IBI and NWS Models

Four sites have been chosen so that a comparison could be carried out between the results obtained for the mean wave power resource from both the IBI and NWS models. The sites are as follows: (1.) NW Irish Coast, (2.) Wave Hub Pembrokeshire Demonstration Zone in the Celtic Sea, (3.) Irish Sea just south of the Isle of Man and (4.) west Wave Development Zone off the west coast of Ireland. These sites can be seen below in Figure 4.14

Two of these sites have been selected because they are locations where WEC's are currently deployed and are being tested, the West Wave site and the Wave Hub Demonstration Zone in Pembrokeshire. The remaining two sites were selected to show the variability in the wave resource in the Irish Sea and also in a coastal location.

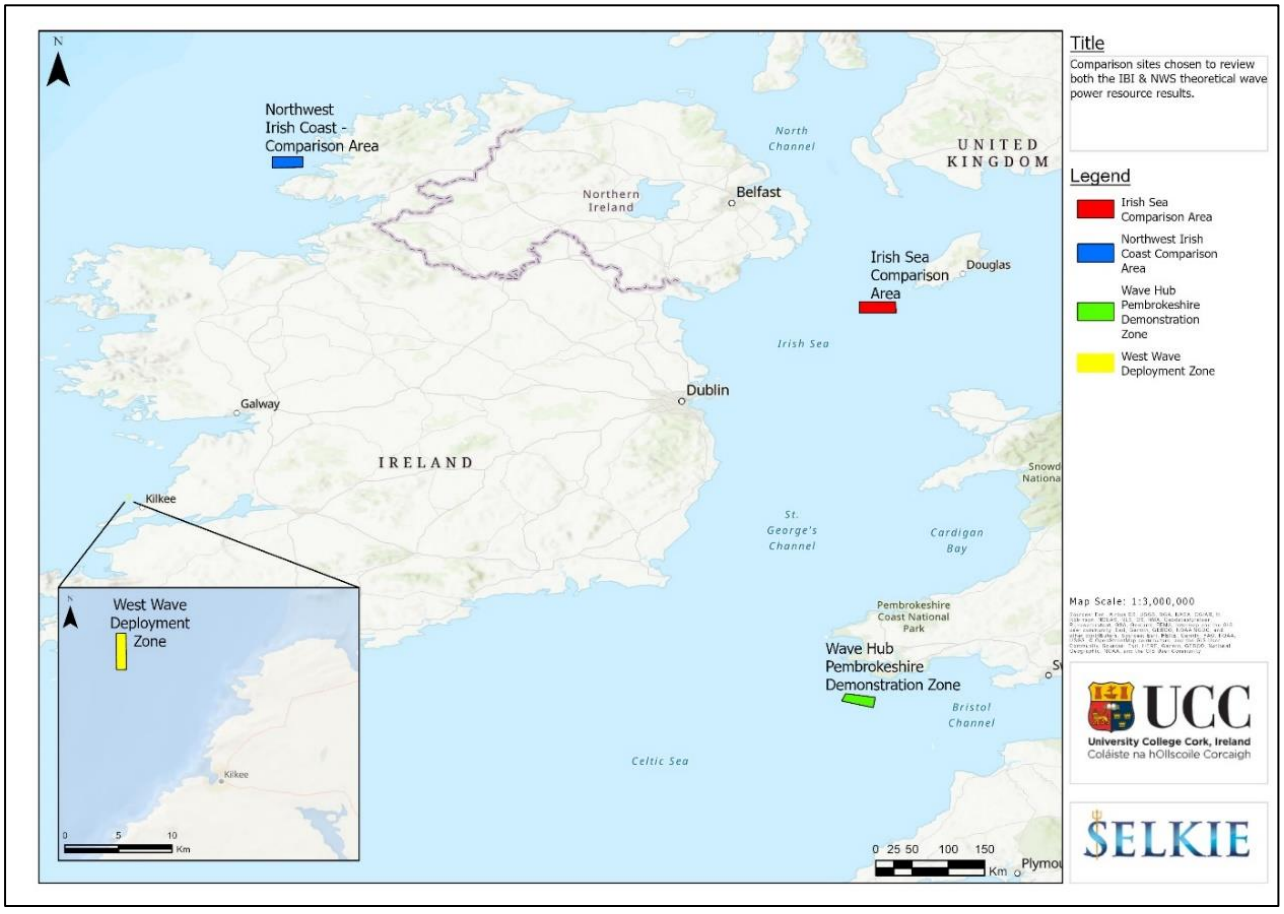



*Figure 4.14 Comparison sites that have been chosen to review the IBI and NWS mean wave power resource results.*

### 4.1.3.1 Comparison Site 1 – Northwest Irish Coast

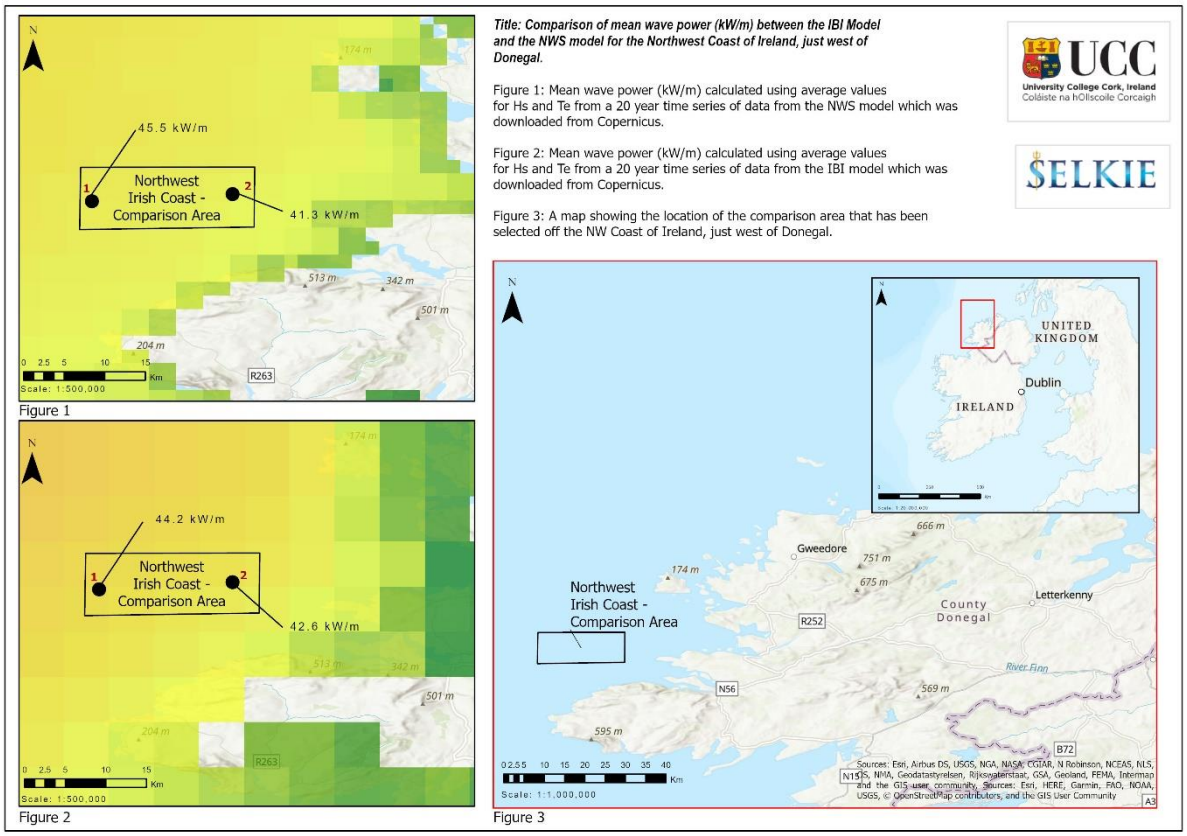



*Figure 4.15 Comparison of mean wave power in kW/m between the IBI Model and the NWS Model for the Northwest Coast of Ireland, just west of Donegal.*

| **Location** | **IBI - Mean Wave Power Resource kW/m** | **NWS - Mean Wave Power Resource kW/m** | **% Difference** |
|---|---|---|---|
| Point 1 - Northwest Irish Coast Comparison Area | 44.2 kW/m | 45.5 kW/m | 2.94% |
| Point 2 - Northwest Irish Coast Comparison Area | 42.6 kW/m | 41.3 kW/m | 3.15% |

*Table 4.8 Comparison table of mean wave power in kW/m between the IBI Model and the NWS Model for the Northwest Coast of Ireland, just west of Donegal.*

The first area that is reviewed for comparison of the wave power resource between the IBI and NWS Models is the northwest Irish Coast, a site that is approximately 10km west of the Donegal coastline (Figure 4.15). The area has been selected as it lies within an area deemed to be suitable for wave device deployment by a project partner, Ocean Energy. In this area it is possible to see the difference in the resolution of both models with proximity to land, it can be seen that the data for the NWS is of a higher resolution and follows the overall trend of the coast much better than the IBI, which is a slightly lower resolution. The values obtained from both models were very similar, with 45.5 kW/m from NWS and 44.2 kW/m in the same location

for the IBI model, a difference of 2.94% (Table 4.8). The point selected closest to the coast shows values of 41.3 kW/m for the NWS model and a slightly higher value of 42.6 kW/m from the IBI model, a difference of 3.15%. Even though this area is in proximity to the coast, there is a very small difference in the results between both models. This shows us that while the models can be less effective in coastal regions, it is only when the data is in very close proximity to the coast, with this area being ~20-30km from the coast. This proves that the models are still very suitable for analysing the wave power resource for potential wave energy sites.

### *4.1.3.2 Comparison Site 2 – Wave Hub Pembrokeshire Demonstration Zone*

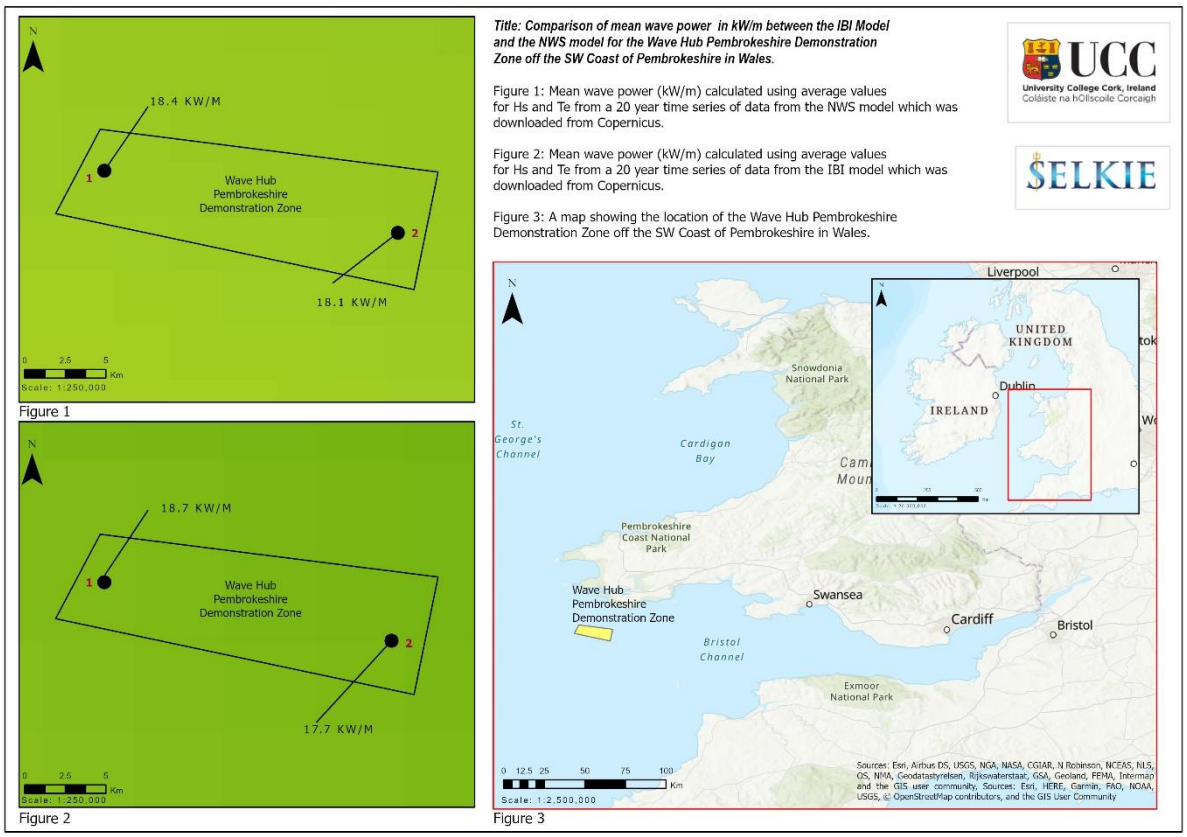



*Figure 4.16 Comparison of mean wave power in kW/m between the IBI Model and the NWS Model for the Wave Hub Pembrokeshire Demonstration Zone off the SW Coast of Pembrokeshire in Wales.*

| Location | IBI - Mean Wave Power Resource kW/m | NWS - Mean Wave Power Resource kW/m | % Difference |
|---|---|---|---|
| Point 1 - Wave Hub Pembrokeshire Demonstration Zone | 18.7 kW/m | 18.4 kW/m | 1.63% |
| Point 2 - Wave Hub Pembrokeshire Demonstration Zone | 17.7 kW/m | 18.1 kW/m | 2.26% |

*Table 4.9 Comparison table of mean wave power in kW/m between the IBI Model and the NWS Model for the Wave Hub Pembrokeshire Demonstration Zone off the SW Coast of Pembrokeshire in Wales.*

The second site that has been chosen for comparison is the Wave Hub Pembrokeshire Demonstration Zone (Celtic Sea Power, 2021) (Figure 4.16). This zone is managed by Wave Hub Ltd and they have stated that the site has a wave power resource of 19 kW/m, it is ~90 sq km in size and has seabed depths of ~50 meters (Marine Energy Wales, 2020). The results from both the IBI and NWS models are generally consistent with what Wave Hub have stated in terms of the mean wave power resource. The NWS model shows results of 18.4 kW/m to the west of the site and 18.1 kW/m to the east of the site, <1 kW/m from what Wave Hub have stated for the site. The IBI model gives results of 18.7 kW/m in the west of the site and 17.7 kW/m in the east of the site, these values are also very consistent with what has been outline by Wave Hub. A difference of 1.63% can be seen between the two models for point 1, and 2.26% for point 2, showing that the correlation between the models in this location is very strong.

### *4.1.3.3 Comparison Site 3 – Irish Sea*

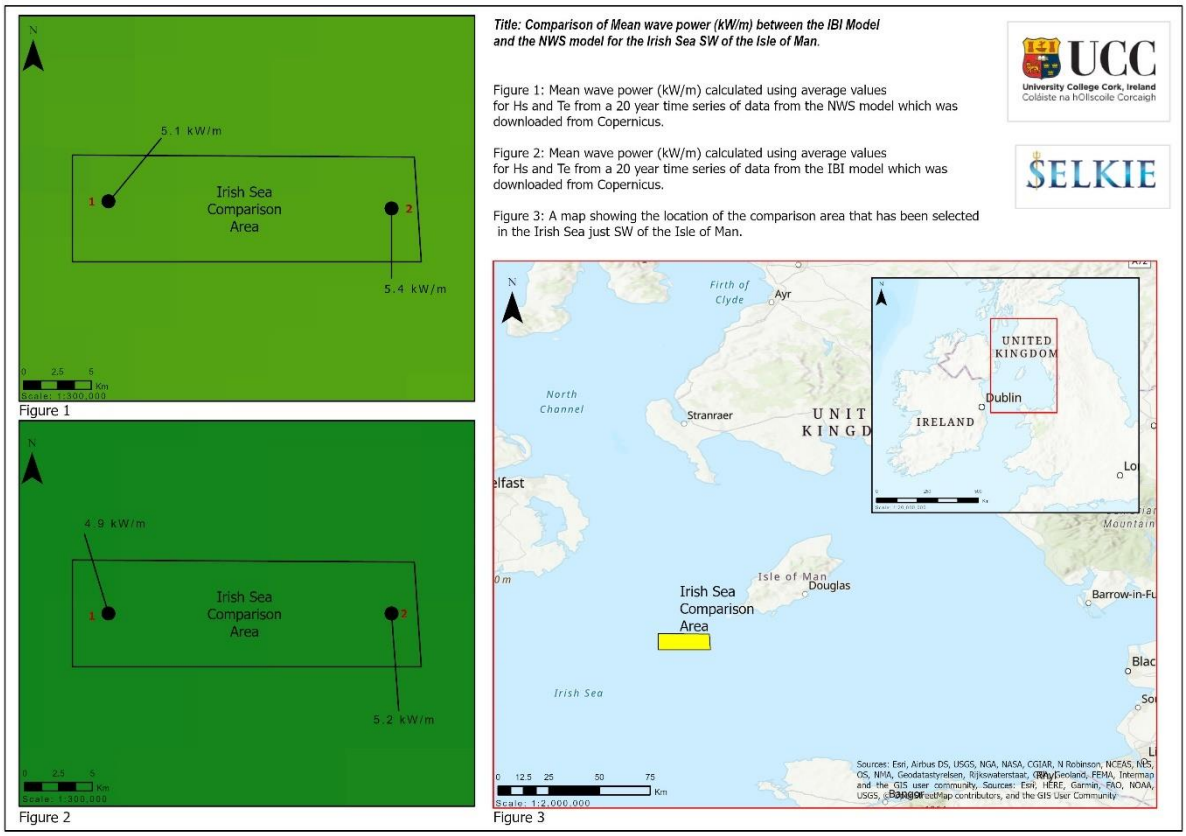



*Figure 4.17 Comparison of mean wave power in kW/m between the IBI Model and the NWS Model for the Irish Sea SW of the Isle of Man.*

| **Location** | **IBI - Mean Wave Power Resource kW/m** | **NWS - Mean Wave Power Resource kW/m** | **% Difference** |
|---|---|---|---|
| Point 1 – Irish Sea Comparison Area | 4.9 kW/m | 5.1 kW/m | 4.08% |
| Point 2 - Irish Sea Comparison Area | 5.2 kW/m | 5.4 kW/m | 3.85% |

*Table 4.10 Comparison table of mean wave power in kW/m between the IBI Model and the NWS Model for the Irish Sea SW of the Isle of Man.*

The third site that has been chosen for comparison is a site in the Irish Sea, just southwest of the Isle of Man (Figure 4.17). This site shows the lowest mean wave power resource out of the four comparison sites, with the general trend of the wave power resource showing a decrease northward into the Irish Sea. For the NWS Model, the results are 5.1 kW/m to the west of the site, and 5.4 kW/m to the east of the site. In comparison, the results from the IBI Model show 4.9 kW/m for the west of the site and 5.2 kW/m for the east of the site, a decrease of 0.2 kW/m for the site for the data from the IBI model. This shows once again that the results from this location are consistent across both models (Table 4.10). The wave power values are

significantly lower here than seen at the other sites, ~13 kW/m lower than the Wave Hub site in the Celtic Sea and ~40 kW/m lower than the site off the northwest coast of Ireland.

#### *4.1.3.4 Comparison Site 4 – West Wave Deployment Zone*

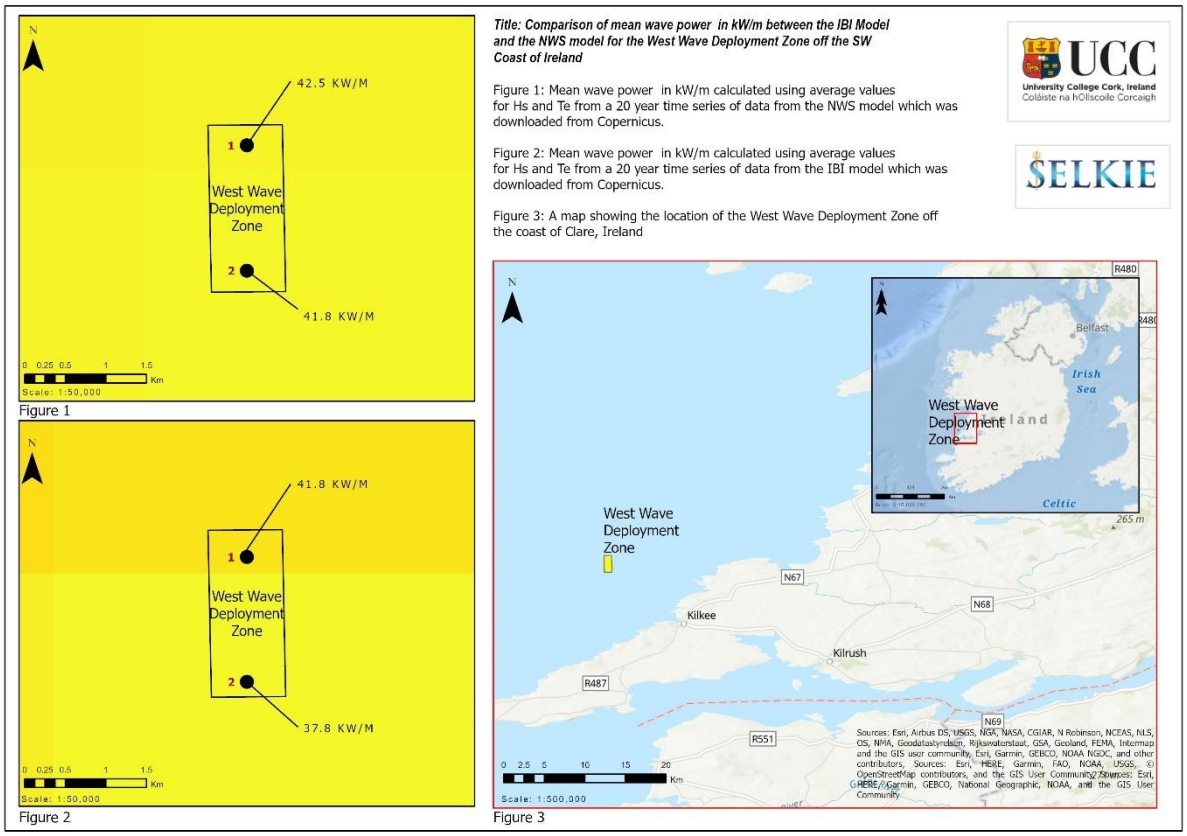



*Figure 4.18 Comparison of mean wave power in kW/m between the IBI Model and the NWS Model for the West Wave Deployment Zone off the SW coast of Ireland.*

| **Location** | **IBI - Mean Wave Power Resource kW/m** | **NWS - Mean Wave Power Resource kW/m** |
|---|---|---|
| Point 1 - West Wave Deployment Zone | 41.8 kW/m | 42.5 kW/m |
| Point 2 - West Wave Deployment Zone | 37.8 kW/m | 41.8 kW/m |

*Table 4.11 Comparison table of mean wave power in kW/m between the IBI Model and the NWS Model for the West Wave Deployment Zone off the SW coast of Ireland.*

The final site that has been chosen for comparison of the mean wave power resource is the West Wave Deployment Zone off the coast of Clare, Ireland (Figure 4.18). The WestWave site is a demonstration project that is being developed by the ESB in Ireland. The site is located ~7km northwest of the town of Kilkee, Co.Clare. The results seen at this site from both models are very similar to those seen at site (1.) northwest coast of Ireland, with values ~40 kW/m from both sites. The data from the NWS model shows values of 42.5 kW/m for the north of the

site and 41.8 kW/m for the south of the site in comparison to values of 41.8 kW/m and 37.8 kW/m respectively from the IBI model. A study by Atan et al (2018) modelled the wave power at the West Wave site using a 12 year time series of data and a SWAN model and the mean value for annual power was 50 kW/m. There is ~17% difference between the values obtained in this study and the values from the Atan et al (2018) study, likely due to difference in the modelling of the data (SWAN versus WAM), grid spacing and time series used.

## 4.2 Tidal Results

In this section, the results of the tidal power analysis are discussed. A comparison of the results is made between both the results from the analysis of the data for this study from the Irish Marine Institute, and the data that is currently available from both the Wales Marine Planning Portal and the Irish Marine Atlas. For the analysis that was completed as part of this study, the Mean Tidal Power ($W/m^2$) was calculated, along with the Mean spring peak current velocity (m/s), the Mean neap peak current velocity (m/s) and the Mean peak current velocity (m/s) - (calculated over the whole year irrespective of mean or spring periods). Several sites have been chosen for an in-depth study and these are discussed in more detail below.

### 4.2.1 Tidal Current Analysis

Analysis of the tidal currents has been undertaken so that a thorough understanding of the spatial nature of the currents within the study area can be achieved. The currents have been analysed for peak flows but have also been separated and modelled as spring and neap cycles.

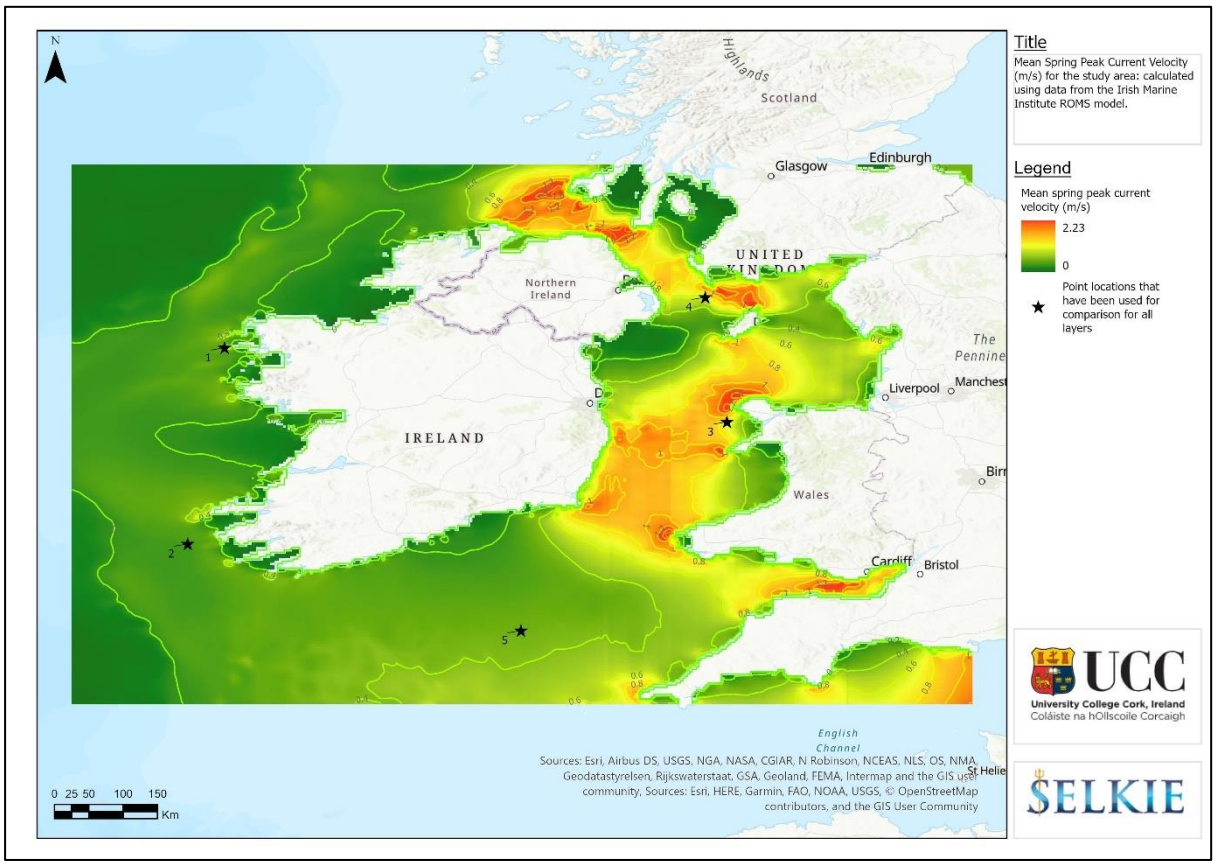



*Figure 4.19 Mean Spring Current Velocity (m/s) that has been calculated using a 1 year time series of data from the Irish Marine Institute ROMS model.*

The analysis of the mean spring current velocities as part of this study have identified a number of sites that would have tidal resource potential based on the mean spring current velocity value, which can be seen in Figure 4.19. A maximum mean spring current velocity of 2.23 m/s can be seen off the northern coast of Ireland between Malin Head and the Island of Islay in Scotland, an area that is well known for its resource potential. A values of 1.97 m/s for the mean spring peak current velocity can be seen off the coast of Ballycastle Northern Ireland, with values of 1.35 – 1.50 m/s seen in the area between the Isle of Man and the Scottish Mainland. Slightly higher values can be seen to the south of the Isle of Man off the Welsh coast, with values of ~1.8 m/s occurring off the western coast of Pembrokeshire and ~1.50 m/s present off the coast of Holyhead. The area off the southeastern coast of Ireland around Arklow/Wexford has mean spring current velocities in the range of ~1.20 m/s. Velocities of ~1.40 m/s can be seen just south of Cardiff in the area close to Penarth. The general spatial distribution of the data is that the values off the western coast of Ireland are the lowest, with values in the range of 0 - 0.6 m/s. Higher values can be seen in areas between land masses such as in the Irish and Celtic Seas and off the northern Irish Coast., between the Isle of Man and Scotland, the area between Northern Ireland and Scotland and the Bristol Channel just south of Cardiff. These results compare very well with the study by Lewis et al (2015) which reported peak spring tide current velocities for the Irish Sea region (Figure 2.31). Higher values >2m/s

where reported in the area around Holyhead Wales, south of Cardiff in the Bristol Channel and in the strait between Isle of Man and Scotland.

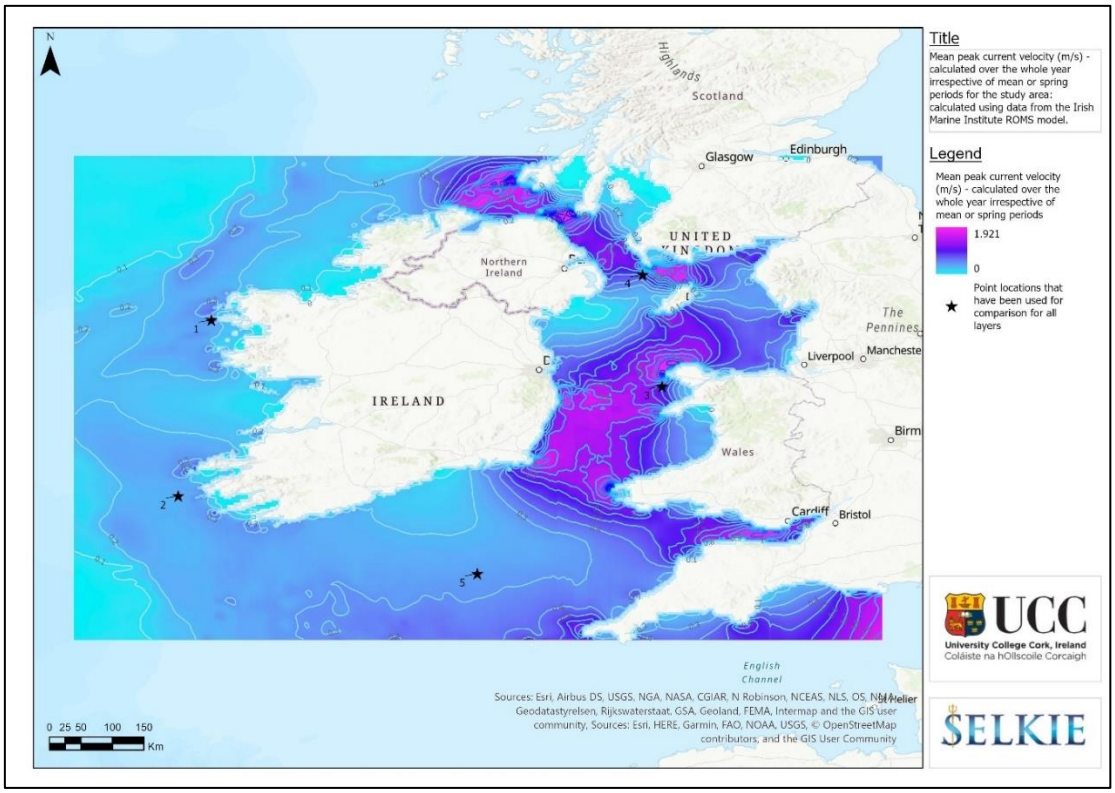



*Figure 4.20 Mean peak current velocity (m/s) - (calculated over the whole year irrespective of mean or spring periods) that has been calculated using a 1 year time series of data from the Irish Marine Institute ROMS model.*

The spatial distribution for the mean peak current velocity and the mean neap peak current velocities are consistent with what is seen with the mean spring peak current velocities. The values encountered in the mean peak current velocity and the mean neap peak current velocity layers are lower than the mean spring current velocity layer, with a maximum value of 1.9 m/s for the mean peak current velocity and 1.6 m/s for the mean neap peak current velocity. The mean peak current velocity can be seen above in Figure 4.20 and the mean neap peak current velocity can be seen in Figure 4.21.

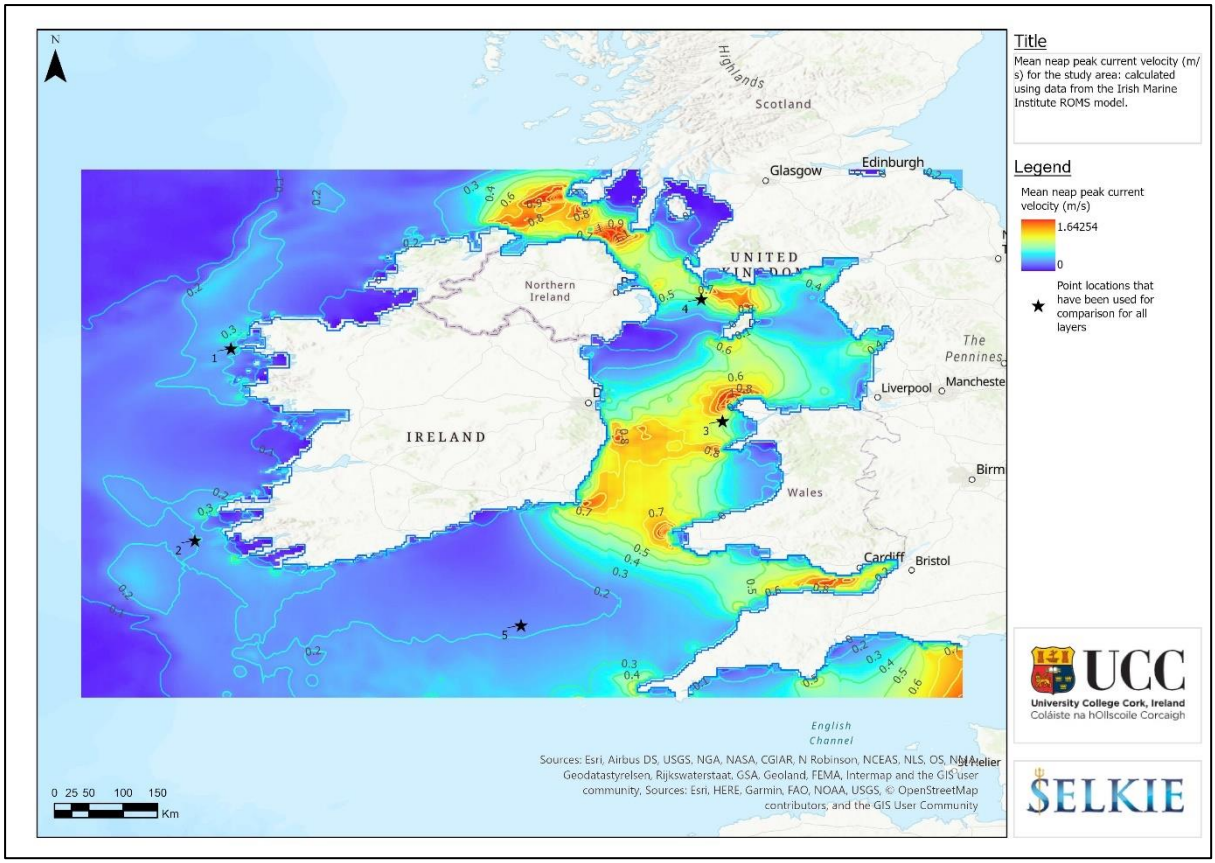



*Figure 4.21 Mean neap peak current velocity (m/s) that has been calculated using a 1 year time series of data from the Irish Marine Institute ROMS model.*

| Location | Mean Spring Peak Current Velocity (m/s) | Mean Peak Current Velocity (m/s) | Mean Neap Peak Current Velocity (m/s) | Max Spring Peak Current Velocity (m/s) | Max Peak Current Velocity (m/s) | Max Neap Peak Current Velocity (m/s) |
|---|---|---|---|---|---|---|
| 1 | 0.35 m/s | 0.31 m/s | 0.27 m/s | 0.93 m/s | 1.00 m/s | 0.88 m/s |
| 2 | 0.24 m/s | 0.22 m/s | 0.19 m/s | 0.70 m/s | 0.70 m/s | 0.59 m/s |
| 3 | 0.72 m/s | 0.62 m/s | 0.52 m/s | 1.07 m/s | 1.07 m/s | 0.89 m/s |
| 4 | 0.69 m/s | 0.58 m/s | 0.47 m/s | 1.15 m/s | 1.15 m/s | 0.83 m/s |
| 5 | 0.33 m/s | 0.26 m/s | 0.18 m/s | 0.55 m/s | 0.55 m/s | 0.40 m/s |

*Table 4.12 Comparison table for the 5 points that have been selected across the study area showing mean and max values for spring current velocity, neap current velocity and peak current velocity.*

### 4.2.2 Tidal Power Resource Analysis

The Mean Tidal Power layer that has been created for the study area can be seen below in Figure 4.22. The analysis of the tidal power shows that the majority of the power resource is located within the Irish and Celtic Seas, with minimum resource values occurring off the

northwest, west and southern coasts of Ireland. This can be seen in the comparison table which shows the values across the five sites for the mean tidal power layers (Table 4.13). These results correspond well with work that has previously been carried out to show the resource in the area, with known resources in the area around Fair Head Northern Ireland (DP Energy, 2021), off the coast of Holyhead Wales (Minesto AB, 2021) and also of the coast of Pembrokeshire, Wales (Morlais Energy, 2021). These sites have been subjected to extensive research over the previous years and the analysis as part of this study backs up the work that has been previously carried out for this area.

The Mean Tidal Power layer shows values in the rage of 400 W/m$^2$ off the southeast coast of Ireland in the area close to Arklow/Wexford. Values off the southwest coast of Ireland are significantly lower with maximum values of ~50 W/m$^2$ seen. The western coast of Pembrokeshire shows higher values with a maximum values of 1600 W/m$^2$ seen. The area to the north of the Isle of Man looks promising with values ~700 W/m$^2$. It was said by Charlier (2003) that large tidal currents are commonly located between land masses or adjacent to headlands, and this can be seen reflected in the tidal power layer, where larger values are seen in areas such as between headlands like north of the Isle of Man and also between Northern Ireland and Scotland. To the east of Ballycastle Northern Ireland, values of ~1500 W/m$^2$ can be seen.

| **Location** | **Mean Tidal Power (W/m$^2$)** | **Mean Spring Tidal Power (W/m$^2$)** | **Mean Neap Tidal Power (W/m$^2$)** |
|---|---|---|---|
| 1 | 17.36 W/m$^2$ | 21.12 W/m$^2$ | 12.04 W/m$^2$ |
| 2 | 5.61 W/m$^2$ | 6.94 W/m$^2$ | 4.05 W/m$^2$ |
| 3 | 95.76 W/m$^2$ | 140.03 W/m$^2$ | 52.68 W/m$^2$ |
| 4 | 83.4 W/m$^2$ | 124.95 W/m$^2$ | 43.22 W/m$^2$ |
| 5 | 8.09 W/m$^2$ | 13.72 W/m$^2$ | 2.71 W/m$^2$ |

*Table 4.13 Comparison table for the 5 points that have been selected across the study area showing hourly mean tidal power, hourly mean spring tidal power and hourly mean neap tidal power.*

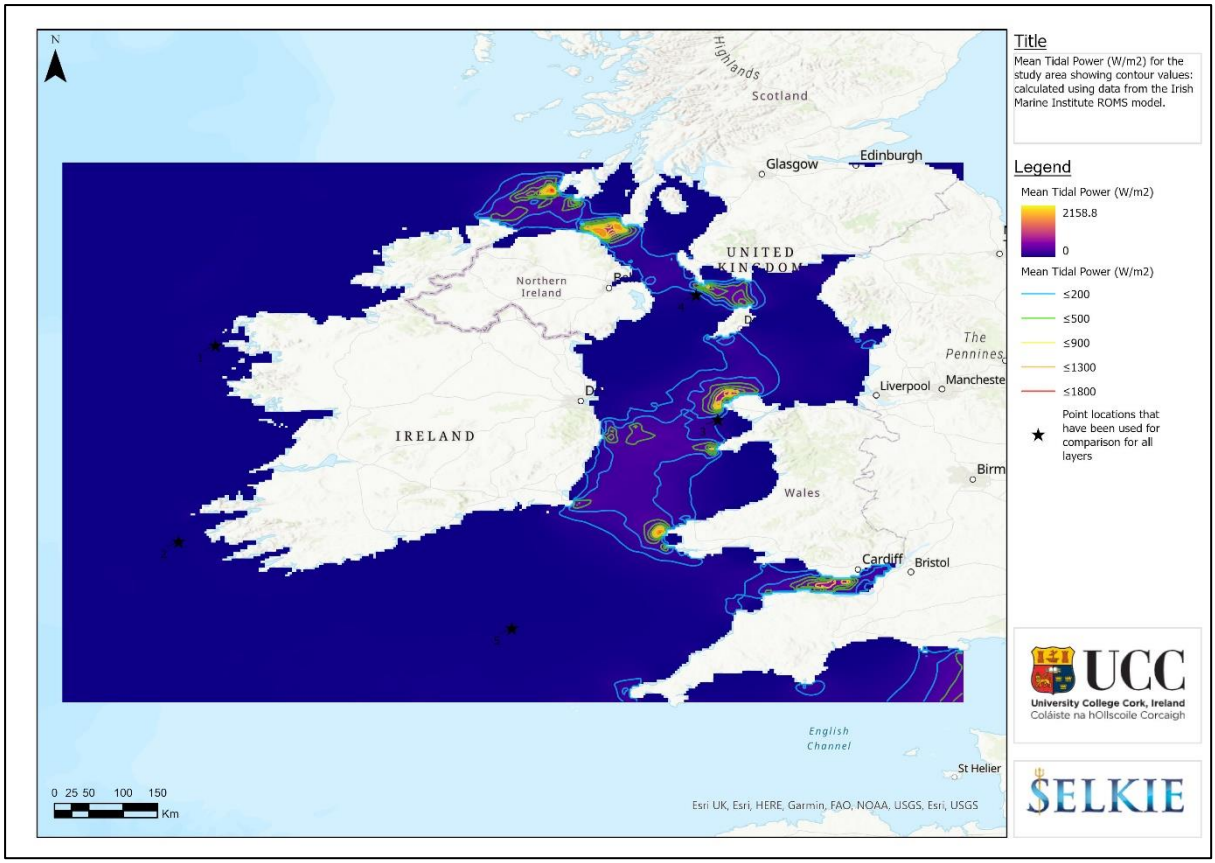



*Figure 4.22 Mean Tidal Power (W/m2).*

Sites of interest can be seen in Figure 4.23 and Figure 4.24 below, where higher tidal power values are present. One area that shows potential for tidal power is the area between Northern Ireland and Mainland UK (including Scotland). This area shows tidal power values in the range of 1500-2000 W/m$^2$, with highest values particularly in the area just southeast of the Isle of Islay, Scotland. Another area of interest is the area just west of Holyhead, Wales, where values of ~1000 W/m$^2$ can be seen. Other areas of interest include the Bristol Channel, the area just west of Pembrokeshire and the eastern coast of Ireland close to Arklow.

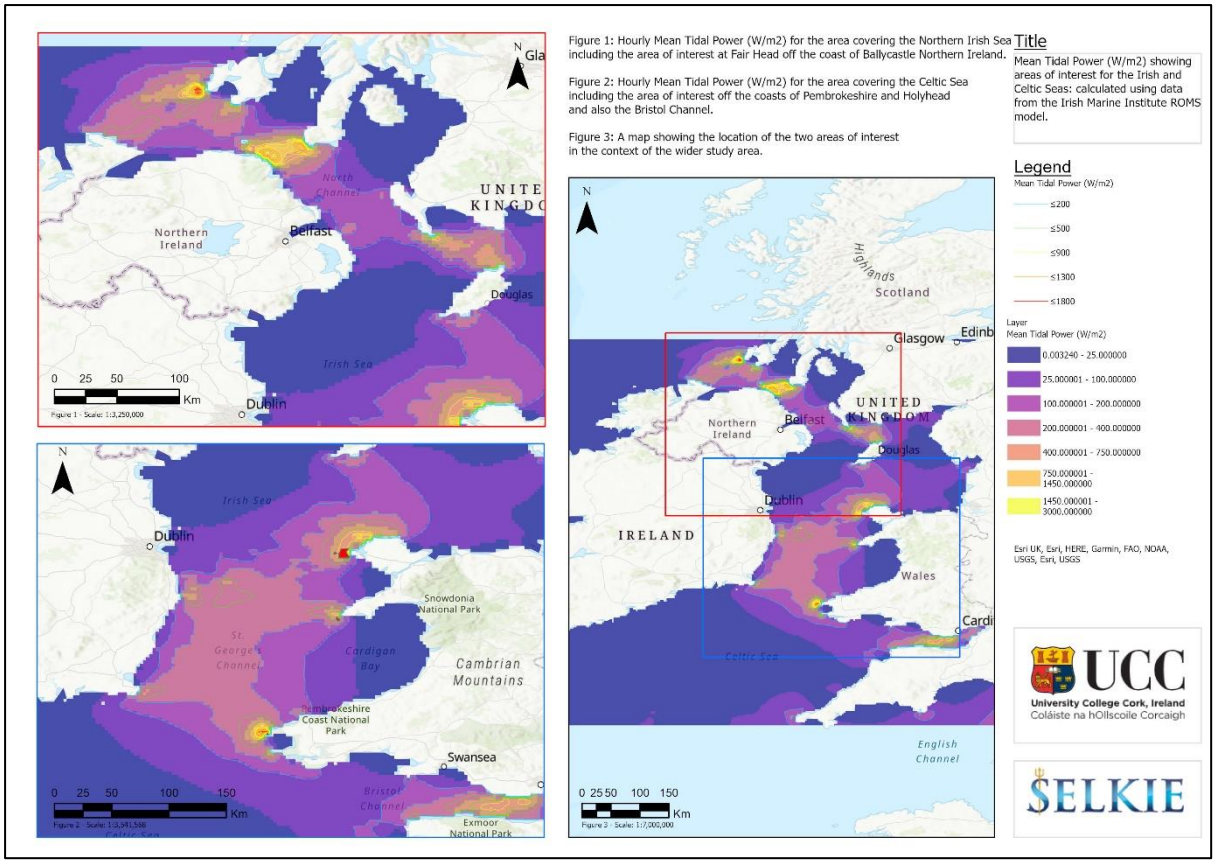



*Figure 4.23 Mean Tidal Power (W/m2) showing areas of interest mainly within the Irish and Celtic Seas.*

Figure 4.24 below shows the main areas of interest for the study area, which are focused in the Irish Sea, the Celtic Sea and off the southeastern coast of Ireland. The tidal resource off the northern Irish coast in the area around Fair Head / Torr Head shows maximum values of 1480 $W/m^2$.

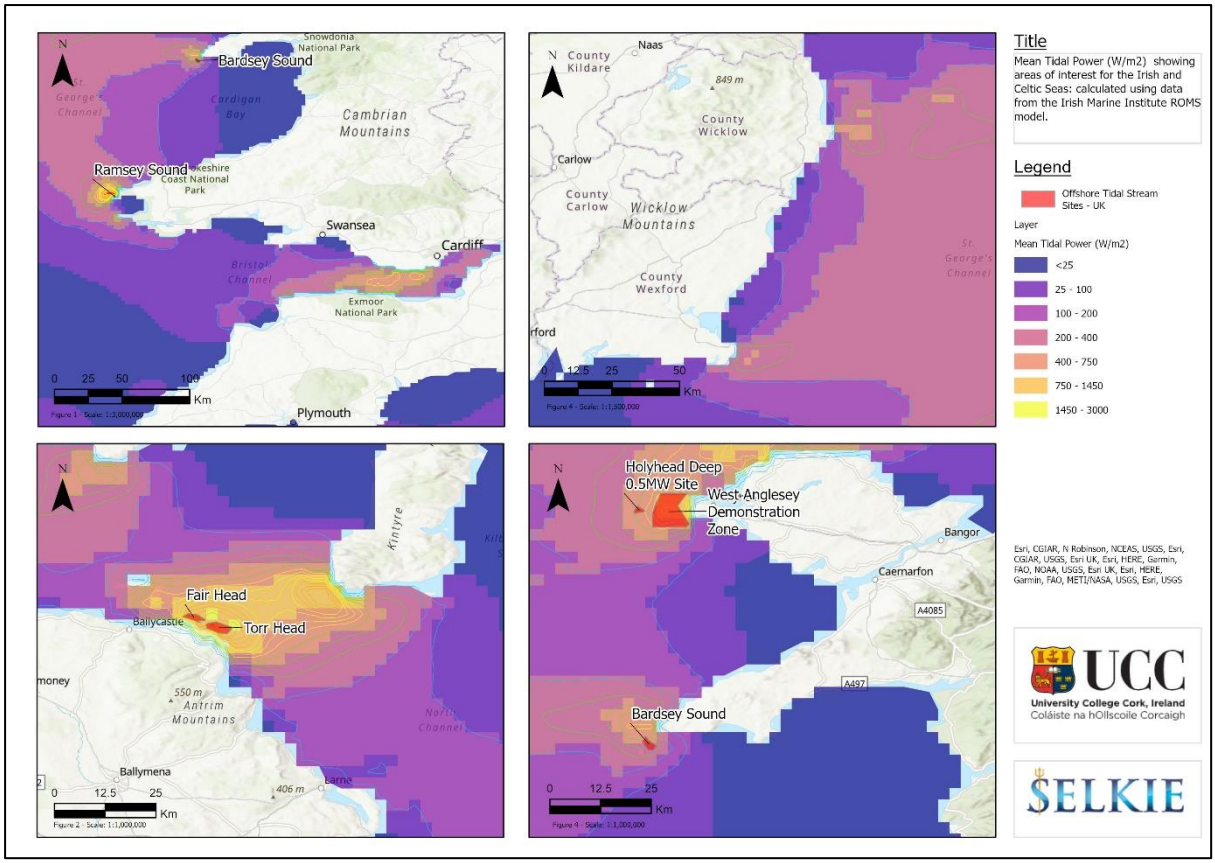



*Figure 4.24 Mean tidal power sites of interest continued.*

It is important to consider not just the mean peak current velocities when calculating power but to also model power using both peak spring and neap current velocities to understand the difference seen in power across the lunar cycle. This is important for tidal developers to understand so they can model where power output will be lower (during neap cycles) and when it is likely to be higher (during spring cycles). The Mean Spring Tidal Power and the Mean Neap Tidal Power can be seen below in Figure 4.25 and Figure 4.26. A notable difference can be seen between both layers, with the power available during the neap cycle significantly lower than during the spring cycle. The maximum power value for the spring cycle is 3068 W/m$^2$ in comparison to 1292 W/m$^2$ for the neap cycle, seen off the northeastern coast off Ireland between Northern Ireland and Scotland. The power values that can be seen in both the spring

and neap power layers follow the same spatial trend as the current value layers, as well as the peak tidal power layer.

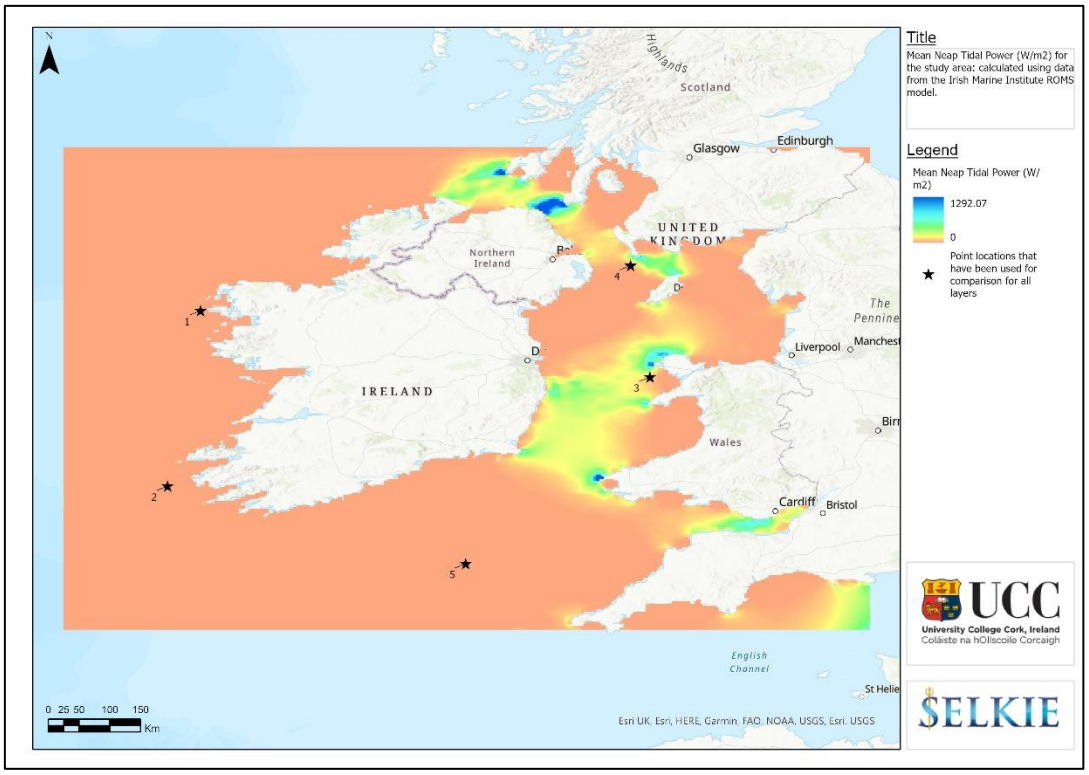



*Figure 4.25 Mean Neap Tidal Power (W/m2).*

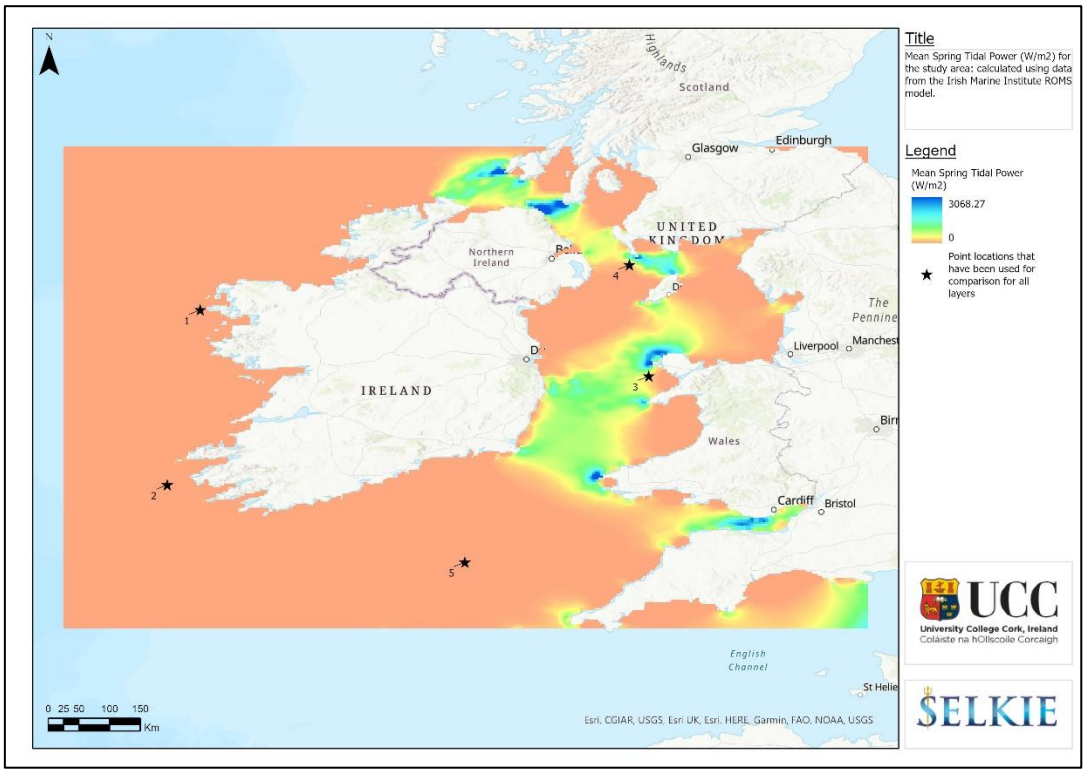



*Figure 4.26 Mean Spring Tidal Power (W/m2).*

### 4.2.3 Total Tidal Energy

The Total Tidal Energy (MWh) layers have been created to show the total amount of power that can be generated in a year in MWh at any given location.

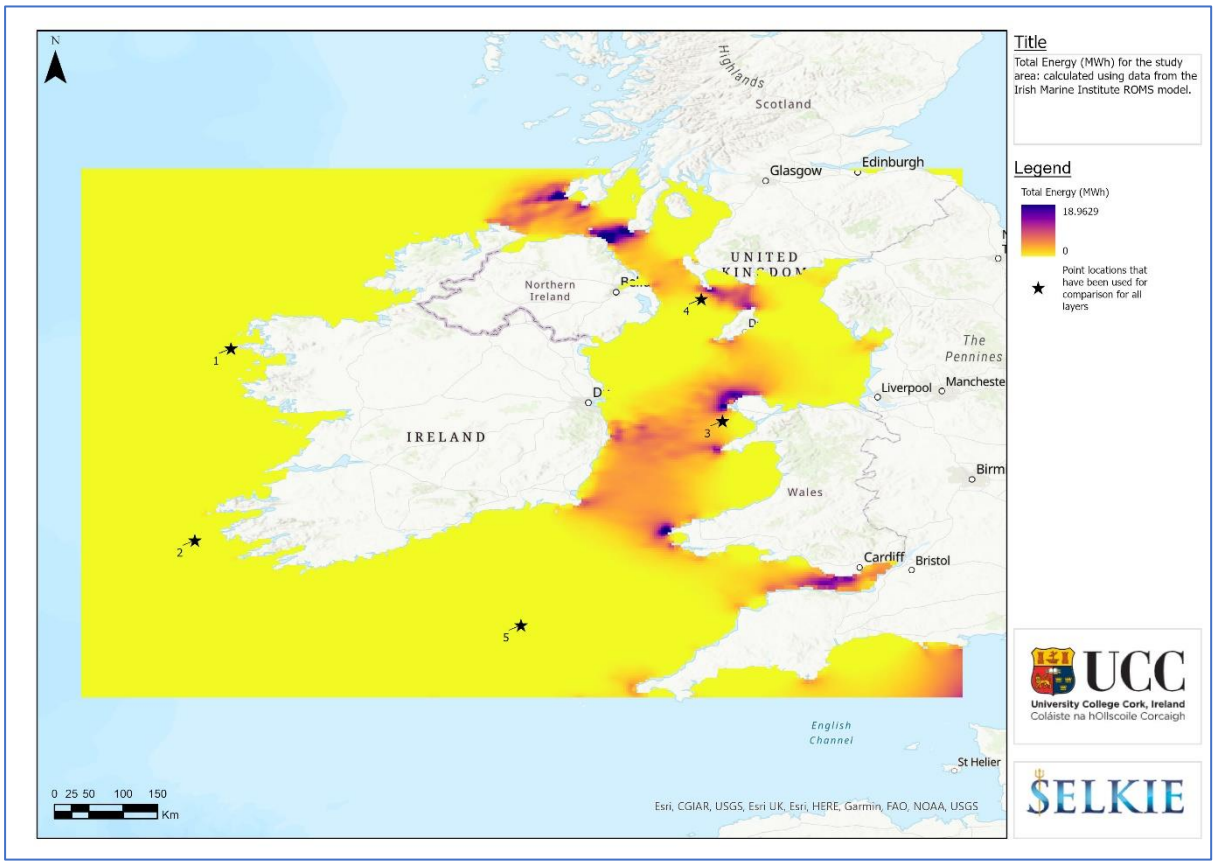



*Figure 4.27 Total Energy (MWh) for the study area: calculated using data from the Irish Marine Institute ROMS model.*

The total tidal energy has the highest value with 18.9 MWh, with lower values of 13 MWH for the spring total energy layer and the lowest values seen for the neap total energy layer of 5.7 MWh. Comparison values from the five sites can be seen for the three layers below in Table 4.14.

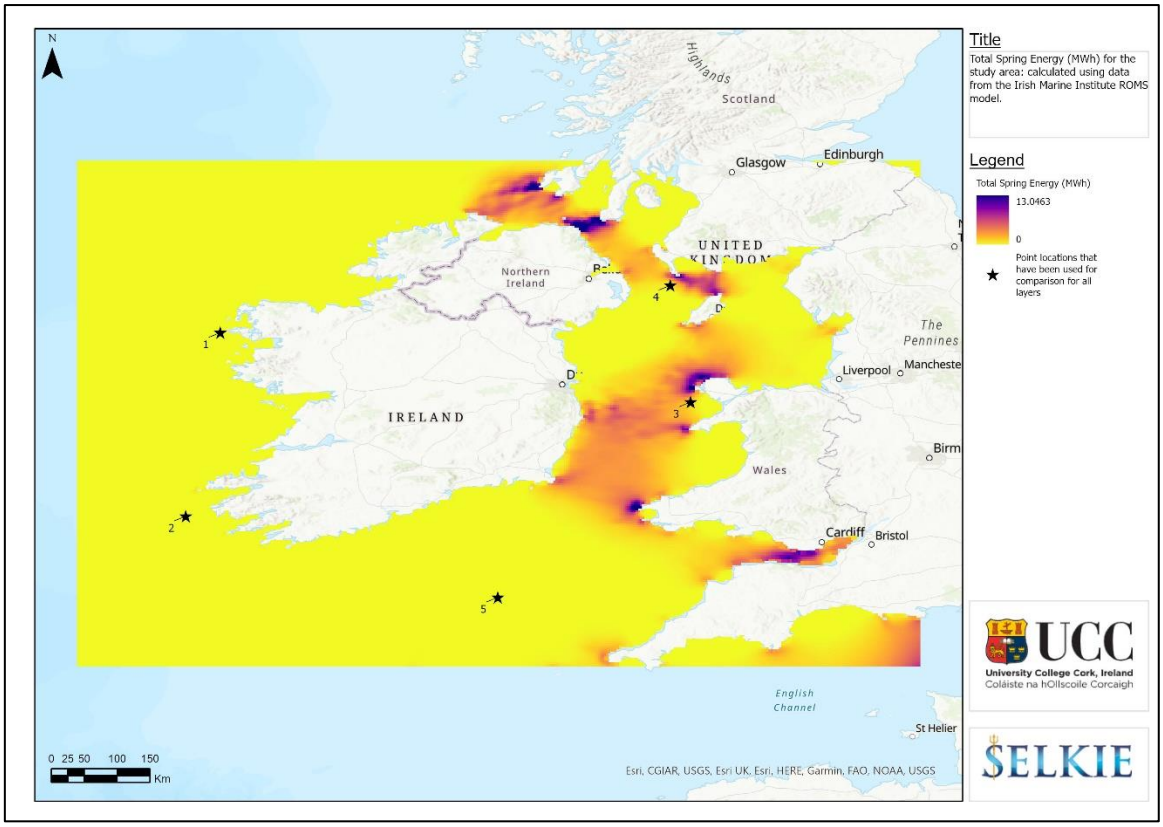



*Figure 4.28 Total Spring Energy (MWh) for the study area: calculated using data from the Irish Marine Institute ROMS model.*

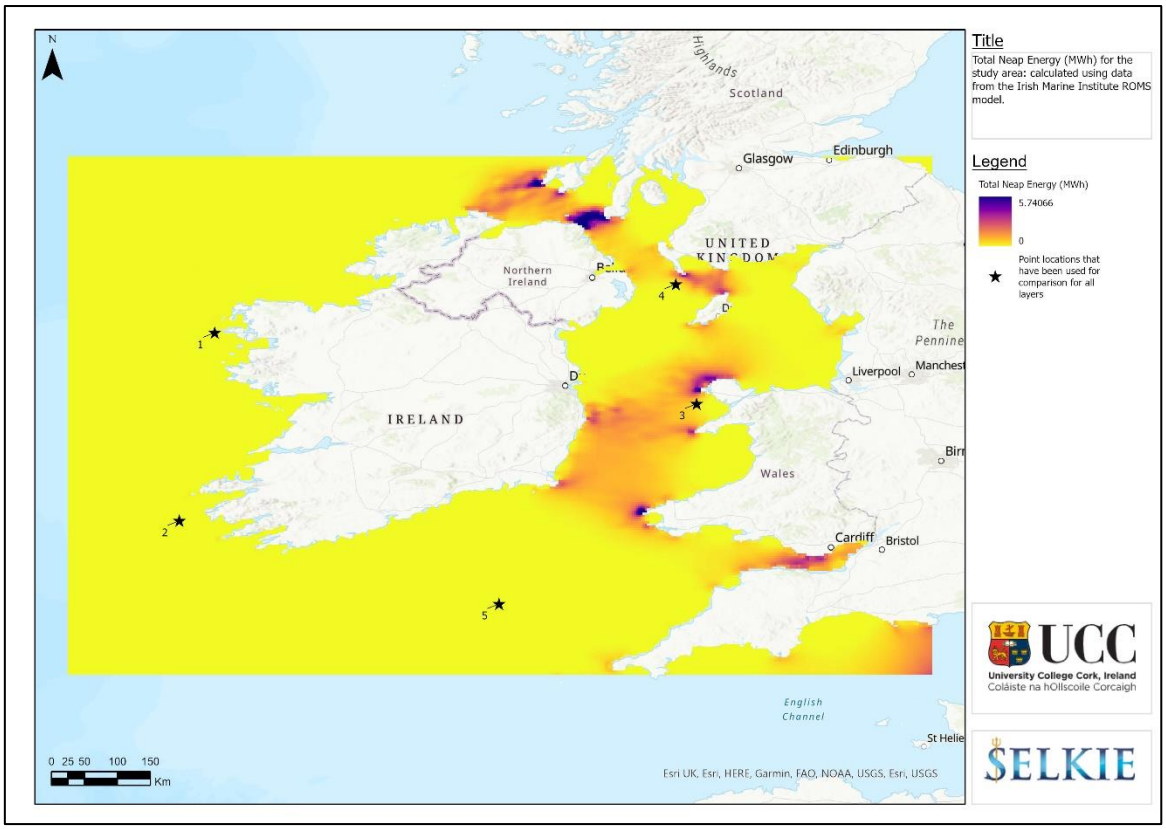



*Figure 4.29 Total Neap Energy (MWh) for the study area: calculated using data from the Irish Marine Institute ROMS model.*

| Location | Annual Tidal Power ($MW/m^2$) | Annual Spring Tidal Power ($MW/m^2$) | Annual Neap Tidal Power ($MW/m^2$) |
|---|---|---|---|
| 1 | 0.15 $MW/m^2$ | 0.089 $MW/m^2$ | 0.053 $MW/m^2$ |
| 2 | 0.049 $MW/m^2$ | 0.029 $MW/m^2$ | 0.017 $MW/m^2$ |
| 3 | 0.84 $MW/m^2$ | 0.60 $MW/m^2$ | 0.22 $MW/m^2$ |
| 4 | 0.73 $MW/m^2$ | 0.53 $MW/m^2$ | 0.187 $MW/m^2$ |
| 5 | 0.071 $MW/m^2$ | 0.058 $MW/m^2$ | 0.012 $MW/m^2$ |

*Table 4.14 Comparison table for the 5 points that have been selected across the study area showing Annual Tidal Power, Annual Spring Tidal Power and Annual Neap Tidal Power.*

## 4.3 Updated Resource Assessment

The updated wave and tidal energy resource assessments that have been completed as part of this study have given new insight into the size and extent of the resource availability, the spatial variability in the resource and detailed seasonal information regarding the parameters needed for assessment. While there currently is resource information available for the study area, these new datasets have been created with up to date, high resolution data.

### 4.3.1 Wave Resource

The results of the wave resource assessment are consistent with work that was previously completed by O'Connell et al., (2020) which showed that using wave spectrum data from numerical models that are available through the Copernicus Marine Service is an accurate and efficient way to model the wave and tidal energy resources. This work has followed on from that study, using data that is a higher resolution and of a longer hindcast, further supporting the methodology and giving the user peace of mind that the data is reliable. The wave resource layers that have been created as part of this study correspond well with work that was previously completed, with the spatial nature of the resource displaying maximum values off the western coast of Ireland with values in the range of 50 – 70 kW/m. Values in the Irish and Celtic Seas are generally lower, with most values in the area being < 50 kW/m.

### 4.3.2 Tidal Resource

The results of the tidal resource analysis will provide tidal power layers as well as spring, neap and peak current velocity layers for the study area for the first time. Currently there are not GIS layers of this type available in online GIS tools for Irish Waters so the development of these layers will be crucial to the advancement of the tidal industry in Ireland going forward. GIS

layers are currently available for UK waters, but the layers were created back in 2008 (ABPmer, 2008) so the improved datasets that have been created as part of this study will be a welcome upgrade to what is currently available. The results of the tidal resource analysis have shown that the greatest resource potential lies mainly within the Irish and Celtic Seas, with high resource potential seen in the areas around Pembrokeshire, Holyhead, and the northern Irish Coast. Resource potential can also be seen in the area off the southeastern Irish coast close to Arklow and Wexford.

## 4.4 Importance for MRE Industry

Analysis of the wave power resource using freely available data through CMEMS has proven to be very effective. Results from both models strongly correlate with each other, and with the in-situ data. This data is openly available and easy to download, which should make wave resource modelling more accessible. It is also available at high resolutions, <3km in some cases and long hindcasts (>20 years), allowing for this and future wave resource modelling to represent the wave climate closer to the coast than with previous Copernicus models, and with greater consideration of historic wave climatic patterns. Analysing the wave data and then converting to GIS allows the users to gain a thorough understanding of the spatial nature of the data. Spatial analysis of the results in GIS has shown that the greatest resource availability is off the west/ northwest cost of Ireland, with lower values seen in the Celtic Sea trending downwards into the Irish Sea. It is understood that waves are generated when winds blow over the ocean, and one parameter that leads to larger more powerful waves is the fetch (the distance the wind travels over the ocean). The wave resource tends to be best in areas where the winds have travelled over long distances, as a result large wave resources can be seen off the west/ northwest coast of Ireland. Reviewing the data spatially also means that patterns can be identified for site selection, such as identifying locations where the resource is abundant, as well as underlying features which may be identified through other GIS layers (proximity to grid connection, underlying bathymetry, bedrock geology etc.). Having these layers available means that developers can now take a first pass look at sites to decide if they have potential, while gaining an understanding of both the resource value but also the seasonal changes in the wave parameters and the resource. This information would inform developers as to times when the resource availability is likely to be higher (eg, in winter months where wave heights are higher and periods are longer), but also where it is more likely to be difficult to access the device for maintenance due to storm conditions or when the device is likely to go into ‘survival

mode'. The time series that has been used to create these layers will also give more reliability to the robustness of the results, with 20 years of data (>175,000 time steps) having been used. A hindcast of this length gives a good understanding of the wave climate, taking into account any seasonal alterations in significant wave heights and wave periods.

The aim of having data such as the wave resource GIS layers that have been created as part of this project is so that they can be added to an open access Web-GIS tool that will help developers make an initial site selection for offshore renewable energy. Wave energy has been identified as a possible source of energy for both Ireland and the UK but it is still at pre-commercialization, so data like this is likely to benefit companies who are interested in entering this energy market. This work aims to give a broad view of the study area so that sites can be selected, but higher resolution modelling at a much finer grid scale (sub – kilometer grid scale) should be completed once a site has been selected. This work has shown that data modelling of the wave energy resource on such a scale can be computationally expensive and complex to carry out, therefore in order to carry out much higher resolution modelling it would be advisable to only do it for a smaller site.

## 4.5 Comparison with other datasets

The wave resource data that is currently available for the study area can be seen below in Figure 4.30. One of the main objectives of this study was to create new up to date, high resolution resource data for an area that covers both the Irish and Celtic Seas and the west coast of Ireland. The figure that has been produced below shows the wave energy resource layer that has been created as part of this study, in comparison to the datasets from the Irish Marine Atlas and the Wales Marine planning portal, both of which had extents that were limited to their own individual jurisdictions. The reason that the data was created to cover both areas is so that a 'whole' view of the study area can be seen, with the aim that developers can gain a comprehensive understanding of the resource availability for the new updated study area.

The resolution has also been improved; the data that has been created for this study has been created at a grid spacing of 0.015 degrees (~3km) for the NWS dataset and a grid spacing of 0.05 degrees (~5km) for the IBI dataset. The time series that was used was a 20 year hindcast from 2000-01-01 00:00:00 to 2019-12-30 23:00:00. The wave resource data from the Irish Marine Atlas that was created in 2005 is described as an initial comparison between several years of hourly wave forecasts (using WAM) on a grid of points located off the Irish coast with

corresponding records from several buoys installed in recent years. This information was then modified slightly to create the technical power resource layers (Marine Institute, 2005). This information is available from the metadata of the layer within the online atlas, but there is limited information given on the source of the wave spectrum data and the grid spacing of the data used. The wave energy resource layer that is available through the Wales Marine Planning Portal was created using wave parameters from both the UK Waters Wave Model which has a spatial resolution of 12km and the Global Waters Wave Model which has a spatial resolution of 60km. The time series used was hourly intervals of data from 1 June 2000 to 31 May 2007 (ABPmer, 2008). The updated wave layers that were created should contain detailed metadata information on the source of the wave parameter data that was used for the resource calculations, the equations that were used and also the hindcasts. This information will give the end user more confidence in the reliability of the dataset when they are using it within an online GIS system.

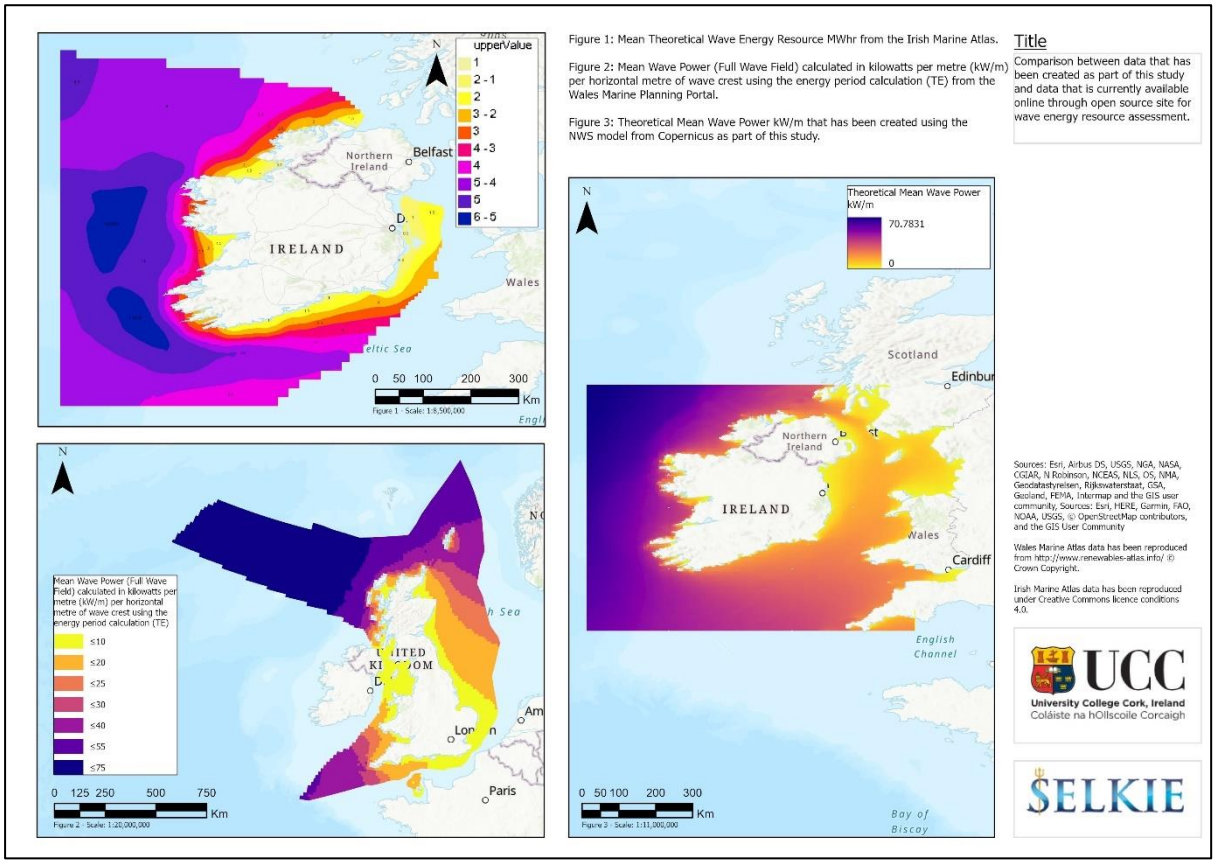



*Figure 4.30 Comparison between wave energy resource dataset that has been created as part of this study and the datasets that are currently available through the Irish Marine Atlas and the Wales Marine Planning Portal.*

The tidal resource data that is currently available for the study area can be seen below in Figure 4.31. As with the wave resource information, the figure below shows a comparison between the new up to date tidal energy resource layer that has been created as part of this study, and the data that is available through the Irish Marine Atlas and the Wales Marine Planning Portal. The tidal data that is available through the Wales Marine Planning portal is comprehensive, but the methodology differs slightly from what was used for this study so a complete comparison cannot be made. For the Wales Marine Planning portal layers, the source data had 32 evenly spaced sigma levels through depth, of which 5 independent levels were used to create the Atlas layers (ABPmer, 2008). In comparison, the layers created as part of this study were created using data that had depth averaged current velocity information. This shows that the source data for the layers was different, meaning that comparing the results wouldn't be accurate. One positive however is that the spatial results from both datasets correlate, with the pattern of the resource availability and also the spatial pattern of the mean spring and neap currents comparing between both datasets. This is encouraging as it shows that the layers that were created as part of this study agree well with data that has previously been created.

The data that has been created as part of this study also correlates very well with the tidal information that is available through the Irish Marine Atlas. There currently isn't a tidal resource layer available from the Irish Marine Atlas, but layers have been created to show the areas with tidal resource potential within Irish Waters. The areas that have been identified include the southeastern coast of Ireland around Arklow/Wexford and an aera off the northern coast of Donegal. This is in strong agreement with the tidal potential power layer that was created for this project, which shows areas of higher tidal power in these areas. The new layers that have been created as part of this study to show the tidal energy resource as well as the detailed layers showing the variability in the tidal currents will be hugely beneficial for tidal device site selection within Irish waters as the data is not currently freely available.

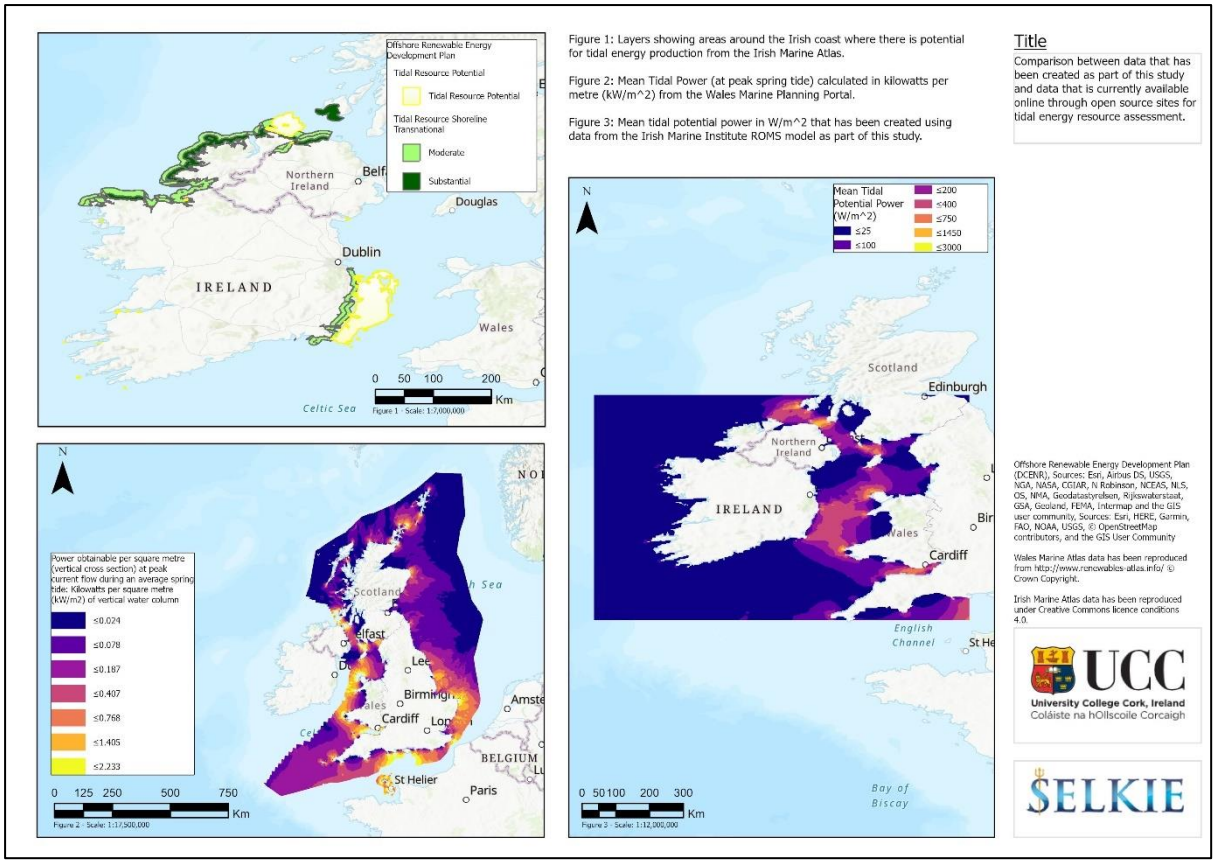



*Figure 4.31 Comparison between tidal energy resource dataset that has been created as part of this study and the datasets that are currently available through the Irish Marine Atlas and the Wales Marine Planning Portal.*

# 5 Conclusions and Recommendations

This section looks at the main conclusions of the study based on the aims and objectives that were outlined at the beginning. Following this it will review the methodology that was undertaken for the study and any limitations there may have been. Finally, it will make recommendations for future work.

- The first objective of this study was to develop a wave resource layer covering the study area of the west and north Atlantic coasts of Ireland as well as the Irish and Celtic Seas. The aim was to use two models from CMEMS, both at different resolutions with the objective of understanding which model works best for wave resource assessment. This objective has successfully been met, with wave resource layers having been developed using both the IBI and NWS models covering the study area. Both the NWS and IBI models proved to be very suitable for wave energy resource assessment at this location, with very good correlation seen between the results of both models at most locations (slightly lower correlation seen in coastal bays). The wave energy resource analysis was carried on from work that was completed by (O'Connell et al., 2020a) which showed that using the data products from CMEMS which contained data assimilation led to accurate and reliable wave energy analysis. The new datasets that have been created as part of this study used a much longer hindcast of 20 years, in comparison to 3 years from the (O'Connell et al., 2020a) study, which make the revised layers more reliable. The results of the wave energy analysis correspond well with work that has previously been done in the area, with the maximum resource potential seen of the western Irish coast, and with resource values decreasing downwards into the Celtic Sea and the lowest resource potential seen in the Irish Sea. Another benefit of this study is the increased study area, with the results now available for both Irish and UK waters.
- The second objective of this study was to carry out detailed seasonal analysis using a 20-year time series of data in order to understand the spatial and temporal patters in the wave resource, as well as in the significant wave heights and the wave periods for the study area. This goal has been accomplished, with layers having been created for both the IBI and NWS models that show the mean results for each season for the significant wave heights, the wave periods and the wave energy resource. The findings of the seasonal analysis showed that in general the largest mean significant wave heights and highest wave periods occur during the winter months, resulting in the largest wave energy resource being available during winter. Results for the months during spring and

autumn were largely similar with values being slightly lower than what was seen during the winter months, with the lowest values occurring during the summer months. Detailed information regarding these results can be seen in Section 4.1.2.

- The third aim was to develop a tidal resource layer covering the study area of the west and north Atlantic coasts of Ireland as well as the Irish and Celtic Seas. The aim was to develop the tidal resource layer using data from a model that is available through the Irish Marine Institute. This objective has been met, with a number of different layers having been developed in order to show the tidal resource for the study area. These layers include the mean tidal potential power, the total tidal potential power, the mean spring tidal power, the total spring tidal power, the mean neap tidal power and the total neap tidal power. These layers aim to give a comprehensive overview of the mean and total potential tidal power that is available for the study area. Based on the analysis the results show that the highest values for both mean and total tidal potential power are generally in the area within the Irish and Celtic Seas, with high values seen in the area between Northern Ireland and Scotland, between the Isle of Man and the mainland, within the Bristol Channel and around the areas of Holyhead and Pembrokeshire. Lower results are seen off the western coasts of Ireland in the Atlantic. For detailed results see section 4.2.2.
- The fourth objective was to carry out detailed analysis of the spring and neap tides to understand the spatial patterns for mean and maximum spring and neap tides for the study area. This objective has been met, with several layers having been created to show the tidal currents for the study area. The layers that have been created include the mean peak current velocity, the maximum peak current velocity, the maximum spring current velocity, the mean spring current velocity, the mean neap current velocity and the maximum neap current velocity. These six layers will give an understanding to the developers of the nature of the peak, spring and neap currents for the study area. The results that have been obtained show that the spatial trend for the tidal currents generally shows that the highest values can be seen within the Irish and Celtic Seas and in areas around headlands for example in the Bristol Channel and in the area between Northern Ireland and Scotland. The lower velocities are seen off the western coast of Ireland in the Atlantic. The trend also shows that the velocities are lower for the neap currents than for the spring currents. The spatial pattern of the current velocities is also reflected

in the results seen for the tidal energy resource layers, in that where there are high current velocities there tends to be higher resource values.

- The fifth objective of this study was to understand both the spatial and temporal nature of the wave and tidal energy resource for the study area. Based on the GIS layers that have been created and the analysis that has been undertaken as part of this study a better understanding of the nature of the wave and tidal energy resources has been gained for the Irish and UK EEZ's. The updated tidal resource assessment that has been completed as part of this study will provide valuable information to tidal device and project developers. The tidal information that has been developed as part of this study will be the first-time that data of its sort will be available for Irish coastal waters within an online GIS tool. As with the wave resource layers, the layers that have been developed with the tidal information cover both UK and Irish waters giving developers a detailed view of the study area. The work that has been carried out as part of this study has given a new up to date view of the nature of the wave and tidal energy resource availability within Irish and western UK waters. The detailed seasonal analysis of both the wave energy resource and the wave parameters (significant wave height and wave energy period) has been improved due to the longer hindcast that has been used as part of this study. The updated study area which now includes both Irish and western UK waters should be very beneficial to device developers when they are undertaking site suitability assessments, as it will provide them with information for the whole of the Irish and Celtic Seas as well as the western Irish coast.
- Finally, the last objective of this study was to determine the capacity for power production from both wave and tidal devices within the study area. The wave and tidal energy resource layers that have been developed were created to show the mean resource availability for the study area. These resource layers will be fed into further analysis work as part of the SELKIE project to determine the technical and accessible resource for a specific area.

## 5.1 Methodology

The methodology that has been developed as part of this project has proven to be an effective method of converting large oceanographic datasets into practical information in the source of GIS layers. The methodology that was developed for the wave resource assessment differed slightly from that of the tidal resource assessment due to the length of the hindcasts. For the

wave resource assessment, the datasets were complex, so processing of the data in both MATLAB and ArcGIS Pro was time consuming and computationally expensive (the datasets were large in size and any processing increased the size dramatically). The study area had to be split into cells of 1 degree x 1 degree in size in order to be downloaded, processed and converted to GIS layers. This method worked well for the study area, but if the study area was larger this process would be very time consuming and repetitive. Further work should be undertaken to better automate this process in the future so that larger study areas can be assessed.

The methodology that was defined for converting the MATLAB results to GIS layers has proven to be very effective. Outputting the data as a GeoTIFF file is a simple and quick process meaning that results can be viewed in GIS as a raster layer almost straight away. A GeoTIFF is also an open-source file type, meaning it can be viewed in any GIS software, not just ArcGIS Pro.

One point to note regarding the methodology is the size of the oceanographic data and the processing difficulties. As technology continues to develop and higher resolution data continues to become more easily available, we will continue to encounter these issues where datasets are almost too large to work with, the realm of 'Big Data'. Huge amounts of information can be extracted from these datasets, but we must fully understand how best to work with them computationally in order the obtain the optimum output. Future work should look at refining the methodology for working with large NetCDF datasets for computing wave energy resource with a long time series.

## 5.2 Data Limitations

While this study has provided new results for the study area which will be hugely beneficial for the offshore renewable energy industry, there have been some limitations to the work, which will be discussed below.

One of the main limitations has been the resolution of the model data that was available to complete both the wave and tidal analysis. For the wave analysis, two models were used from CMEMS. These two models were the highest resolution models that are currently available for the study area, but it has been noted that the resolution is not accurate enough for modeling near shore conditions.

Another limitation has been with the post processing of the data in both MATLAB and ArcGIS. The NetCDF files that were downloaded from CMEMS were very large (due to large study area and long hindcast) and post processing of the data was very time consuming.

## 5.3 Recommendations for future work

Based on the work that has been completed as part of this study and the limitations that have been identified there are a number of recommendations for future work.

The analysis that was undertaken as part of this study has shown that the grid resolution is most important when close to the shoreline. In particular, the comparison that was undertaken for the wave resource analysis with the IBI and NWS models has shown that the small variations in model resolution are most noticeable close to the shoreline and not in deeper waters. As a result of this it would be recommended for future work that higher resolution modelling be carried out at sites closer to the shoreline in order to obtain more accurate estimates of nearshore conditions. The resolution used for both the wave and tidal datasets for this study was > 1km so it would be advised that higher resolution modelling would be carried out at a test site close to the shore to test this.

In terms of the tidal work that was carried out, it was only possible to complete the analysis with one dataset, the ROMS model that was provided by the Irish Marine Institute. Analysis should be undertaken using data from a Copernicus Marine Service model that has been identified as being suitable for tidal energy resource assessment, the Atlantic - European North West Shelf - Ocean Physics Analysis and Forecast (Product Identifier: NWSHELF_ANALYSISFORECAST_PHY_LR_004_001). Determining the tidal energy resource using this data would allow a comparison to be carried out between it and the Irish Marine Institute ROMS model dataset. This work had been planned as part of this study but due to time constraints it was unable to be completed.

While this work has carried out seasonal analysis of the wave spectrum parameters and the tidal currents, it has not looked in depth at the occurrence of extreme events such as storms. In order to have a complete view of the conditions that are likely to occur at a site, in particular maximum events during winter months when storms are more likely, further work must be undertaken to model and analyze extreme events within the study area. Extreme analysis of the wave and tidal parameters should be undertaken so that a better understanding of site conditions

can be obtained. Parameters to look at would be extreme wave heights during each season, extreme wave periods etc.

The GIS layers that have been created as part of this study are 2-Dimensional in terms of time, meaning that they only show mean/max/min values, rather than a time series of data. It would be hugely beneficial for developers to be able to view parameters such as significant wave heights/wave periods or spring/neap current velocities as an interactive dataset that would change through time. This capability is relatively new to Online GIS and any future work should consider adding datasets that have time information to the Web-GIS tool in the form of a multidimensional raster dataset. Having the ability to view multidimensional data in an online GIS tool would enable developers to better understand the nature of the parameters as they change through the season, which would help them to plan for device maintenance schedules.

The datasets that have been created as part of this project are static, meaning that they will not be regularly updated in order to show the most up to date scenario. The CMEMS models that have been used to model the wave energy resource get updated bi-annually providing an additional six months to the hindcast. This means that in six months' time, the datasets that have been created as part of this study will technically be out of date. It would be recommended that an update schedule be developed so that the layers within the online GIS can be updated once new information is available via the Copernicus Models. It should also be noted within the layer metadata when the layer is technically 'out-of-date' so that the user knows that they are not looking at the most up to date version of the dataset.

# References

A Level Geographhy, 2018. *Waves*. [online] Available at: <https://www.alevelgeography.com/waves/> [Accessed 9 Oct. 2021].

ABPmer, 2008. *Atlas of UK Marine Renewable Energy Resources*. Atlas of UK Marine Renewable Energy Resources. Available at: https://www.renewables-atlas.info/

Arancha Amo Baladrón, Bruno Levier & Marcos García Sotillo, 2020. Product User ManualAvailable at: https://catalogue.marine.copernicus.eu/documents/PUM/CMEMS-IBI-PUM-005-006.pdf

Ainsworth, T. and Juneau, N., 2009. *"Significant Wave Height" A closer look at wave forecasts*. National Oceanic and Atmospheric Association. November 16, 2009. https://slideplayer.com/slide/7778637/

Anon 2021. *CMEMS*. [online] Available at: <https://resources.marine.copernicus.eu/?option=com_cswview=detailsproduct_id=IBI_MULTIYEAR_WAV_005_006> [Accessed 25 Aug. 2021].

Anon 2021. *Ireland's Marine Atlas*. [online] Available at: <https://atlas.marine.ie/#?c=53.9043:-15.8862:6> [Accessed 25 Jun. 2021].

Aquaret, 2008. *Aquaret*. [online] Available at: <https://aquaret.com/images/stories/aquaret/pdf/wven_red.pdf> [Accessed 14 Jun. 2021].

Aquaret, 2012a. *European Resource Map*. [online] Available at: <https://aquaret.com/index525f.html?option=com_content&view=article&id=136&Itemid=279&lang=en>.

Aquaret, 2012b. *Wave Technologies*. [online] Available at: <https://aquaret.com/indexea3d.html?option=com_content&view=article&id=203&Itemid=344&ang=en#Animations>.

Atan, R., Goggins, J. and Nash, S., 2018. Galway Bay – The 1/4 scale wave energy test site? A detailed wave energy resource assessment and investigation of scaling factors. *Renewable Energy*, 119, pp.217-234.

AWS Ocean Energy, 2021a. *Archimedes Waveswing - AWS Ocean Energy*. [online] Available at: <https://www.awsocean.com/archimedes-waveswing/> [Accessed 18 Oct. 2021].

AWS Ocean Energy, 2021b. *Gallery - AWS Ocean Energy*. [online] Available at: <https://www.awsocean.com/project-gallery-nwec-iii/> [Accessed 12 Oct. 2021].

Blunden, L.S. and Bahaj, A.S., 2007. Tidal energy resource assessment for tidal stream generators: *http://dx.doi.org/10.1243/09576509JPE332*, [online] 221(2), pp.137–146. https://doi.org/10.1243/09576509JPE332.

Bombora, 2020. *Global potential for wave*. [online] Available at: <https://bomborawave.com/wave-energy/>.

British Crown and OceanWise Ltd, 2020. *Wales Marine Planning Portal*. [online] Available at: <http://lle.gov.wales/apps/marineportal/#lat=52.5630&on=-4.2737&z=7&tgt=false&layers=390,231,62> [Accessed 11 Oct. 2021].

Cahill, B. and Lewis, T., 2014. *Wave Period Ratios and the Calculation of Wave Power*. *Marine Energy Technology Symposium*. Proceedings of the 2nd Marine Energy Technology Symposium METS2014 April 15-18, 2014, Seattle, WA.

Celtic Sea Power, 2021. *Renewable energy technology test site in Pembrokeshire, South Wales*. [online] Available at: <https://www.celticseapower.co.uk/our-projects/pembrokeshire-wave-zone> [Accessed 11 Oct. 2021].

Charlier, R.H., 2003. A “sleeper” awakes: Tidal current power. *Renewable and Sustainable Energy Reviews*, 7(6), pp.515–529. https://doi.org/10.1016/S1364-0321(03)00079-0.

Copernicus, 2021. *Data | Copernicus Marine*. [online] Available at: <https://resources.marine.copernicus.eu/products> [Accessed 11 Oct. 2021].

DP Energy, 2021. *N. Ireland: Fair Head Tidal Energy Park - North Antrim Coast - DP Energy - Energy is in our nature*. [online] Available at: <https://www.dpenergy.com/projects/wind/n-ireland-fair-head-tidal-energy-park-north-antrim-coast/> [Accessed 24 Aug. 2021].

EMEC, 2021a. *Flumill : EMEC: European Marine Energy Centre*. [online] Available at: <https://www.emec.org.uk/about-us/our-tidal-clients/flumill/> [Accessed 12 Oct. 2021].

EMEC, 2021b. *Kawasaki Heavy Industries : EMEC: European Marine Energy Centre*. [online] Available at: <http://www.emec.org.uk/about-us/our-tidal-clients/kawasaki-heavy-industries/> [Accessed 23 Jun. 2021].

EMEC, 2021c. *Marine Energy*. [online] Available at: <http://www.emec.org.uk/marine-energy/> [Accessed 24 Jun. 2021].

EMEC, 2021d. *Tidal devices : EMEC: European Marine Energy Centre*. [online] Available at: <http://www.emec.org.uk/marine-energy/tidal-devices/> [Accessed 23 Jun. 2021].

Environmental Systems Research Institute, Inc., 2016. *What is raster data?—Help | ArcGIS for Desktop*. [online] Available at: <https://desktop.arcgis.com/en/arcmap/10.3/manage-data/raster-and-images/what-is-raster-data.htm> [Accessed 13 Jul. 2021].

European Union, 2021. *European Atlas of the Seas*. [online] Available at: <https://ec.europa.eu/maritimeaffairs/atlas/maritime_atlas/#lang=EN;p=w;bkgd=5;theme=4:0.75;c=1224514.3987259883,6446275.841017013;z=4> [Accessed 11 Oct. 2021].

Falcão, A.F.O. and Henriques, J.C.C., 2016. Oscillating-water-column wave energy converters and air turbines: A review. *Renewable Energy*, 85, pp.1391–1424. https://doi.org/10.1016/J.RENENE.2015.07.086.

Folley, M., Babarit, A., Child, B., Forehand, D., O'boyle, L., Silverthorne, K., Spinneken, J., Stratigaki, V. and Troch, P., 2012. *A Review of Numerical Modelling of Wave Energy Converter Arrays.* [online] Available at: <http://www.asme.org/about-asme/terms-of-use>.

Gleizon, P., Campuzano, F., Carracedo, P., Martinez, A., Goggins, J., Atan, R. and Nash, S., 2017. Wave energy resources along the European Atlantic Coast. In: *Marine Renewable Energy: Resource Characterization and Physical Effects*. Springer International Publishing.pp.37–69. https://doi.org/10.1007/978-3-319-53536-4_2.

Guillou, N., Lavidas, G. and Chapalain, G., 2020. *Wave Energy Resource Assessment for Exploitation—A Review*. J. Mar. Sci. Eng. 2020, 8(9), 705; https://doi.org/10.3390/jmse8090705

Hendershott, M., 2004. *Lecture 1: Introduction to ocean tides*. Woods Hole Oceanographic Institute, Tech Report., WHOI-2005-08.

Hofer, B., 2014. Uses of online geoprocessing technology in analyses and case studies: a systematic analysis of literature. *http://dx.doi.org/10.1080/17538947.2014.962632*, [online] 8(11), pp.901–917. https://doi.org/10.1080/17538947.2014.962632.

Investopedia. 2022. *What a Z-Score Tells Us*. [online] Available at: <https://www.investopedia.com/terms/z/zscore.asp#:~:text=What%20Is%20a%20Z%2DScore,identical%20to%20the%20mean%20score.> [Accessed 26 April 2022].

Langlee Wave Power AS, 2013. *Media Centre | Langlee Wave Power*. [online] Available at: <http://www.langleewp.com/?q=media-centre> [Accessed 12 Oct. 2021].

Lavelle, John & Kofoed, J., 2021. *Experimental Testing of the Langlee Wave Energy Converter*. [online] Available at: <https://www.researchgate.net/publication/267863519_Experimental_Testing_of_the_Langlee_Wave_Energy_Converter> [Accessed 9 Aug. 2021].

Lewis, M., Neill, S.P., Robins, P.E. and Hashemi, M.R., 2015. Resource assessment for future generations of tidal-stream energy arrays. *Energy*, [online] 83, pp.403–415. https://doi.org/10.1016/j.energy.2015.02.038.

Malczewski, J., 2007. GIS-based multicriteria decision analysis: a survey of the literature. *https://doi.org/10.1080/13658810600661508*, [online] 20(7), pp.703–726. https://doi.org/10.1080/13658810600661508.

Marine Energy Wales, 2020. *The Resource | Marine Energy Wales*. [online] Available at: <https://www.marineenergywales.co.uk/marine-energy-in-wales/the-resource/> [Accessed 11 Oct. 2021].

Marine Institute, 2005. *Irish Spatial Data Exchange - Marine Institute*. [online] Available at: <https://www.isde.ie/geonetwork/srv/eng/catalog.search#/metadata/8b10d123-1e3a-42e7-90fa-dba4974cbfe1> [Accessed 25 Jun. 2021].

Marine Institute, 2015. *Ireland's Marine Atlas*. [online] Available at: <https://atlas.marine.ie/#?c=53.9043:-15.8643:6> [Accessed 11 Oct. 2021].

Marine Institute, 2020. *Ocean Forecasts | Marine Institute*. [online] Available at: <http://www.marine.ie/Home/site-area/data-services/marine-forecasts/ocean-forecasts> [Accessed 25 Jun. 2021].

Minesto AB, 2021a. *Holyhead Deep – the world's first low-flow tidal stream project | Minesto*. [online] Available at: <https://minesto.com/projects/holyhead-deep> [Accessed 26 Aug. 2021].

Minesto AB, 2021b. *Ocean Energy | Minesto*. [online] Available at: <https://minesto.com/ocean-energy> [Accessed 11 Oct. 2021].

Minesto AB, 2021c. *Project and technology development | Minesto*. [online] Available at: <https://minesto.com/projects> [Accessed 24 Jun. 2021].

Morlais Energy, 2021. *Morlais | Anglesey Marine Energy*. [online] Available at: <https://www.morlaisenergy.com/> [Accessed 26 Aug. 2021].

NOAA, 2021. What are tides? [online] Available at: <https://oceanservice.noaa.gov/facts/tides.html> [Accessed 22 Jun. 2021].

Ocean Energy - Europe, 2021. *Wave Energy*. [online] https://www.oceanenergy-europe.eu/ocean-energy/wave-energy/. Available at: <https://www.oceanenergy-europe.eu/ocean-energy/wave-energy/>.

OceanEnergy, 2020a. *Air Turbine Technology* . [online] Available at: <https://oceanenergy.ie/air-turbine-technology/> [Accessed 11 Oct. 2021].

OceanEnergy, 2020b. *OE35 - OceanEnergy*. [online] Available at: <https://oceanenergy.ie/oe35/> [Accessed 11 Oct. 2021].

O'Connell, R., de Montera, L., Peters, J.L. and Horion, S., 2020a. An updated assessment of Ireland's wave energy resource using satellite data assimilation and a revised wave period ratio. *Renewable Energy,* 160, pp.1431–1444. https://doi.org/10.1016/j.renene.2020.07.029.

O'Connell, R., de Montera, L., Peters, J.L. and Horion, S., 2020b. An updated assessment of Ireland's wave energy resource using satellite data assimilation and a revised wave period ratio. *Renewable Energy,* 160, pp.1431–1444. https://doi.org/10.1016/j.renene.2020.07.029.

O'Halloran, B., 2020. Baby, it's cold outside: Electricity consumption hits record high. [online] Available at: <https://www.irishtimes.com/business/energy-and-resources/baby-it-s-cold-outside-electricity-consumption-hits-record-high-1.4427946 >.

O'Rourke, F., Boyle, F. and Reynolds, A., 2010. Tidal current energy resource assessment in Ireland: Current status and future update. *Renewable and Sustainable Energy Reviews*, [online] 14(9), pp.3206–3212. https://doi.org/10.1016/j.rser.2010.07.039.

Paul Webb, 2021. *11.3 Tide Classification – Introduction to Oceanography*. [online] Available at: <https://rwu.pressbooks.pub/webboceanography/chapter/11-3-tide-classification/> [Accessed 11 Oct. 2021].

Regen, 2019. *Energy Generation in Wales*. [online] Available at: <https://gov.wales/sites/default/files/publications/2019-10/energy-generation-in-wales-2018.pdf> [Accessed 10 Dec. 2020].

Sabella, 2021. *Photos | Sabella*. [online] Available at: <https://www.sabella.bzh/en/media-center/photos> [Accessed 12 Oct. 2021].

Santo, H., Taylor, P.H. and Stansby, P.K., 2020. The performance of the three-float M4 wave energy converter off Albany, on the south coast of western Australia, compared to Orkney (EMEC) in the U.K. *Renewable Energy*, [online] 146, pp.444–459. https://doi.org/10.1016/J.RENENE.2019.06.146.

SEAI, 2004. Tidal & Current Energy Resources in Ireland. Available at: https://www.seai.ie/publications/Tidal_Current_Energy_Resources_in_Ireland_Report.pdf

Simec Atlantis, 2021. SeaGen-S 2MW Proven and commercially viable tidal energy generation. Available at: https://simecatlantis.com/2019/07/26/meygen-operational-update-3-2/

Tethys, 2021. *Wave Dragon Pre-Commercial Demonstration Project | Tethys*. [online] Available at: <https://tethys.pnnl.gov/project-sites/wave-dragon-pre-commercial-demonstration-project> [Accessed 12 Oct. 2021].

The Liquid Grid, 2018. *Wave Energy Converters*. https://theliquidgrid.com/marine-clean-technology/wave-energy-converters/.

Tonani, M. & Saulter, A., 2021. Product User Manual for NWS Ocean Waves Reanalysis Product NWSHELF_REANALYSIS_WAV_004_015. Issue: 1.1

Tucker, M. and Pitt, E., 2001. *Waves in ocean engineering.* Amsterdam: Elsevier.

Wave Dragon, 2017. *Technology*. [online] Available at: <https://www.wavedragon.co.uk/technology-2/> [Accessed 27 Sep. 2021].

Webb, P., 2021a. *11.1 Tidal Forces*. "Tidal Forces" by Paul Webb, Available at: https://geo.libretexts.org/@go/page/4458

Webb, P., 2021b. *11.3 Tide Classification*. "Tide Classification" by Paul Webb, Available at: https://geo.libretexts.org/@go/page/4460 [Accessed April 26, 2022].

Wello, 2021. *The Penguin - Wello Oy*. [online] Available at: <https://wello.eu/the-penguin-2/> [Accessed 11 Oct. 2021].

WP Marine, 2021. *Tidal Stream Energy*. [online] Available at: <http://www.esru.strath.ac.uk/EandE/Web_sites/10-11/Tidal/tidal.html> [Accessed 25 Jun. 2021].

Zhao, P., Foerster, T. and Yue, P., 2012. The Geoprocessing Web. *Computers and Geosciences*, 47, pp.3–12. https://doi.org/10.1016/J.CAGEO.2012.04.021.

# Appendix

## 1 - Publication of Paper related to research

Proceedings of the 14th CoastGIS International Symposium
CoastGIS 2021
16-17 September 2021, Raseborg, Finland

### An assessment of newly available Copernicus sea surface wave products for mapping wave energy in Irish and UK waters

Ross O'Connell, Rebecca Furlong

MaREI Centre for Marine and Renewable Energy, Beaufort Building, Environmental Research Institute, University College Cork, Ringaskiddy, Ireland

ross.oconnell@ucc.ie| rebecca.furlong55@gmail.com

**Abstract**

Accurate and up-to-date wave energy resource assessments are crucial to wave energy project developers. High resolution products for representing sea surface wave parameters in European waters are now available via the Copernicus Marine Environment Monitoring Service (CMEMS). Here, the accuracy of two such products is assessed against in-situ wave buoy measurements at specific sites of interest to the wave energy sector. Each product is then used to map the parameters pertinent to the wave energy sector, these are; the significant wave height and the wave energy period. Based on these parameters, a spatial calculation of the wave energy resource is performed using both products for comparison and spatio-temporal analysis. The study area focused on Irish and Western UK waters and the time series of data used was 20 years. In the accuracy assessment, both models perform well overall for representing both parameters. The overall difference in significant wave height bias between the two products is found to be on the order of 8 cm, and the difference in wave energy period is 0.02 s. Spatially, the highest resource values were seen along the west coast of Ireland, particularly the northwest, and the temporal analysis revealed winter to be the season with the most abundant resource. This work can be used to inform wave energy farm site selection and project feasibility analysis.

## Introduction

High resolution data that is currently available through the Copernicus Marine Monitoring Service (CMEMS) is invaluable when it comes to the future of wave energy resource assessments. This study aims to show how wave parameters from two of the Copernicus numerical wave models can be used to carry out a high resolution wave energy resource assessment, with the aim of converting the data into GIS layers so that they can be used in multi-criteria decision analysis tools such as the Web-GIS tool that this being developed as part of the SELKIE wave and tidal energy project. CMEMS provides datasets from different numerical models which have been developed using *in-situ* measurements, altimeter and satellite data. The data is now available for a range of oceanographic parameters including significant wave height and wave period. Long hindcasts of more than twenty years at different time steps, usually one or three hourly, can be selected.

## Data and Methodology

### Model Data

Two products were identified to be suitable for the wave energy resource assessment in this study. The first was Atlantic – Iberian Biscay Irish – Ocean Wave Reanalysis (Product Identifier - IBI_MULTIYEAR_WAV_005_006). The model is based on the MFWAM model developed by Meteo-France (MF). It is fed by the ERA 5 reanalysis wind data from ECMWF, covers the extents 19°W – 5°W; 56°N – 26°N and has a spatial resolution of 0.05degree x 0.05degree, or ~ 3 to 5 km. The second product that was identified to be suitable for the wave resource modelling was the Atlantic – European North West Shelf – Wave Physics Reanalysis model. This model gives a hindcast for the European Northwest Shelf area beginning from 1980 – 01 – 01 to Present. The underlying wave model is WaveWatch III, which covers the extents of 16°W – 13°W; 62.75°N – 46°N and the resolution is 0.017degree x 0.017degree, or ~ 1.5 to 3 km.

### *In-Situ* Data

The *in-situ* data for the accuracy assessment was derived from three separate buoys that were independent of the model, i.e. the data was not fed into either of the models. The location of each in the context of the study area is shown in Fig. 1. The data from the WestWave buoy was derived from the Marine Institute (2021), the data from West Pembrokeshire was derived from CEFAS (2021), and the

data from WaveHub was obtained through the NNRCMP (2021). A one-year time-series for each was downloaded for each point.

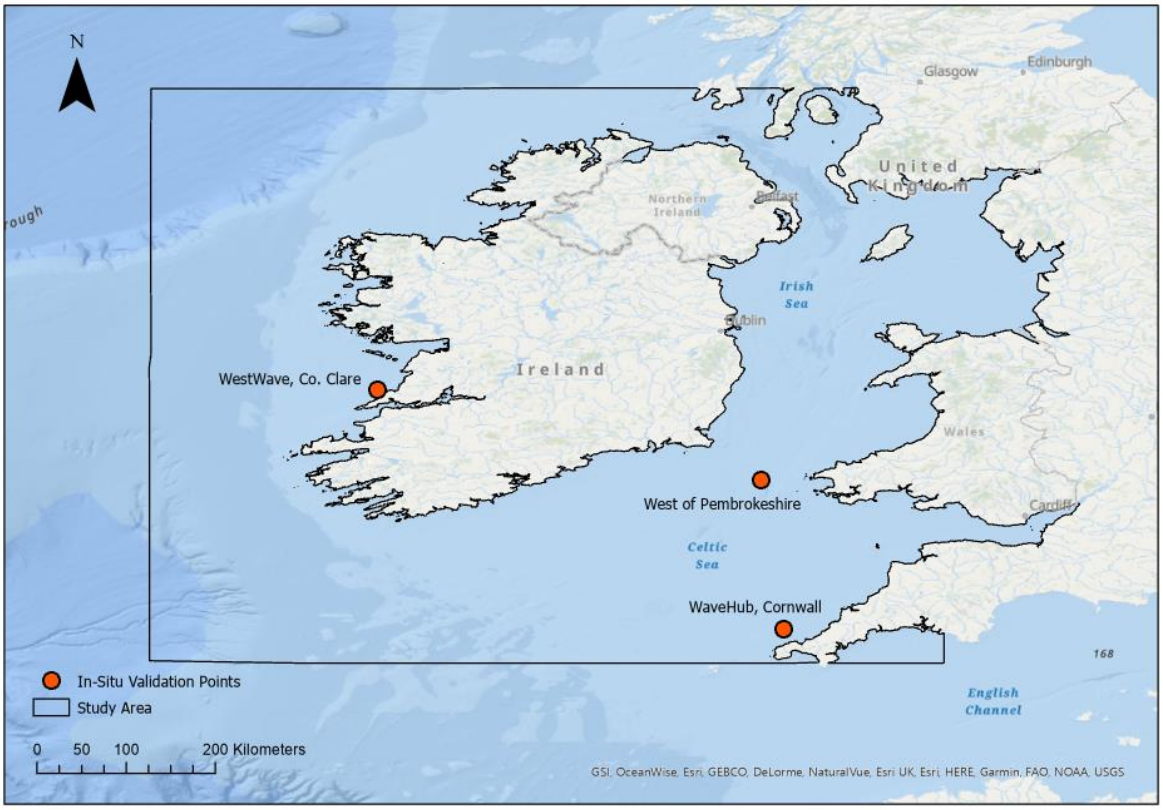



**Fig. 1.** Extent of the study area and location of the *in-situ* validation points.

Resource Computation

The variables that affect wave energy are the significant wave height ($H^2m0$) and wave energy period ($T_e$) (O'Connell et al., 2020b). The theoretical wave power resource was calculated using the 20 year hindcast of $H^2m0$ and $T_e$ data from both the NWS and IBI models discussed above. Both the average annual average wave power and seasonal average wave power were computed using these parameters. The theoretical wave power was calculated using the following equation from (Cahill and Lewis, 2014):

$$P = 0.49\, H^2 m0\, T_e \quad (1)$$

where P is the power per unit width of wave crest.

Validation

The *in-situ* data was compared against the grid of model data closest to the coordinates of each validation site using a co-location script in MATLAB. Only the data closest in time to each other, and no more than 30 minutes apart, was selected for the comparison. The bias (Equation 2), root mean square error (RMSE; Equation 3), scatter index (SI; Equation 4) and correlation coefficient (*R*; Equation 5) were then calculated for each.

$$Bias = \frac{1}{N}\sum_{i=1}^{N} e_i \quad (2)$$

$$RMSE = \sqrt{\frac{1}{N}\sum_{i=1}^{N} {e_i}^2} \quad (3)$$

$$SI = \frac{RMSE}{U} \quad (4)$$

$$R = \frac{1}{\sigma_U \sigma_u (N-1)} \sum_{i=1}^{N} (U_i - U)(u_i - u) \quad (5)$$

where $U$ and $u$ denote the mean of the *in-situ* and modelled significant wave height or wave period respectively, $\sigma_U$ and $\sigma_u$ their standard deviations, and $N$ the number of match up samples/data pairs.

**Results**

Theoretical Wave Energy Resource

The results of the theoretical wave power resource modelling can be seen in Fig. 2 below. Both models show a similar spatial trend with the resource being greatest off the Northwest coast of Ireland. High values are also notable off the west and southwest coasts of Ireland. The resource can be seen to reduce in magnitude with increasing proximity to land in all areas. A reduction in power can be seen moving along the Celtic Sea northwards into the Irish Sea. Power values off the west coast of Ireland tend to be between 50-72 kW/m, with those in the Irish Sea being generally less than 10 kW/m. There is a difference of ~2 kW/m seen between the two models, with the maximum value from the NWS model being 70.8 kW/m and the highest value from the IBI model being 72.3 kW/m, which proves good agreement between both datasets. However, one area with a difference in the results is along the coasts, where the finer grid cells of the NWS model show more detail in coastal areas. The contours from both datasets can be seen to be trending almost North – South in the Atlantic off the Western Irish coast, with wave power values decreasing to the east.

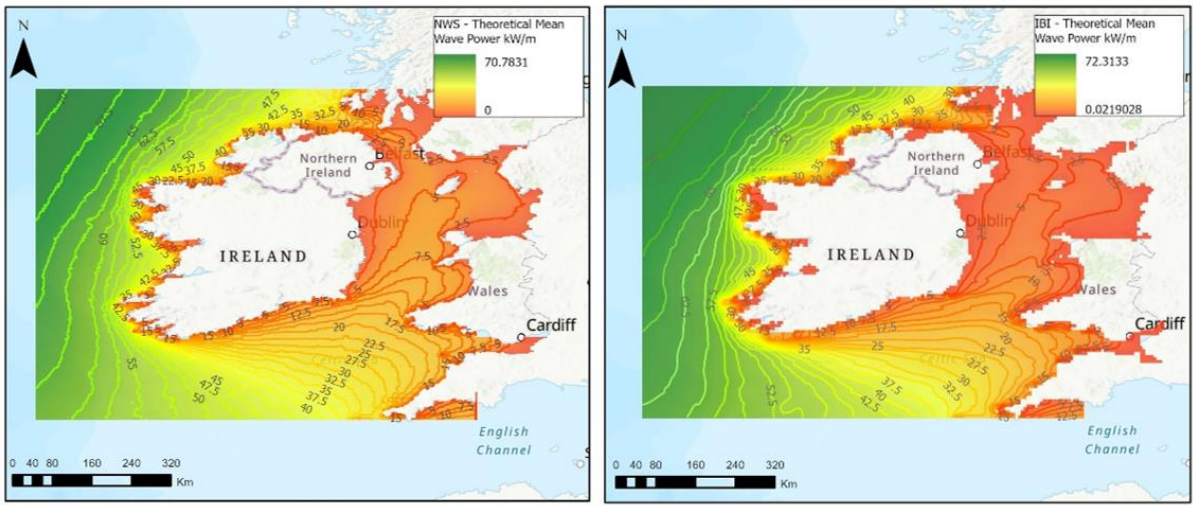



**Fig. 2.** Theoretical Wave Power Resource from both the NWS and IBI models.

Seasonality of the Wave Energy Resource

The results of the seasonal modelling can be seen in Fig. 3 and Fig. 4 below. For both models, the resource is seen to be most abundant in winter months of December, January, and February, with maximum values of 134.4 kW/m for the NWS model and 140 kW/m for the IBI model being observed off the Northwest coast of Ireland for this period. The resource values for each model in both Spring (March, April and May) and Autumn (September, October and November) are very similar, with 50-70 kW/m seen off the west coast of Ireland, though slightly higher along coastal areas for the NWS model, again likely due to the finer resolution. The same spatial trend of the highest values presenting off the Northwest coast of Ireland persists for these periods. The Summer months of June, July and August show the lowest wave power resource for both models, with the highest value of ~ 20 kW/m seen again off the Northwest coast of Ireland and values in the Irish and Celtic seas not exceeding 15 kW/m. The greatest variability can be seen between the seasons of Winter and Summer, with a variance of ~100 kW/m evident off the Northwest coast of Ireland.

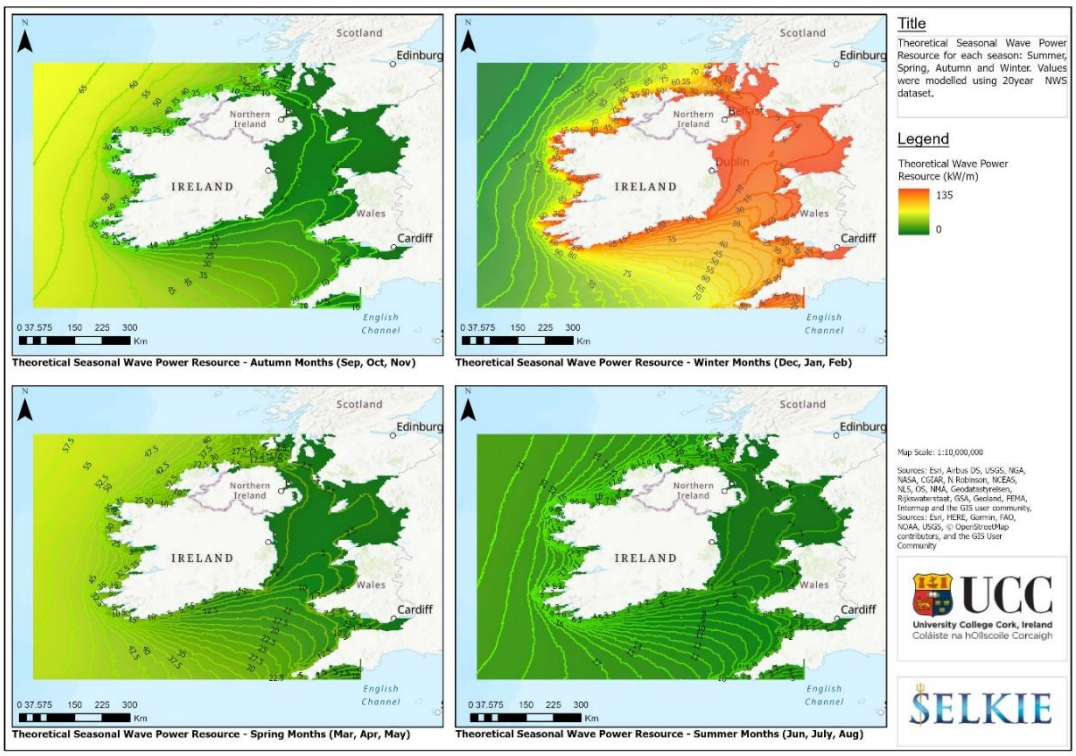



**Fig. 3.** Seasonal modelling of the theoretical wave power resource using data from the NWS model.

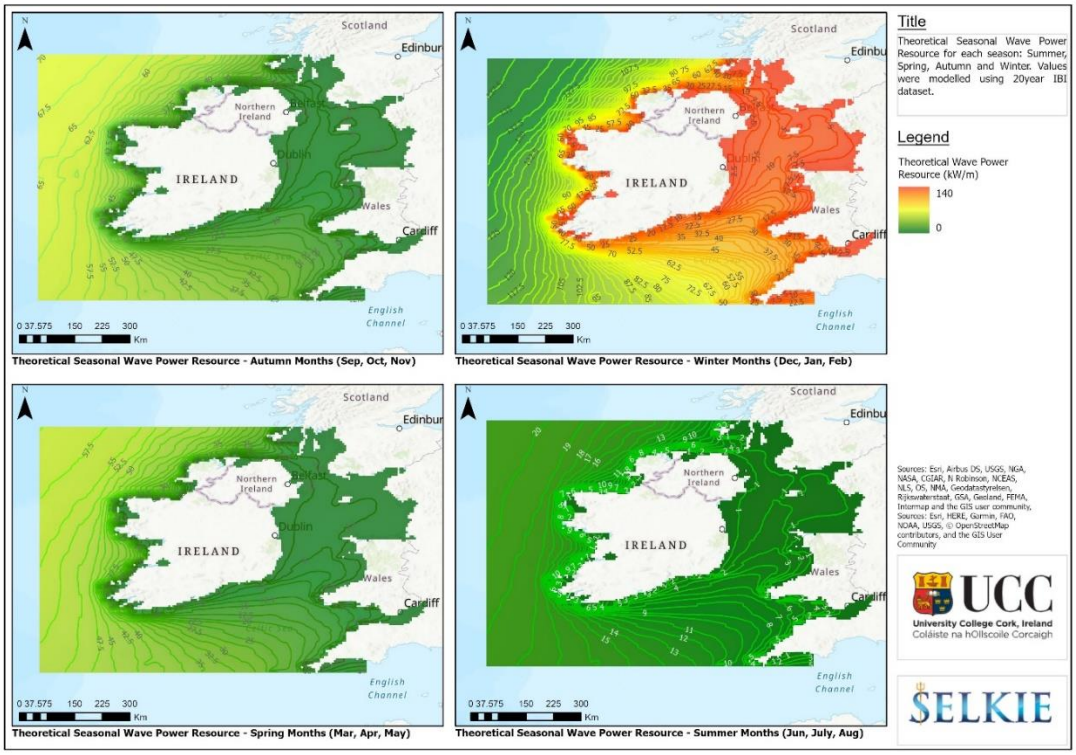



**Fig. 4.** Seasonal modelling of the theoretical wave power resource using data from the IBI model.

## Accuracy Assessment

A strong correlation between the modelled significant wave height and the measured significant wave height was observed with each of the two products. The average significant wave height correlation coefficient across the three sites was 0.97 for both models (Table 1). Despite having the same overall *R* value, the RMSE for the IBI product was slightly greater than that of the NWS product with values of 0.35m and 0.31m, respectively. The NWS product also had the lowest overall significant wave height bias at 0.11 compared to 0.20 for the IBI product, and the lowest overall significant wave height SI at 0.16 compared to 0.18. Despite this, the overall bias, RMSE, SI and *R* values did not show much differentiation in value between the two products. Also noteworthy in terms of bias is that none of the products are overpredicting the mean significant wave height at any of the three validation points. Overall, both products systematically showed very accurate significant wave height results for all of the selected accuracy indicators. The scatterplot diagrams also testify to this, with very good agreement evident for both the NWS model in Fig. 4(a) and the IBI model in Fig. 4(b).

**Table 1.** Accuracy assessment results for (a) the NWS product and (b) the IBI product: results are shown for significant wave height and wave energy period.

(a)

| Significant Wave Height | | | | | |
|---|---|---|---|---|---|
| Buoy | $\bar{x}$ (m) | Bias (m) | RMSE | SI | *R* |
| WestWave | 2.3497 | 0.2399 | 0.4175 | 0.1777 | 0.9739 |
| WaveHub | 1.9881 | 0.0256 | 0.2666 | 0.1341 | 0.9729 |
| WestPem | 1.6660 | 0.0625 | 0.2582 | 0.1549 | 0.9709 |
| Wave Energy Period | | | | | |
| Buoy | $\bar{x}$ (s) | Bias (s) | RMSE | SI | *R* |
| WestWave | 7.1070 | -0.4990 | 0.8882 | 0.1250 | 0.8876 |
| WaveHub | 5.8662 | 0.1394 | 0.6752 | 0.1151 | 0.8932 |
| WestPem | 4.9107 | 0.4419 | 0.7517 | 0.1531 | 0.8853 |

(b)

| Significant Wave Height | | | | | |
|---|---|---|---|---|---|
| Buoy | $\bar{x}$ (m) | Bias (m) | RMSE | SI | *R* |
| WestWave | 2.2447 | 0.3459 | 0.4773 | 0.2126 | 0.9807 |
| WaveHub | 1.9271 | 0.0879 | 0.2846 | 0.1477 | 0.9721 |
| WestPem | 1.5824 | 0.1441 | 0.2959 | 0.1870 | 0.9715 |
| Wave Energy Period | | | | | |
| Buoy | $\bar{x}$ (s) | Bias (s) | RMSE | SI | *R* |
| WestWave | 7.1867 | -0.5784 | 0.8828 | 0.1228 | 0.9134 |
| WaveHub | 6.1137 | -0.1081 | 0.7410 | 0.1212 | 0.8923 |
| WestPem | 5.0130 | 0.3340 | 0.7170 | 0.1430 | 0.8754 |

The agreement between modelled wave period and observed wave period was slightly lower than that of the significant wave height, with overall *R* values of 0.88 for both the NWS and IBI products (Table 1). The overall RMSE was very slightly lower for the NWS product at 0.77 compared to 0.78 for the IBI product. Unlike with significant wave height, the models were underestimating wave energy period values as shown with the negative bias values for both products at the WestWave site, and also at the WaveHub site for the IBI product. The overall wave energy period SI was 0.13 for both models. Both products show accurate wave energy period results across the study area for each of the indicators assessed, again evident in the scatterplots (Fig. 5).

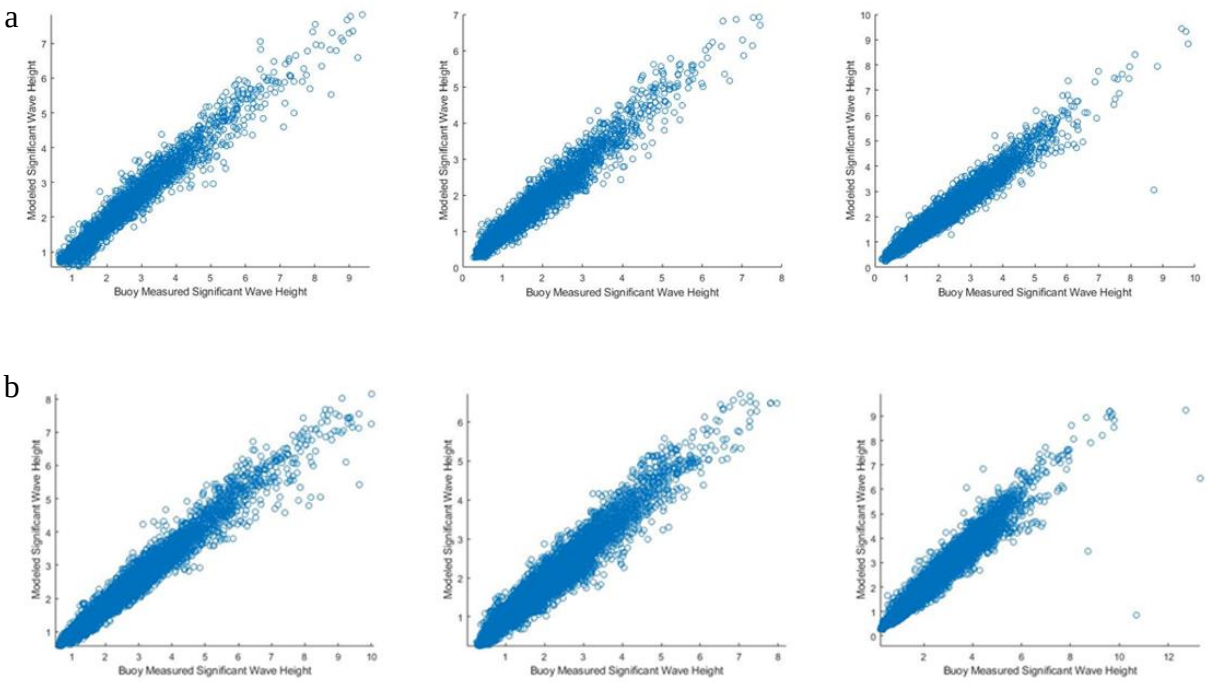



**Fig. 4.** Scatterplot diagrams for modelled v buoy measured significant wave height at each site for (a) the NWS model and (b) the IBI model.

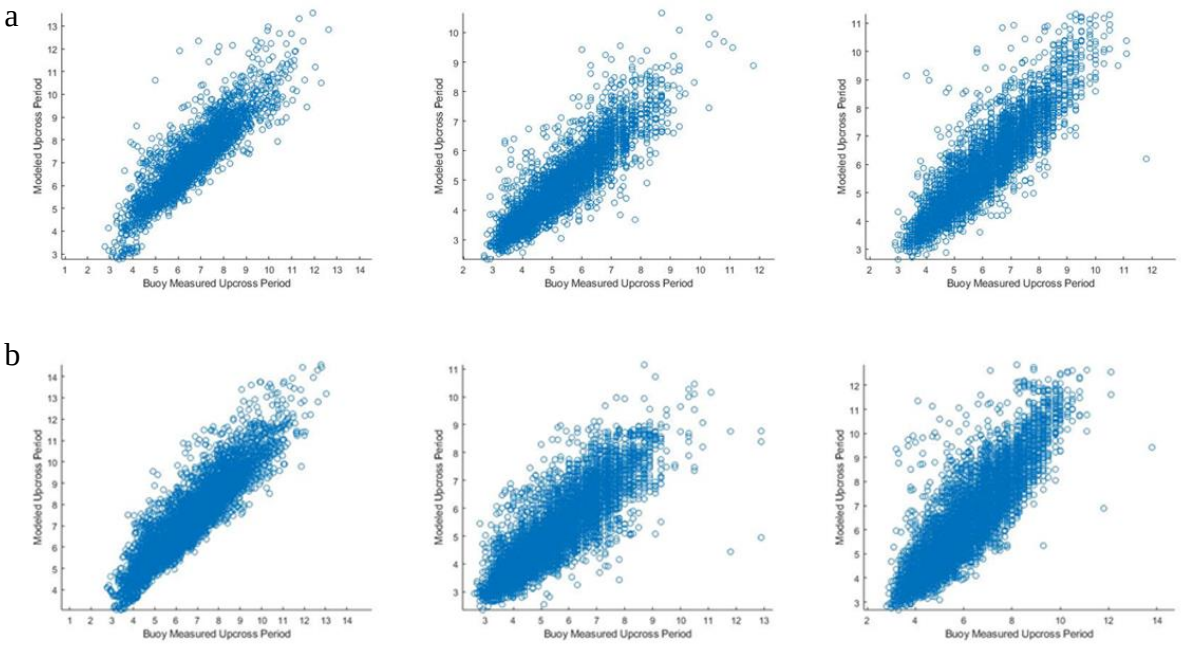



**Fig. 5.** Scatterplot diagrams for modelled v buoy measured wave energy period at each site for (a) the NWS model and (b) the IBI model.

**Discussion and Conclusion**

Modelling of the wave power resource using freely available data from CMEMS has proven to be very effective. Results from both models strongly correlate with each other, and with the in-situ data. This data is openly available and easy to download, which should make wave resource modelling more accessible. It is also available at high resolutions, <3km in some cases, and with long hindcasts (>20 years), allowing for this and future wave resource modelling to represent the wave climate closer to the coast than with previous Copernicus models, and with greater consideration of historic wave climatic patterns. Modelling the wave data and then converting to GIS layers allows the users to gain a thorough understanding of the spatial nature of the data. Spatial analysis of the results in GIS has shown that the greatest resource availability is in the North Atlantic off the West coast of Ireland (particularly the Northwest), with lower values seen in the Celtic Sea and into the Irish Sea.

Waves are generated when winds blow over the ocean, and one parameter that leads to larger more powerful waves is the fetch (the distance the wind travels over the ocean). In agreement with this, the wave resource proved to be most abundant where this fetch is greatest, i.e. off Atlantic coasts. Having these layers available means that developers can now take a first pass look at sites to decide if they have potential, while gaining a better understanding of not just the resource value, but also its associated parameters and seasonal changes. This information would inform developers as to times when the resource availability is likely to be higher (e.g. in Winter months where wave heights are higher and periods are longer), and also when and where it is more likely to be difficult to access the device for maintenance due to storm conditions or when the device is likely to go into 'survival mode', the latter requiring further computation in MATLAB, but for which the same data could be used.

The time series that has been used to create these layers will also give more reliability to the robustness of the results, with 20 years of data (>175,000 time steps) giving a good understanding of the wave climate by taking into account intra-annual alterations in significant wave heights and wave periods. Analysis that has not been taken into account, and perhaps would be worth looking at in the future, is the effect of climate change and how it may lead to larger storms and increasing significant wave heights (Wolf and Woolf, 2006), which in turn can have an effect on the wave resource and the viability of a device at a specific location.

The aim of having data such as the wave resource GIS layers that have been created as part of this project is so that they can be added to an open access Web-GIS tool that will allow users to take a first-glance look at choosing sites for offshore renewable energy. Wave energy has been identified as a possible future source of clean energy for both Ireland and the UK, but it is still at the pre-commercial stage. Therefore, data such as this is likely to benefit those interested in entering this energy market in the years to come. The work gives a broad view of the study area so that sites can be selected, but higher resolution modelling at an even finer grid scale (sub – kilometer) could be completed once a specific site has been selected. However, the data modelling of the wave energy resource on such a scale can be computationally expensive and complex to carry out, therefore in order to carry out any higher resolution modelling, it would be advisable to only do so for a much smaller study area.

The accuracy assessment proved that the models are generally agreeing well with the observed *in-situ* data from the met-ocean buoys. It is apparent that the agreement is slightly better for the NWS product than the IBI product, possibly owing to the finer resolution of the former. With both products, there appears to be better agreement between modelled and measured data for significant wave height than wave period, the reasons for which are unknown to the authors. One potential reason for this with the IBI model is that data assimilation from satellites is being used for the modelling of significant wave height but not for wave period, a theory discussed in a study by O'Connell et al. (2020). However, this does not explain the same pattern of results seen with the NWS product, since satellite data assimilation is not being performed for significant wave height modelling there. Although the validation results proved a high level of accuracy, the WestWave site generally produced the least accurate results of the

three sites for both products representing both parameters (significant wave height and wave period). This may be explained by the fact that the WestWave site is that closest to the coast, leading to the slightly poorer representation of coastal processes (i.e. difficulty to account for coastal sheltering) in comparison to offshore processes.

**Acknowledgements**

This research has been undertaken as part of the SELKIE project, a €4.2m cross-border project aiming to boost the marine energy industry in Wales and Ireland. The project has been funded under the European Regional Development Fund. The data received from CMEMS as well as the technical support from the team there was imperative to the success of this work. Data and/or assistance provided the Irish Marine Institute, the Channel Coastal Observatory and CEFAS is also gratefully acknowledged.

**References**

Cahill, B., andsnd Lewis, T. (2014). WAVE PERIOD RATIOS AND THE CALCULATION OF WAVE POWER. In *Marine Energy Technology Symposium*.

CEFAS (2021) *Cefas - WaveNet interactive map* [online] Available at: <http://wavenet.cefas.co.uk/Map> [Accessed 1 July 2021].

*CMEMS*. (n.d.-a). Retrieved August 25, 2021, from https://resources.marine.copernicus.eu/?option=com_cswandsndview=detailsandsndproduct_id=NWSHELF_REANALYSIS_WAV_004_015

*CMEMS*. (n.d.-b). Retrieved August 25, 2021, from https://resources.marine.copernicus.eu/?option=com_cswandsndview=detailsandsndproduct_id=IBI_MULTIYEAR_WAV_005_006

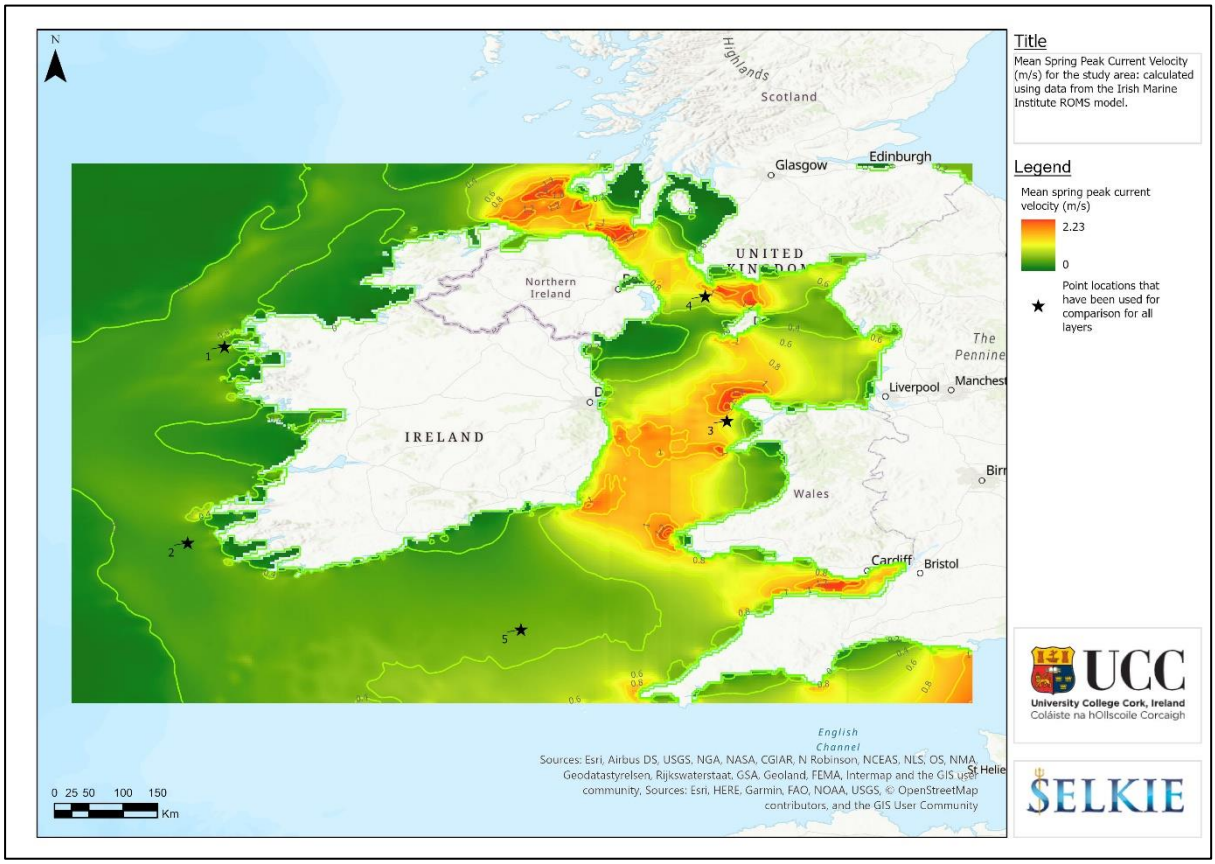
Marine Institute (2021) *Wave Buoy Observations* [online] Available at: http://www.marine.ie/Home/site-area/data-services/real-time-observations/wave-buoy-observations [Accessed: 12 Jul. 2021].

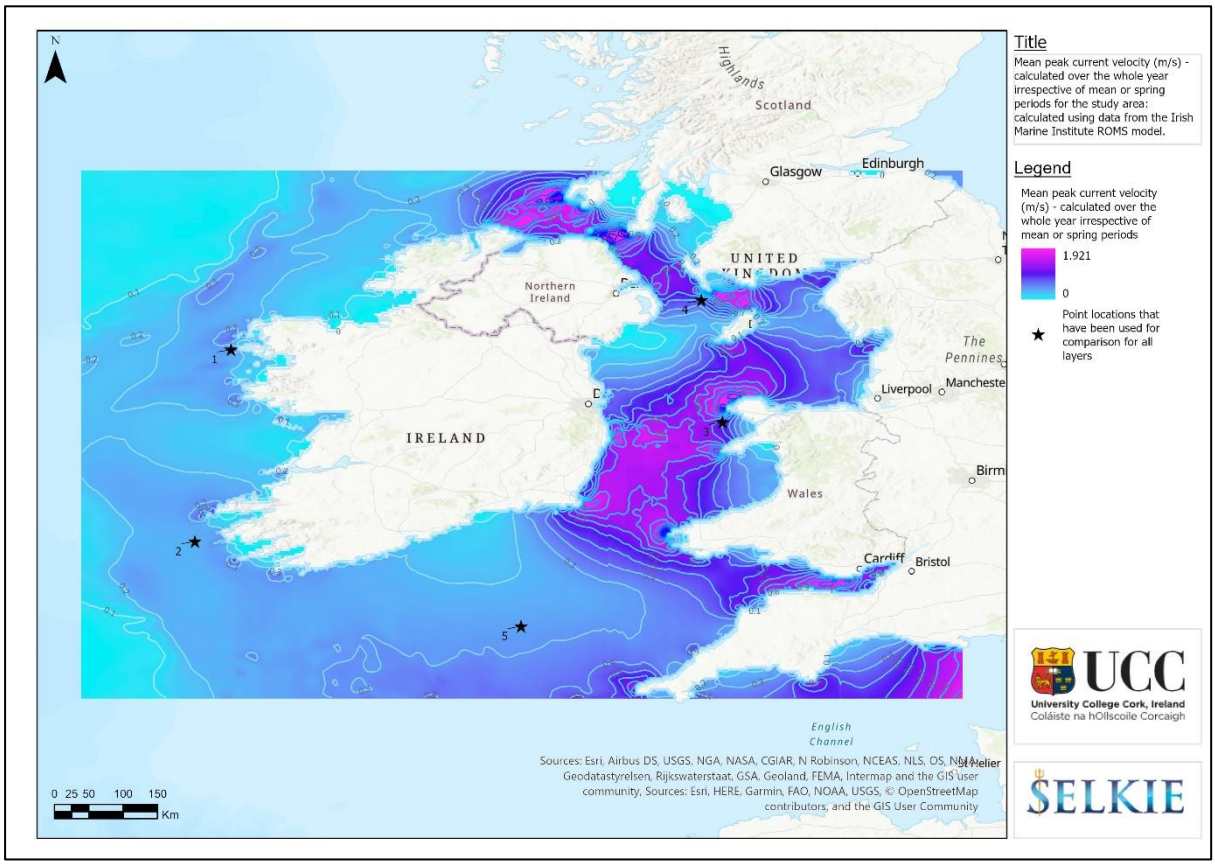
NNRCMP (2021) *Channel Coastal Observatory - Wave Hub* [online] Coastalmonitoring.org Available at: <https://coastalmonitoring.org/realtimedata/?chart=116andsndtab=wavesandsndrange=yearandsnddisp_option=1andsnduser_indate=01-01-2016andsnddatum=chart> [Accessed 1 July 2021].

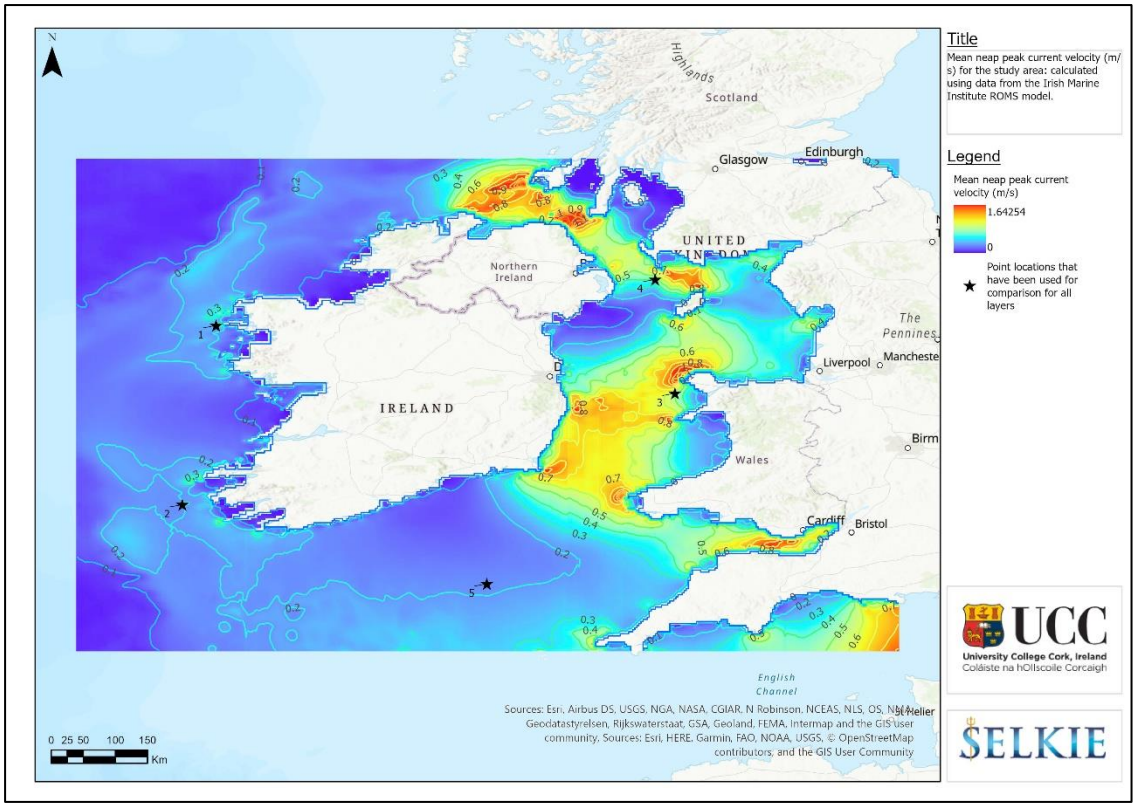
O'Connell, R., de Montera, L., Peters, J. L., andsnd Horion, S. (2020). An updated assessment of Ireland's wave energy resource using satellite data assimilation and a revised wave period ratio. *Renewable Energy*, *160*, 1431–1444. https://doi.org/10.1016/j.renene.2020.07.029

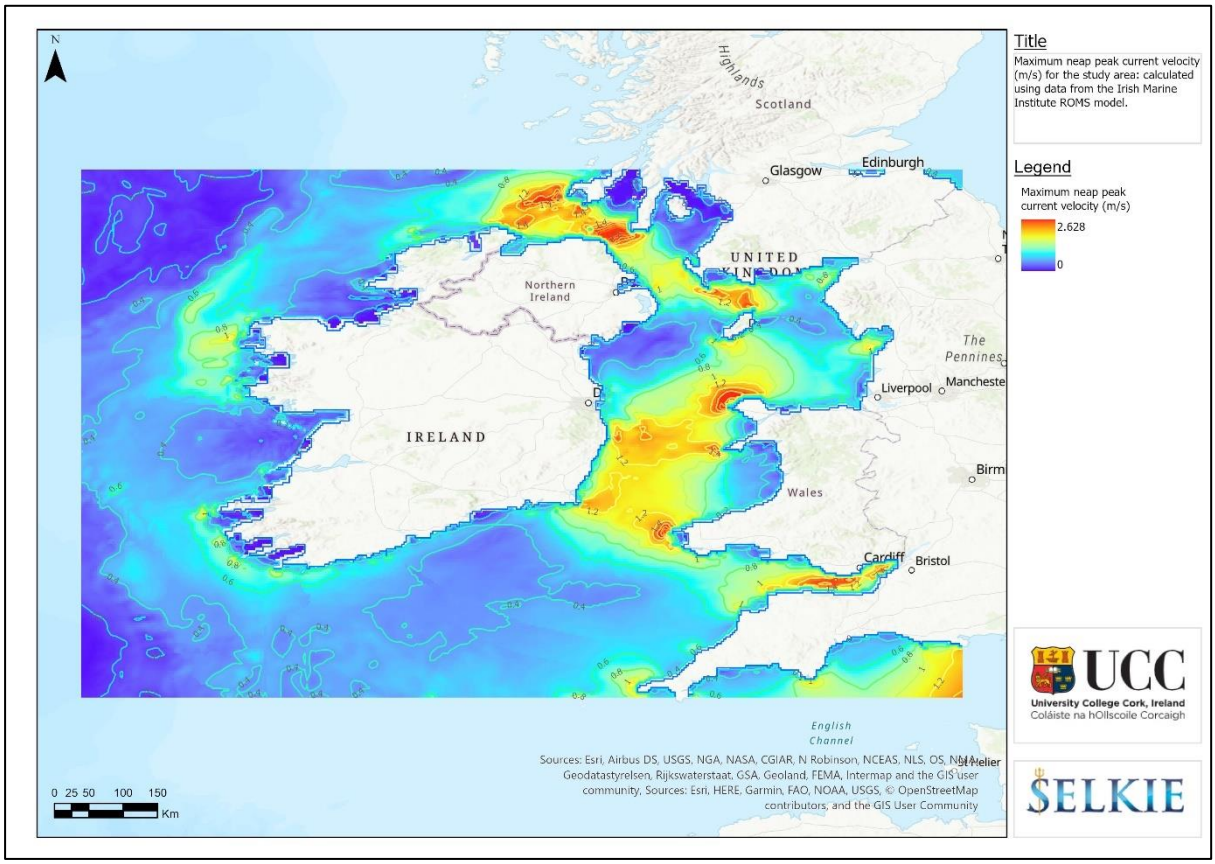
Wolf, J. and Woolf, D. (2006) Waves and climate change in the north-east Atlantic. *Geophysical Research Letters*, 33(6).

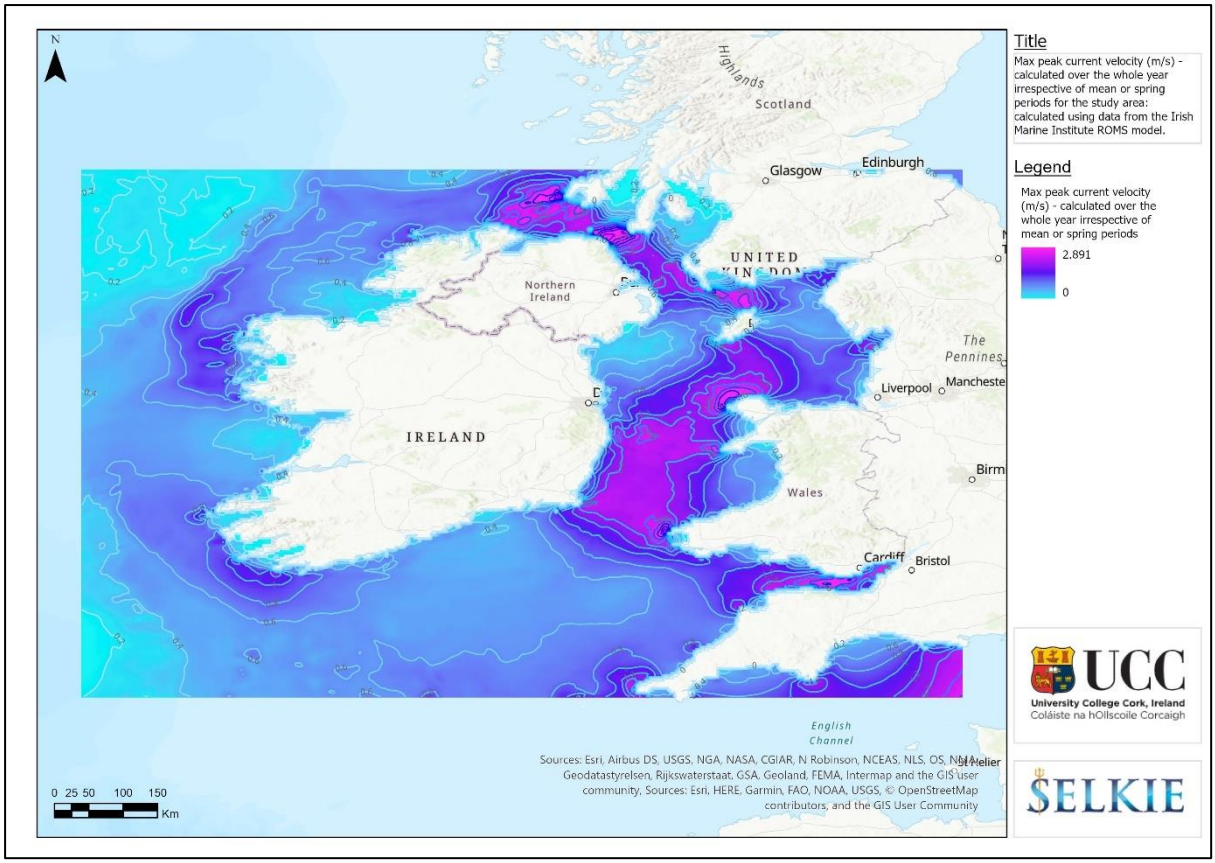
## 2 – Figures

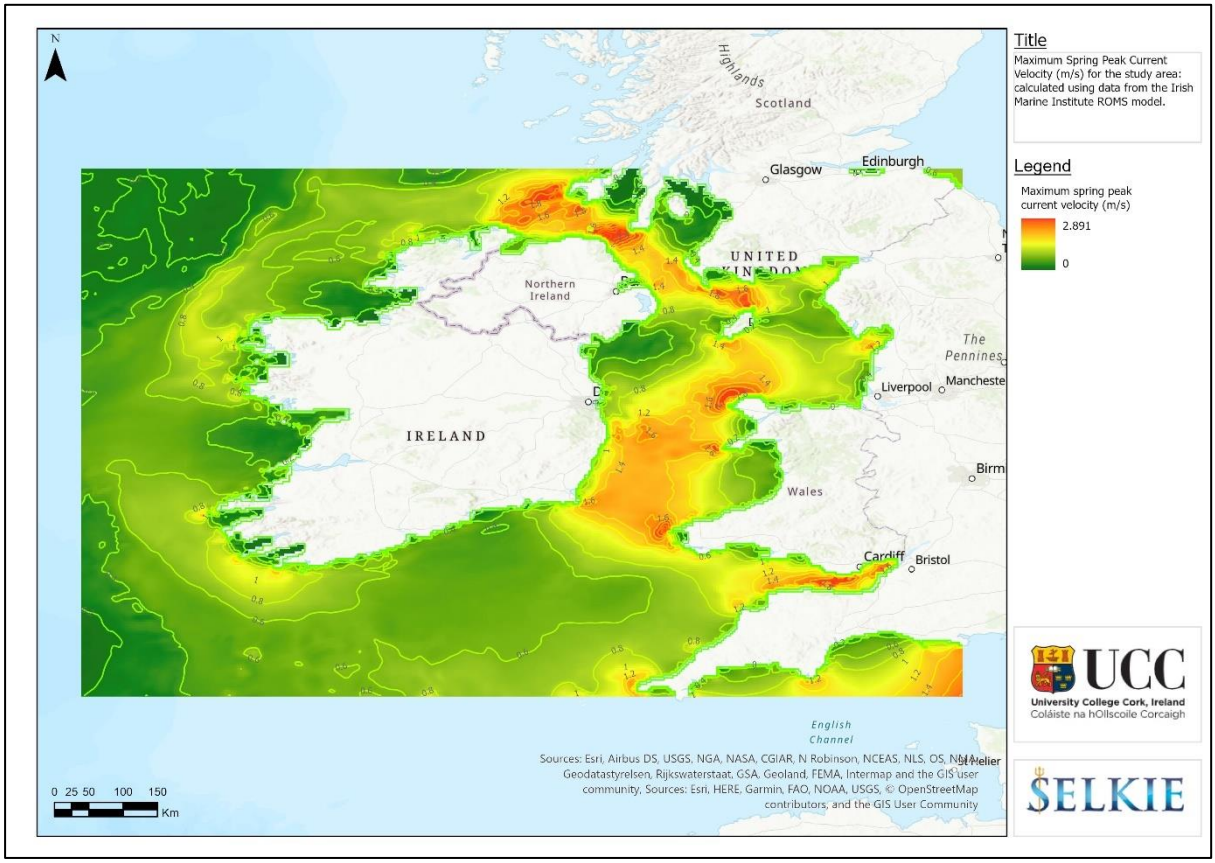

Title
Mean Spring Peak Current Velocity (m/s) for the study area: calculated using data from the Irish Marine Institute ROMS model.
Legend
Mean spring peak current velocity (m/s)
2.23
0
Point locations that have been used for comparison for all layers
Highlands
Scotland
Glasgow
Edinburgh
Northern Ireland
IRELAND
Wales
Liverpool
Cardiff
Bristol
English Channel
0 25 50 100 150
Km
UCC
University College Cork, Ireland
Coláiste na hOllscoile Corcaigh
SELKIE

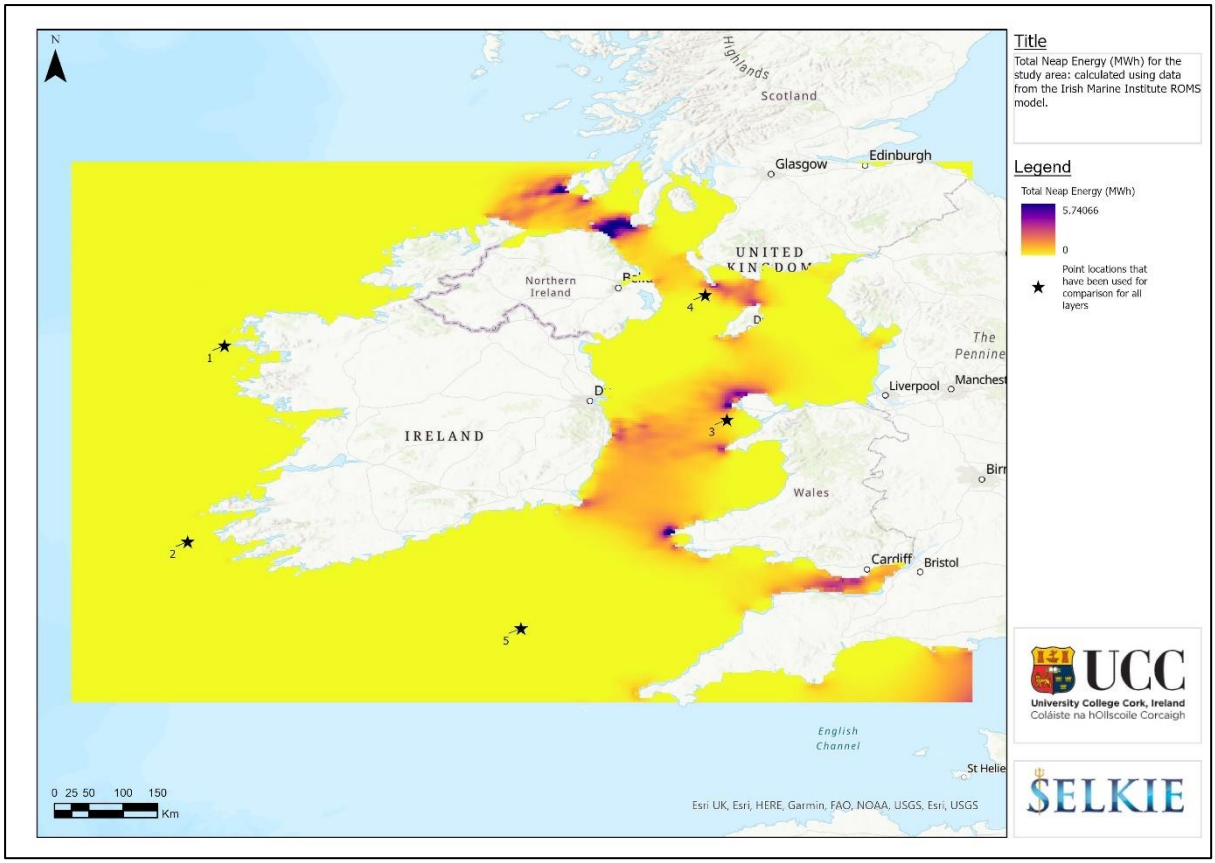

Title
Mean peak current velocity (m/s) - calculated over the whole year irrespective of mean or spring periods for the study area: calculated using data from the Irish Marine Institute ROMS model.
Legend
Mean peak current velocity (m/s) - calculated over the whole year irrespective of mean or spring periods
1.921
0
Point locations that have been used for comparison for all layers
Highlands
Scotland
Glasgow
Edinburgh
Northern Ireland
IRELAND
Wales
Liverpool
Cardiff
Bristol
English Channel
0 25 50 100 150
Km
UCC
University College Cork, Ireland
Coláiste na hOllscoile Corcaigh
SELKIE

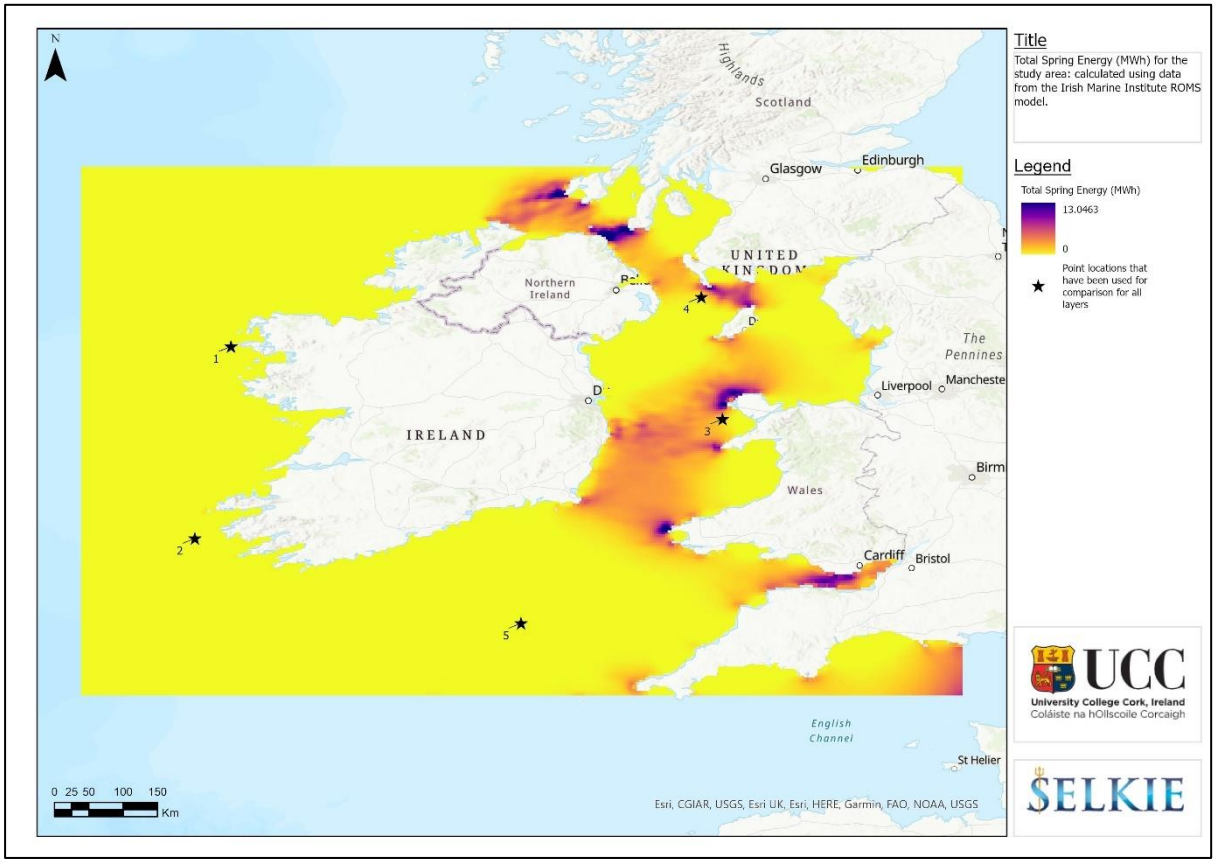

Title
Mean neap peak current velocity (m/s) for the study area: calculated using data from the Irish Marine Institute ROMS model.
Legend
Mean neap peak current velocity (m/s)
1.64254
0
Point locations that have been used for comparison for all layers
Highlands
Scotland
Glasgow
Edinburgh
Northern Ireland
The Pennines
Liverpool
Manchester
IRELAND
Wales
Birmingham
Cardiff
Bristol
English Channel
St Helier
0 25 50 100 150
Km
Sources: Esri, Airbus DS, USGS, NGA, NASA, CGIAR, N Robinson, NCEAS, NLS, OS, NMA, Geodatastyrelsen, Rijkswaterstaat, GSA, Geoland, FEMA, Intermap and the GIS user community, Sources: Esri, HERE, Garmin, FAO, NOAA, USGS, © OpenStreetMap contributors, and the GIS User Community
UCC
University College Cork, Ireland
Coláiste na hOllscoile Corcaigh
SELKIE

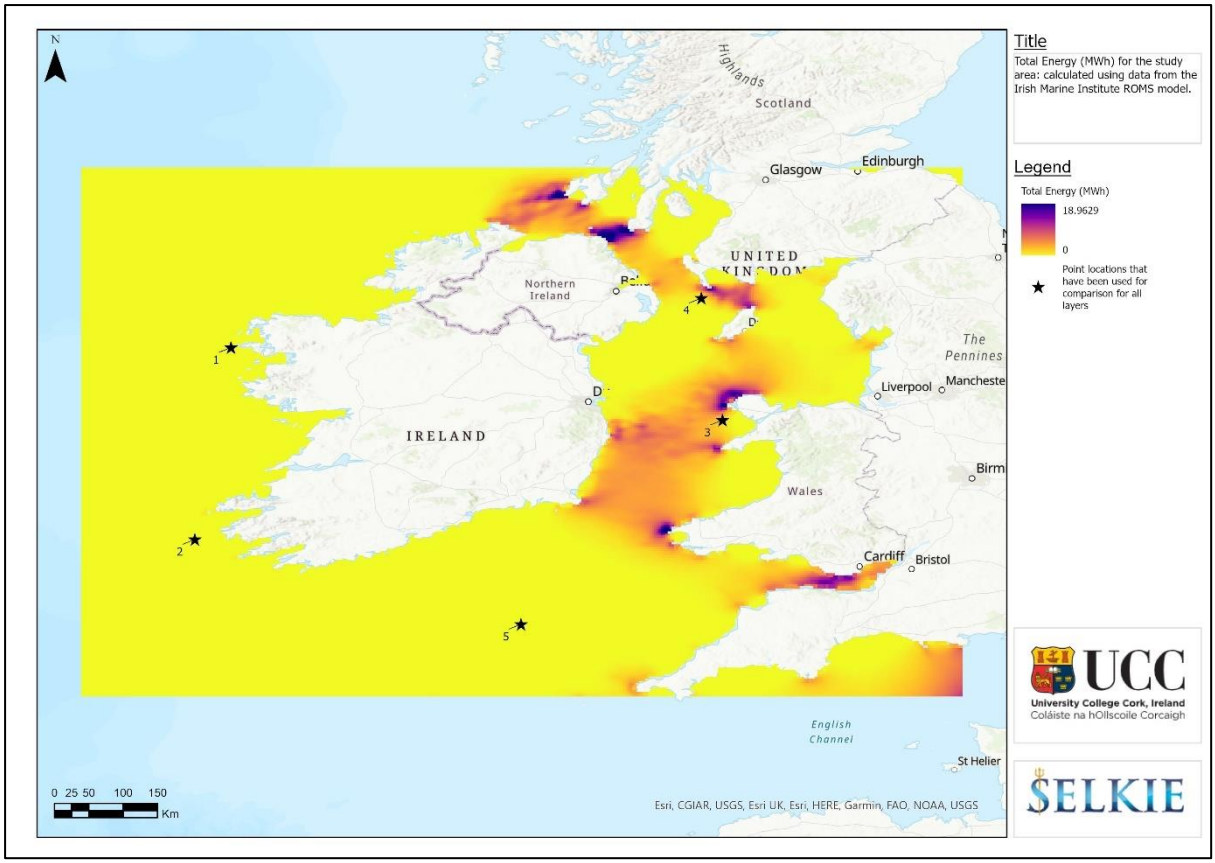

Title
Maximum neap peak current velocity (m/s) for the study area: calculated using data from the Irish Marine Institute ROMS model.
Legend
Maximum neap peak current velocity (m/s)
2.628
0
Highlands
Scotland
Glasgow
Edinburgh
Northern Ireland
The Pennines
Liverpool
Manchester
IRELAND
Wales
Birmingham
Cardiff
Bristol
English Channel
St Helier
0 25 50 100 150
Km
Sources: Esri, Airbus DS, USGS, NGA, NASA, CGIAR, N Robinson, NCEAS, NLS, OS, NMA, Geodatastyrelsen, Rijkswaterstaat, GSA, Geoland, FEMA, Intermap and the GIS user community, Sources: Esri, HERE, Garmin, FAO, NOAA, USGS, © OpenStreetMap contributors, and the GIS User Community
UCC
University College Cork, Ireland
Coláiste na hOllscoile Corcaigh
SELKIE

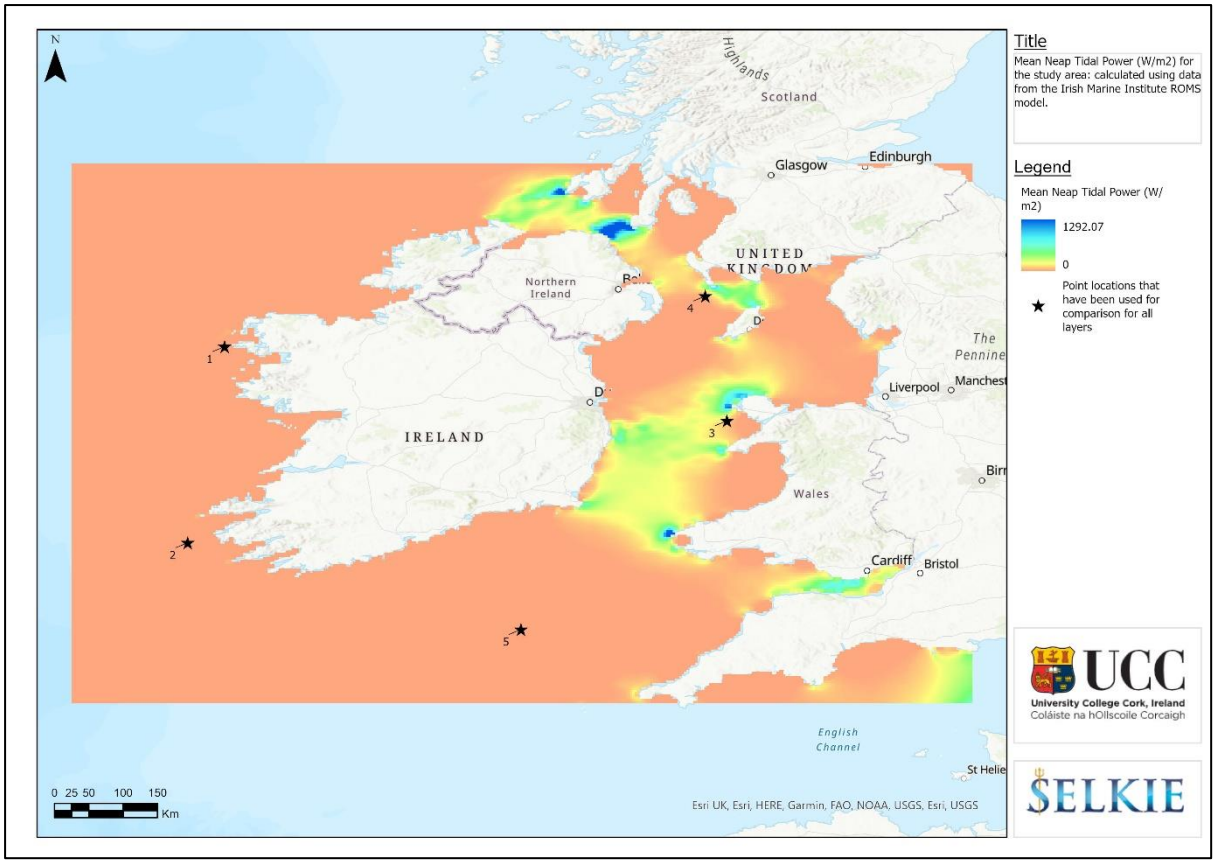

N
Highlands
Scotland
Glasgow
Edinburgh
UNITED KINGDOM
Northern Ireland
The Pennines
Liverpool
Manchester
IRELAND
Birmingham
Wales
Cardiff
Bristol
English Channel
St Helier
0 25 50 100 150
Km
Sources: Esri, Airbus DS, USGS, NGA, NASA, CGIAR, N Robinson, NCEAS, NLS, OS, NMA, Geodatastyrelsen, Rijkswaterstaat, GSA, Geoland, FEMA, Intermap and the GIS user community, Sources: Esri, HERE, Garmin, FAO, NOAA, USGS, © OpenStreetMap contributors, and the GIS User Community
Title
Max peak current velocity (m/s) - calculated over the whole year irrespective of mean or spring periods for the study area: calculated using data from the Irish Marine Institute ROMS model.
Legend
Max peak current velocity (m/s) - calculated over the whole year irrespective of mean or spring periods
2.891
0
UCC
University College Cork, Ireland
Coláiste na hOllscoile Corcaigh
SELKIE

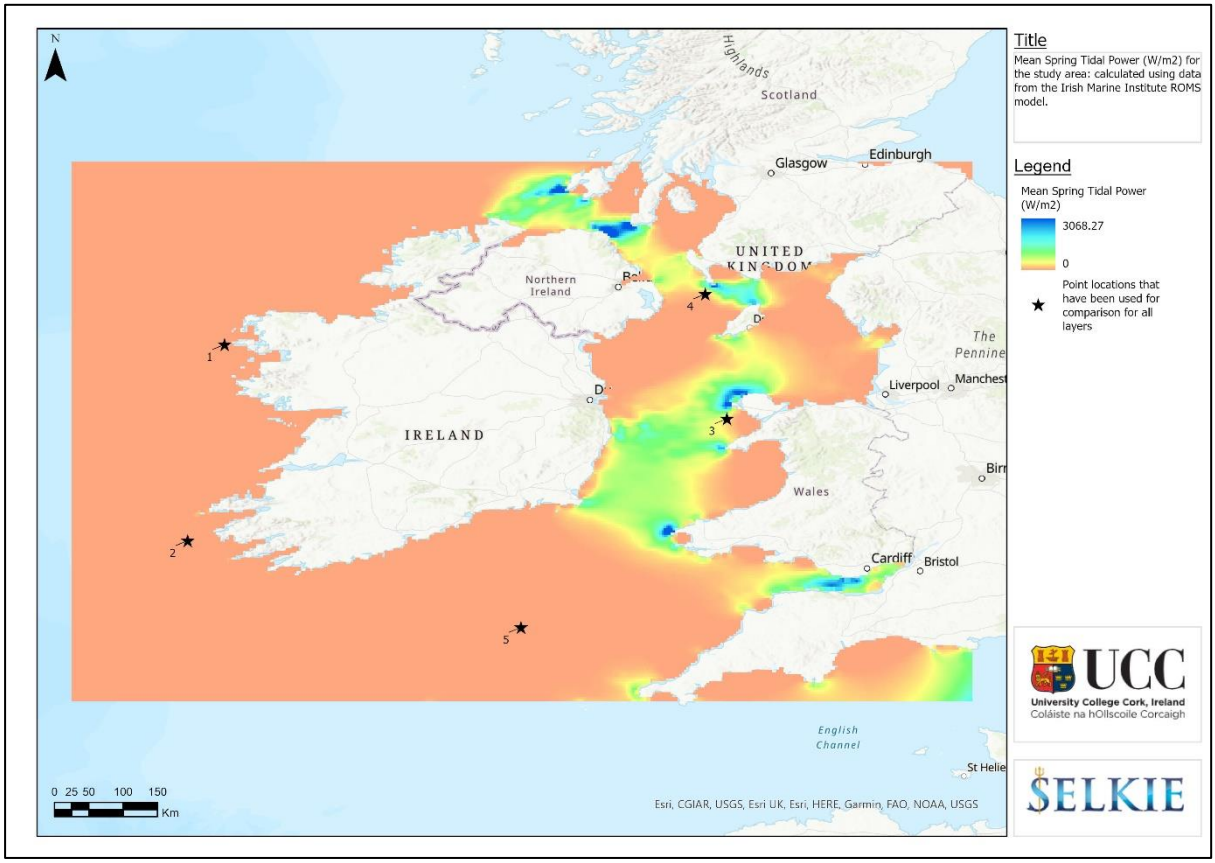

N
Highlands
Scotland
Glasgow
Edinburgh
UNITED KINGDOM
Northern Ireland
The Pennines
Liverpool
Manchester
IRELAND
Birmingham
Wales
Cardiff
Bristol
English Channel
St Helier
0 25 50 100 150
Km
Sources: Esri, Airbus DS, USGS, NGA, NASA, CGIAR, N Robinson, NCEAS, NLS, OS, NMA, Geodatastyrelsen, Rijkswaterstaat, GSA, Geoland, FEMA, Intermap and the GIS user community, Sources: Esri, HERE, Garmin, FAO, NOAA, USGS, © OpenStreetMap contributors, and the GIS User Community
Title
Maximum Spring Peak Current Velocity (m/s) for the study area: calculated using data from the Irish Marine Institute ROMS model.
Legend
Maximum spring peak current velocity (m/s)
2.891
0
UCC
University College Cork, Ireland
Coláiste na hOllscoile Corcaigh
SELKIE

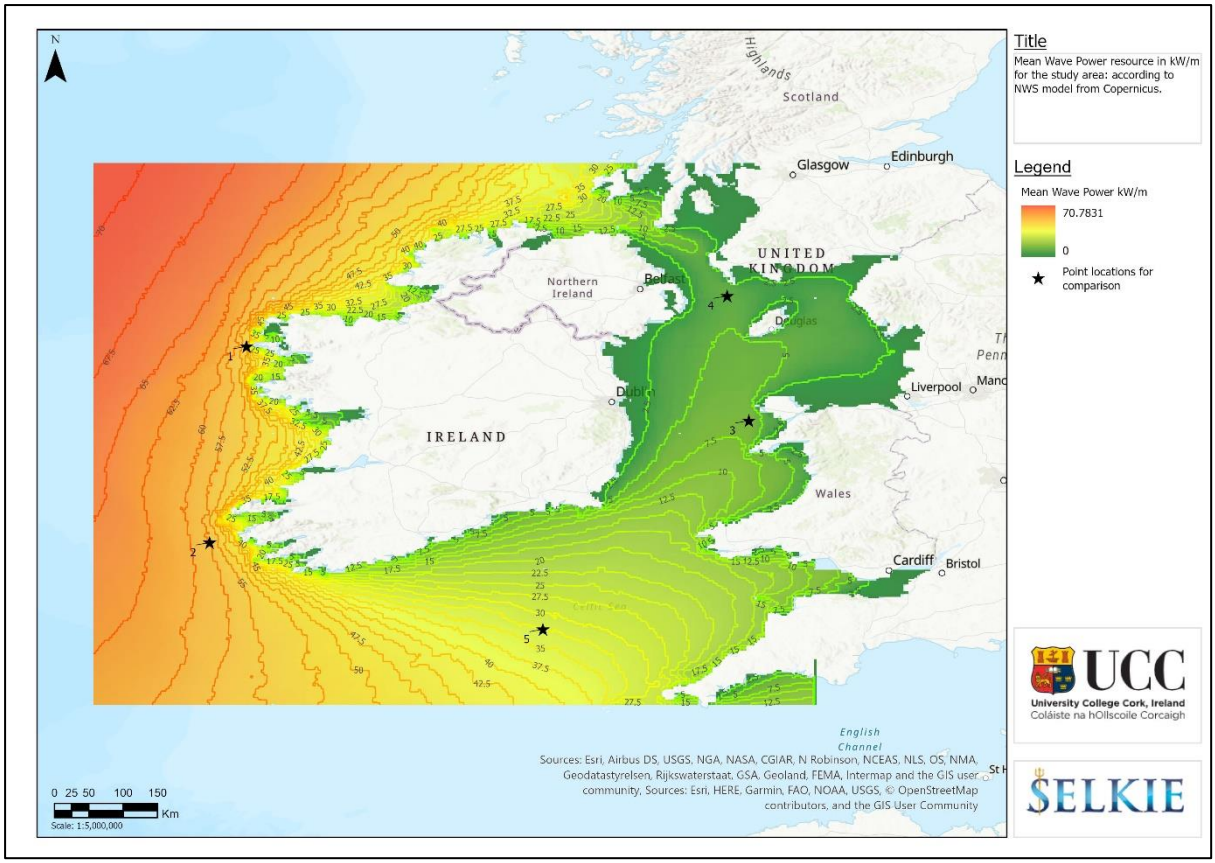

Title
Total Neap Energy (MWh) for the study area: calculated using data from the Irish Marine Institute ROMS model.
Legend
Total Neap Energy (MWh)
5.74066
0
Point locations that have been used for comparison for all layers
Highlands
Scotland
Glasgow
Edinburgh
UNITED KINGDOM
Northern Ireland
IRELAND
The Pennines
Liverpool
Manchester
Wales
Cardiff
Bristol
English Channel
St Helier
1
2
3
4
5
0 25 50 100 150
Km
Esri UK, Esri, HERE, Garmin, FAO, NOAA, USGS, Esri, USGS
UCC
University College Cork, Ireland
Coláiste na hOllscoile Corcaigh
SELKIE

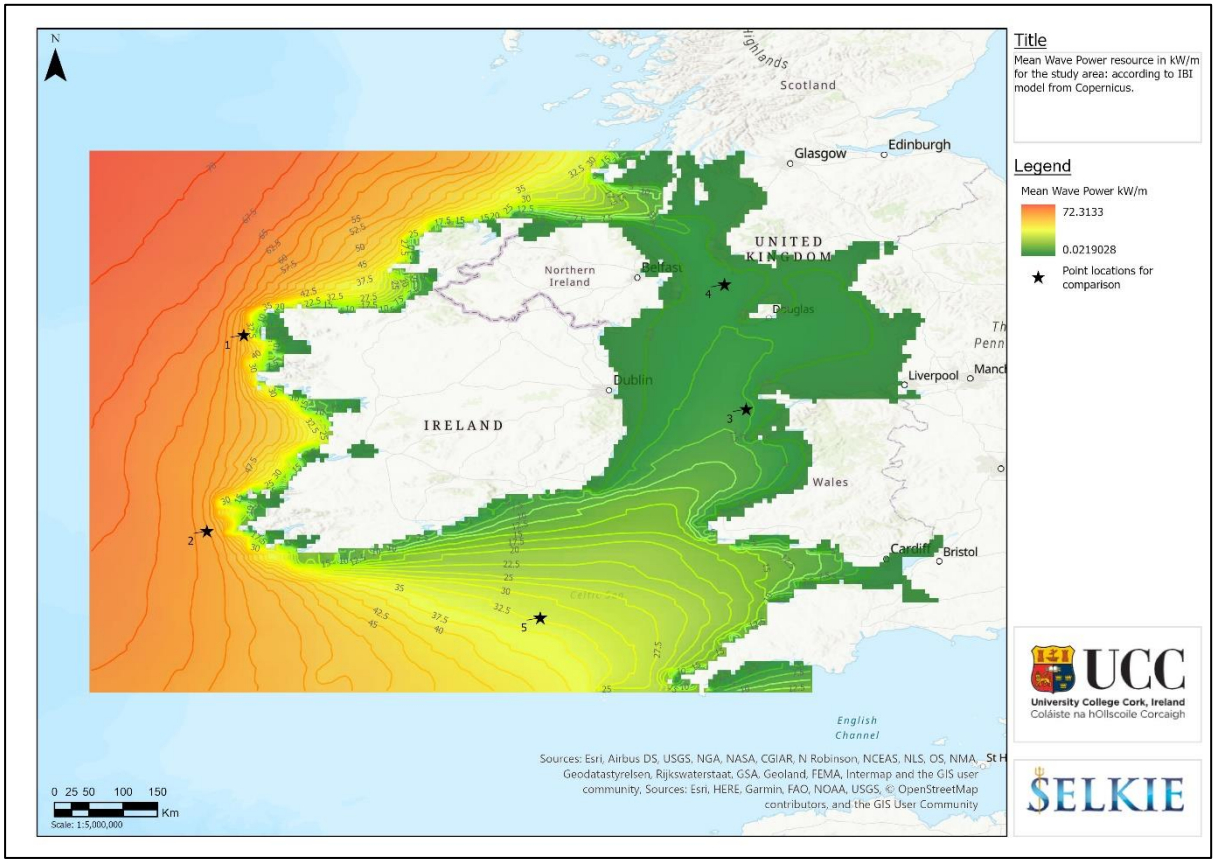

Title
Total Spring Energy (MWh) for the study area: calculated using data from the Irish Marine Institute ROMS model.
Legend
Total Spring Energy (MWh)
13.0463
0
Point locations that have been used for comparison for all layers
Highlands
Scotland
Glasgow
Edinburgh
UNITED KINGDOM
Northern Ireland
IRELAND
The Pennines
Liverpool
Manchester
Wales
Cardiff
Bristol
English Channel
St Helier
1
2
3
4
5
0 25 50 100 150
Km
Esri, CGIAR, USGS, Esri UK, Esri, HERE, Garmin, FAO, NOAA, USGS
UCC
University College Cork, Ireland
Coláiste na hOllscoile Corcaigh
SELKIE

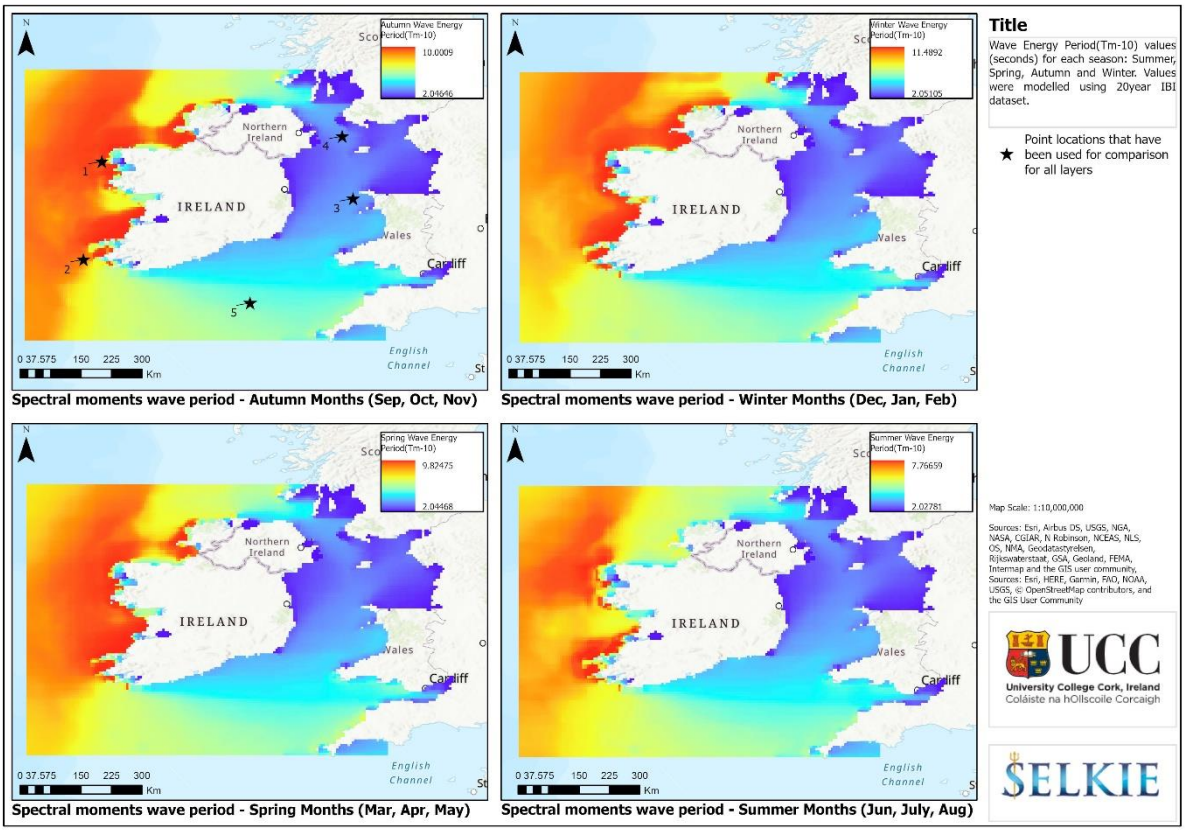

N
Highlands
Scotland
Glasgow
Edinburgh
UNITED KINGDOM
Northern Ireland
The Pennines
Liverpool
Manchester
IRELAND
Wales
Birmingham
Cardiff
Bristol
English Channel
St Helier
1
2
3
4
5
0 25 50 100 150
Km
Esri, CGIAR, USGS, Esri UK, Esri, HERE, Garmin, FAO, NOAA, USGS
Title
Total Energy (MWh) for the study area: calculated using data from the Irish Marine Institute ROMS model.
Legend
Total Energy (MWh)
18.9629
0
Point locations that have been used for comparison for all layers
UCC
University College Cork, Ireland
Coláiste na hOllscoile Corcaigh
SELKIE


N
Highlands
Scotland
Glasgow
Edinburgh
UNITED KINGDOM
Northern Ireland
The Pennine
Liverpool
Manchest
IRELAND
Wales
Cardiff
Bristol
English Channel
St Helie
0 25 50 100 150
Km
Esri UK, Esri, HERE, Garmin, FAO, NOAA, USGS, Esri, USGS
Title
Mean Neap Tidal Power (W/m2) for the study area: calculated using data from the Irish Marine Institute ROMS model.
Legend
Mean Neap Tidal Power (W/m2)
1292.07
0
Point locations that have been used for comparison for all layers
UCC
University College Cork, Ireland
Coláiste na hOllscoile Corcaigh
SELKIE


N
Highlands
Scotland
Glasgow
Edinburgh
UNITED KINGDOM
Northern Ireland
The Pennine
Liverpool
Manchest
IRELAND
Wales
Cardiff
Bristol
English Channel
St Helie
0 25 50 100 150
Km
Esri, CGIAR, USGS, Esri UK, Esri, HERE, Garmin, FAO, NOAA, USGS
Title
Mean Spring Tidal Power (W/m2) for the study area: calculated using data from the Irish Marine Institute ROMS model.
Legend
Mean Spring Tidal Power (W/m2)
3068.27
0
Point locations that have been used for comparison for all layers
UCC
University College Cork, Ireland
Coláiste na hOllscoile Corcaigh
SELKIE


N
Highlands
Scotland
Glasgow
Edinburgh
UNITED KINGDOM
Northern Ireland
Belfast
Douglas
Liverpool
Dublin
IRELAND
Wales
Cardiff
Bristol
English Channel
1
2
3
4
5
0 25 50 100 150
Km
Scale: 1:5,000,000
Sources: Esri, Airbus DS, USGS, NGA, NASA, CGIAR, N Robinson, NCEAS, NLS, OS, NMA, Geodatastyrelsen, Rijkswaterstaat, GSA, Geoland, FEMA, Intermap and the GIS user community, Sources: Esri, HERE, Garmin, FAO, NOAA, USGS, © OpenStreetMap contributors, and the GIS User Community
Title
Mean Wave Power resource in kW/m for the study area: according to NWS model from Copernicus.
Legend
Mean Wave Power kW/m
70.7831
0
Point locations for comparison
UCC
University College Cork, Ireland
Coláiste na hOllscoile Corcaigh
SELKIE


N
Highlands
Scotland
Glasgow
Edinburgh
UNITED KINGDOM
Northern Ireland
Belfast
Douglas
Liverpool
Dublin
IRELAND
Wales
Cardiff
Bristol
English Channel
1
2
3
4
5
0 25 50 100 150
Km
Scale: 1:5,000,000
Sources: Esri, Airbus DS, USGS, NGA, NASA, CGIAR, N Robinson, NCEAS, NLS, OS, NMA, Geodatastyrelsen, Rijkswaterstaat, GSA, Geoland, FEMA, Intermap and the GIS user community, Sources: Esri, HERE, Garmin, FAO, NOAA, USGS, © OpenStreetMap contributors, and the GIS User Community
Title
Mean Wave Power resource in kW/m for the study area: according to IBI model from Copernicus.
Legend
Mean Wave Power kW/m
72.3133
0.0219028
Point locations for comparison
UCC
University College Cork, Ireland
Coláiste na hOllscoile Corcaigh
SELKIE

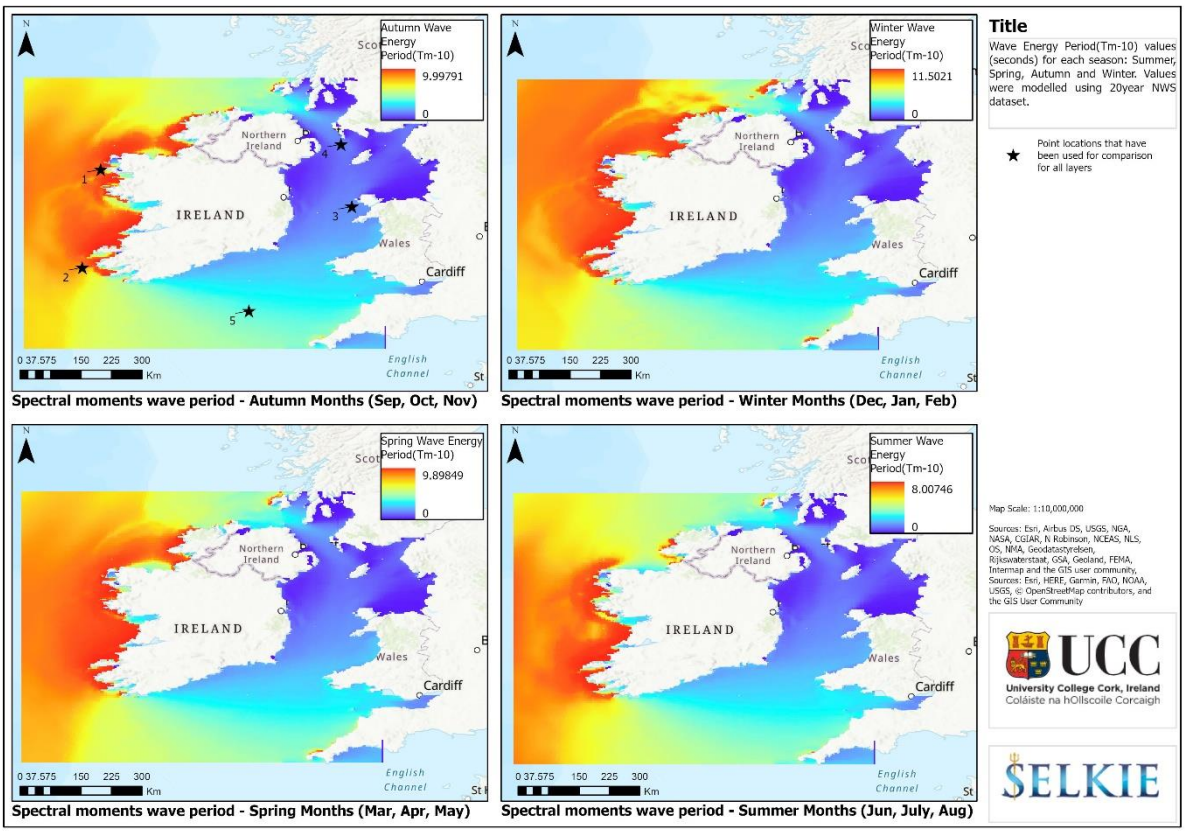



Spectral moments wave period - Autumn Months (Sep, Oct, Nov)

Spectral moments wave period - Winter Months (Dec, Jan, Feb)

Spectral moments wave period - Spring Months (Mar, Apr, May)

Spectral moments wave period - Summer Months (Jun, July, Aug)

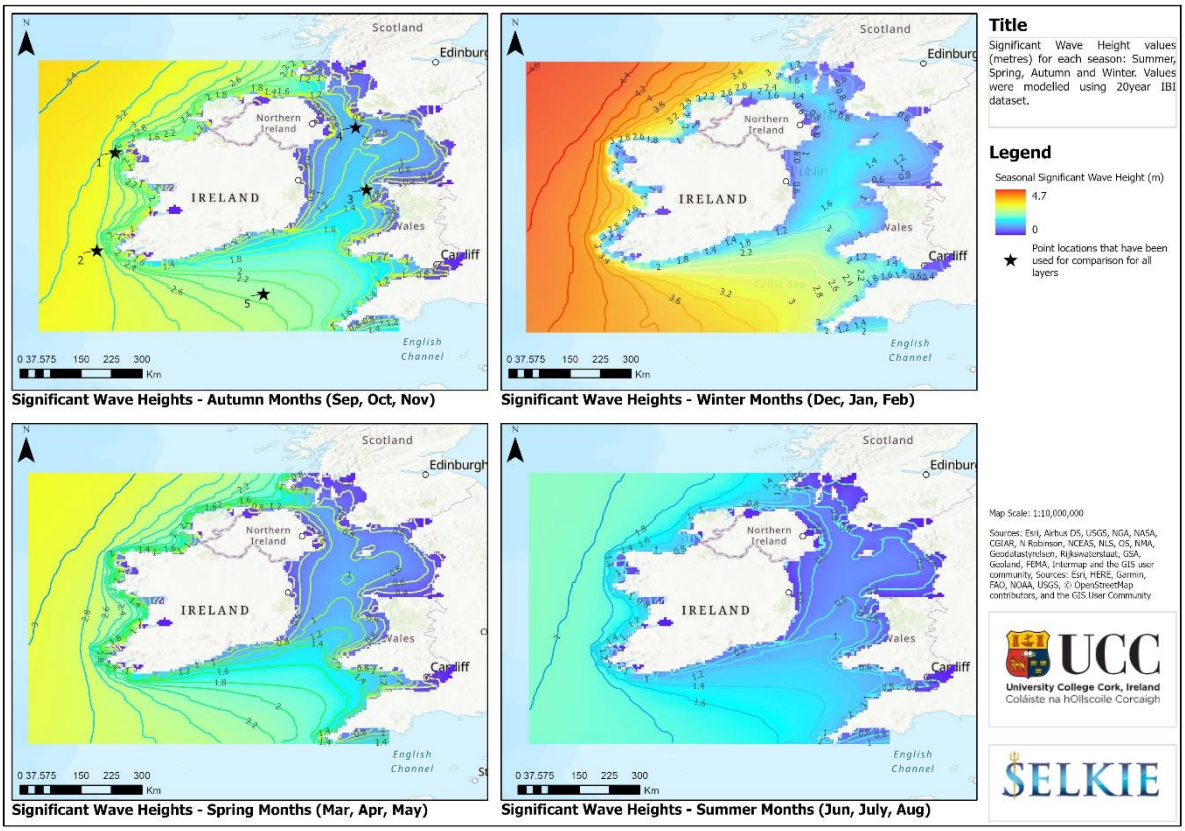


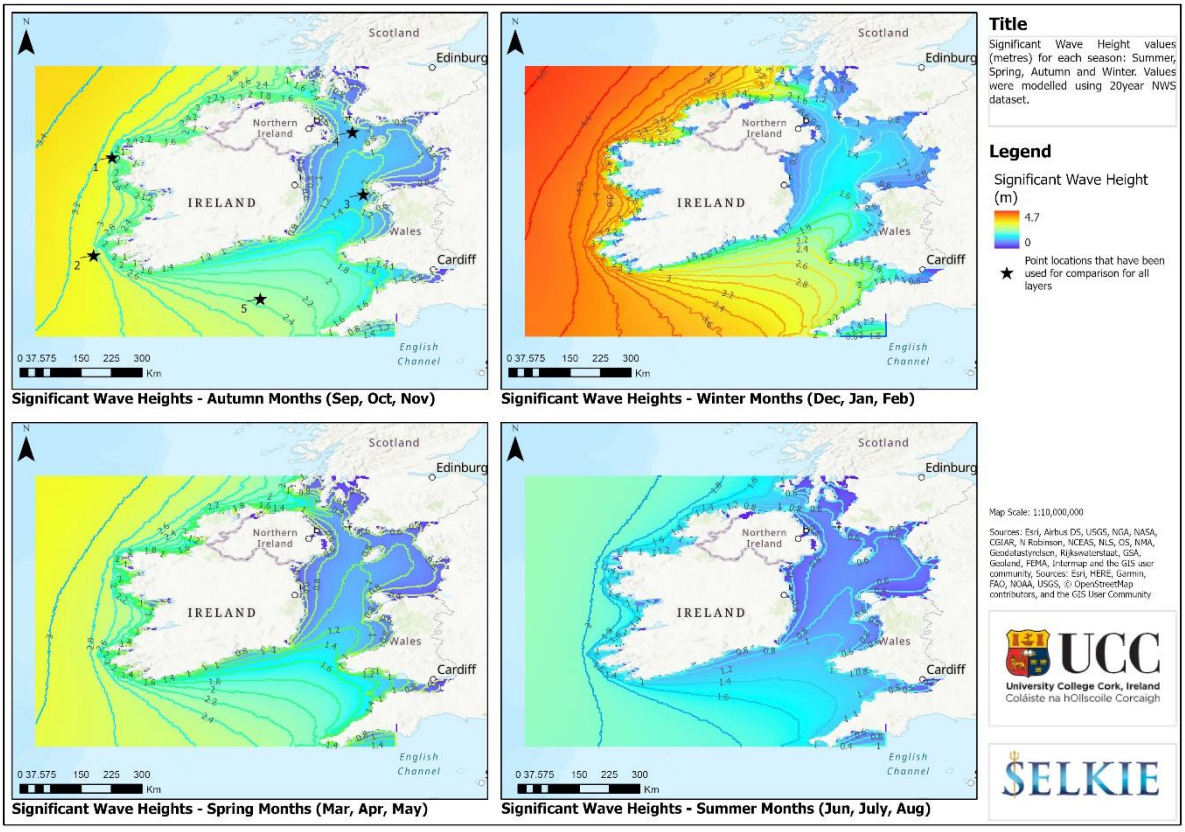

Spectral moments wave period - Autumn Months (Sep, Oct, Nov)

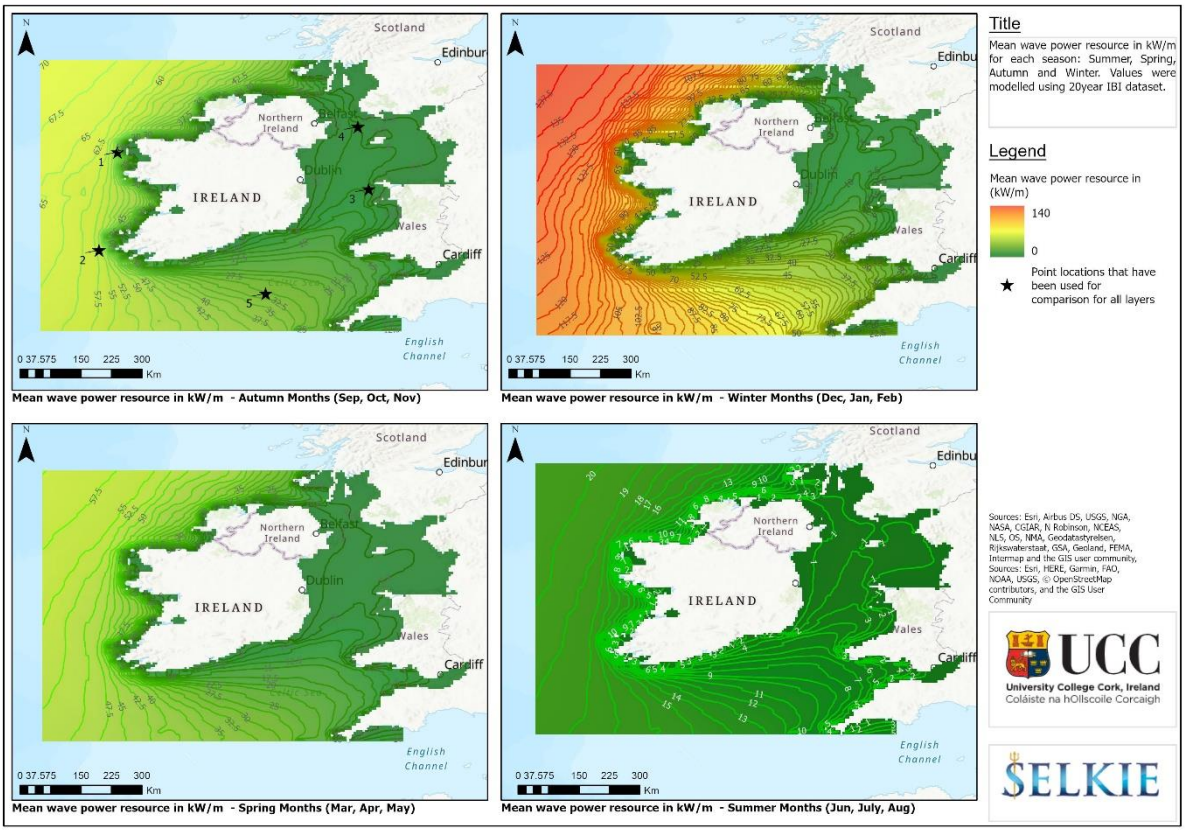
Spectral moments wave period - Winter Months (Dec, Jan, Feb)

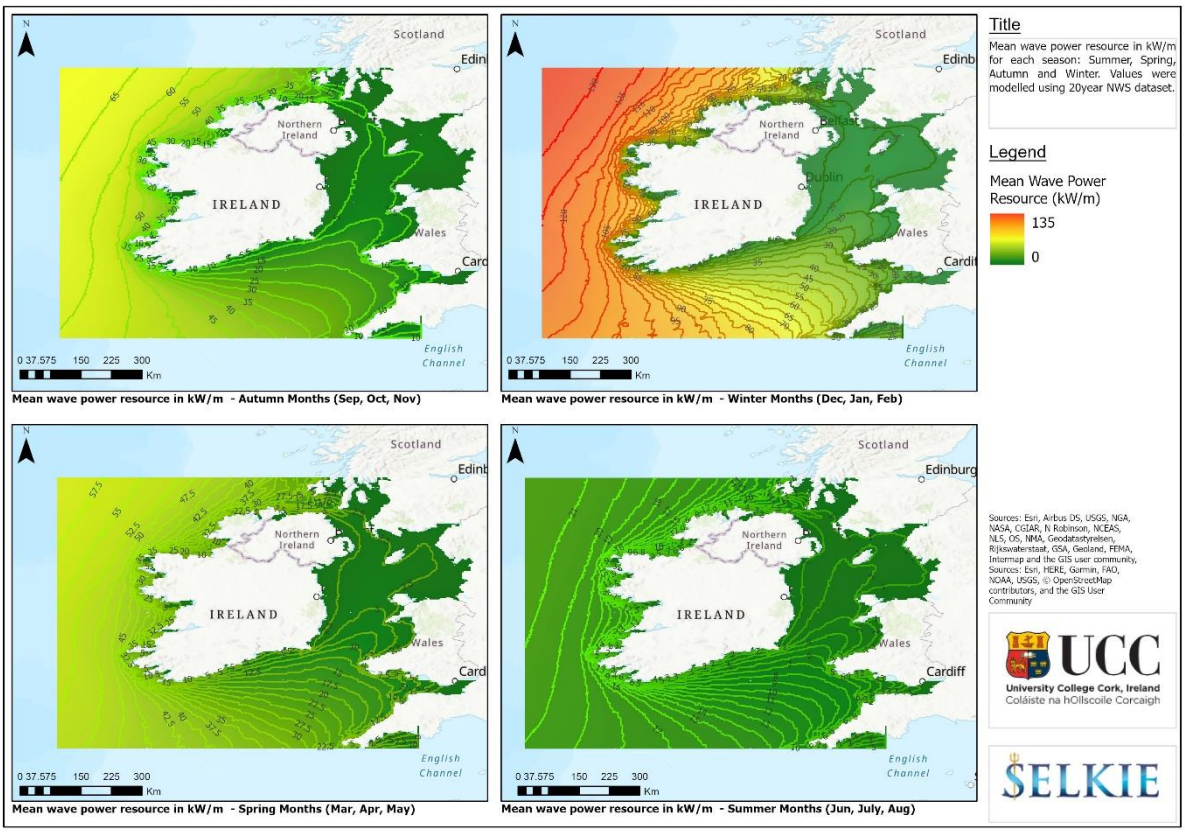
Spectral moments wave period - Spring Months (Mar, Apr, May)

Spectral moments wave period - Summer Months (Jun, July, Aug)


Scotland
Edinburgh
Northern Ireland
IRELAND
Wales
Cardiff
English Channel
0 37.575 150 225 300
Km
Significant Wave Heights - Autumn Months (Sep, Oct, Nov)
Significant Wave Heights - Winter Months (Dec, Jan, Feb)
Significant Wave Heights - Spring Months (Mar, Apr, May)
Significant Wave Heights - Summer Months (Jun, July, Aug)
Title
Significant Wave Height values (metres) for each season: Summer, Spring, Autumn and Winter. Values were modelled using 20year IBI dataset.
Legend
Seasonal Significant Wave Height (m)
4.7
0
Point locations that have been used for comparison for all layers
Map Scale: 1:10,000,000
Sources: Esri, Airbus DS, USGS, NGA, NASA, CGIAR, N Robinson, NCEAS, NLS, OS, NMA, Geodatastyrelsen, Rijkswaterstaat, GSA, Geoland, FEMA, Intermap and the GIS user community, Sources: Esri, HERE, Garmin, FAO, NOAA, USGS, © OpenStreetMap contributors, and the GIS User Community
UCC
University College Cork, Ireland
Coláiste na hOllscoile Corcaigh
SELKIE

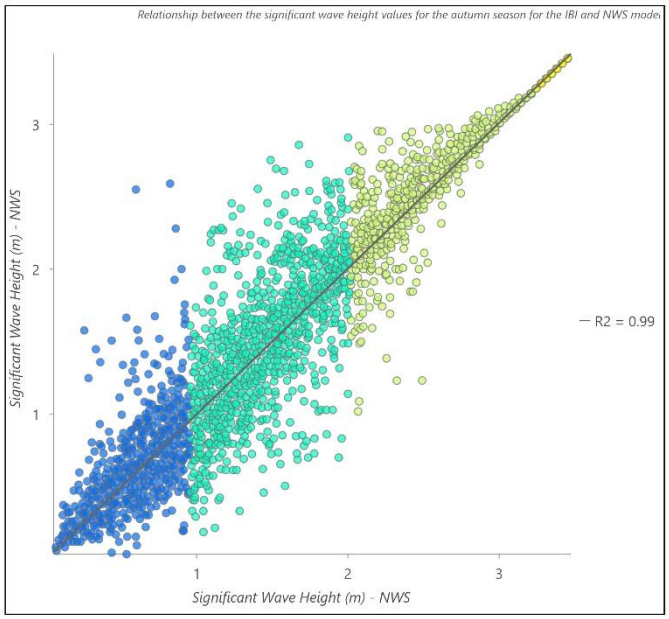

Scotland
Edinburgh
Northern Ireland
IRELAND
Wales
Cardiff
English Channel
0 37.575 150 225 300
Km
Significant Wave Heights - Autumn Months (Sep, Oct, Nov)
Significant Wave Heights - Winter Months (Dec, Jan, Feb)
Significant Wave Heights - Spring Months (Mar, Apr, May)
Significant Wave Heights - Summer Months (Jun, July, Aug)
Title
Significant Wave Height values (metres) for each season: Summer, Spring, Autumn and Winter. Values were modelled using 20year NWS dataset.
Legend
Significant Wave Height (m)
4.7
0
Point locations that have been used for comparison for all layers
Map Scale: 1:10,000,000
Sources: Esri, Airbus DS, USGS, NGA, NASA, CGIAR, N Robinson, NCEAS, NLS, OS, NMA, Geodatastyrelsen, Rijkswaterstaat, GSA, Geoland, FEMA, Intermap and the GIS user community, Sources: Esri, HERE, Garmin, FAO, NOAA, USGS, © OpenStreetMap contributors, and the GIS User Community
UCC
University College Cork, Ireland
Coláiste na hOllscoile Corcaigh
SELKIE

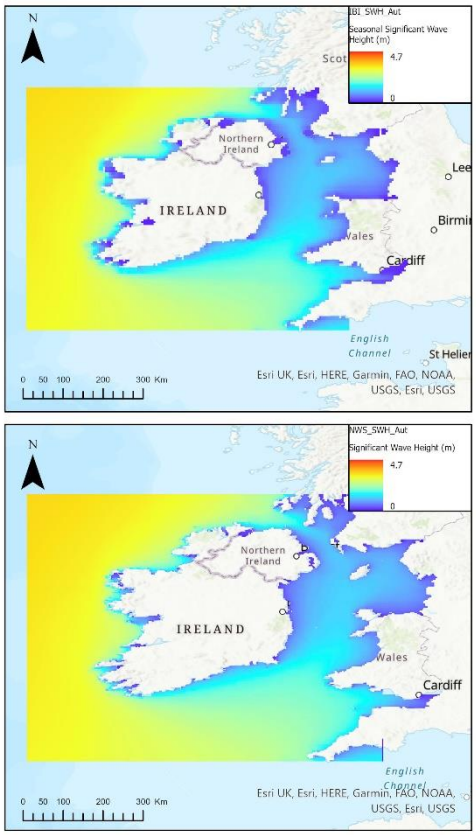

Scotland
Edinburgh
Northern Ireland
Belfast
IRELAND
Dublin
Wales
Cardiff
English Channel
0 37.575 150 225 300
Km
Mean wave power resource in kW/m - Autumn Months (Sep, Oct, Nov)
Mean wave power resource in kW/m - Winter Months (Dec, Jan, Feb)
Mean wave power resource in kW/m - Spring Months (Mar, Apr, May)
Mean wave power resource in kW/m - Summer Months (Jun, July, Aug)
Title
Mean wave power resource in kW/m for each season: Summer, Spring, Autumn and Winter. Values were modelled using 20year IBI dataset.
Legend
Mean wave power resource in (kW/m)
140
0
Point locations that have been used for comparison for all layers
Sources: Esri, Airbus DS, USGS, NGA, NASA, CGIAR, N Robinson, NCEAS, NLS, OS, NMA, Geodatastyrelsen, Rijkswaterstaat, GSA, Geoland, FEMA, Intermap and the GIS user community, Sources: Esri, HERE, Garmin, FAO, NOAA, USGS, © OpenStreetMap contributors, and the GIS User Community
UCC
University College Cork, Ireland
Coláiste na hOllscoile Corcaigh
SELKIE


Scotland
Northern Ireland
IRELAND
Wales
English Channel
0 37.575 150 225 300
Km
Mean wave power resource in kW/m - Autumn Months (Sep, Oct, Nov)
Mean wave power resource in kW/m - Winter Months (Dec, Jan, Feb)
Mean wave power resource in kW/m - Spring Months (Mar, Apr, May)
Mean wave power resource in kW/m - Summer Months (Jun, July, Aug)
Title
Mean wave power resource in kW/m for each season: Summer, Spring, Autumn and Winter. Values were modelled using 20year NWS dataset.
Legend
Mean Wave Power Resource (kW/m)
135
0
Sources: Esri, Airbus DS, USGS, NGA, NASA, CGIAR, N Robinson, NCEAS, NLS, OS, NMA, Geodatastyrelsen, Rijkswaterstaat, GSA, Geoland, FEMA, Intermap and the GIS user community, Sources: Esri, HERE, Garmin, FAO, NOAA, USGS, © OpenStreetMap contributors, and the GIS User Community
UCC
University College Cork, Ireland
Coláiste na hOllscoile Corcaigh
SELKIE

Title

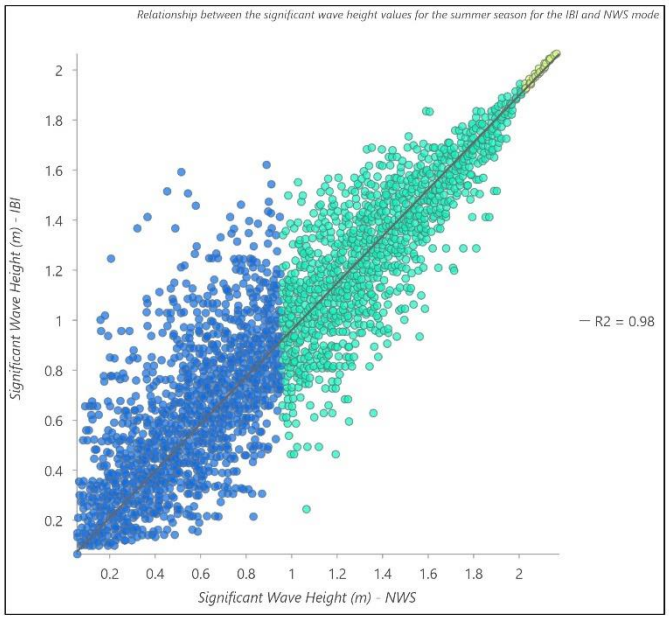
Scatter plot showing the relationship between the mean significant wave height (m) for the autumn months for the IBI and NWS models, with the IBI model showing in the map on the top right and the NWS map on the bottom left of the page.

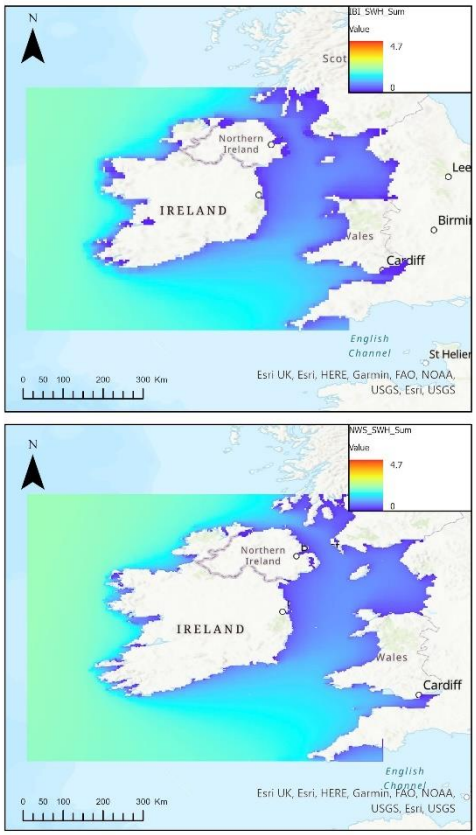



Title

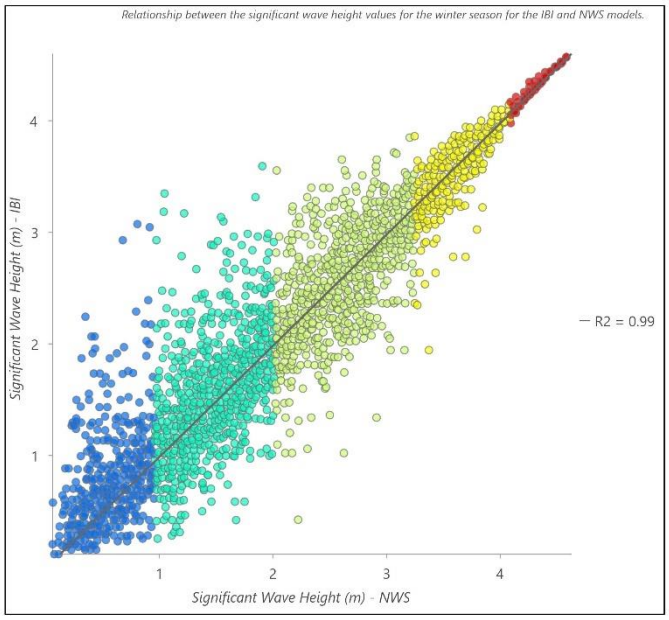
Scatter plot showing the relationship between the mean significant wave height (m) for the summer months for the IBI and NWS models, with the IBI model showing in the map on the top right and the NWS map on the bottom left of the page.

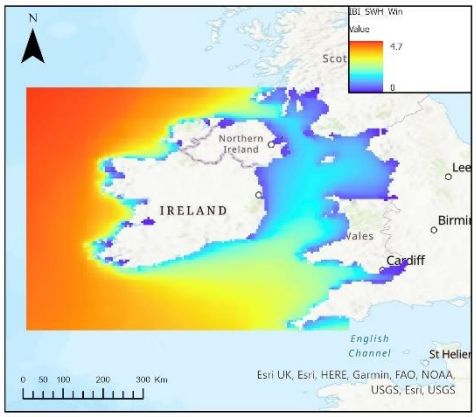


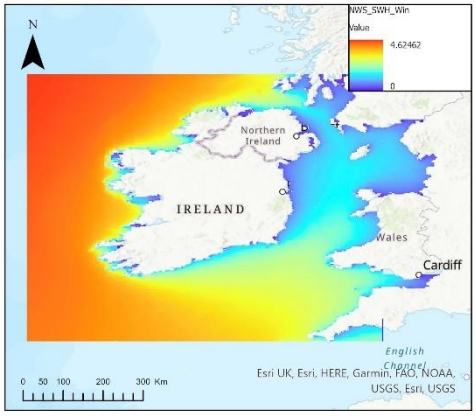



Title

Scatter plot showing the relationship between the mean significant wave height (m) for the winter months for the IBI and NWS models, with the IBI model showing in the map on the top right and the NWS map on the bottom left of the page.

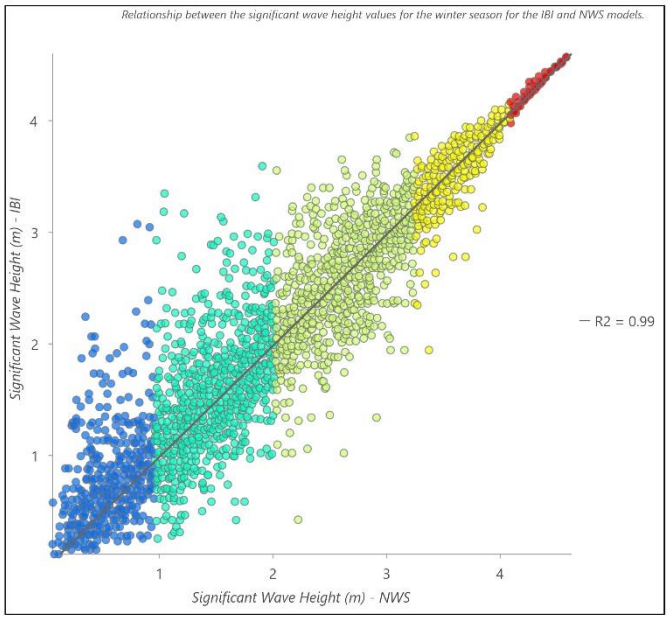


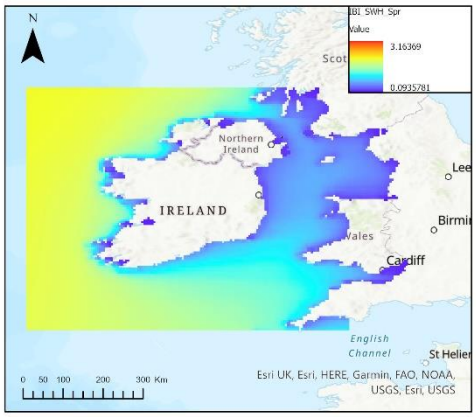



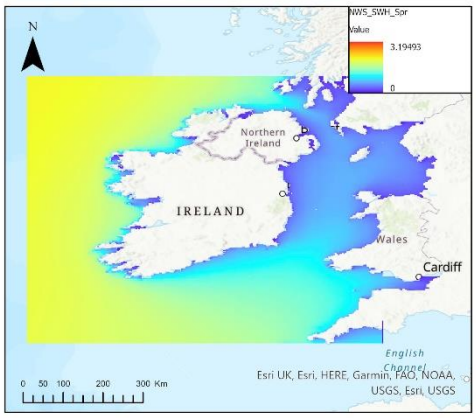




Title

Scatter plot showing the relationship between the mean significant wave height (m) for the spring months for the IBI and NWS models, with the IBI model showing in the map on the top right and the NWS map on the bottom left of the page.

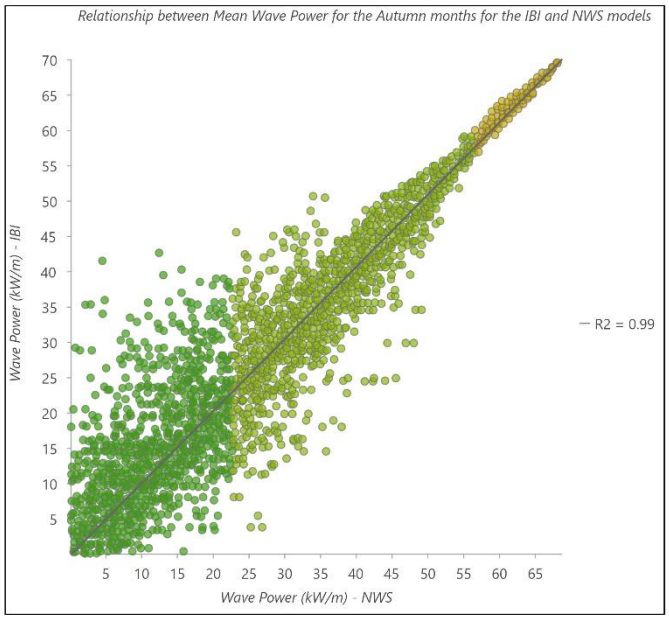


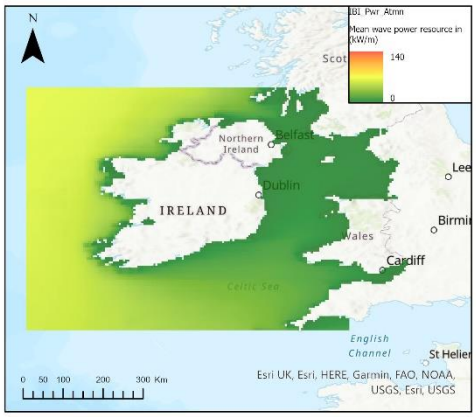



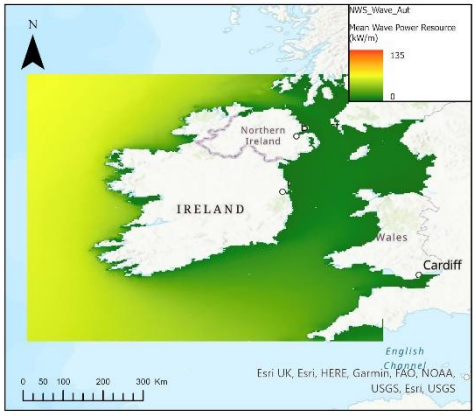



Title

Scatter plot showing the relationship between the mean wave power (kW/m) for the autumn months for the IBI and NWS models, with the IBI model showing in the map on the top right and the NWS map on the bottom left of the page.

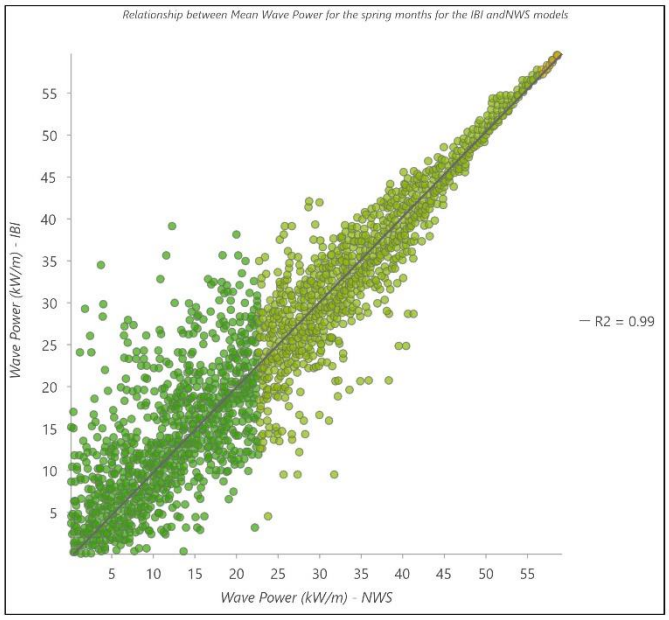


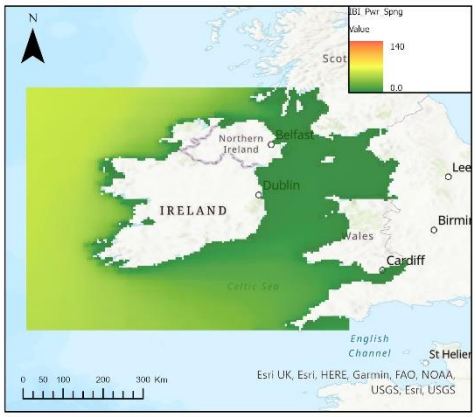



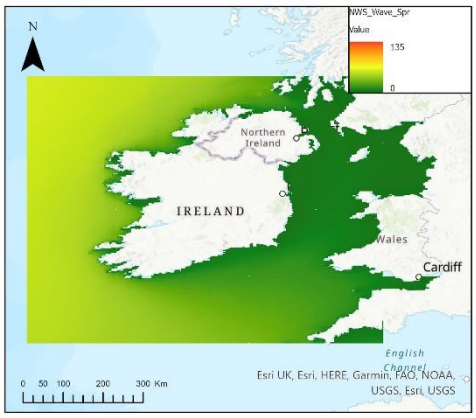




Title

Scatter plot showing the relationship between the mean wave power (kW/m) for the spring months for the IBI and NWS models, with the IBI model showing in the map on the top right and the NWS map on the bottom left of the page.

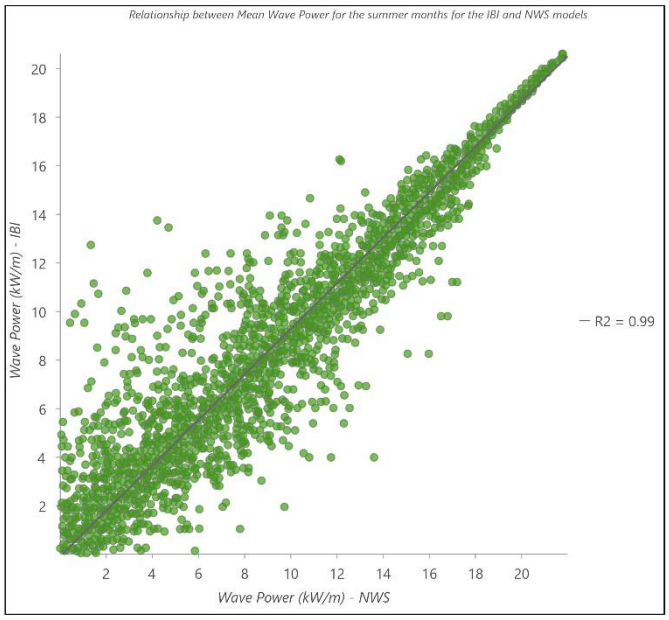


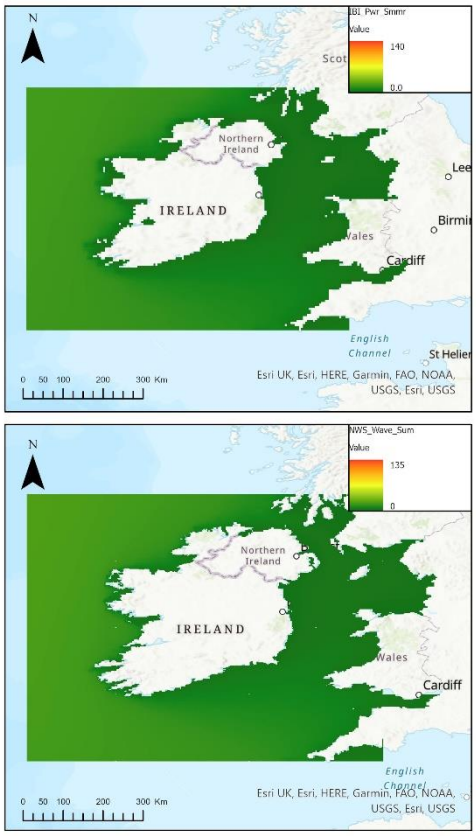



Title

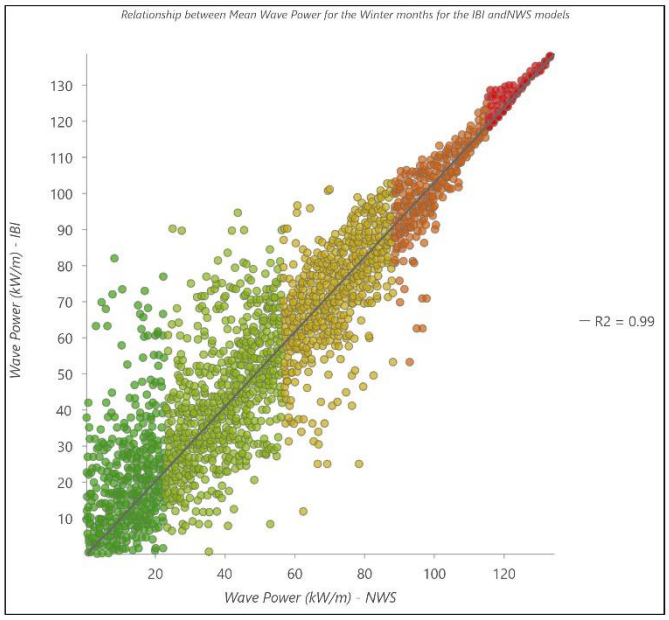
Scatter plot showing the relationship between the mean wave power (kW/m) for the summer months for the IBI and NWS models, with the IBI model showing in the map on the top right and the NWS map on the bottom left of the page.

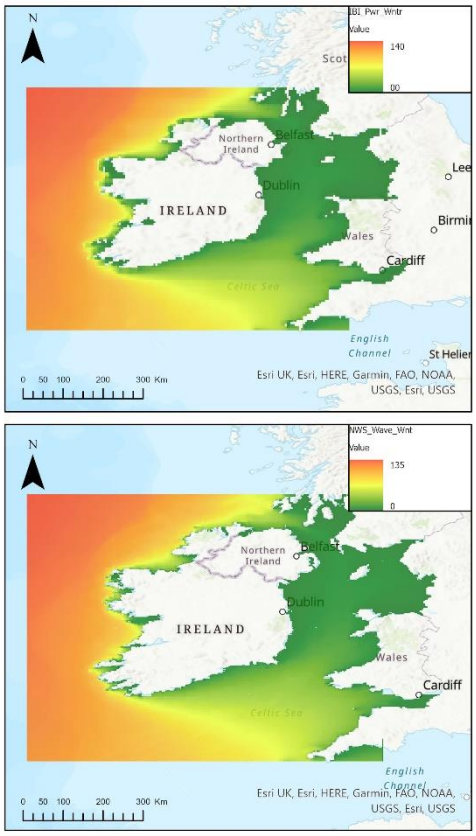


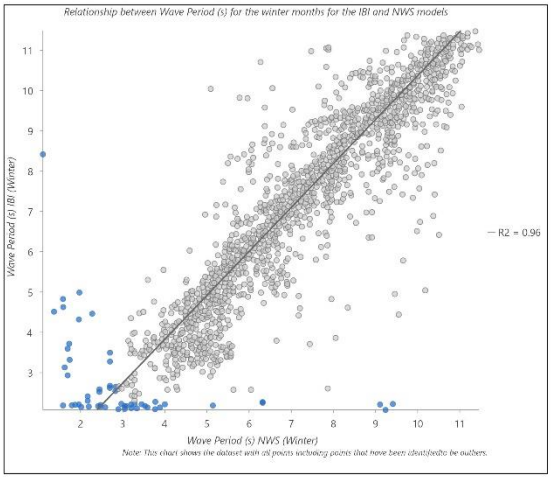

Title

Scatter plot showing the relationship between the mean wave power (kW/m) for the winter months for the IBI and NWS models, with the IBI model showing in the map on the top right and the NWS map on the bottom left of the page.



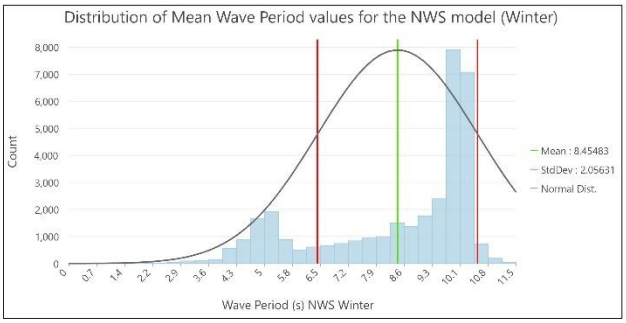



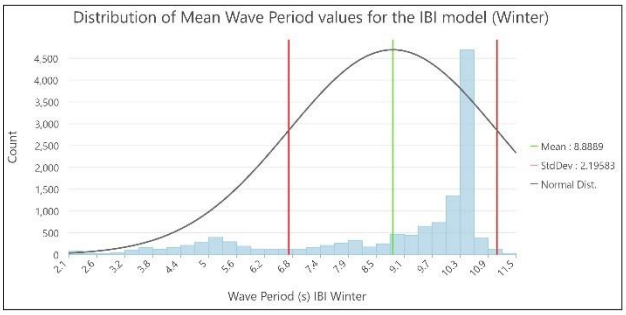



**Title**

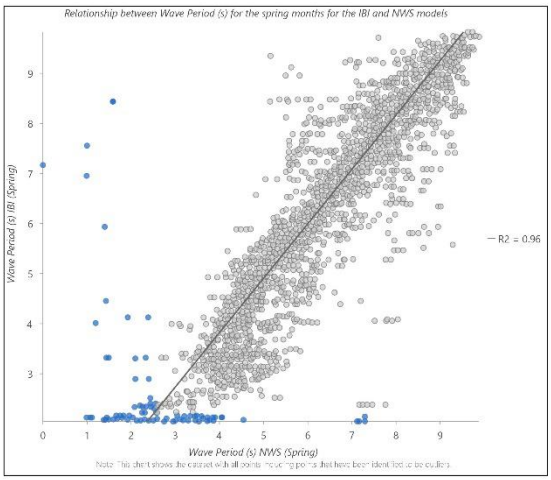
This figure aims to show the statistics of the IBI and NWS models for the winter data, including the mean and standard deviations in the histograms, as well as the correlation between both models in the scatter plot. Z-Scores have been calculated for both datasets and these have been used to identify any outliers in the data, which can be seen in the map.



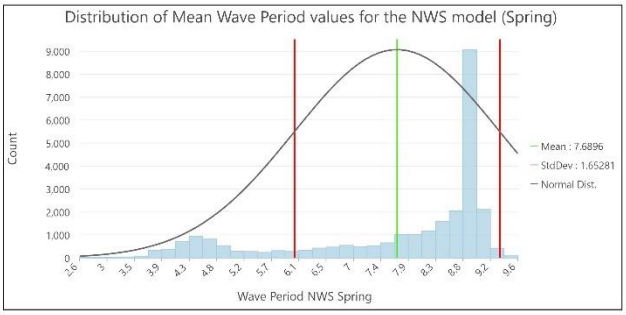


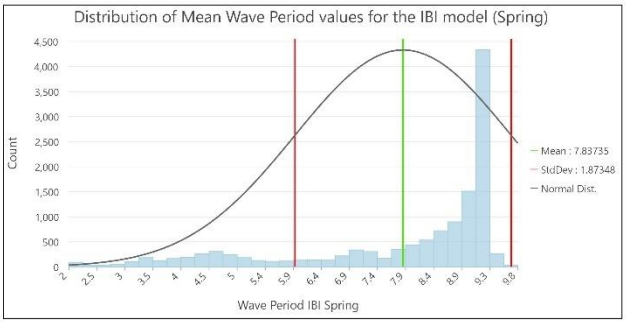





**Title**

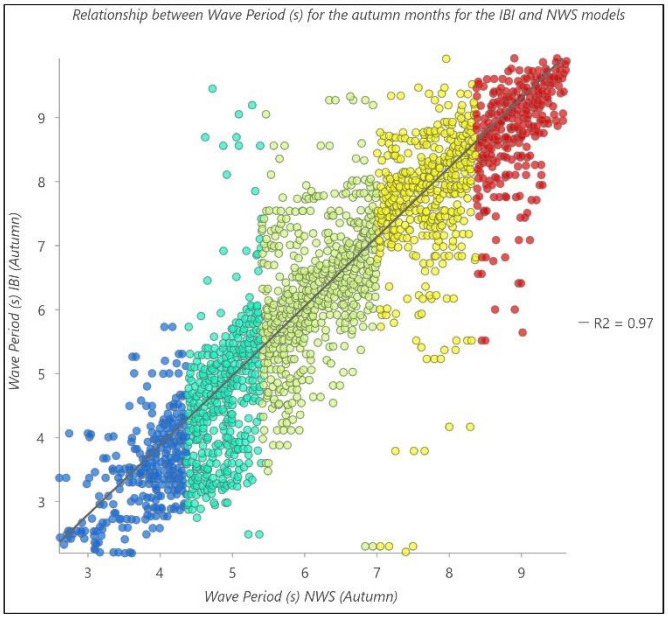
This figure aims to show the statistics of the IBI and NWS models for the spring data, including the mean and standard deviations in the histograms, as well as the correlation between both models in the scatter plot. Z-Scores have been calculated for both datasets and these have been used to identify any outliers in the data, which can be seen in the map.

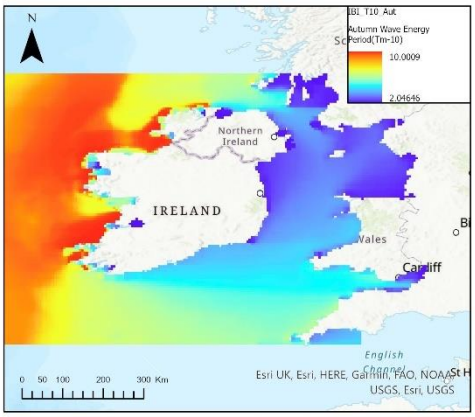


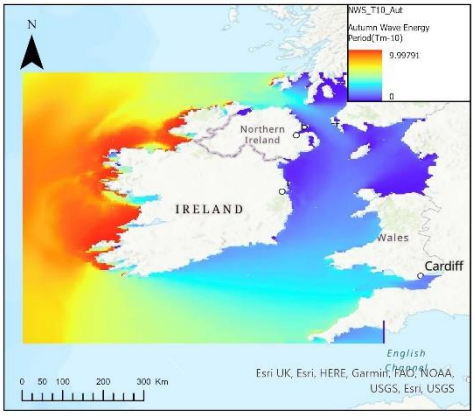



Title

Scatter plot showing the relationship between the mean wave period (s) for the autumn months for the IBI and NWS models, with the IBI model showing in the map on the top right and the NWS map on the bottom left of the page.

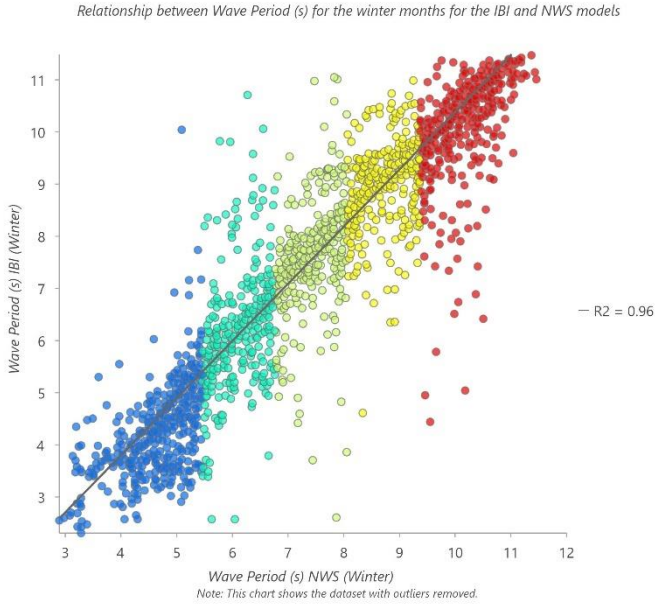


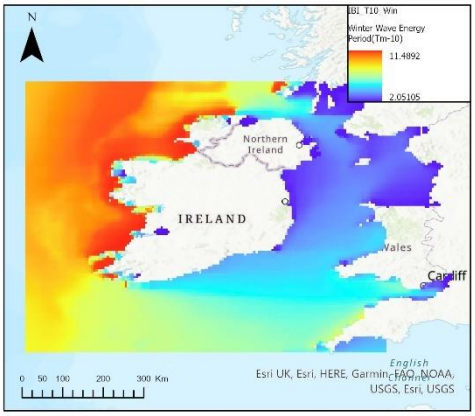



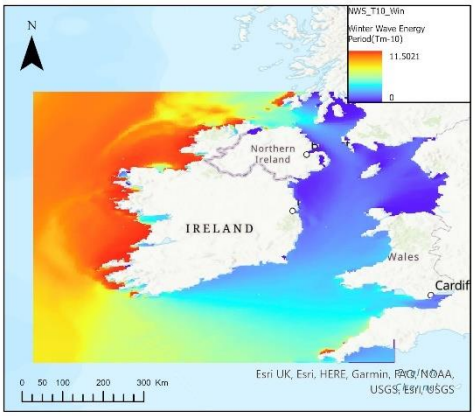




Title

Scatter plot showing the relationship between the mean wave period (s) for the winter months for the IBI and NWS models, with the IBI model showing in the map on the top right and the NWS map on the bottom left of the page.

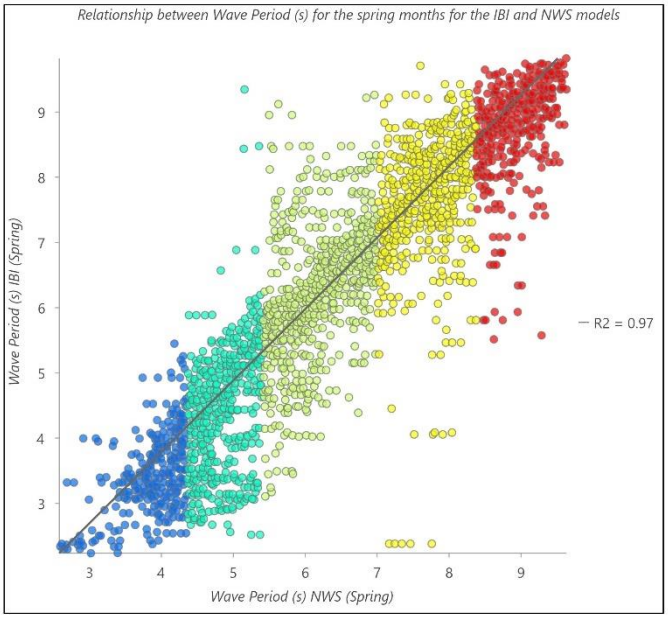


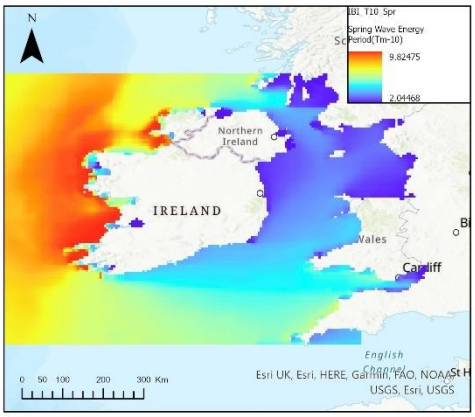



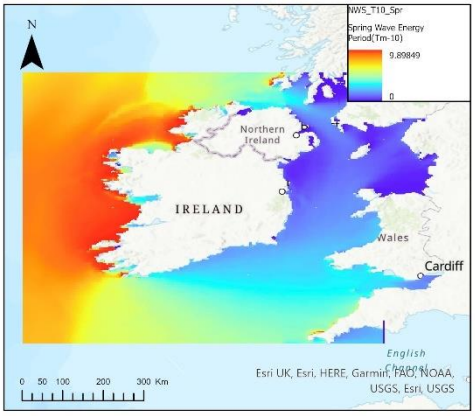



Title

Scatter plot showing the relationship between the mean wave period (s) for the spring months for the IBI and NWS models, with the IBI model showing in the map on the top right and the NWS map on the bottom left of the page.

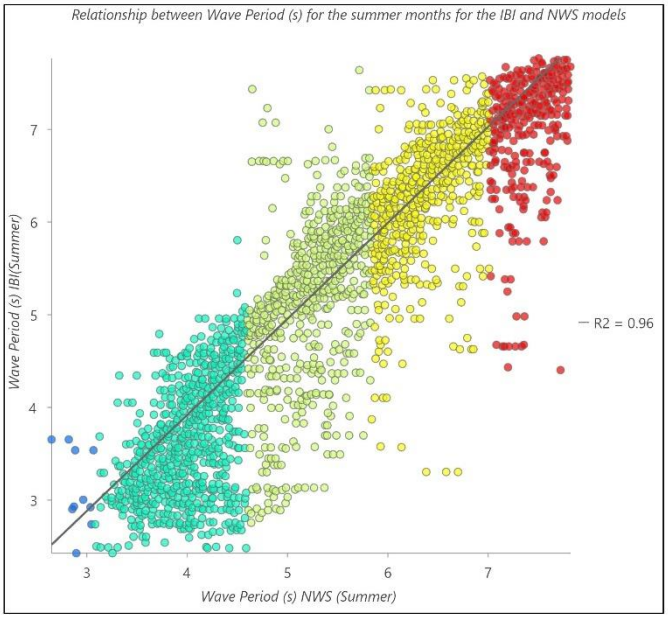


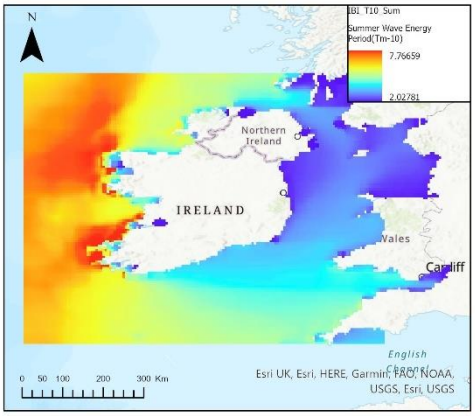



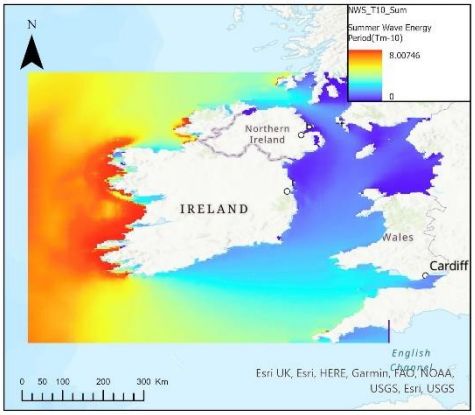




Title

Scatter plot showing the relationship between the mean wave period (s) for the summer months for the IBI and NWS models, with the IBI model showing in the map on the top right and the NWS map on the bottom left of the page.



## 3 – Tables

| ***Layer Name*** | ***Description*** |
|---|---|
| Mean wave power kW/m | A layer showing the calculated mean wave power in kW/m which has been derived using the wave power equation (see Section 2.1.1). The layer was created using a 20 year time series of data. |
| Mean Winter Wave Power kW/m | A layer showing the mean wave power in kW/m for the winter months. Each grid point displays a mean value that has been calculated using a 20 year time series. |
| Mean Summer Wave Power kW/m | A layer showing the mean wave power in kW/m for the summer months. Each grid point displays a mean value that has been calculated using a 20 year time series. |
| Mean Spring Wave Power kW/m | A layer showing the mean wave power in kW/m for the spring months. Each grid point displays a mean value that has been calculated using a 20 year time series. |
| Mean Autumn Wave Power kW/m | A layer showing the mean wave power in kW/m for the autumn months. Each grid point displays a mean value that has been calculated using a 20 year time series. |
| Mean Winter Significant Wave Heights (m) | A layer showing the mean significant wave heights in metres for the winter months. Each grid point displays a mean value that has been calculated using a 20 year time series. |
| Mean Summer Significant Wave Heights (m) | A layer showing mean significant wave heights in metres for the summer months. Each grid point displays a mean value that has been calculated using a 20 year time series. |

| | |
|---|---|
| Mean Spring Significant Wave Heights (m) | A layer showing the mean significant wave heights in metres for the spring months. Each grid point displays a mean value that has been calculated using a 20 year time series. |
| Mean Autumn Significant Wave Heights (m) | A layer showing the mean significant wave heights in metres for the autumn months. Each grid point displays a mean value that has been calculated using a 20 year time series. |
| Mean Winter Wave Energy Period (s) | A layer showing the mean wave period in seconds for the winter months. Each grid point displays a mean value that has been calculated using a 20 year time series. |
| Mean Summer Wave Energy Period (s) | A layer showing the mean wave period in seconds for the summer months. Each grid point displays a mean value that has been calculated using a 20 year time series. |
| Mean Spring Wave Energy Period (s) | A layer showing the mean wave period in seconds for the spring months. Each grid point displays a mean value that has been calculated using a 20 year time series. |
| Mean Autumn Wave Energy Period (s) | A layer showing the mean wave period in seconds for the autumn months. Each grid point displays a mean value that has been calculated using a 20 year time series. |

| ***Layer Name*** | ***Description*** |
|---|---|
| Maximum spring peak current velocity (m/s) - | Maximum value for the peak flow of the spring current for the time series – values are in metres per second. |
| Maximum neap peak current velocity (m/s) | Maximum value for the peak flow of the neap current for the time series – values are in metres per second. |

| | |
|---|---|
| Mean spring peak current velocity (m/s) | Average value for the peak flow of the spring current for the time series – values are in metres per second. |
| Mean neap peak current velocity (m/s) | Average value for the peak flow of the neap current for the time series – values are in metres per second. |
| Mean peak current velocity (m/s) | Average value for the peak flow of the current irrespective of spring/neap cycles for the time series – values are in metres per second. |
| Max peak current velocity (m/s) | Maximum value for the peak flow of the current irrespective of spring/neap cycles for the time series – values are in metres per second. |
| Mean Tidal Power ($W/m^2$) | Average value for tidal power (irrespective of the device swept area) for the time series – values are in $W/m^2$ |
| Total Energy (MWh) | The total annual energy that is available per $m^2$ in megawatt – hours. |
| Total Spring Energy (MWh) | The total annual energy that is available per $m^2$ in megawatt- hours, with current values only taken from spring tidal cycles. |
| Total Neap Energy (MWh) | The total annual energy that is available per $m^2$ in megawatt - hours, with current values only taken from neap tidal cycles. |
| Mean Spring Tidal Power ($W/m^2$) | Average value for tidal power (irrespective of the device swept area) for the time series – values are in $W/m^2$. Current values that were used to calculate the power values were take only from spring tidal cycles. |
| Mean Neap Tidal Power ($W/m^2$) | Average value for tidal power (irrespective of the device swept area) for the time series – values are in $W/m^2$. Current values that were used to calculate the power values were take only from neap tidal cycles. |

*Mean Wave Power*

```
clear all
close all

% address the netcdf file with the model data
ncfile = 'cmems_mod_ibi_wav_55.5_55_11_10.nc';

% call the longitude from the model
long = ncread(ncfile,'longitude');

% call the latitude from the model
lat = ncread(ncfile,'latitude');

% call the time values from the netcdf file for the model
time = ncread(ncfile,'time');

% change time format from 'hours since 1950-1-1 00:00:00'
to normal date
% and time
%time_formatted_model = datestr(time/24+datenum('1950-01-
01 00:00:00'));

% convert from 'datestring' to 'datetime' for readability
%time = datetime(time_formatted_model);

% call the significant wave height values from the netcdf
file for the
%model
SWH = ncread(ncfile,'VHM0');

% call the wave period values from the netcdf file for
the model
T10 = ncread(ncfile,'VTM10');

% calculate the wave power
Wave_Power = 0.49*(SWH.^2).*(T10);

% define the dimension for which to sum the values of
S = sum(Wave_Power,3);

% divide by the number of time sets to get the average
S = S/175296;

% create the inverse for matrix dimension agreement
S = S';
```

```
mymap = pcolor(long, lat, S)

% Get geo referenced
R =
georasterref('RasterSize',size(S),'LatitudeLimits',[55,55
.5],'LongitudeLimits',[-11,-10]);
%S = flipud(S) ;
% write to tiff file
tiffile =
'cmems_mod_ibi_wav_55.5_55_11_10_wave_power.tif' ;
geotiffwrite(tiffile,S,R)
%% Read geotiff file
[S, R] = geotiffread(tiffile);
```

*Winter Months Wave Power*

```
clear all
close all

% address the netcdf file with the model data
ncfile = 'cmems_mod_ibi_wav_53_52.5_12_11.nc';

% call the longitude from the model
long = ncread(ncfile,'longitude');

% call the latitude from the model
lat = ncread(ncfile,'latitude');

% call the time values from the netcdf file for the model
time = ncread(ncfile,'time');

% change time format from 'hours since 1950-1-1 00:00:00'
to normal date
% and time
time_formatted_model = datestr(time/24+datenum('1950-01-
01 00:00:00'));

% convert from 'datestring' to 'datetime' for readability
time = datetime(time_formatted_model);

% convert from 'datetime' 'datevec' for readability
dv = datevec(time);

% define the start and end times
month = dv(:,2);
```

```
for i = 1:4
    i
    if i ==4
        winter = find (month==12 | month ==1 | month==2);
    end
end

% call the wave period values from the netcdf file for
the model
T10 = ncread(ncfile,'VTM10');

% Extract winter data from sst
T10Winter = T10(:,:,winter)

% call the significant wave height values from the netcdf
file for the model
SWH = ncread(ncfile,'VHM0');

% Extract winter data from sst
swhWinter = SWH(:,:,winter)

% calculate the wave power
Wave_Power = 0.49*(swhWinter.^2).*(T10Winter);

% define the dimension for which to sum the values of
S = sum(Wave_Power,3);

% divide by the number of time sets to get the average
S = S/(43296);

% create the inverse for matrix dimension agreement
S = S';

% create pseudocolor plot of matrix
pcolor(long,lat,S);

% Get geo referenced
R =
georasterref('RasterSize',size(S),'LatitudeLimits',[52.5,
53],'LongitudeLimits',[-12,-11]);
%S = flipud(S) ;
% write to tiff file
tiffile =
'cmems_mod_ibi_wav_53_52.5_12_11_winter_wave_power.tif' ;
geotiffwrite(tiffile,S,R)
%Read geotiff file
[S, R] = geotiffread(tiffile);
```

*Winter Months Significant Wave Height*

```
clear all
close all

% address the netcdf file with the model data
ncfile = 'cmems_mod_ibi_wav_51_50.5_11_10.nc';

% call the longitude from the model
long = ncread(ncfile,'longitude');

% call the latitude from the model
lat = ncread(ncfile,'latitude');

% call the time values from the netcdf file for the model
time = ncread(ncfile,'time');

% change time format from 'hours since 1950-1-1 00:00:00'
to normal date
% and time
time_formatted_model = datestr(time/24+datenum('1950-01-
01 00:00:00'));

% convert from 'datestring' to 'datetime' for readability
time = datetime(time_formatted_model);

% convert from 'datetime' 'datevec' for readability
dv = datevec(time);

% define the start and end times
month = dv(:,2);

for i = 1:4
    i
    if i ==4
        winter = find (month==12 | month ==1 | month==2);
    end
end

% call the significant wave height values from the netcdf
file for the model
SWH = ncread(ncfile,'VHM0');

% Extract winter data from sst
swhWinter = SWH(:,:,winter)
```

```
% define the dimension for which to sum the values of
S = sum(swhWinter,3);

% divide by the number of time sets to get the average
S = S/(43296);

% create the inverse for matrix dimension agreement
S = S';

% create pseudocolor plot of matrix
pcolor(long,lat,S);

% Get geo referenced
R =
georasterref('RasterSize',size(S),'LatitudeLimits',[50.5,
51],'LongitudeLimits',[-11,-10]);
%S = flipud(S) ;
% write to tiff file
tiffile =
'cmems_mod_ibi_wav_51_50.5_11_10_winter_swh_v2.tif' ;
geotiffwrite(tiffile,S,R)
%Read geotiff file
[S, R] = geotiffread(tiffile);
```

*Winter Months Spectral Wave Period*

```
clear all
close all

% address the netcdf file with the model data
ncfile = 'cmems_mod_ibi_wav_56_55.5_12_11.nc';

% call the longitude from the model
long = ncread(ncfile,'longitude');

% call the latitude from the model
lat = ncread(ncfile,'latitude');

% call the time values from the netcdf file for the model
time = ncread(ncfile,'time');

% change time format from 'hours since 1950-1-1 00:00:00'
to normal date
% and time
```

```
time_formatted_model = datestr(time/24+datenum('1950-01-
01 00:00:00'));

% convert from 'datestring' to 'datetime' for readability
time = datetime(time_formatted_model);

% convert from 'datetime' 'datevec' for readability
dv = datevec(time);

% define the start and end times
month = dv(:,2);

for i = 1:4
    i
    if i ==4
        winter = find (month==12 | month ==1 | month==2);
    end
end

% call the wave period values from the netcdf file for
the model
T10 = ncread(ncfile,'VTM10');

% Extract winter data from sst
T10Winter = T10(:,:,winter)

% define the dimension for which to sum the values of
S = sum(T10Winter,3);

% divide by the number of time sets to get the average
S = S/(43296);

% create the inverse for matrix dimension agreement
S = S';

% create pseudocolor plot of matrix
pcolor(long,lat,S);

% Get geo referenced
R =
georasterref('RasterSize',size(S),'LatitudeLimits',[55.5,
56],'LongitudeLimits',[-12,-11]);
%S = flipud(S) ;
% write to tiff file
tiffile =
'cmems_mod_ibi_wav_56_55.5_12_11_winter_T10.tif' ;
geotiffwrite(tiffile,S,R)
%Read geotiff file
```

```
[S, R] = geotiffread(tiffile);
```

*Autumn Months Wave Power*

```
clear all
close all

% address the netcdf file with the model data
ncfile = 'cmems_mod_ibi_wav_53_52.5_12_11.nc';

% call the longitude from the model
long = ncread(ncfile,'longitude');

% call the latitude from the model
lat = ncread(ncfile,'latitude');

% call the time values from the netcdf file for the model
time = ncread(ncfile,'time');

% change time format from 'hours since 1950-1-1 00:00:00'
to normal date
% and time
time_formatted_model = datestr(time/24+datenum('1950-01-
01 00:00:00'));

% convert from 'datestring' to 'datetime' for readability
time = datetime(time_formatted_model);

% convert from 'datetime' 'datevec' for readability
dv = datevec(time);

% define the start and end times
month = dv(:,2);

for i = 1:4
    i
    if i ==3
        autumn = find (month==9 | month ==10 |
month==11);
    end
end

% call the wave period values from the netcdf file for
the model
T10 = ncread(ncfile,'VTM10');
```

```
% Extract winter data from sst
T10Autumn = T10(:,:,autumn)

% call the significant wave height values from the netcdf
file for the model
SWH = ncread(ncfile,'VHM0');

% Extract winter data from sst
swhAutumn = SWH(:,:,autumn)

% calculate the wave power
Wave_Power = 0.49*(swhAutumn.^2).*(T10Autumn);

% define the dimension for which to sum the values of
S = sum(Wave_Power,3);

% divide by the number of time sets to get the average
S = S/(43680);

% create the inverse for matrix dimension agreement
S = S';

% create pseudocolor plot of matrix
pcolor(long,lat,S);

% Get geo referenced
R =
georasterref('RasterSize',size(S),'LatitudeLimits',[52.5,
53],'LongitudeLimits',[-12,-11]);
%S = flipud(S) ;
% write to tiff file
tiffile =
'cmems_mod_ibi_wav_53_52.5_12_11_autumn_wave_Power.tif' ;
geotiffwrite(tiffile,S,R)
%Read geotiff file
[S, R] = geotiffread(tiffile);
```

*Autumn Months Significant Wave Height*

```
clear all
close all

% address the netcdf file with the model data
ncfile = 'cmems_mod_ibi_wav_56_55.5_12_11.nc';
```

```
% call the longitude from the model
long = ncread(ncfile,'longitude');

% call the latitude from the model
lat = ncread(ncfile,'latitude');

% call the time values from the netcdf file for the model
time = ncread(ncfile,'time');

% change time format from 'hours since 1950-1-1 00:00:00'
to normal date
% and time
time_formatted_model = datestr(time/24+datenum('1950-01-
01 00:00:00'));

% convert from 'datestring' to 'datetime' for readability
time = datetime(time_formatted_model);

% convert from 'datetime' 'datevec' for readability
dv = datevec(time);

% define the start and end times
month = dv(:,2);

for i = 1:4
    i
    if i ==3
        autumn = find (month==9 | month ==10 |
month==11);
    end
end

% call the significant wave height values from the netcdf
file for the model
SWH = ncread(ncfile,'VHM0');

% Extract winter data from sst
swhAutumn = SWH(:,:,autumn)

% define the dimension for which to sum the values of
S = sum(swhAutumn,3);

% divide by the number of time sets to get the average
S = S/(43680);

% create the inverse for matrix dimension agreement
S = S';
```

```
% create pseudocolor plot of matrix
pcolor(long,lat,S);

% Get geo referenced
R =
georasterref('RasterSize',size(S),'LatitudeLimits',[55.5,
56],'LongitudeLimits',[-12,-11]);
%S = flipud(S) ;
% write to tiff file
tiffile =
'cmems_mod_ibi_wav_56_55.5_12_11_autumn_swh.tif' ;
geotiffwrite(tiffile,S,R)
%Read geotiff file
[S, R] = geotiffread(tiffile);
```

*Autumn Months Spectral Wave Period*

```
clear all
close all

% address the netcdf file with the model data
ncfile = 'cmems_mod_ibi_wav_56_55.5_12_11.nc';

% call the longitude from the model
long = ncread(ncfile,'longitude');

% call the latitude from the model
lat = ncread(ncfile,'latitude');

% call the time values from the netcdf file for the model
time = ncread(ncfile,'time');

% change time format from 'hours since 1950-1-1 00:00:00'
to normal date
% and time
time_formatted_model = datestr(time/24+datenum('1950-01-
01 00:00:00'));

% convert from 'datestring' to 'datetime' for readability
time = datetime(time_formatted_model);

% convert from 'datetime' 'datevec' for readability
dv = datevec(time);
```

```
% define the start and end times
month = dv(:,2);

for i = 1:4
    i
    if i ==3
        autumn = find (month==9 | month ==10 |
month==11);
    end
end

% call the wave period values from the netcdf file for
the model
T10 = ncread(ncfile,'VTM10');

% Extract winter data from sst
T10Autumn = T10(:,:,autumn)

% define the dimension for which to sum the values of
S = sum(T10Autumn,3);

% divide by the number of time sets to get the average
S = S/(43680);

% create the inverse for matrix dimension agreement
S = S';

% create pseudocolor plot of matrix
pcolor(long,lat,S);

% Get geo referenced
R =
georasterref('RasterSize',size(S),'LatitudeLimits',[55.5,
56],'LongitudeLimits',[-12,-11]);
%S = flipud(S) ;
% write to tiff file
tiffile =
'cmems_mod_ibi_wav_56_55.5_12_11_autumn_T10.tif' ;
geotiffwrite(tiffile,S,R)
%Read geotiff file
[S, R] = geotiffread(tiffile);
```

*Spring Months Wave Power*

```
clear all
```

```
close all

% address the netcdf file with the model data
ncfile = 'cmems_mod_ibi_wav_53_52.5_12_11.nc';

% call the longitude from the model
long = ncread(ncfile,'longitude');

% call the latitude from the model
lat = ncread(ncfile,'latitude');

% call the time values from the netcdf file for the model
time = ncread(ncfile,'time');

% change time format from 'hours since 1950-1-1 00:00:00'
to normal date
% and time
time_formatted_model = datestr(time/24+datenum('1950-01-
01 00:00:00'));

% convert from 'datestring' to 'datetime' for readability
time = datetime(time_formatted_model);

% convert from 'datetime' 'datevec' for readability
dv = datevec(time);

% define the start and end times
month = dv(:,2);

for i = 1:4
    i
    if i ==1
        spring = find (month==3 | month ==4 | month==5);
    end
end

% call the wave period values from the netcdf file for
the model
T10 = ncread(ncfile,'VTM10');

% Extract winter data from sst
T10Spring = T10(:,:,spring)

% call the significant wave height values from the netcdf
file for the model
SWH = ncread(ncfile,'VHM0');

% Extract winter data from sst
```

```
swhSpring = SWH(:,:,spring)

% calculate the wave power
Wave_Power = 0.49*(swhSpring.^2).*(T10Spring);

% define the dimension for which to sum the values of
S = sum(Wave_Power,3);

% divide by the number of time sets to get the average
S = S/(44160);

% create the inverse for matrix dimension agreement
S = S';

% create pseudocolor plot of matrix
pcolor(long,lat,S);

% Get geo referenced
R =
georasterref('RasterSize',size(S),'LatitudeLimits',[52.5,
53],'LongitudeLimits',[-12,-11]);
%S = flipud(S) ;
% write to tiff file
tiffile =
'cmems_mod_ibi_wav_53_52.5_12_11_spring_wave_power.tif' ;
geotiffwrite(tiffile,S,R)
%Read geotiff file
[S, R] = geotiffread(tiffile);
```

*Spring Months Significant Wave Heights*

```
clear all
close all

% address the netcdf file with the model data
ncfile = 'cmems_mod_ibi_wav_56_55.5_12_11.nc';

% call the longitude from the model
long = ncread(ncfile,'longitude');

% call the latitude from the model
lat = ncread(ncfile,'latitude');

% call the time values from the netcdf file for the model
time = ncread(ncfile,'time');
```

```
% change time format from 'hours since 1950-1-1 00:00:00'
to normal date
% and time
time_formatted_model = datestr(time/24+datenum('1950-01-
01 00:00:00'));

% convert from 'datestring' to 'datetime' for readability
time = datetime(time_formatted_model);

% convert from 'datetime' 'datevec' for readability
dv = datevec(time);

% define the start and end times
month = dv(:,2);

for i = 1:4
    i
    if i ==1
        spring = find (month==3 | month ==4 | month==5);
    end
end

% call the significant wave height values from the netcdf
file for the model
SWH = ncread(ncfile,'VHM0');

% Extract summer data from sst
swhSpring = SWH(:,:,spring)

% define the dimension for which to sum the values of
S = sum(swhSpring,3);

% divide by the number of time sets to get the average
S = S/(44160);

% create the inverse for matrix dimension agreement
S = S';

% create pseudocolor plot of matrix
pcolor(long,lat,S);

% Get geo referenced
R =
georasterref('RasterSize',size(S),'LatitudeLimits',[55.5,
56],'LongitudeLimits',[-12,-11]);
%S = flipud(S) ;
% write to tiff file
```

```
tiffile =
'cmems_mod_ibi_wav_56_55.5_12_11_spring_swh.tif' ;
geotiffwrite(tiffile,S,R)
%Read geotiff file
[S, R] = geotiffread(tiffile);
```

*Spring Months Spectral Wave Period*

```
clear all
close all

% address the netcdf file with the model data
ncfile = 'cmems_mod_ibi_wav_56_55.5_12_11.nc';

% call the longitude from the model
long = ncread(ncfile,'longitude');

% call the latitude from the model
lat = ncread(ncfile,'latitude');

% call the time values from the netcdf file for the model
time = ncread(ncfile,'time');

% change time format from 'hours since 1950-1-1 00:00:00'
to normal date
% and time
time_formatted_model = datestr(time/24+datenum('1950-01-
01 00:00:00'));

% convert from 'datestring' to 'datetime' for readability
time = datetime(time_formatted_model);

% convert from 'datetime' 'datevec' for readability
dv = datevec(time);

% define the start and end times
month = dv(:,2);

for i = 1:4
    i
    if i ==1
        spring = find (month==3 | month ==4 | month==5);
    end
end
```

```
% call the wave period values from the netcdf file for
the model
T10 = ncread(ncfile,'VTM10');

% Extract winter data from sst
T10Spring = T10(:,:,spring)

% define the dimension for which to sum the values of
S = sum(T10Spring,3);

% divide by the number of time sets to get the average
S = S/(44160);

% create the inverse for matrix dimension agreement
S = S';

% create pseudocolor plot of matrix
pcolor(long,lat,S);

% Get geo referenced
R =
georasterref('RasterSize',size(S),'LatitudeLimits',[55.5,
56],'LongitudeLimits',[-12,-11]);
%S = flipud(S) ;
% write to tiff file
tiffile =
'cmems_mod_ibi_wav_56_55.5_12_11_spring_T10.tif' ;
geotiffwrite(tiffile,S,R)
%Read geotiff file
[S, R] = geotiffread(tiffile);
```

*Summer Months Wave Power*

```
clear all
close all

% address the netcdf file with the model data
ncfile = 'cmems_mod_ibi_wav_53_52.5_12_11.nc';

% call the longitude from the model
long = ncread(ncfile,'longitude');

% call the latitude from the model
lat = ncread(ncfile,'latitude');
```

```
% call the time values from the netcdf file for the model
time = ncread(ncfile,'time');

% change time format from 'hours since 1950-1-1 00:00:00'
to normal date
% and time
time_formatted_model = datestr(time/24+datenum('1950-01-
01 00:00:00'));

% convert from 'datestring' to 'datetime' for readability
time = datetime(time_formatted_model);

% convert from 'datetime' 'datevec' for readability
dv = datevec(time);

% define the start and end times
month = dv(:,2);

for i = 1:4
    i
    if i ==2
        summer = find (month==6 | month ==7 | month==8);
    end
end

% call the wave period values from the netcdf file for
the model
T10 = ncread(ncfile,'VTM10');

% Extract winter data from sst
T10Summer = T10(:,:,summer)

% call the significant wave height values from the netcdf
file for the model
SWH = ncread(ncfile,'VHM0');

% Extract winter data from sst
swhSummer = SWH(:,:,summer)

% calculate the wave power
Wave_Power = 0.49*(swhSummer.^2).*(T10Summer);

% define the dimension for which to sum the values of
S = sum(Wave_Power,3);

% divide by the number of time sets to get the average
S = S/(44160);
```

```
% create the inverse for matrix dimension agreement
S = S';

% create pseudocolor plot of matrix
pcolor(long,lat,S);

% Get geo referenced
R =
georasterref('RasterSize',size(S),'LatitudeLimits',[52.5,
53],'LongitudeLimits',[-12,-11]);
%S = flipud(S) ;
% write to tiff file
tiffile =
'cmems_mod_ibi_wav_53_52.5_12_11_summer_wave_power.tif' ;
geotiffwrite(tiffile,S,R)
%Read geotiff file
[S, R] = geotiffread(tiffile);
```

*Summer Months Significant Wave Heights*

```
clear all
close all

% address the netcdf file with the model data
ncfile = 'cmems_mod_ibi_wav_56_55.5_12_11.nc';

% call the longitude from the model
long = ncread(ncfile,'longitude');

% call the latitude from the model
lat = ncread(ncfile,'latitude');

% call the time values from the netcdf file for the model
time = ncread(ncfile,'time');

% change time format from 'hours since 1950-1-1 00:00:00'
to normal date
% and time
time_formatted_model = datestr(time/24+datenum('1950-01-
01 00:00:00'));

% convert from 'datestring' to 'datetime' for readability
time = datetime(time_formatted_model);

% convert from 'datetime' 'datevec' for readability
```

```
dv = datevec(time);

% define the start and end times
month = dv(:,2);

for i = 1:4
    i
    if i ==2
        summer = find (month==6 | month ==7 | month==8);
    end
end

% call the significant wave height values from the netcdf
file for the model
SWH = ncread(ncfile,'VHM0');

% Extract winter data from sst
swhSummer = SWH(:,:,summer)

% define the dimension for which to sum the values of
S = sum(swhSummer,3);

% divide by the number of time sets to get the average
S = S/(44160);

% create the inverse for matrix dimension agreement
S = S';

% create pseudocolor plot of matrix
pcolor(long,lat,S);

% Get geo referenced
R =
georasterref('RasterSize',size(S),'LatitudeLimits',[55.5,
56],'LongitudeLimits',[-12,-11]);
%S = flipud(S) ;
% write to tiff file
tiffile =
'cmems_mod_ibi_wav_56_55.5_12_11_summer_swh.tif' ;
geotiffwrite(tiffile,S,R)
%Read geotiff file
[S, R] = geotiffread(tiffile);
```

*Summer Months Spectral Wave Period*

```
clear all
close all

% address the netcdf file with the model data
ncfile = 'cmems_mod_ibi_wav_56_55.5_12_11.nc';

% call the longitude from the model
long = ncread(ncfile,'longitude');

% call the latitude from the model
lat = ncread(ncfile,'latitude');

% call the time values from the netcdf file for the model
time = ncread(ncfile,'time');

% change time format from 'hours since 1950-1-1 00:00:00'
to normal date
% and time
time_formatted_model = datestr(time/24+datenum('1950-01-
01 00:00:00'));

% convert from 'datestring' to 'datetime' for readability
time = datetime(time_formatted_model);

% convert from 'datetime' 'datevec' for readability
dv = datevec(time);

% define the start and end times
month = dv(:,2);

for i = 1:4
    i
    if i ==2
        summer = find (month==6 | month ==7 | month==8);
    end
end

% call the wave period values from the netcdf file for
the model
T10 = ncread(ncfile,'VTM10');

% Extract winter data from sst
T10Summer = T10(:,:,summer)

% define the dimension for which to sum the values of
S = sum(T10Summer,3);
```

```
% divide by the number of time sets to get the average
S = S/(44160);

% create the inverse for matrix dimension agreement
S = S';

% create pseudocolor plot of matrix
pcolor(long,lat,S);

% Get geo referenced
R =
georasterref('RasterSize',size(S),'LatitudeLimits',[55.5,
56],'LongitudeLimits',[-12,-11]);
%S = flipud(S) ;
% write to tiff file
tiffile =
'cmems_mod_ibi_wav_56_55.5_12_11_summer_T10.tif' ;
geotiffwrite(tiffile,S,R)
%Read geotiff file
[S, R] = geotiffread(tiffile);
```

## 5 – NWS Scripts

### *Mean Wave Power*

```
clear all
close all

% address the netcdf file with the model data
ncfile = 'MetO-NWS-WAV-RAN_50.5_50_11_10_v2.nc';

% call the longitude from the model
long = ncread(ncfile,'longitude');

% call the latitude from the model
lat = ncread(ncfile,'latitude');

% call the time values from the netcdf file for the model
time = ncread(ncfile,'time');

% change time format from 'hours since 1950-1-1 00:00:00'
to normal date
% and time
%time_formatted_model = datestr(time/24+datenum('1950-01-
01 00:00:00'));
```

```
% convert from 'datestring' to 'datetime' for readability
%time = datetime(time_formatted_model);

% call the significant wave height values from the netcdf
file for the
%model
SWH = ncread(ncfile,'VHM0');

% call the wave period values from the netcdf file for
the model
T10 = ncread(ncfile,'VTM10');

% calculate the wave power
Wave_Power = 0.49*(SWH.^2).*(T10);

% define the dimension for which to sum the values of
S = sum(Wave_Power,3);

% divide by the number of time sets to get the average
S = S/(58440);

% create the inverse for matrix dimension agreement
S = S';

mymap = pcolor(long, lat, S)

% Get geo referenced
R =
georasterref('RasterSize',size(S),'LatitudeLimits',[50,50
.5],'LongitudeLimits',[-11,-10]);
%S = flipud(S) ;3
% write to tiff file
tiffile = 'MetO-NWS-WAV-
RAN_50.5_50_11_10_v2_wave_power_test.tif' ;
geotiffwrite(tiffile,S,R)
%% Read geotiff file
[S, R] = geotiffread(tiffile);
```

*Winter Months Wave Power*

```
clear all
close all

% address the netcdf file with the model data
ncfile = 'MetO-NWS-WAV-RAN_51_50.5_10_9.nc'
```

```
 ncdisp (ncfile)

% call the longitude from the model
long = ncread(ncfile,'longitude');

% call the latitude from the model
lat = ncread(ncfile,'latitude');

% call the time values from the netcdf file for the model
time = ncread(ncfile,'time');

%convert time to double
td = double(time)

% change time format from 'hours since 1950-1-1 00:00:00'
to normal date
% and time
time_formatted_model = datestr(td/24+datenum('2000-01-01
00:00:00'));

% convert from 'datestring' to 'datetime' for readability
time = datetime(time_formatted_model);

% convert from 'datetime' 'datevec' for readability
dv = datevec(time);

% define the start and end times
month = dv(:,2);

for i = 1:4
    i
    if i ==4
        winter = find (month==12 | month ==1 | month==2);
    end
end

% call the wave period values from the netcdf file for
the model
T10 = ncread(ncfile,'VTM10');

% Extract winter data from sst
T10Winter = T10(:,:,winter)

% call the significant wave height values from the netcdf
file for the model
SWH = ncread(ncfile,'VHM0');

% Extract winter data from sst
```

```
swhWinter = SWH(:,:,winter)

% calculate the wave power
Wave_Power = 0.49*(swhWinter.^2).*(T10Winter);

% define the dimension for which to sum the values of
S = sum(Wave_Power,3);

% divide by the number of time sets to get the average
S = S/(14440);

% create the inverse for matrix dimension agreement
S = S';

% create pseudocolor plot of matrix
pcolor(long,lat,S);

% Get geo referenced
R =
georasterref('RasterSize',size(S),'LatitudeLimits',[50.5,
51],'LongitudeLimits',[-10,-9]);
%S = flipud(S) ;
% write to tiff file
tiffile = 'MetO-NWS-WAV-
RAN_51_50.5_10_9_winter_wave_power.tif' ;
geotiffwrite(tiffile,S,R)
%Read geotiff file
[S, R] = geotiffread(tiffile);
```

*Winter Months Significant Wave Heights*

```
clear all
close all

% address the netcdf file with the model data
ncfile = 'MetO-NWS-WAV-RAN_54_53.5_4.5_3.5.nc';

% call the longitude from the model
long = ncread(ncfile,'longitude');

% call the latitude from the model
lat = ncread(ncfile,'latitude');

% call the time values from the netcdf file for the model
time = ncread(ncfile,'time');

%convert time to double
```

```
td = double(time)

% change time format from 'hours since 1950-1-1 00:00:00'
to normal date
% and time
time_formatted_model = datestr(td/86400+datenum('1970-01-
01 00:00:00'));

% convert from 'datestring' to 'datetime' for readability
time = datetime(time_formatted_model);

% convert from 'datetime' 'datevec' for readability
dv = datevec(time);

% define the start and end times
month = dv(:,2);

for i = 1:4
    i
    if i ==4
        winter = find (month==12 | month ==1 | month==2);
    end
end

% call the significant wave height values from the netcdf
file for the model
SWH = ncread(ncfile,'VHM0');

% Extract winter data from sst
swhWinter = SWH(:,:,winter)

% define the dimension for which to sum the values of
S = sum(swhWinter,3);

% divide by the number of time sets to get the average
S = S/(14440);

% create the inverse for matrix dimension agreement
S = S';

% create pseudocolor plot of matrix
pcolor(long,lat,S);

% Get geo referenced
R =
georasterref('RasterSize',size(S),'LatitudeLimits',[53.5,
54],'LongitudeLimits',[-4.5,-3.5]);
%S = flipud(S) ;
```

```
% write to tiff file
tiffile = 'MetO-NWS-WAV-
RAN_54_53.5_4.5_3.5_winter_swh_.tif' ;
geotiffwrite(tiffile,S,R)
%Read geotiff file
[S, R] = geotiffread(tiffile);
```

*Winter Months Spectral Wave Period*

```
clear all
close all

% address the netcdf file with the model data
ncfile = 'MetO-NWS-WAV-RAN_54_53.5_4.5_3.5.nc';

% call the longitude from the model
long = ncread(ncfile,'longitude');

% call the latitude from the model
lat = ncread(ncfile,'latitude');

% call the time values from the netcdf file for the model
time = ncread(ncfile,'time');

%convert time to double
td = double(time)

% change time format from 'hours since 1950-1-1 00:00:00'
to normal date
% and time
time_formatted_model = datestr(td/86400+datenum('1970-01-
01 00:00:00'));

% convert from 'datestring' to 'datetime' for readability
time = datetime(time_formatted_model);

% convert from 'datetime' 'datevec' for readability
dv = datevec(time);

% define the start and end times
month = dv(:,2);

for i = 1:4
    i
    if i ==4
        winter = find (month==12 | month ==1 | month==2);
    end
```

```
end

% call the wave period values from the netcdf file for
the model
T10 = ncread(ncfile,'VTM10');

% Extract winter data from sst
T10Winter = T10(:,:,winter)

% define the dimension for which to sum the values of
S = sum(T10Winter,3);

% divide by the number of time sets to get the average
S = S/(14440);

% create the inverse for matrix dimension agreement
S = S';

% create pseudocolor plot of matrix
pcolor(long,lat,S);

% Get geo referenced
R =
georasterref('RasterSize',size(S),'LatitudeLimits',[53.5,
54],'LongitudeLimits',[-4.5,-3.5]);
%S = flipud(S) ;
% write to tiff file
tiffile = 'MetO-NWS-WAV-
RAN_54_53.5_4.5_3.5_winter_T10.tif' ;
geotiffwrite(tiffile,S,R)
%Read geotiff file
[S, R] = geotiffread(tiffile);
```

*Autumn Months Wave Power*

```
clear all
close all

% address the netcdf file with the model data
ncfile = 'MetO-NWS-WAV-RAN_54_53.5_4.5_3.5.nc';

% call the longitude from the model
long = ncread(ncfile,'longitude');

% call the latitude from the model
lat = ncread(ncfile,'latitude');
```

```
% call the time values from the netcdf file for the model
time = ncread(ncfile,'time');

%convert time to double
td = double(time)

% change time format from 'hours since 1950-1-1 00:00:00'
to normal date
% and time
time_formatted_model = datestr(td/86400+datenum('1970-01-
01 00:00:00'));

% convert from 'datestring' to 'datetime' for readability
time = datetime(time_formatted_model);

% convert from 'datetime' 'datevec' for readability
dv = datevec(time);

% define the start and end times
month = dv(:,2);

for i = 1:4
    i
    if i ==3
        autumn = find (month==9 | month ==10 |
month==11);
    end
end

% call the wave period values from the netcdf file for
the model
T10 = ncread(ncfile,'VTM10');

% Extract winter data from sst
T10Autumn = T10(:,:,autumn)

% call the significant wave height values from the netcdf
file for the model
SWH = ncread(ncfile,'VHM0');

% Extract winter data from sst
swhAutumn = SWH(:,:,autumn)

% calculate the wave power
Wave_Power = 0.49*(swhAutumn.^2).*(T10Autumn);

% define the dimension for which to sum the values of
S = sum(Wave_Power,3);
```

```
% divide by the number of time sets to get the average
S = S/(14560);

% create the inverse for matrix dimension agreement
S = S';

% create pseudocolor plot of matrix
pcolor(long,lat,S);

% Get geo referenced
R =
georasterref('RasterSize',size(S),'LatitudeLimits',[53.5,
54],'LongitudeLimits',[-4.5,-3.5]);
%S = flipud(S) ;
% write to tiff file
tiffile = 'MetO-NWS-WAV-
RAN_54_53.5_4.5_3.5_autumn_wave_Power.tif' ;
geotiffwrite(tiffile,S,R)
%Read geotiff file
[S, R] = geotiffread(tiffile);
```

*Autumn Months Significant Wave Heights*

```
clear all
close all

% address the netcdf file with the model data
ncfile = 'MetO-NWS-WAV-RAN_54_53.5_4.5_3.5.nc';

% call the longitude from the model
long = ncread(ncfile,'longitude');

% call the latitude from the model
lat = ncread(ncfile,'latitude');

% call the time values from the netcdf file for the model
time = ncread(ncfile,'time');

%convert time to double
td = double(time)

% change time format from 'hours since 1950-1-1 00:00:00'
to normal date
% and time
time_formatted_model = datestr(td/86400+datenum('1970-01-
01 00:00:00'));
```

```
% convert from 'datestring' to 'datetime' for readability
time = datetime(time_formatted_model);

% convert from 'datetime' 'datevec' for readability
dv = datevec(time);

% define the start and end times
month = dv(:,2);

for i = 1:4
    i
    if i ==3
        autumn = find (month==9 | month ==10 |
month==11);
    end
end

% call the significant wave height values from the netcdf
file for the model
SWH = ncread(ncfile,'VHM0');

% Extract winter data from sst
swhAutumn = SWH(:,:,autumn)

% define the dimension for which to sum the values of
S = sum(swhAutumn,3);

% divide by the number of time sets to get the average
S = S/(14560);

% create the inverse for matrix dimension agreement
S = S';

% create pseudocolor plot of matrix
pcolor(long,lat,S);

% Get geo referenced
R =
georasterref('RasterSize',size(S),'LatitudeLimits',[53.5,
54],'LongitudeLimits',[-4.5,-3.5]);
%S = flipud(S) ;
% write to tiff file
tiffile = 'MetO-NWS-WAV-
RAN_54_53.5_4.5_3.5_autumn_swh.tif' ;
geotiffwrite(tiffile,S,R)
%Read geotiff file
[S, R] = geotiffread(tiffile);
```

*Autumn Months Spectral Wave Period*

```
clear all
close all

% address the netcdf file with the model data
ncfile = 'MetO-NWS-WAV-RAN_54_53.5_4.5_3.5.nc';

% call the longitude from the model
long = ncread(ncfile,'longitude');

% call the latitude from the model
lat = ncread(ncfile,'latitude');

% call the time values from the netcdf file for the model
time = ncread(ncfile,'time');

%convert time to double
td = double(time)

% change time format from 'hours since 1950-1-1 00:00:00'
to normal date
% and time
time_formatted_model = datestr(td/86400+datenum('1970-01-
01 00:00:00'));

% convert from 'datestring' to 'datetime' for readability
time = datetime(time_formatted_model);

% convert from 'datetime' 'datevec' for readability
dv = datevec(time);

% define the start and end times
month = dv(:,2);

for i = 1:4
    i
    if i ==3
        autumn = find (month==9 | month ==10 |
month==11);
    end
end

% call the wave period values from the netcdf file for
the model
T10 = ncread(ncfile,'VTM10');
```

```
% Extract winter data from sst
T10Autumn = T10(:,:,autumn)

% define the dimension for which to sum the values of
S = sum(T10Autumn,3);

% divide by the number of time sets to get the average
S = S/(14560);

% create the inverse for matrix dimension agreement
S = S';

% create pseudocolor plot of matrix
pcolor(long,lat,S);

% Get geo referenced
R =
georasterref('RasterSize',size(S),'LatitudeLimits',[53.5,
54],'LongitudeLimits',[-4.5,-3.5]);
%S = flipud(S) ;
% write to tiff file
tiffile = 'MetO-NWS-WAV-
RAN_54_53.5_4.5_3.5_autumn_T10.tif' ;
geotiffwrite(tiffile,S,R)
%Read geotiff file
[S, R] = geotiffread(tiffile);
```

*Spring Months Wave Power*

```
clear all
close all

% address the netcdf file with the model data
ncfile = 'MetO-NWS-WAV-RAN_54_53.5_4.5_3.5.nc';

% call the longitude from the model
long = ncread(ncfile,'longitude');

% call the latitude from the model
lat = ncread(ncfile,'latitude');

% call the time values from the netcdf file for the model
time = ncread(ncfile,'time');

%convert time to double
td = double(time)
```

```
% change time format from 'hours since 1950-1-1 00:00:00'
to normal date
% and time
time_formatted_model = datestr(td/86400+datenum('1970-01-
01 00:00:00'));

% convert from 'datestring' to 'datetime' for readability
time = datetime(time_formatted_model);

% convert from 'datetime' 'datevec' for readability
dv = datevec(time);

% define the start and end times
month = dv(:,2);

for i = 1:4
    i
    if i ==1
        spring = find (month==3 | month ==4 | month==5);
    end
end

% call the wave period values from the netcdf file for
the model
T10 = ncread(ncfile,'VTM10');

% Extract winter data from sst
T10Spring = T10(:,:,spring)

% call the significant wave height values from the netcdf
file for the model
SWH = ncread(ncfile,'VHM0');

% Extract winter data from sst
swhSpring = SWH(:,:,spring)

% calculate the wave power
Wave_Power = 0.49*(swhSpring.^2).*(T10Spring);

% define the dimension for which to sum the values of
S = sum(Wave_Power,3);

% divide by the number of time sets to get the average
S = S/(14720);

% create the inverse for matrix dimension agreement
S = S';
```

```
% create pseudocolor plot of matrix
pcolor(long,lat,S);

% Get geo referenced
R =
georasterref('RasterSize',size(S),'LatitudeLimits',[53.5,
54],'LongitudeLimits',[-4.5,-3.5]);
%S = flipud(S) ;
% write to tiff file
tiffile = 'MetO-NWS-WAV-
RAN_54_53.5_4.5_3.5_spring_wave_power.tif' ;
geotiffwrite(tiffile,S,R)
%Read geotiff file
[S, R] = geotiffread(tiffile);
```

*Spring Months Significant Wave Heights*

```
clear all
close all

% address the netcdf file with the model data
ncfile = 'MetO-NWS-WAV-RAN_54_53.5_4.5_3.5.nc';

% call the longitude from the model
long = ncread(ncfile,'longitude');

% call the latitude from the model
lat = ncread(ncfile,'latitude');

% call the time values from the netcdf file for the model
time = ncread(ncfile,'time');

%convert time to double
td = double(time)

% change time format from 'hours since 1950-1-1 00:00:00'
to normal date
% and time
time_formatted_model = datestr(td/86400+datenum('1970-01-
01 00:00:00'));

% convert from 'datestring' to 'datetime' for readability
time = datetime(time_formatted_model);

% convert from 'datetime' 'datevec' for readability
dv = datevec(time);
```

```
% define the start and end times
month = dv(:,2);

for i = 1:4
    i
    if i ==1
        spring = find (month==3 | month ==4 | month==5);
    end
end

% call the significant wave height values from the netcdf
file for the model
SWH = ncread(ncfile,'VHM0');

% Extract summer data from sst
swhSpring = SWH(:,:,spring)

% define the dimension for which to sum the values of
S = sum(swhSpring,3);

% divide by the number of time sets to get the average
S = S/(14720);

% create the inverse for matrix dimension agreement
S = S';

% create pseudocolor plot of matrix
pcolor(long,lat,S);

% Get geo referenced
R =
georasterref('RasterSize',size(S),'LatitudeLimits',[53.5,
54],'LongitudeLimits',[-4.5,-3.5]);
%S = flipud(S) ;
% write to tiff file
tiffile = 'MetO-NWS-WAV-
RAN_54_53.5_4.5_3.5_spring_swh.tif' ;
geotiffwrite(tiffile,S,R)
%Read geotiff file
[S, R] = geotiffread(tiffile);
```

*Spring Months Spectral Wave Period*

```
clear all
close all
```

```
% address the netcdf file with the model data
ncfile = 'MetO-NWS-WAV-RAN_54_53.5_4.5_3.5.nc';

% call the longitude from the model
long = ncread(ncfile,'longitude');

% call the latitude from the model
lat = ncread(ncfile,'latitude');

% call the time values from the netcdf file for the model
time = ncread(ncfile,'time');

%convert time to double
td = double(time)

% change time format from 'hours since 1950-1-1 00:00:00'
to normal date
% and time
time_formatted_model = datestr(td/86400+datenum('1970-01-
01 00:00:00'));

% convert from 'datestring' to 'datetime' for readability
time = datetime(time_formatted_model);

% convert from 'datetime' 'datevec' for readability
dv = datevec(time);

% define the start and end times
month = dv(:,2);

for i = 1:4
    i
    if i ==1
        spring = find (month==3 | month ==4 | month==5);
    end
end

% call the wave period values from the netcdf file for
the model
T10 = ncread(ncfile,'VTM10');

% Extract winter data from sst
T10Spring = T10(:,:,spring)

% define the dimension for which to sum the values of
S = sum(T10Spring,3);

% divide by the number of time sets to get the average
```

```
S = S/(14720);

% create the inverse for matrix dimension agreement
S = S';

% create pseudocolor plot of matrix
pcolor(long,lat,S);

% Get geo referenced
R =
georasterref('RasterSize',size(S),'LatitudeLimits',[53.5,
54],'LongitudeLimits',[-4.5,-3.5]);
%S = flipud(S) ;
% write to tiff file
tiffile = 'MetO-NWS-WAV-
RAN_54_53.5_4.5_3.5_spring_T10.tif' ;
geotiffwrite(tiffile,S,R)
%Read geotiff file
[S, R] = geotiffread(tiffile);
```

*Summer Months Wave Power*

```
clear all
close all

% address the netcdf file with the model data
ncfile = 'MetO-NWS-WAV-RAN_54_53.5_4.5_3.5.nc';

% call the longitude from the model
long = ncread(ncfile,'longitude');

% call the latitude from the model
lat = ncread(ncfile,'latitude');

% call the time values from the netcdf file for the model
time = ncread(ncfile,'time');

%convert time to double
td = double(time)

% change time format from 'hours since 1950-1-1 00:00:00'
to normal date
% and time
time_formatted_model = datestr(td/86400+datenum('1970-01-
01 00:00:00'));

% convert from 'datestring' to 'datetime' for readability
```

```
time = datetime(time_formatted_model);

% convert from 'datetime' 'datevec' for readability
dv = datevec(time);

% define the start and end times
month = dv(:,2);

for i = 1:4
    i
    if i ==2
        summer = find (month==6 | month ==7 | month==8);
    end
end

% call the wave period values from the netcdf file for
the model
T10 = ncread(ncfile,'VTM10');

% Extract winter data from sst
T10Summer = T10(:,:,summer)

% call the significant wave height values from the netcdf
file for the model
SWH = ncread(ncfile,'VHM0');

% Extract winter data from sst
swhSummer = SWH(:,:,summer)

% calculate the wave power
Wave_Power = 0.49*(swhSummer.^2).*(T10Summer);

% define the dimension for which to sum the values of
S = sum(Wave_Power,3);

% divide by the number of time sets to get the average
S = S/(14720);

% create the inverse for matrix dimension agreement
S = S';

% create pseudocolor plot of matrix
pcolor(long,lat,S);

% Get geo referenced
R =
georasterref('RasterSize',size(S),'LatitudeLimits',[53.5,
54],'LongitudeLimits',[-4.5,-3.5]);
```

```
%S = flipud(S) ;
% write to tiff file
tiffile = 'MetO-NWS-WAV-
RAN_54_53.5_4.5_3.5_summer_wave_power.tif' ;
geotiffwrite(tiffile,S,R)
%Read geotiff file
[S, R] = geotiffread(tiffile);
```

*Summer Months Significant Wave Heights*

```
clear all
close all

% address the netcdf file with the model data
ncfile = 'MetO-NWS-WAV-RAN_54_53.5_4.5_3.5.nc';

% call the longitude from the model
long = ncread(ncfile,'longitude');

% call the latitude from the model
lat = ncread(ncfile,'latitude');

% call the time values from the netcdf file for the model
time = ncread(ncfile,'time');

%convert time to double
td = double(time)

% change time format from 'hours since 1950-1-1 00:00:00'
to normal date
% and time
time_formatted_model = datestr(td/86400+datenum('1970-01-
01 00:00:00'));

% convert from 'datestring' to 'datetime' for readability
time = datetime(time_formatted_model);

% convert from 'datetime' 'datevec' for readability
dv = datevec(time);

% define the start and end times
month = dv(:,2);

for i = 1:4
    i
    if i ==2
        summer = find (month==6 | month ==7 | month==8);
```

```
    end
end

% call the significant wave height values from the netcdf
file for the model
SWH = ncread(ncfile,'VHM0');

% Extract winter data from sst
swhSummer = SWH(:,:,summer)

% define the dimension for which to sum the values of
S = sum(swhSummer,3);

% divide by the number of time sets to get the average
S = S/(14720);

% create the inverse for matrix dimension agreement
S = S';

% create pseudocolor plot of matrix
pcolor(long,lat,S);

% Get geo referenced
R =
georasterref('RasterSize',size(S),'LatitudeLimits',[53.5,
54],'LongitudeLimits',[-4.5,-3.5]);
%S = flipud(S) ;
% write to tiff file
tiffile = 'MetO-NWS-WAV-
RAN_54_53.5_4.5_3.5_summer_swh.tif' ;
geotiffwrite(tiffile,S,R)
%Read geotiff file
[S, R] = geotiffread(tiffile);
```

*Summer Months Spectral Wave Period*

```
clear all
close all

% address the netcdf file with the model data
ncfile = 'MetO-NWS-WAV-RAN_54_53.5_4.5_3.5.nc';

% call the longitude from the model
long = ncread(ncfile,'longitude');

% call the latitude from the model
lat = ncread(ncfile,'latitude');
```

```
% call the time values from the netcdf file for the model
time = ncread(ncfile,'time');

%convert time to double
td = double(time)

% change time format from 'hours since 1950-1-1 00:00:00'
to normal date
% and time
time_formatted_model = datestr(td/86400+datenum('1970-01-
01 00:00:00'));

% convert from 'datestring' to 'datetime' for readability
time = datetime(time_formatted_model);

% convert from 'datetime' 'datevec' for readability
dv = datevec(time);

% define the start and end times
month = dv(:,2);

for i = 1:4
    i
    if i ==2
        summer = find (month==6 | month ==7 | month==8);
    end
end

% call the wave period values from the netcdf file for
the model
T10 = ncread(ncfile,'VTM10');

% Extract winter data from sst
T10Summer = T10(:,:,summer)

% define the dimension for which to sum the values of
S = sum(T10Summer,3);

% divide by the number of time sets to get the average
S = S/(14720);

% create the inverse for matrix dimension agreement
S = S';

% create pseudocolor plot of matrix
pcolor(long,lat,S);
```

```
% Get geo referenced
R =
georasterref('RasterSize',size(S),'LatitudeLimits',[53.5,
54],'LongitudeLimits',[-4.5,-3.5]);
%S = flipud(S) ;
% write to tiff file
tiffile = 'MetO-NWS-WAV-
RAN_54_53.5_4.5_3.5_summer_T10.tif' ;
geotiffwrite(tiffile,S,R)
%Read geotiff file
[S, R] = geotiffread(tiffile);
```